Oestrogen regulation of NKCC1, NHERF3 and ENaC-β in oestrogen-dependent breast cancer

Thesis submitted for the degree of Doctor of Philosophy

Hasithi Anjalika Umagiliya Bandara

Northern Institute for Cancer Research,
Faculty of Medical Sciences,
Newcastle University

September 2015

Abstract

Oestrogen plays a major role in the development and progression of oestrogen receptor-positive breast cancers. Previously, a set of nineteen oestrogen-regulated genes was identified in oestrogen-responsive breast cancer cells. Seventeen were upregulated and two were downregulated. Oestrogen altered the expression of genes that encode proteins involved in the regulation of ion transport. *SLC12A2* encodes NKCC1, a Na^+-K^+-Cl^- co-transporter. *PDZK1* encodes the scaffolding protein NHERF3 and *SCNNIB* encodes the β-subunit of the epithelial Na^+ channel (ENaC). Expression of the oestrogen-regulated gene *SLC12A2* decreased whilst *PDZK1* and *SCNNIB* expression increased.

The purpose of this study is to investigate the oestrogen regulation of NKCC1, NHERF3 and ENaC-β protein expression in oestrogen-responsive breast cancer cells by western transfer analysis. NKCC1 expression decreased whereas the expression of NHERF3 and ENaC-β increased in response to oestrogen in all three cell lines MCF-7, EFM-19 and EFF-3. Immunofluorescence data confirmed the localisation of NKCC1 to the cell membrane. NHERF3 and ENaC-β were located mainly in the cytoplasm and there was evidence for vesicular localisation.

Functional activity of NKCC1, assessed by $^{86}Rb^+$ (K^+) influx, revealed low activity of NKCC1 which was then enhanced by hypertonicity. NKCC1 activity was decreased more by oestrogen treatment in EFM-19 cells than in MCF-7. Intracellular pH was measured with a pH-sensitive dye BCECF-AM to evaluate Na^+/H^+ exchange. Oestrogen increased the capacity of EFM-19 cells to regulate pH_i.

The oestrogenic and anti-oestrogenic effects of several anti-oestrogens were assessed. Notably, bazedoxifene was agonistic for NKCC1 expression. Tamoxifen, 4-hydroxytamoxifen, toremifene and lasofoxifene were partially agonistic for NHERF3. The antagonistic activities of the anti-oestrogens were more complex and varied between cell lines for all three proteins. Fulvestrant was unable to reverse the oestrogen-induced expression of ENaC-β.

In conclusion, this study confirmed that oestrogen alters the expression and activity of proteins involved in ion transport. Modification of this cell phenotype may favour breast cancer progression.

I dedicate this work to,

my beloved parents

Erald and **Rohini**

my wonderful sister

Ruvini

and

my amazing husband

Udena

Acknowledgements

Firstly, I would like to express my sincere thanks to my supervisors Dr Felicity May and Professor Nicholas Simmons, for their continued guidance and support throughout the duration of my PhD. I am forever grateful for your encouragement and advice in assisting me in writing this thesis.

A special thanks goes out to all my friends and colleagues Mercedes, Marina, Farah, Barry, Sanjay and Brendan for making my time in the NICR a memorable and enjoyable one. I would like to thank Noel and Git for providing me with protocols and tips regarding the BCECF assay.

Last but not least, I would like to thank my family without whom none of this would be possible. Words cannot describe how grateful I am to my beloved father and mother for being my pillars of strength and courage, and also for generously providing the research funding. Thanks to my sister, Ruvini for cheering me up and constantly reminding me that every cloud has a silver lining. I deeply appreciate the emotional support of my loving husband, Udena who provided the greatest motivation to make this PhD a success.

Table of Contents

List of Figures

List of Tables

Chapter 1. Introduction

1.1 Breast Cancer

1.1.1 Normal breast structure

The human breast contains epithelial ducts and lobules. The lobules are the glands that produce breast milk and the ducts carry the milk produced by the lobules to the nipple. A network of small ducts connects to larger ducts which then join to one main duct that transports milk to the nipple. The lobules and ducts of the breast are surrounded by stroma consisting of adipose tissue, fibrous connective tissue, lymphatics and blood capillaries. The ducts and lobules are lined by two cell layers of epithelium: the inner layer of ductal or lobular epithelial cells and the non-continuous outer layer of myoepithelial cells. These epithelia are supported by a basement membrane, hence separating them from the surrounding stroma (Figure 1.1). The epithelial cells of ducts and lobules within the breast are responsive to circulating hormones such as oestrogen. Breasts undergo structural changes during puberty and further development occurs during pregnancy and lactation.

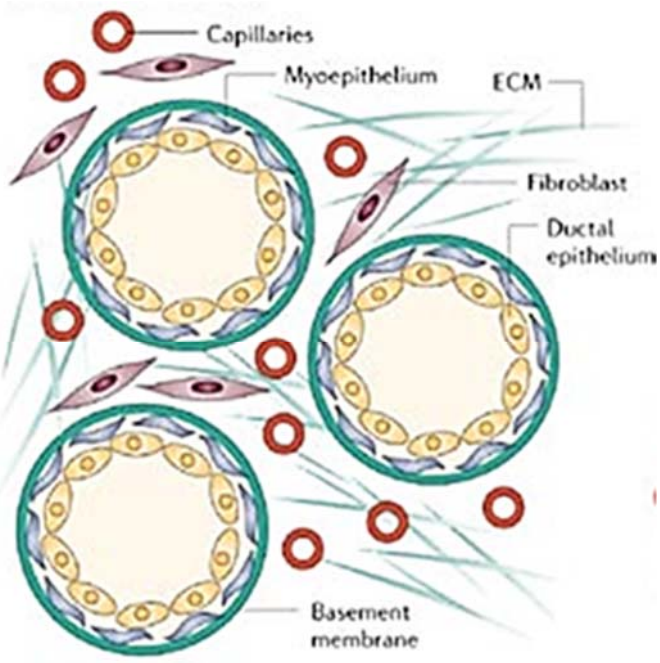

Figure 1.1 Components of normal breast tissue. The lobular and ductal epithelia along with the myoepithelial cells are supported by a basement membrane. The surrounding stroma

consists of capillaries, fibroblasts and extracellular matrix (ECM). Figure taken from (Kalluri and Zeisberg, 2006).

1.1.2 Breast cancer - Incidence and mortality

Breast cancer is the most common cancer in females in the UK, accounting for about 30% of all cases diagnosed. In women, the lifetime risk of developing breast cancer is 1 in 8 (Sasieni *et al.*, 2011). Approximately 49,900 females and 350 males were diagnosed with breast cancer in the UK in 2011 (*Cancer Statistics, CRUK*, 2014). The incidence rates of breast cancer in females in the UK continue to rise. This increase could possibly be due to early detection through current effective breast screening and awareness programmes running across the UK.

In 2012, over 522,000 women died from breast cancer worldwide. Currently, breast cancer is the second leading cause of death from cancer in females after lung cancer, and accounts for 15% of cancer-related deaths (Figure 1.2). In the UK, almost 11,600 women and 75 men died from breast cancer in 2012 (*Cancer Statistics, CRUK*, 2014). The mortality rates have dropped markedly due to improvements in diagnosis and treatment. The survival rates have been increasing and presently more than 8 in 10 women survive breast cancer beyond 5 years.

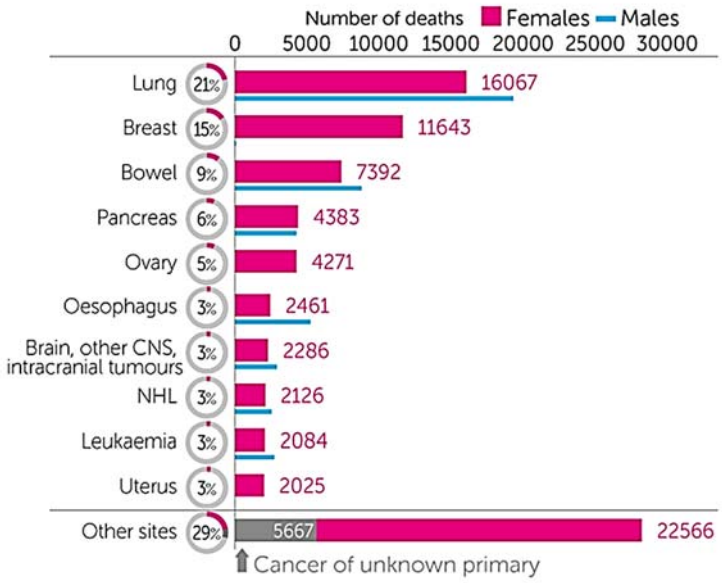

Figure 1.2 Most common causes of cancer death. Lung cancer, followed by breast and bowel cancers are the main causes of female cancer-related mortality. Figure obtained from (*Cancer Statistics, CRUK*, 2014).

1.1.3 Breast cancer - Risk factors

Several key risk factors have been associated with increased probability of developing breast cancer. The details of these risk factors are outlined in the following sub-sections.

1.1.3.1 Gender

The highest risk factor for developing breast cancer is being female. Worldwide about 1.7 million women were diagnosed with breast cancer in year 2012 (GLOBOCAN, 2012). Men have about a 100-fold decreased risk of developing breast cancer than females. In 2011, the incidence rates for males were less than 1% of all breast cancer cases reported.

1.1.3.2 Age

Age is one of the stronger risk factors. The likelihood of being diagnosed with breast cancer increases with age in both women and men. Women over the age of 50 are diagnosed most commonly, whereas most men are over the age of 75 when diagnosed with breast cancer (*Cancer Statistics, CRUK*, 2014). Between year 2009 and 2011, over 80% of breast cancer cases arose in women over 50 years of age (Figure 1.3A). For men approximately 36% of cases occurred over the age of 75 (Figure 1.3B). Females up to the ages of 20, 49 and 69 have an estimated risk of 1 in 2000, 1 in 50 and 1 in 13 respectively, of developing breast cancer.

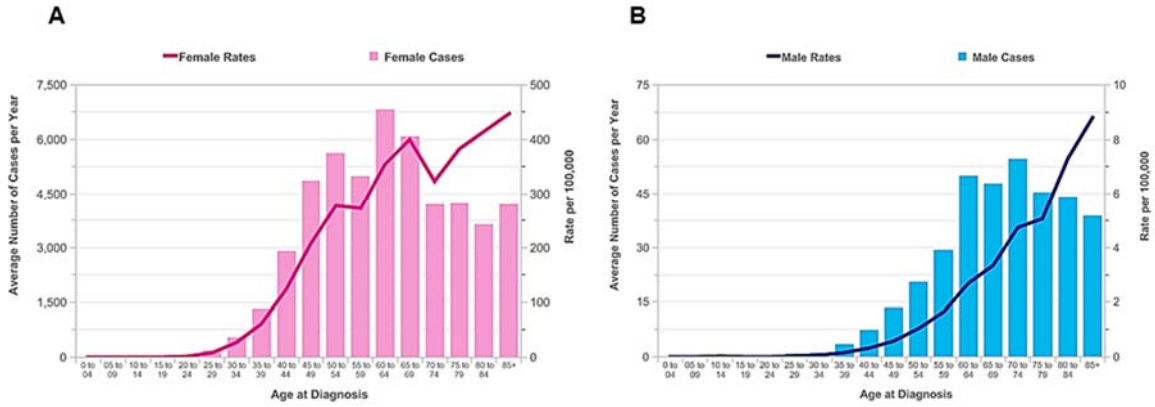

Figure 1.3 Age specific incidence for females and males in the UK. The risk of developing breast cancer increases with age and the majority is over the age of 50 and 75 for women and men, respectively. Figure obtained from (*Cancer Statistics, CRUK*, 2014).

1.1.3.3 Reproduction

There are several reproductive factors that increase or decrease the chances of developing breast cancer. Child bearing and breast feeding lowers the risk whereas early age at menarche and late menopause tend to increase the risk. As the parity of a woman increases, there is a decrease in the probability of developing breast cancer. Breastfeeding is a well known protective factor, and is shown to reduce the risk by 4.3% if a child is breastfed for at least 12 months (Parkin, 2011). Breast cancer incidence is more common in the developed world, than in developing countries. One of the possible explanations for this increase in risk is that women in developed countries have fewer children and breast feed for a shorter period of time compared to women in developing countries. Early menarche before the age of 12 years and late menopause on or after 50 years increase the risk, primarily due to the prolonged exposure to the actions of endogenous oestrogens (Pike *et al.*, 1993).

1.1.3.4 Hormones

Exogenous hormonal factors such as oral contraceptive use and hormone replacement therapy have been associated with increased risk of breast cancer. Oral contraceptives usage and the development of breast cancer remain controversial. For current users of oral contraceptives, there is an increased risk compared to never-users, whilst the risk is reduced the longer the duration of discontinued use (CGHFBC, 1996). Studies have shown that the age at first oral contraceptive use is correlated positively with the age at diagnosis with breast cancer. This suggests that there is an increased risk of developing breast cancer earlier in life, if a female has started to use oral contraceptive at a younger age (Imkampe and Bates, 2012). Increased duration of hormone replacement therapy use seems to cause an increase in the risk of being diagnosed with breast cancer. Current users of combined oestrogen and progestin hormone replacement therapy have a greater risk than users of drugs consisting of oestrogen alone (Rossouw *et al.*, 2002; Beral, 2003).

Higher levels of endogenous hormones such as oestrogen and progesterone may also play a role in increasing breast cancer risk. Although pre-menopausal

women with high concentrations of circulating oestrogen do not show an association with increased risk, post-menopausal women with high oestrogens levels have a 2-3 times higher risk of developing breast cancer than those with low levels of endogenous oestrogen (Key *et al.*, 2002; Walker *et al.*, 2011). The development of oestrogen receptor-α positive (ERα+) tumours have been associated with exposure to other circulating hormones such as insulin. Insulin-like growth factor 1 (IGF-1) and insulin have been implicated with the development of breast cancer in pre-menopausal and post-menopausal women. Also obesity and type 2 diabetes mellitus have been correlated with an increase in breast cancer risk. Higher circulating levels of insulin increases the risk of developing breast cancer in obese women with diabetes (Gunter *et al.*, 2009; Liao *et al.*, 2011).

1.1.3.5 Hereditary factors and family history

Hereditary factors contribute to a small proportion of breast cancer; the vast majority of breast cancers arise sporadically. Hereditary mutations account for about 5-10% of all cancer cases reported (Deng, 2006). Mutations in hereditary tumour suppressor genes *BRCA1* and *BRCA2* are implicated as breast cancer causative genes and contribute to an increase in risk of developing breast cancer. BRCA1 and BRCA2 are involved in homologous recombination and DNA double strand break repair. Women carrying a germ-line mutation in either *BRCA1* or *BRCA2* genes have a 45% to 65% risk of developing breast cancer by the age of 70 (Antoniou *et al.*, 2003). The presence of mutations in other genes such as *p53*, *ATM* and *PTEN* confers an increase in breast cancer risk (Elledge and Allred, 1998; Inskip *et al.*, 1999).

Genome wide association studies (GWAS) have led to the discovery of low penetrance alleles that contribute to the familial risk of breast cancer. Several studies have reported the identification of new breast cancer susceptibility loci that were associated significantly with breast cancer risk (Easton *et al.*, 2007; Hunter *et al.*, 2007; Stacey *et al.*, 2007). These susceptibility loci are single nucleotide polymorphisms (SNPs) within *FGFR2*, *TNRC9*, *CASC8*, *CASC16*, *CASC21* and *LSP1*. The genes have two alleles with SNPs, one of which is a

high-risk allele and the other a low-risk allele. The SNPs in intron 2 of the *FGFR2* gene were the most significantly associated with risk. The *FGFR2* gene encodes a receptor tyrosine kinase that belongs to the Fibroblast Growth Factor Receptor family. The relative-risk per allele is 1.26 and 1.20 for *FGFR2* and *TNRC9*, respectively (Easton *et al.*, 2007). The *FGFR2* SNPs were associated only with oestrogen receptor positive cancers, whereas *TNRC9* was observed to be associated with both oestrogen receptor positive and oestrogen receptor negative tumours. More recently, another 78 loci have been discovered through GWAS. Most of these loci were associated with risk of oestrogen receptor positive tumours. In contrast, *TERT*, *RALY*, *MDM4*, *LGR6* and *FTO* were largely associated with risk of oestrogen receptor negative tumours (Haiman *et al.*, 2011; Siddiq *et al.*, 2012; Couch *et al.*, 2013; Garcia-Closas *et al.*, 2013). *BABAM1* and *ANKLE1* were more commonly associated with risk of triple negative breast cancers (Antoniou *et al.*, 2010). Ghoussaini *et al.* (2012) identified three new susceptibility loci at 12p11, 12q24 and 21q21 which were associated with breast cancer risk. The 12p11 and 12q24 loci contained the genes *PTHLH* and *TBX3*, respectively, both of which are known to play a role in the development of mammary glands (Wysolmerski and Stewart, 1998; Davenport *et al.*, 2003). The 21q21 locus was closest to the gene *NRIP1* which acts as a repressor of ERα activity and inhibits cell growth.

Familial breast cancer is another important factor, as the risk doubles if there is one first-degree relative such as mother or sister who is affected by breast cancer. In women, with an affected first-degree relative the breast cancer incidence rate is 5.5%, whereas if there are two or more first-degree relatives affected the incidence rate increases to 13.3% (CGHFBC, 2001).

1.1.3.6 Lifestyle

Diet, smoking, alcohol consumption, exercise and obesity are included in this broad category of lifestyle factors. They are considered potentially avoidable risk factors. The consumption of alcohol and smoking increases the risk of developing breast cancer. In comparison to women who do not smoke, cigarette smoking women conveys a 10-20% increased risk (Xue *et al.*, 2011). Alcohol

consumption is associated with approximately 6% of breast cancers in women in the UK. The risk of breast cancer has been shown to increase by 12% for every additional 10 g increase in the daily intake of alcohol (Allen *et al.*, 2009). Despite inadequate evidence, some studies suggest a direct link between dietary saturated fat intake and breast cancer (Boyd *et al.*, 2003; Sieri *et al.*, 2008). Another risk factor for developing breast cancer is obesity. In overweight and obese post-menopausal women the risk is estimated to increase by 10-20% and 30%, respectively (Parkin and Boyd, 2011). This increase in risk is correlated directly to increased synthesis of oestrogen in excess adipose tissue (Lorincz and Sukumar, 2006). Other harmful factors contributing to an increase in breast cancer risk include exposure to mutagenic agents such as ionising radiation. In the UK, approximately 1% of breast cancers occur due to exposure to x-rays or gamma radiation (Parkin and Darby, 2011). Carcinogenic ionising radiation causes damage to DNA which may be repaired aberrantly leading to mutations that predispose to increased risk of breast cancer.

Other factors such as appropriately controlled diet and exercise are beneficial, and may reduce an individual's risk of breast cancer. Post-menopausal women who tend to be more physically active have a reduction in breast cancer risk by 15-20% (Monninkhof *et al.*, 2007). This decrease in risk may be associated to active post-menopausal women having lower concentrations of circulating hormones such as oestrogen in blood, than the less active post-menopausal women.

1.1.4 Breast cancer - Types

Breast cancer is broadly categorised into two main groups according to its histological appearance and invasion of the stroma. Invasive carcinoma and non-invasive carcinoma are these two main groups (Fabbri, 2008). Adenocarcinomas of the breast cancer arise from epithelial cells lining the ducts or lobules within the breast.

Invasive or infiltrating carcinomas are malignant tumours that have the ability to break through the myoepithelial cell layer, and invade into the surrounding tissue. Such invasive adenocarcinomas are either invasive ductal (IDC) which is the most common type of breast cancer, or invasive lobular (ILC) which comprises about 15% of all breast cancers (Kumar V, 2004). Invasive carcinomas have the potential to metastasise through the blood circulation and lymphatic system, into other parts of the body. IDC of no special type (IDC NST), also known as IDC not otherwise specified (IDC NOS) accounts for the majority of 80% of breast carcinomas diagnosed.

Non-invasive or carcinoma *in-situ* stay in the place of origin and do not invade into adjacent tissue stroma. These carcinomas include ductal carcinoma *in situ* (DCIS) or lobular carcinomas *in situ* (LCIS) (Kumar V, 2004; Fabbri, 2008). *In-situ* carcinomas do not infiltrate into surrounding breast tissue and instead remain within an intact myoepithelial cell layer. Because both DCIS and LCIS do not have the capacity to break through the myoepithelium they do not metastasise into other parts of the body.

1.1.5 Breast cancer - Classification

1.1.5.1 Molecular classification

In addition to the aforementioned histological classification, breast tumours are further classified according to their molecular receptor expression. Breast cancer cells can express the oestrogen receptor (ER), the progesterone receptor (PgR) and the human epidermal growth factor receptor 2 (EGFR2, HER2 or neu).

Tumours that express the oestrogen receptor-α are referred to as “oestrogen receptor-α-positive” or ERα+, whereas breast cancers that express progesterone receptor are identified as “progesterone receptor-positive” or PgR+. Tumours which overexpress HER2 are termed “HER2-positive”. Additionally tumours that do not express any of these three receptors are known as “triple-negative” breast cancers.

Breast cancer is widely considered as a highly heterogeneous disease. Therefore more recently, extensive molecular and genetic profiling had been investigated to determine detailed analysis of prognosis and to predict response to treatments. Analyses of gene expression arrays have identified five distinct molecular subtypes of breast cancer (Perou *et al.*, 2000; Sorlie *et al.*, 2003). These subdivisions include luminal A, luminal B, HER2 enriched, basal-like and normal-like tumours. The luminal A subtype express ER and have a low proliferation rate, whilst luminal B subtype also express the ER, but have higher rate of proliferation. Luminal A has a better prognosis than luminal B. The HER2 enriched breast cancers have HER2 gene amplification and overexpress HER2, but test negative for ER and PgR. Basal-like tumours are triple-negative and do not express ER, PgR or HER2. Such cancers are highly proliferative and have worst prognosis. The normal-like breast cancers often relate to gene clusters of normal breast cells. These normal-like tumours express genes that are distinctive of basal epithelial cells.

A recent study based on integrated analysis of genome and transcriptome data has led to the identification of ten novel molecular subtypes of breast cancer (Curtis *et al.*, 2012). In this study, 2000 breast tumours were analysed by joint clustering of data from gene expression and copy number data. The 10 subgroups were categorised as Integrative Cluster (IntClust) 1-10. The IntClust 2 subtype are high risk oestrogen receptor positive breast cancers that have amplifications of known driver genes such as *CCND1* and *EMSY*. The IntClust 3 and IntClust 4 subgroups generally had tumours with good prognosis. The IntClust 3 comprised oestrogen receptor positive cases, whilst IntClust 4 had both oestrogen receptor positive and oestrogen receptor negative cases. The IntClust 4 subgroup was also called the “CNA-devoid” subgroup, due to the lack

of copy number aberrations. IntClust 1, 6, and 9 consisted mostly of oestrogen receptor positive tumours with intermediate prognosis. Moreover, the IntClust 10 subgroup comprised basal-like tumours, whereas the IntClust 5 consisted of HER2-enriched breast tumours. Each of the subtypes are associated with different prognosis and are proposed to require different therapeutic strategies.

The cancer genome atlas (TCGA) network has analysed tumour and germline DNA samples from 825 patients, and combined data from different platforms. The platforms included exome sequencing, mRNA arrays, microRNA, DNA methylation, protein expression and copy number variant arrays (Cancer Genome Atlas, 2012). Four main classes of breast cancer were identified with a high degree of heterogeneity within each of the classes. The four groups were luminal A, luminal B, HER2 enriched and basal-like. The genes *TP53*, *PIK3CA* and *GATA3* were mutated in 37 %, 36 % and 11 % of breast tumours, respectively. Mutations were more prevalent in luminal A and luminal B tumours than in HER2-enriched and basal-like groups. *PIK3CA* gene was mutated in 45 % of luminal A tumours and 29 % of luminal B tumours, making it one of the most frequently mutated genes in breast cancer. The *TP53* gene was mutated in 12 % of luminal A and 29 % of luminal B tumours. The more frequently mutated genes were specific to the different subgroups. Mutations in the *TP53* gene was observed in 72 % of HER2-enriched cases and in 80 % of basal-like tumours. *MAP3K1* and *MAP2K4* genes which encode proteins belonging to the serine/threonine kinase family, were amongst the more frequently mutated genes, particularly specific to luminal tumours. Additionally the TCGA identified several novel genes which were mutated significantly in the breast tumours analysed. The genes include *RUNX1*, *PTPN22*, *NF1*, *CCND3*, *AFF2* and *TBX3* to name a few (Cancer Genome Atlas, 2012).

1.1.5.2 TNM stage

Clinical staging of breast cancer is based upon the tumour size (T), the spread to lymph nodes (N) and the presence of distant metastasis (M). This staging system is called the Tumour, lymph Node and Metastases (TNM) staging (Edge, 2010). This TNM staging system guides the clinician through

classification of the breast tumour to determine the best treatment options for individuals.

- The T (tumour) stage

This T staging system is grouped into six main categories: TX, T0, T1, T2, T3 and T4. The inability to assess the primary tumour is specified by the TX notation. If there is no evidence of a primary tumour it is designated as T0. Additionally, T1 classifies, breast tumours that are less than 2 cm in size and includes further subdivisions T1mi, T1a, T1b and T1c. T1mi signifies a tumour less than 0.1 cm, whilst T1a and T1b tumours are larger than 0.1 cm and 0.5 cm, respectively. T1c tumours are larger than 1 cm but smaller than 2 cm. Tumours larger than 2 cm but no more than 5 cm across are grouped as T2, whereas T3 cancers are more than 5 cm across in their greatest dimension. Any tumours that have spread directly to the chest wall or into the skin are designated as T4.

- The N (nodes) stage

The nodal stage assesses whether the tumour has extended to the lymph nodes and is classified into five groups namely, NX, N0, N1, N2 and N3 (Edge, 2010). In the case where lymph nodes have been removed previously or are inaccessible, the cancer is specified as NX. N0 stands for cancers that have not spread to any lymph nodes nearby. The presence of cancerous cells in 1-3 axillary nodes of the underarm or in the internal mammary lymph nodes are indicated as N1. N2 signifies that the tumours have spread to one or more mammary lymph nodes and to at least 4-9 lymph nodes in the underarm. N2 has two subdivisions, in which N2a denotes tumours present in the axillary lymph nodes which are attached to surrounding tissues. N2b stands for any cancer cells that are not present in the axillary lymph nodes, but present in the internal mammary lymph nodes behind the sternum. N3 consists of three subgroups namely; N3a, N3b and N3c. tumours that are classified as N3a have either spread to 10 or more axillary lymph nodes and also to the infraclavicular lymph nodes beneath the collar bone. Cancerous cells present in both internal mammary lymph nodes and axillary lymph nodes are categorised as N3b. in

contrast to N3a, any tumour metastasis detected in the supraclavicular lymph nodes above the collar bone are referred to as N3c.

- The M (metastasis) stage

This stage is the simplest to classify as it contains only two groups: M0 and M1. No distant metastasis exhibited by clinical or radiographic signs are indicated as M0. If any distant metastasis that is metastases in other parts of the body other than the breast and surrounding lymph nodes is observed, then the tumour is designated as M1 (Edge, 2010).

1.1.6 Breast cancer - Therapy

Patients with breast cancer are treated dependent upon the clinical stage and prognosis of their breast cancer type. The choice of treatment depends also on the receptor status of the cancer cells, that is whether they express any of the following receptors: ER, PgR or HER2/neu. Treatment of breast cancer consists of a single or combination of treatment procedures.

1.1.6.1 Surgical treatment

Surgical resection is still the most widely used mode of treatment. Several pathological factors including size and grade of tumour, involvement of the lymph nodes and invasion to lymphatics, are taken into account when making a decision about surgical treatment. Surgery may involve complete removal of the breast in which case it is termed “total mastectomy”, or breast conserving surgeries such as removal of small tumour lumps and parts of the breast where the procedure is known as “lumpectomy” or “wide local excision” (Sabel, 2009). Depending on the degree of invasiveness and metastasis of the tumour, lymph nodes may also be removed surgically. Patients may be treated with neoadjuvant therapies such as radiation therapy and chemotherapy, prior to surgical resection. These neoadjuvant therapies will aid in the shrinkage of the tumour and potentially allow for breast conservation surgery.

1.1.6.2 Radiotherapy

Following breast conservation surgery, patients are often treated with radiation therapy. Radiotherapy involves the use of radiation such as X-rays to kill tumour cells, in residual breast tissue (Lin and Tripuraneni, 2011). Irradiation is usually used as an adjuvant therapy, which refers to any treatment administered post-operatively. Radiotherapy is also used to successfully prevent or treat tumour metastases. A recent report highlighted that post-surgical radiation therapy reduces greatly the risk of disease recurrence (Early Breast Cancer Trialists' Collaborative *et al.*, 2011a).

1.1.6.3 Chemotherapy

Chemotherapy is the use of cytotoxic drugs to kill or prevent the growth and division of cancer cells. Chemotherapeutic agents are used as neoadjuvant and adjuvant breast cancer treatments. Neoadjuvant chemotherapy may induce tumour shrinkage, prior to surgery. Cyclophosphamide, epirubicin and doxorubicin are examples of chemotherapeutic drugs, which target and destroy fast replicating cancer cells (Tabuchi *et al.*, 2009). These drugs induce DNA damage by intercalating with DNA. Other agents such as docetaxel and paclitaxel inhibit polymerisation of microtubules, thus preventing cell division. They then promote apoptosis. Chemotherapy has potential adverse effects, as it does not only target fast-growing cancer cells, but also fast-growing normal cells. The resulting side effects are fatigue, hair loss and nausea.

1.1.6.4 Endocrine therapy

Hormones such as oestrogen are responsible for both the pathogenesis and the progression of breast cancer. Another form of systemic therapy in addition to chemotherapy is endocrine therapy. Breast cancers that express the oestrogen receptor and/or progesterone receptor are treated with endocrine receptor-based therapy. Endocrine therapy is considered the most effective form of systemic treatment and has led to improvements in patient recovery from breast cancer (Pritchard, 2005). Hormonal therapy includes potential chemopreventative agents that either inhibit the production of oestrogens or

block the functional oestrogen receptor. Anti-oestrogenic drugs such as tamoxifen and fulvestrant have been administered widely to patients with oestrogen receptor-positive tumours mainly due to their specificity of action.

Tamoxifen

Anti-oestrogens such as tamoxifen target and compete with oestrogen and block their mode of action, thus inhibiting oestrogen receptor activity. Because oestrogen induces the expression of genes that promote cell growth and proliferation, tamoxifen treatment thereby, leads to an arrest of cell proliferation. The cell cycle is blocked at the G_1 phase, in cells treated with tamoxifen (Dalvai and Bystricky, 2010).

Adjuvant treatment with tamoxifen for 5-years reduces the relative risk of recurrence and prolongs the disease-free survival particularly in pre-menopausal women with ER-positive breast cancer (Early Breast Cancer Trialists' Collaborative, 2001). However, the extensive use of tamoxifen has both its advantages and disadvantages. Tamoxifen has oestrogenic actions on bones, which is advantageous because it prevents osteoporosis. Conversely, the use of tamoxifen causes side effects such as fatigue, hot flushes, sweating and lowering of serum cholesterol levels. Other disadvantages include the increased risk of developing endometrial cancer because tamoxifen has partial agonist activity in the endometrium. Tamoxifen has been in use for the past 4 decades. Alternative drugs that have greater anti-oestrogenic effects on tumours than tamoxifen have been developed. Hormonal treatment agents that do not cross the blood brain barrier, hence proven not to induce hot flushes were established (O'Regan and Jordan, 2001).

4-hydroxytamoxifen

4-hydroxytamoxifen is one of the active metabolites of tamoxifen. It has a 25-100 fold stronger binding affinity for ER than tamoxifen (Favoni and de Cupis, 1998). The binding affinity of 4-hydroxytamoxifen to ER is similar to that of 17β-oestradiol.

Fulvestrant

A more selective anti-oestrogen is fulvestrant also known as ICI 182,780 or Faslodex. It is a pure anti-oestrogen and does not induce any oestrogen-like activity in the uterus or in bones (Platet *et al.*, 2004). Fulvestrant is a steroidal anti-oestrogen and as shown in Figure 1.4, its structure is quite similar to that of 17β-oestradiol, apart from the additional long-chain alkyl moiety at the 7-alpha position. Fulvestrant has an ER binding affinity which is about 100 times more than that of tamoxifen (Howell *et al.*, 2004). Its mechanism of action involves rapid degradation of the ER and it has been termed a selective oestrogen receptor downregulator (SERD). It has minimal side effects, but has been shown to be effective treatment for prevention of breast cancer recurrence. In comparison to tamoxifen, fulvestrant does not cross the blood brain barrier hence does not induce hot flushes.

Raloxifene

Raloxifene is a benzothiophene that causes blockage of the ER. It is a second generation selective oestrogen receptor modulator (SERM). Raloxifene exerts anti-oestrogenic effects on breast tissue and displays weak antagonism in the endometrium. Similar to tamoxifen, raloxifene is capable of preventing osteoporosis, as it increases the density of bones (Ettinger *et al.*, 1999).

Bazedoxifene

Another anti-oestrogen bazedoxifene belongs to the 3rd generation of partial anti-oestrogens and was developed using raloxifene as a template. The chemical structures of raloxifene and bazedoxifene are quite similar. The benzothiophene group (C_8H_6S) of raloxifene highlighted in green in Figure 1.4, is substituted with an indole ring (C_8H_7N). Bazedoxifene inhibits growth and proliferation of oestrogen-stimulated breast cancer cells MCF-7 and T47D (Komm *et al.*, 2005; Lewis-Wambi *et al.*, 2011). Bazedoxifene also increases the degradation of ER in MCF-7 cells. Bazedoxifene is a ‘raloxifene-like’ drug and has been shown to increase bone density (Miller *et al.*, 2008). Bazedoxifene is used widely in the clinic as a treatment and prevention of osteoporosis. Unlike other anti-oestrogens, bazedoxifene did not induce hot

flushes, and also showed beneficial antagonistic effects in ovarian, endometrial and breast tissue (Ronkin *et al.*, 2005; Archer *et al.*, 2009).

Toremifene

Toremifene is an analogue of tamoxifen, and is very similar in structure apart from the chlorine (Cl) atom at the 4th position (circled in red in Figure 1.4). The binding affinity of toremifene for the ER is also similar to tamoxifen. Toremifene inhibited the growth of oestrogen responsive cell lines and is currently used in the clinic as a treatment for advanced metastatic breast cancer (Robinson and Jordan, 1989; Pyrhonen *et al.*, 1999). The agonist activity of toremifene on bone was similar to that of tamoxifen (Saarto *et al.*, 2001).

Lasofoxifene

Lasofoxifene is a third generation anti-oestrogen used in the treatment of osteoporosis and vaginal atrophy. It exerts antagonistic effects in breast and uterine tissue (Rosati *et al.*, 1998). Clinical studies have shown a 65-85% reduction in relative risk of developing breast cancer in patients to whom lasofoxifene was administered (Gennari *et al.*, 2010). Compared to raloxifene, lasofoxifene exerts an additional benefit of decreasing the risk of coronary heart disease (Cummings *et al.*, 2010). A substantial reduction in cholesterol levels contribute to this decrease in risk.

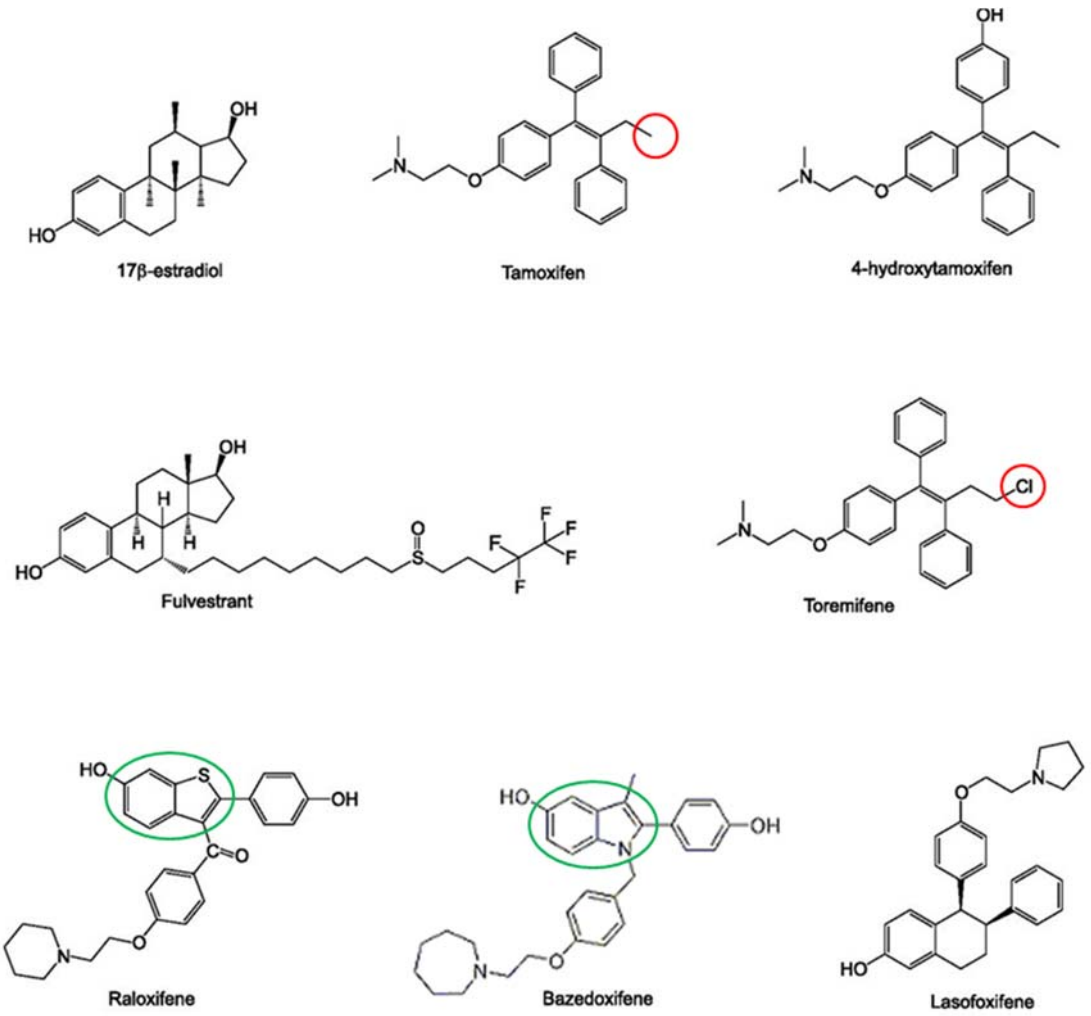

Figure 1.4 Chemical structures of oestrogen receptor ligands. The structure of oestradiol, tamoxifen, 4-hydroxytamoxifen, fulvestrant, bazedoxifene, toremifene, raloxifene and lasofoxifene are shown. Red circles highlight structural differences between tamoxifen and toremifene. Green circles highlight structural differences between raloxifene and bazedoxifene. Figure modified from (Burris *et al.*, 2013).

Another form of endocrine therapy is the use of steroidal and non-steroidal aromatase inhibitors. Aromatase also known as oestrogen synthase is the enzyme that converts androgens to oestrogens. Aromatase belongs to the cytochrome P450 superfamily and is expressed in many tissues, including ovaries, breast, liver, placenta and adipose tissue (Brueggemeier *et al.*, 2005; Bhatnagar, 2007). High levels of aromatase are detected in endometrial and breast cancers. There are two types of aromatase inhibitors: steroidal and nonsteroidal (Lonning, 2011). The steroidal aromatase inhibitors bind to the aromatase enzyme irreversibly. In contrast, the nonsteroidal aromatase inhibitors bind to aromatase reversibly and are more potent than the steroidal

aromatase inhibitors (Miller and Dixon, 2000). Third generation steroidal aromatase inhibitor exemestane and non-steroidal aromatase inhibitors anastrozole and letrozole inhibit the enzyme aromatase and hence prevent the biosynthesis of oestrogen. This inhibition of aromatisation leads to a minimal production of oestrogen. Aromatase inhibitors are used as an adjuvant treatment for oestrogen receptor-positive breast cancers mainly in post-menopausal women and have been reported to prevent reappearance of disease (Winer *et al.*, 2005).

1.1.6.5 Other targeted therapy

Breast cancer is a highly heterogeneous disease and it is of vital importance to identify the receptor status of an individual's cancer. There is a greater need to target cancer cells in a specific manner, without harming normal cells. One way this specificity can be achieved is by using molecular targeted therapy. Such targeted therapies could either be in the form of monoclonal antibodies or of tyrosine kinase inhibitors. Better systemic actions are provided for by these selective inhibitors as they have a precise and more efficient mode of action. These molecular targeted inhibitors tend to block growth and proliferation of cancer cells and prevent tumour cell metastasis.

Endocrine therapy is administered to patients with ER and PgR expressive cancers, whereas HER2 over-expressive cancers are treated with trastuzumab (Herceptin) (Spector and Blackwell, 2009). Trastuzumab is a humanised monoclonal antibody against the HER2 receptor and is generally administered in combination with chemotherapy. Pertuzumab is another monoclonal antibody against the HER2 receptor that is used in the treatment of metastatic breast cancer (Perez and Spano, 2012). Selective inhibitors that target different members of the epidermal growth factor receptor family (EGFR) are lapatinib and gefitinib, both of which are tyrosine kinase inhibitors.

Current research focus is on identifying other suitable targets. Other potential receptors that could be targeted include the vascular endothelial growth factor receptor (VEGF) and insulin-like growth factor receptor. The monoclonal antibody, Bevacizumab targets the vascular endothelial growth factor and

blocks tumour angiogenesis (Hampton, 2005). Several recently developed antibodies and inhibitor molecules are undergoing clinical trials.

Currently, there are several other targeted agents that interfere with signal transduction pathways such as PI3K/AKT/mTOR and Ras/Raf/MAPK. It is proposed that these targeted therapies will be particularly effective in the treatment of oestrogen receptor positive breast cancers. The *PIK3CA* gene that encodes the catalytic subunit of PI3K have been shown to be mutated commonly in oestrogen receptor positive breast cancers (Cancer Genome Atlas, 2012). This observation suggest that inhibitors that target PI3K would be effective to treat cancer progression and resistance to current treatment regimes in oestrogen receptor positive breast cancer. Pictilisib is a selective inhibitor of PI3K, which was evaluated in combination with fulvestrant in a randomised phase II study. Results indicated that the progression-free survival of patients in the combination arm was not significantly different to that of the fulvestrant alone arm. mTOR inhibitors such as everolimus have been combined with exemestane, an aromatase inhibitor, and have been proven successful at improving progression-free survival compared to patients treated with exemestane alone (Piccart *et al.*, 2014). Everolimus is usually administered to postmenopausal women with advanced breast cancer.

Resistance to endocrine therapy has been reported to develop through activation of the Ras/MEK/MAPK pathway. MEK inhibitors such as selumetinib have been combined with fulvestrant to test their effectiveness in the treatment of patients with advanced breast cancers that developed after endocrine therapy with aromatase inhibitors (Zaman *et al.*, 2015). The combination treatment did not improve overall survival and resulted in several adverse events such as vomiting, skin disorders and oedema. Another MEK inhibitor, trametinib has been tested in combination with an AKT inhibitor, afuresertib in a phase I study (Tolcher *et al.*, 2015).

Drugs that target CDK4/6 prevent cell cycle progression from G_1 to S phase. A CDK4/6 inhibitor palbociclib has been shown to be effective at inhibiting growth of oestrogen receptor positive, HER2-negative breast cancers (Turner *et al.*, 2015). Other CDK4/6 inhibitors, abemaciclib and ribociclib are undergoing

clinical trials and will be tested in combination with fulvestrant or aromatase inhibitors such as anastrozole and letrozole (Lu, 2015).

1.2 Role of oestrogen in the development of breast cancer

Steroid hormones such as oestrogens are crucial for the regulation of lipid metabolism, neuronal homeostasis, female and male fertility, bone development and also for efficient functioning of the cardiovascular system (Shao and Brown, 2004). Normal breast tissue development does not occur in aromatase-deficient women who have lower levels of circulating oestrogens. However, normal pre- and post- pubertal breast growth and development take place when these women were treated with oestrogen therapy. This observation illustrates the importance of oestrogen for the normal development of the breast. The roles played by oestrogen is not limited to the breast, but extend to the uterus, liver, ovary and bones. Oestrogen is known to stimulate growth and proliferation of breast cancer cells and plays an extensive role in facilitating the progression and metastasis of breast cancer. Because oestrogens mediate their action via interaction with the oestrogen receptor, anti-oestrogenic drugs that target the oestrogen receptor are beneficial in the treatment of breast cancer.

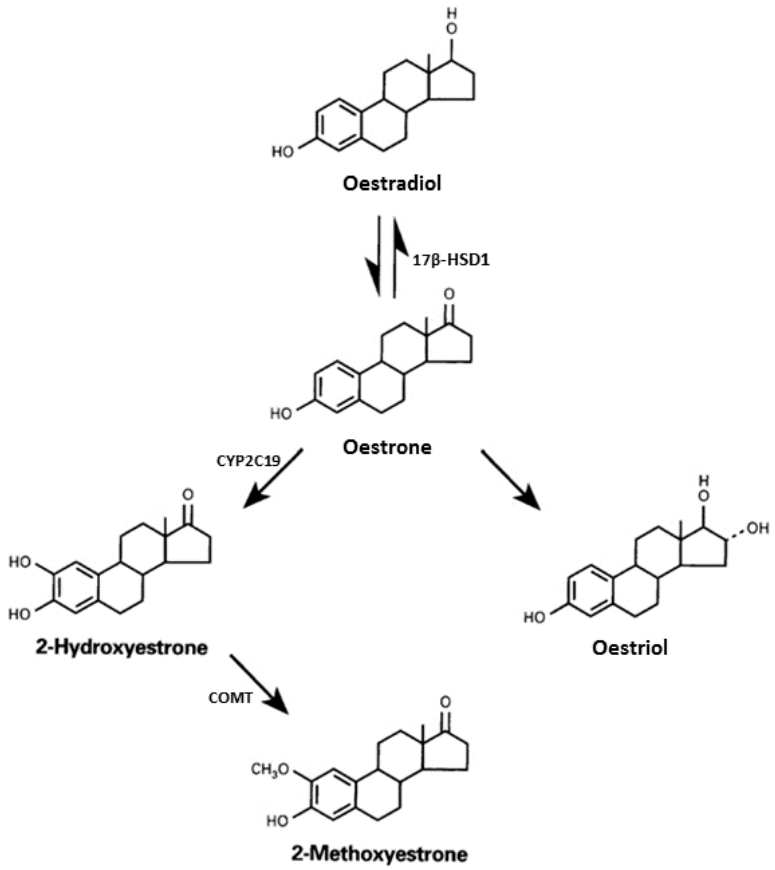

Figure 1.5 Different forms of oestrogen. Oestrone, oestradiol and oestriol consist of one, two and three hydroxyl (OH) groups respectively. Oestrone can be inter-converted to 17β-oestradiol by the enzyme 17β-hydroxysteroid dehydrogenase type 1 (17β-HSD1). Oestrone can be broken down further into oestriol and 2-hydroxyestrone. The hydroxylation of oestrone to 2-hydroxyestrone is catalysed by a member of cytochrome P450 family, CYP2C19. 2-hydroxyestrone is methylated to 2-methoxyestrone by catechol-o-methyltransferase (COMT). Figure adapted from (Ackerman and Carr, 2002).

There are three different types of endogenous oestrogens: oestrone (E_1), 17β-oestradiol (E_2) and oestriol (E_3), which contain one, two and three hydroxyl (OH) groups respectively (Figure 1.5). Out of the three oestrogens, 17β-oestradiol is the most biologically active and is produced primarily in the ovaries in pre-menopausal women. In post-menopausal women oestradiol is produced in adipose tissue, bone, brain and in vascular endothelial cells. The enzyme 17β-hydroxysteroid dehydrogenase type 1 (17β-HSD) aids the conversion of oestrone to oestradiol. The catechol metabolites 2-hydroxyestrone and 2-methoxyestrone are catabolic degradation products of oestrogens. The oestrogens exert their actions by binding to oestrogen receptors.

1.2.1 Oestrogen Receptors

Oestrogen receptors belong to the superfamily of nuclear receptors and are characterised as ligand-dependent-transcription factors (Platet *et al.*, 2000; Huang *et al.*, 2010). There are two different oestrogen receptors ERα and ERβ which have distinct functions (Osborne and Schiff, 2005). ERα is encoded by the gene ESR1 located on chromosome 6 and ERβ is encoded by the gene ESR2 which is located in chromosome 14. ERα was cloned in 1985, whereas ERβ was discovered later in 1996. The 66 kDa ERα consists of 595 amino acid residues and is larger than the ERβ which contains 530 amino acids and has a molecular weight of 59 kDa. It is well known that the expression of ERα in breast cancer cells is critical for the progression of the tumour. In contrast, the function of ERβ is understood poorly. Human tissues including the spleen, thymus, ovary and testis express ERβ (Mosselman *et al.*, 1996). The binding affinity of oestradiol to oestrogen receptors is higher than that of oestrone and oestriol, therefore oestrone and oestriol are weaker agonists for the ER in comparison to oestradiol. Due to its high binding affinity, 17β-oestradiol concentrations of less than 10^{-9} M can activate both ERα and ERβ. Yet ERβ requires a higher 10^{-10} M concentration of 17β oestradiol to reach half maximal activity, in comparison to the 10^{-11} M oestradiol concentration required by ERα (Mosselman *et al.*, 1996).

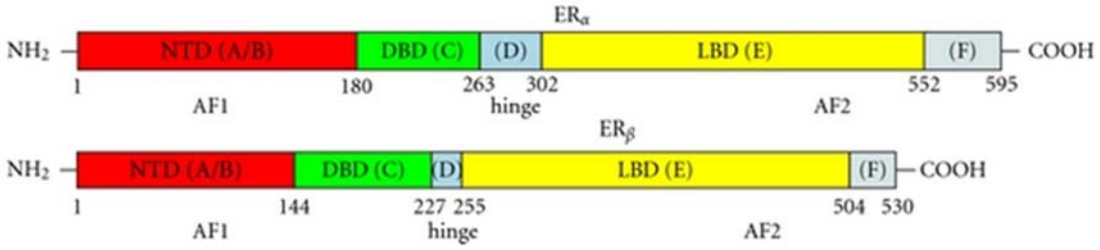

Figure 1.6 Organisation of the functional domains of oestrogen receptors: ERα and ERβ. The five different domains are indicated. NTD refers to the amino terminal domain (red), DBD is the DNA binding domain (green), hinge region (blue), LBD is the ligand binding domain (yellow) and the F-region located at the C-terminal end (grey). The numbers indicate the amino acid sequence position for each domain. Figure taken from (Kumar *et al.*, 2011) .

As shown in Figure 1.6, both oestrogen receptors are organized into five distinct regions. They are amino terminal domain (NTD), DNA binding domain (DBD),

hinge region, ligand binding domain (LBD) and the F-region which is located at the C-terminal end. The NTD contains the transcriptional activation function domain AF-1, which is a regulator of transcription. The NTD is considered to be in a dynamic structural state that is intrinsically disordered which allows in recognition and providing a surface that encourages binding of specific target molecules (Warnmark *et al.*, 2001). Upon binding of the interaction complexes, the molecules will rearrange themselves into the correct conformation. The DNA-binding domain binds to short palindromic sequences of DNA known as oestrogen response elements (EREs). The binding affinity of the oestrogen receptor is regulated by the DBD. It also assists in the recruitment and direction of co-activators to the transcription site. The hinge region acts as a flexible connector between the DBD and the LBD. Binding of ligands such as oestrogen exposes the nuclear localisation signal present in the hinge region (Kumar *et al.*, 2011). The LBD also known as the “E” domain follows the hinge region. This LBD is the key region which determines the activity of the oestrogen receptor and its ligand. This functional domain comprises of a ligand binding cavity and impacts binding of co-activators and co-repressors. The LBD is made up of 12 helices, of which helices 10 and 11 are involved in the formation of dimers. The dimer interaction surface formed allows the binding of agonistic and antagonistic ligands to the oestrogen receptor. The activation function domain AF-2 is located in the LBD. In comparison to the AF-1 situated in the NTD which is constitutively active, the AF-2 requires binding of hormone for it to be activated (Platet *et al.*, 2000). The LBD of both ERα and ERβ share about 55% sequence homology. The “F” region within the C-terminus is known to regulate gene transcription and interaction with other proteins. In the presence of 17β-oestradiol this F domain was shown to inhibit receptor dimerisation (Yang *et al.*, 2008). Complete deletion of the F region was required to remove the agonist activity of 4-hydroxytamoxifen which suggests a role in selective modulation of the oestrogen receptor (Koide *et al.*, 2007).

1.2.2 Mechanism of action

Oestrogen exerts its actions via two pathways: one which is the classical pathway and the other non-classical pathway. The classical pathway is also

termed genomic pathway whereas the non-classical pathway is also known as non-genomic pathway. The effects of oestrogen via these pathways lead to a range of cellular processes including cell proliferation, survival, differentiation and apoptosis. The development and progression of oestrogen receptor positive breast cancers occur via the contribution of both these pathways.

The binding of ligands such as oestrogen to the oestrogen receptor causes its dissociation from the chaperone heat shock proteins. The induction of a conformational change causes homodimerisation of the ER, thus leading to an interaction between the EREs present in the promoter regions of the target genes and ER (Miyoshi *et al.*, 2010). Phosphorylation of the serine residues in the AF-1 region of the NTD is essential for full activation of the ER. The dimeric receptor can bind either directly or indirectly. Formation of an active ER complex allows for and recruitment of coactivator complexes such as CBP, P300 to other DNA-bound transcription factors such as c-fos and c-jun, thus allowing transcription of oestrogen-responsive genes. The indirect binding of the activated ER occurs through different non-oestrogen-response-element (non-ERE) sites of promoter regions such as the activator protein-1 (AP-1) and specificity protein-1 (SP-1) also lead to transcription of genes (Kushner *et al.*, 2000; Safe, 2001).

Oestrogen may also mediate its actions via formation of cell membrane bound complexes. These oestrogen receptors may form complexes with other adaptor proteins such as focal adhesion kinase (FAK) and Src homology domain containing protein (SHC). Such non-genomic interactions may include actions mediated through receptors such as the type 1 IGF receptor and EGF receptor (Razandi *et al.*, 2003; Song *et al.*, 2004). The formation of macromolecular complexes activates the IGF and EGF receptors and sends signals further downstream. This signal transduction is reported to occur via stimulation of the mitogen-activated protein kinase (MAPK) pathway (Le Romancer *et al.*, 2010).

1.3 Oestrogen stimulates cell proliferation and invasion

Studies have shown that there is an increase in proliferation and invasion of cells in response to oestrogen as well as the presence of oestrogen receptor (Chalbos *et al.*, 1982; Jakesz *et al.*, 1984). Oestradiol was shown to increase invasiveness of MCF-7 cells in *in vitro* studies using Matrigel (Thompson *et al.*, 1988). Although the majority of studies have shown the stimulatory effects of oestrogen on cell proliferation and invasion, some studies have reported contradictory effects of oestrogen, indicating reduced metastatic potential and invasion ability of breast cancer cell lines. Several studies stated that high expression of ERα may lead to a reduction in invasion. Results from a study in MCF-7 cells indicated that there was an increase in cell migration and invasion in response to anti-oestrogens; tamoxifen and 4-hydroxytamoxifen. Despite the increase in cell migration, the addition of anti-oestrogens inhibited cell proliferation (Thompson *et al.*, 1988). In addition to this, the presence of ERα and ERβ has been shown to reduce invasion by 3-fold and 2-fold, respectively in ERα-negative MDA-MB-231 cells cotransfected with an ERα expression vector (Platet *et al.*, 2000).

1.4 Genes regulated by oestrogen

Oestrogen binding to the ER leads to altered transcription of a large number of genes that play a role in a number of cellular processes including growth, differentiation, angiogenesis and apoptosis. Oestrogen-regulated genes are crucial in causing breast tumourigenesis. The exact function of such oestrogen-regulated genes is yet to be elucidated. Whole genome expression profiling led to the discovery of numerous oestrogen-regulated genes (Frasor *et al.*, 2003). Expression analyses including those based on microarray technologies has identified a series of nineteen genes in oestrogen-responsive breast cancer cells. The genes were either upregulated or downregulated by oestrogen (Westley and May, 2006). However, the roles of about ten of these oestrogen-regulated genes remain unclear.

1.5 Genes that regulate vesicle trafficking and exocytosis leading to tumourigenesis

Many characteristics of cancer such as cell cycle regulation, angiogenesis, invasion and metastasis depend on changes in vesicle trafficking that occur in tumour cells (Steeg, 2005; Wright, 2008). The effects of oestradiol have been studied using scanning and transmission electron microscopy in MCF-7 cells in culture. The study indicated that oestrogen treatment of 2-11 days caused the formation of an extensive network of microvilli at the cell surface (Vic *et al.*, 1982). Upon treatment with oestrogen, there was an observable difference in cellular structures such as mitochondria, Golgi body and rough endoplasmic reticulum. The clear mitochondria, rough endoplasmic reticulum and Golgi complexes were detected initially in the cytoplasm, but as oestrogen treatment continued to about day 8, the cellular structures were located near the cell membrane. These changes in structure suggest that the breast cancer cells had acquired a secretory cell phenotype. There appears to be a link between the modulation of exocytosis and tumourigenesis (Chan and Weber, 2002). A gene expression study in breast cancer cells has identified a set of oestrogen-regulated genes, out of which 5 genes involved in vesicle trafficking have been studied in greater detail (Wright *et al.*, 2009). Expression microarray analyses identified 147 genes associated with vesicle trafficking including exocytosis. One of such oestrogen-regulated genes is *SLC12A2* which encodes for the Na^+-K^+-Cl^- co-transporter NKCC1. The mRNA levels of *SLC12A2* were shown to decrease when oestrogen-responsive MCF-7, EFM-19 and EFF-3 cells were treated with oestrogen for 48 hours.

1.6 Role of ion transporters in the development of cancer

Ion transporters are specialised membrane proteins or signal transduction molecules that play a major role in a wide range of cellular activities including gene expression, secretion, solute transport, intercellular communication, hormone secretion, proliferation, cell volume regulation, migration and invasion (Fraser *et al.*, 2005). Defects in ion transporter structure or function are

associated with the development of cancer and many other diseased states (Li and Xiong, 2011). Hallmarks of cancer pathogenesis including uncontrolled cell growth, invasion, angiogenesis, metastasis and reduction in apoptosis have been shown to be linked to aberrations of membrane ion transporters (Kunzelmann, 2005; Prevarskaya *et al.*, 2010). The actions of ion transporters are known to stimulate motility and cell migration. Therefore malignant tumour cells that acquire such motility cause detrimental effects. Although the process through which cell motility occurs is not understood fully, it is thought to be mediated by changes in cytosolic Ca^{2+} activity. Movement of osmotically active ions Na^+ and K^+ is thought to encourage cell motility. Functional ion channels and exchangers are crucial for the regulation of cell volume. The movement of ions results in loss or gain of water by osmosis. This in turn leads either to cell swelling or cell shrinkage (Cuddapah and Sontheimer, 2011).

This research project will focus on three proteins; NKCC1, a Na^+-K^+-Cl^- co-transporter that assists in the active transport of sodium, potassium and chloride ions into cells, a sodium hydrogen exchange regulatory factor, NHERF3 which is a PDZ-containing scaffold protein involved in the regulation of transporters such as sodium hydrogen exchangers at the plasma membrane, and finally ENaC which is an epithelial sodium channel.

1.7 *SLC12A2* (NKCC1)

The electroneutral Na^+-K^+-Cl^- co-transporter is a member of the solute carrier 12 (SLC12) family of transporters. The gene *SLC12A1* encodes the protein NKCC2, whereas the *SLC12A2* gene encodes NKCC1. Both NKCC1 and NKCC2 belong to the Na^+ dependent subgroup *SLC12A* gene family. In humans, the *SLC12A2* gene is located on chromosome 5, location 5q23.3 (Payne *et al.*, 1995).

NKCC1 is ubiquitously expressed in the basolateral membranes of many different secretory epithelial cells including airway, testes, breast, colon, inner ear, vascular smooth muscle and salivary gland (Xu *et al.*, 1994; Payne *et al.*, 1995). NKCC1 is expressed in other cells such as glial cells which reside in

neural tissue. NKCC2 expression is limited to the apical surface of cells in the thick ascending limb of the loop of Henle in the kidney. NKCC1 corresponding to a transcript size of 7.4 kb is larger than NKCC2 and is made up of about 1200 amino acid residues. The transcript size of NKCC2 is approximately 5.2 kb and it consists of 1000 amino acids. NKCC1 has a molecular mass of 195 kDa, and NKCC2 is of 121 kDa (Russell, 2000). The two NKCC proteins share approximately 58% identity.

1.7.1 Structure

Studies have shown that NKCC1 comprises 12 α-helical transmembrane spanning domains (Xu *et al.*, 1994). It consists of three regions which include an amino-terminal region, a central hydrophobic region and a carboxy-terminal region as illustrated in Figure 1.7. Early studies recognised several N-glycosylation sites. These potential extracellular hydrophilic segments of NKCC1 assist in glycan linkage and are located within the large extracellular loop between transmembrane (TM) 7 and TM8. The amino-terminal domain contains one phosphorylation site, whereas the carboxy-terminal region has multiple phosphorylation sites. Site-directed mutagenesis studies revealed that mutational changes that occur in TM2 cause changes in the binding affinity of cations. This suggested that TM2 is important for binding and transport of the cations Na^+ and K^+. TM4 and TM7 control the transport of the anion Cl^- (Isenring *et al.*, 1998). The stoichiometry at which NKCC transports the three types of ions is at 1 Na^+: 1 K^+: 2 Cl^- (Geck *et al.*, 1980).

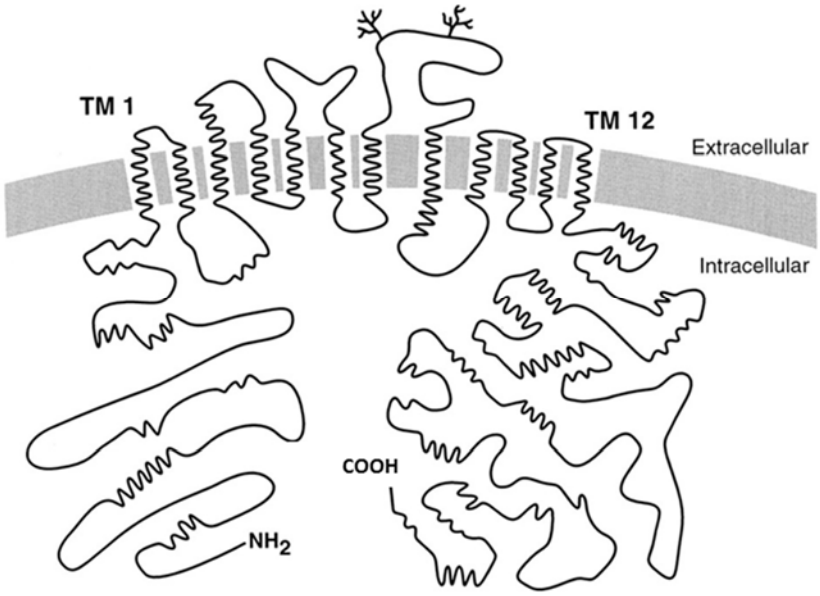

Figure 1.7 Graphical representation of the structure of NKCC1. NKCC1 is divided into three main regions including an amino terminal domain, a central hydrophobic domain and a carboxy-terminal domain. The central hydrophobic domain consists of 12 transmembrane spanning α-helices (TM1 to TM12). The amino-terminal domain has one phosphorylation site, whereas the carboxy-terminal domain has multiple phosphorylation sites. The mutational changes that occur in TM2 have led to a change in the affinity of cations. The affinity to the anion chloride was affected by point mutations in TM4 to TM7. Figure taken from (Russell, 2000).

1.7.2 Function

The main functions of ion transporters such as NKCC1 are the maintenance of epithelial ion secretion and regulation of cell volume (Hebert *et al.*, 2004). Activation of NKCC1 occurs by the accumulation of Cl^- ions within the cell. By allowing ions into the cell, NKCC1 is responsible for the maintenance of an electrochemical gradient. This ionic gradient results in loss of water by osmosis and hence leads to cell shrinkage. The loss of water and cell shrinkage activates NKCC (Russell, 2000). This activation is thought to be mediated by the phosphorylation of serine and threonine residues (Lytle and Forbush, 1992). Dephosphorylation of SPS1-related proline/alanine-rich kinase (SPAK) / oxidative stress-responsive kinase 1 (OSR1) or an increase in intracellular Cl^- concentration leads to the inactivation of NKCC (Breitwieser *et al.*, 1990; Gillen and Forbush, 1999). Such effects of SPAK/OSR1 are mediated via the with no lysine kinase (WNK) signalling pathway in response to hypertonic stress (Thastrup *et al.*, 2012). The migration of cells through narrow confined spaces is brought about by cell shrinkage. In human glioma cells, NKCC1 has been shown to assist in regaining cell volume subsequent to migration through

narrow spaces (Haas and Sontheimer, 2010). Loop diuretics such as bumetanide and furosemide inhibit NKCC1 (Figure 1.8). This inhibition is mediated by the binding of the loop diuretic to the transmembrane domains TM2 to TM7 and TM11 to TM12 at a stoichiometry of one inhibitory molecule per transporter protein (Isenring *et al.*, 1998). The order of potency is bumetanide > piretanide > furosemide (Reyes and Leary, 1993).

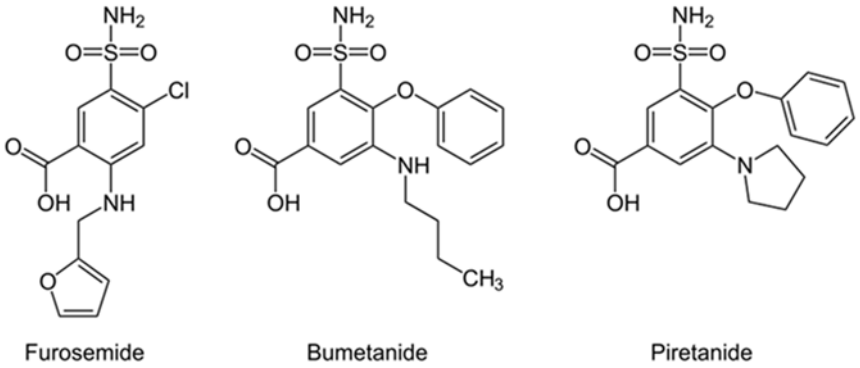

Figure 1.8 Chemical structures of loop diuretics. The structure of furosemide, bumetanide and piretanide are shown.

The mammary gland is a highly metabolic tissue. It expresses a range of membrane-bound transporters such as NKCC1. In mammary ducts, NKCC1 was expressed mainly at the plasma membrane. There was no expression observed in the cytoplasm of epithelial cells (Shillingford *et al.*, 2002). NKCC1 expressed in these ductal epithelial cells was shown to mediate Cl^- ion secretion (Selvaraj *et al.*, 2000). In rat mammary tissue, NKCC1 has been shown to be important in secretion and transport of milk constituents during lactation (Shennan, 1989; Shennan and McNeillie, 1990). The regulation of Cl^- ion secretion and cell volume suggests that NKCC1 is important in ductal morphogenesis of the breast. NKCC1 plays a role in the development of ducts as evidence showed that actively dividing epithelial cells express less NKCC1 (Shillingford *et al.*, 2002). There could be a potential role of NKCC1 in the development of breast cancer.

1.8 *PDZK1* (NHERF3)

The oestrogen-responsive gene *PDZK1* is located on chromosome 1, location 1q21. This gene encodes the Na^+-H^+ exchange regulatory co-factor 3 (NHERF3). Epithelial cells of proximal tubules of the kidney, pancreas, adrenal cortex, breast and gastrointestinal tract have been shown to express NHERF3 (Kocher *et al.*, 1998). The protein NHERF3 consists of 519 amino acids and has a molecular mass of 63 kDa.

1.8.1 Structure

NHERF3 consists of an N-terminal domain, four PDZ domains, namely, PDZ1, PDZ2, PDZ3 and PDZ4 and a C-terminal region (Figure 1.9). These PDZ domains can interact concurrently with other proteins. They can coordinate the interaction of several proteins which are present at the cell membrane such as the membrane-associated protein 17 (MAP17). The NHERF family has four members: NHERF1, NHERF2, NHERF3 and NHERF4. NHERF1 and NHERF2 have two PDZ domains. The other two members NHERF3 and NHERF4 that belong to this family have four PDZ domains.

Figure 1.9 Schematic model diagram of the NHERF3 protein. NHERF3 has a short N-terminal domain, four PDZ domains named PDZ1, PDZ2, PDZ3 and PDZ4 followed by a C-terminal region. Figure adapted from (Fenske *et al.*, 2009).

1.8.2 Function

Proteins that belong to the PDZ family are known to regulate various cellular functions. These include ion transport, signal transduction, cell proliferation and differentiation. The NHERF proteins facilitate the organisation of membrane associated proteins at the cell membrane (Figure 1.10). Therefore NHERF proteins are termed scaffolding proteins. Within the gastrointestinal tract, NHERF3 and the other PDZ adaptor proteins NHERF1, NHERF2 and NHERF4

have been implicated in mediating ion transport and anion secretion (Lamprecht and Seidler, 2006).

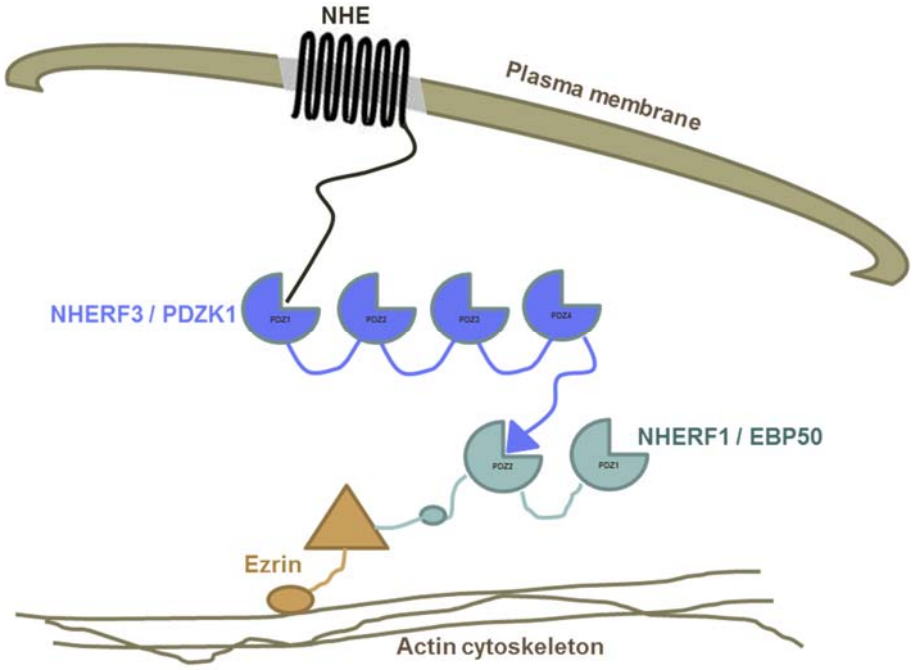

Figure 1.10 Schematic diagram of the formation of a complex. The interaction of the NHERF3-NHERF1-ezrin complex. The tail of NHERF3 binds to NHERF1, which in turn binds to ezrin. The carboxy-terminal of ezrin interacts with the cytoskeletal F-actin.

Cancers that originate from epithelial cells tend to have an overexpression of NHERF3. The protein MAP17, which interacts with NHERF3, was overexpressed in several carcinomas including breast, colon, kidney and prostate (Guijarro *et al.*, 2007). Oestrogen receptor positive breast cancers more commonly overexpressed NHERF3 in comparison to oestrogen receptor negative breast cancers (Ghosh *et al.*, 2000). Some studies have shown the effects of oestradiol in the alternation of membrane structures such as microvilli. Therefore it could be speculated that the induction of NHERF3 plays a role in facilitating the response to oestrogen in ER positive breast cancers. A study confirmed that siRNA knockdown of PDZK1 inhibited the oestrogen-induced increase of both oestrogen receptors. These results further clarified that the actions mediated by oestrogen on NHERF3 acts through the ERα and ERβ receptors (Kim *et al.*, 2012). In skin specimens taken from patients with melasma, oestrogen induced the expression of tyrosinase, which is an enzyme

that catalyses the oxidation of tyrosine along with the expression of NHERF3. Moreover, treatments with increasing concentrations of oestrogen from 10 nM to 100 nM, lead to an increase in expression of other NHERF3 interacting ion transporters such as the Na^+-H^+ exchanger (NHE) and cystic fibrosis transmembrane conductance regulator (CFTR).

1.9 *SCNN1B* (ENaC-β)

Epithelial sodium channels (ENaC) are expressed mainly on the apical surface of epithelial cells within the lung, colon and kidney (Garty and Palmer, 1997). In the mammalian kidney, ENaC is located primarily in the distal convoluted tubules and in the cortical collecting ducts (Gambling *et al.*, 2004). Our gene of interest *SCNN1B* is situated on chromosome 16 location 16p12.2-p12.1 and encodes the β-subunit of ENaC. ENaC-β has a molecular mass of approximately 72 kDa.

1.9.1 Structure

ENaC consists of three different subunits named, ENaC-α, ENaC-β and ENaC-γ. More recently, a fourth subunit ENaC-δ has been isolated (Yamamura *et al.*, 2008). Each of the three α, β and γ subunits comprises two transmembrane segments that span the apical membrane of epithelial cells (Figure 1.11). The amino-terminals and the carboxy-terminals of the subunits are located intracellularly.

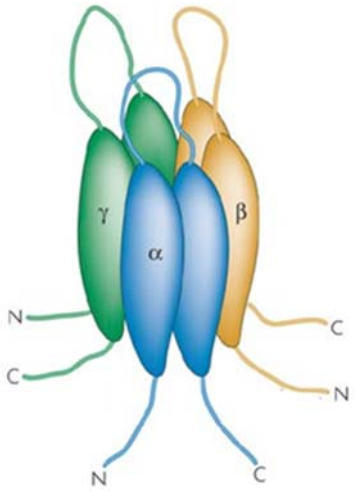

Figure 1.11 Structure of the epithelial sodium channel (ENaC). It is made up of three heterotrimeric subunits named α, β and γ. Each subunit consists of two transmembrane helices. ENaC has an intracellular amino-terminal region followed by a transmembrane domain, a large extracellular loop, a second transmembrane segment and an intracellular carboxy-terminal tail. Figure adapted from (Gamper and Shapiro, 2007).

1.9.2 Function

The main function of ENaC is the maintenance of sodium homeostasis and also the regulation of blood volume and blood pressure (Rossier *et al.*, 2002). Several hormones present in the kidney such as vasopressin, aldosterone, catecholamines and insulin control the activity of ENaC. They induce a rapid increase in Na^+ transport by altering the subcellular localisation of ENaC to the plasma membrane (Loffing *et al.*, 2001). These effects are facilitated by the secondary messengers: serum glucocorticoid kinase 1 (SGK), cyclic adenosine monophosphate (cAMP) and inositol-1,4,5 triphosphate (IP3). The mRNA levels of ENaC-α, ENaC-β and ENaC-γ are regulated by hormones such as aldosterone and vasopressin, with resulting changes in expression of the three ENaC subunits. Vasopressin has been shown to increase the expression of ENaC-β and ENaC-γ subunits mRNAs, in the lung and renal collecting ducts of rats (Nicco *et al.*, 2001). This increase in expression led to an increase in vasopressin mediated Na^+ transport. Hormones such as oestrogen and progesterone may play a role in modulating the renal handling of Na^+ and assist in the retention of sodium and water. The role of hormones such as oestrogen was proposed based on studies that have observed that renal regulation of Na^+ varies during the oestrous cycle of rats and humans (Hartley and Forsling, 2002; Pechere-Bertschi *et al.*, 2002).

One of the key features of cancer pathogenesis is migration of cells. ENaC is involved in cell migration and regulation of cell volume. Cells lose volume and shrink in size in order to invade through narrow intercellular spaces. ENaC allows cells to regain cell volume after cell shrinkage. This increase in cell volume is termed “regulatory volume increase”. A study in human glioma cells has shown that one of the main roles of ENaC is to aid in the process of regulatory volume increase (Ross *et al.*, 2007). Knockdown of ENaC-α and ENaC-γ inhibited the migration of glioma cells (Kapoor *et al.*, 2009). This observation provides evidence of the potential relationship between cell migration and channels that transport ions.

The amiloride-sensitive ENaC is responsible for the presence of the low Na^+ ion concentration in milk. The role of ENaC in the mammary ductal epithelia has been demonstrated in studies of murine models. With the aid of Ussing chambers, in which planar sheets of bovine mammary epithelial cells were grown on permeable filter matrices which were clamped forming a barrier between two half-chambers, Quesnell et al confirmed that ENaC-β and ENaC-γ responded to glucocorticoids such as dexamethasone and cortisol. These actions were mediated via the glucocorticoid receptor (Quesnell *et al.*, 2007b). The mammary epithelial cells under evaluation exhibited an increase in short circuit currents in the presence of cortisol and dexamethasone. The increase in short circuit current is a direct measure of net ion transport. In cells that were previously induced by corticosteroids, a decrease in short circuit current was observed when the apical membranes were exposed to 10 μM amiloride or 1 μM Benzamil. Amiloride is an epithelial sodium channel blocker and benzamil is a sodium-calcium exchange blocker in addition to being a potent ENaC blocker.

The following Figure 1.12 shows a model diagram of the mediation of ion transport in a secretory mammary duct epithelial cell. NKCC1 located in the basolateral membrane transports Na^+, K^+ and 2 Cl^- ions into the cell. A Na^+ ion gradient is generated by the ATP-driven Na^+/K^+ pump, which pumps Na^+ ions out and K^+ ions into the cell, against their concentration gradients (Shennan and Peaker, 2000). A low Na^+ ion concentration inside the cell is maintained by the ouabain-sensitive Na^+/K^+ ATPase which is located in the basolateral membrane of the cell (Kimura, 1969; Linzell and Peaker, 1971). NHERF3 facilitates organisation of membrane associated proteins such as the Na^+/H^+ exchangers (NHEs) (Thomson *et al.*, 2005). The NHEs are responsible for regulation of intracellular pH and transports ions at a stoichiometry of 1 Na^+ : 1 H^+. The amiloride-sensitive ENaC is localised to the apical membrane and transports Na^+ ions into the cell. In lactating tissue, secretion of milk constituents is dependent upon the polarised transport of ions determined by the transepithelial ionic concentration gradients.

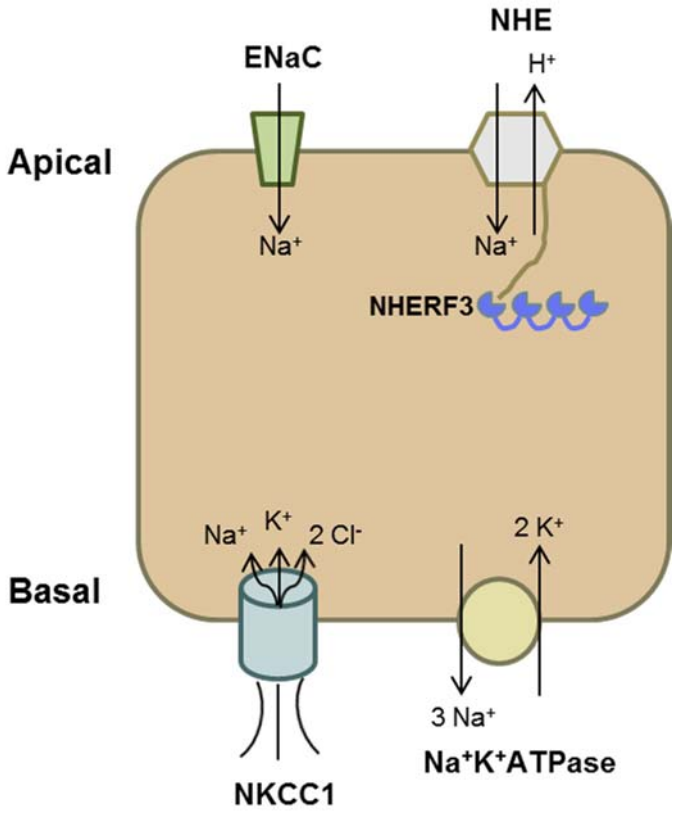

Figure 1.12 Schematic diagram of a mammary duct epithelial cell. NKCC1 is located in the basolateral membrane and transports Na^+, K^+ and $2Cl^-$ ions. The epithelial Na^+ channel (ENaC) that transports Na^+ ions is located in the apical membrane. The Na^+, K^+ ATPase pumps 3 Na^+ out and takes 2 K^+ ions in. NHERF3 provides a scaffold to other membrane associated proteins such as the Na^+/H^+ exchanger (NHE).

1.10 Ion transporters as therapeutic targets

It has been suggested that ion channels and transporters could be potential therapeutic targets for cancer (Li and Xiong, 2011). Inhibition of ion transporters could aid in preventing the progression of cancer. It has been proposed that gliomas including primary brain tumours could be treated with chlorotoxin, which is a peptide derived from the death-stalker scorpion (Soroceanu *et al.*, 1998). Chlorotoxin is a Cl^- channel inhibitor that binds specifically to glioma cells and cells in tumours originating from the neuroectoderm (Lyons *et al.*, 2002).

Another gene *KCNK5* which is induced by oestradiol, encodes for a potassium channel known as TASK2. In oestrogen-responsive breast cancer cells MCF-7 and T47D, this potassium channel played a role in the regulation of cell proliferation (Alvarez-Baron *et al.*, 2011). Moreover, siRNA knockdown of *KCNK5* resulted in attenuation of cell proliferation by cell cycle arrest at the G_1/S phase. Inhibitors that have the ability to target TASK2 specifically would be beneficial in treatment of ER positive breast tumours.

The association of molecules involved in organisation of transport proteins at the cell surface, or of transport proteins or ion channels in cancer cell function suggests that inhibitors or modulators of ion transporters such as NKCC1, ENaC and the scaffold protein NHERF3 could eventually lead to new breast tumour treatments. Although it is a long term prospect, this project will provide the initial basis.

1.11 Hypothesis

We hypothesise that oestrogen alters the expression of specific genes *SLC12A2*, *SCNN1B* and *PDZK1* that encode proteins involved in ion transport. The alteration of protein expression induced by oestrogens, leads to polarised transport of ions. Modifications in membrane transporter abundance and to their polarised location will likely impact on cellular ion homeostasis. Ion transporters have been implicated in many pathophysiological processes of cancer such as uncontrolled growth, decreased apoptosis and increased migration and invasion.

The associated phenotypic changes in ion transport and any change in the polarised organisation of transport activity may favour breast cancer progression. We aim to understand how ion transporters and scaffolding proteins relate to each other in the context of altering the cell phenotype in response to oestrogen.

1.12 Aims

The main objectives of this project were to;

- Measure the expression of oestrogen-regulated genes *SLC12A2*, *PDZK1* and *SCNN1B* in oestrogen-responsive cell lines MCF-7, EFM-19 and EFF-3. The protein expression of NKCC1, NHERF3 and ENaC-β was analysed by western transfer.
- Study the oestrogen regulation of proteins NKCC1, NHERF3 and ENaC-β. Steroid hormone withdrawal studies will enable study of the effects of oestrogen on breast cancer cells.
- Evaluate expression of the proteins NKCC1, NHERF-3 and ENaC-β in the absence and presence of different anti-oestrogens such as tamoxifen, fulvestrant, 4-hydroxytamoxifen, raloxifene, toremifene etc.
- Investigate the cellular localisation of membrane transporters and scaffolding proteins by immunofluorescence and confocal microscopy in polarised cell monolayers and determine the effects of oestrogens.
- Determine the functional regulatory roles of the protein encoded by the oestrogen-regulated gene *SLC12A2*. The activity of NKCC1 was assessed with the $^{86}Rb^{+}$ (K^{+}) influx assay. Pharmacological agents such as ouabain and loop-diuretics furosemide and bumetanide which inhibit NKCC1 were used.
- Test the importance of the NHERF3 protein in regulation of Na^{+}/H^{+} exchange. This was assessed in the context of cellular control of pH using the pH-sensitive dye BCECF-AM.

Chapter 2. Materials and Methods

2.1 Tissue Culture

2.1.1 Cell lines

Human breast cancer cell lines were purchased from the American Type Culture Collection (ATCC). Cells were cultured in sterile tissue culture flasks (Corning, UK) of varying growth surface areas of 25 cm^2, 75 cm^2 and 175 cm^2 (T-25, T-75 and T-175).

2.1.2 Routine cell culture

Oestrogen responsive human breast cancer cell lines were MCF-7, EFM-19, EFF-3, BT-474, T-47D and ZR-75. Oestrogen non-responsive cell lines were MDA-MB-231, SKB-R3, BT-20, Hs578T and HBL-100. These cells were cultured in Dulbecco's modified Eagle's medium (DMEM) containing 10 % foetal calf serum (FCS) and 1 µg/ml (0.17 µM) insulin. Cell lines were incubated at 37°C in a humidified 5% CO_2 incubator and usually grown to 70 % confluence. Prior to trypsinisation, cells were washed twice with autoclaved phosphate buffered saline (PBS) comprising 0.14 M NaCl, 0.01 M PO_4 buffer and 0.003 M KCl. Cells were detached from tissue culture flask surfaces with 50 mg/ml porcine trypsin and 20 mg/ml EDTA (1:3 trypsin/EDTA) solution diluted in PBS. Once detached, cells were centrifuged (Beckman Allegra X-12 R rotor SX 4750) for 5 minutes at 1500 rpm at room temperature, in sterile BD FalconTM tubes (BD Biosciences, UK). Cells were then seeded into fresh flasks at dilutions between 1:2 and 1:9 in fresh tissue culture medium. Cell lines were tested for mycoplasma contamination on a regular basis.

2.1.3 Cryopreservation of cells

As mentioned previously, once cells were trypsinised, they are resuspended in DMEM supplemented with 20% (v/v) foetal bovine serum and 10% (v/v) DMSO. The cell suspension was added to sterile polypropylene cryo-vials (Invitrogen Life Technologies, UK) in 0.5 ml aliquots. For short-term storage cells were kept

in a -70°C freezer and for long-term storage cells were transferred to liquid nitrogen.

When required, cell aliquots were thawed rapidly and added to pre-warmed cell culture medium in T25 flasks. The medium was replaced 24 hours after seeding.

2.1.4 Preparation of dextran-coated charcoal stripped serum (DCCS)

Twenty grams of charcoal (Sigma, UK) and 0.2 g of dextran T70 (Pharmacia, UK) were mixed thoroughly and suspended in 250 ml of sterile distilled water. This was followed by 10 minute incubation at room temperature and centrifugation for 15 minutes at 7000 rpm at 4 ^{o}C (JA17 rotor, Beckman J2-21 centrifuge). The supernatant was aspirated carefully and the process was repeated. The dextran-coated charcoal was resuspended in 200 ml of newborn calf serum (Invitrogen Life Technologies, UK). The contents were transferred to conical flasks and incubated at 55 ^{o}C in a shaking waterbath for 40 minutes. After incubation, the contents were centrifuged at 10,000 rpm at 4 ^{o}C for 30 minutes. The serum was carefully transferred to clean centrifuge bottles and centrifuged at 10000 rpm at 4 ^{o}C for 30 minutes to remove any remaining charcoal. Then the dextran-coated charcoal stripped calf serum (DCC-CS) was filter sterilised through a 0.45 µm filter unit (Corning, UK) and was stored in a freezer at -20 ^{o}C.

2.1.5 Withdrawal of cells

Cells were plated onto 12-well or 24-well plates in routine culture medium and were allowed to attach for 24 hours. Withdrawal from steroids in the culture medium was by culture for 5 days in phenol red-free DMEM containing 1 µg/ml (0.17 µM) insulin and 10 % newborn calf serum which had been treated with dextran-coated charcoal. This medium is steroid depleted and does not contains any cytokines. Throughout the first 3 days of serum withdrawal, cells were washed twice with PBS and fresh steroid-depleted medium was added. During the next 2 days, medium was changed daily.

2.1.6 Treatment of cells

Following the 5 day withdrawal of cells from steroids, cells were treated with oestrogen diluted to a concentration of 10^{-9} M in withdrawal media for 6 hours to 10 days. Media were changed daily. For oestrogen concentration dependent experiments, different concentrations of oestrogen were used ranging from 10^{-7} M to 10^{-13} M.

For anti-oestrogen dependent experiments, several anti-oestrogens were used at the concentrations given below.

Anti-oestrogen	Concentration	Manufacturer
Tamoxifen	10^{-7} M $5x10^{-6}$ M	Sigma
4-Hydroxytamoxifen	10^{-8} M	Sigma
Fulvestrant	10^{-8} M	Sigma
Bazedoxifene	10^{-7} M	Cayman chemical
Toremifene	10^{-7} M	Santa Cruz
Raloxifene	10^{-7} M	Cayman chemical
Lasofoxifene	10^{-8} M	Santa Cruz

Table 2.1 List of anti-oestrogens and concentrations. The anti-oestrogens and manufacturers are listed.

2.2 Preparation of cell lysates

2.2.1 Protein Extraction

Cells were washed twice with ice-cold PBS. Cells were then lysed in radioimmunoprecipitation assay (RIPA) lysis buffer containing 150 mM NaCl, 50 mM Tris pH 7.5, 1 mM EDTA, 1% NP-40 and 0.25% Sodium deoxycholate supplemented with the protease inhibitors 1 µg/ml aprotinin, 1 µg/ml leupeptin, 1 µg/ml pepstatin, 2 mM sodium orthovanadate, 2 mM sodium fluoride and 2

mM phenyl methyl sulphonyl fluoride (PMSF) (Sigma, UK) on ice. Then cells were agitated for 30 minutes on ice and centrifuged at 14,000 rpm for 10 minutes at 4^{o}C to remove any insoluble cellular debris. Once centrifugation was complete, the supernatant was removed to a fresh eppendorf tube and labelled accordingly. These lysates were stored in a -20 ^{o}C freezer. Then the protein concentration was measured with bicinchoninic acid assay (Thermo Scientific, UK) using BSA as the standard.

2.2.2 Measurement of protein concentration

The protein concentrations of the cell lysates were measured using bicinchoninic acid (BCA) assay. BCA is a detergent based upon bicinchoninic and is used for quantification of total protein. BCA reagents A and B (Thermo Scientific, UK) were mixed at a ratio of 50:1 to produce a working dilution. Standards of 0, 0.025, 0.05, 0.1, 0.2, 0.5, 1 and 2 mg/ml bovine serum albumin (BSA) were prepared in a 1:10 dilution of RIPA buffer and made into aliquots of 5 µl each. Cell lysate aliquots of 0.5 µl were diluted in a 1:10 ratio in 4.5 µl of SDW. Ninety five microliters of the BCA reagent mixture was added to 5 µl of each of the protein standards and diluted lysates. The samples were vortexed and incubated in a water bath at 37 ^{o}C for 30 minutes.

This BCA assay uses a colorimetric detection system which shows a strong absorbance at 562 nm. The proteins present in an alkaline medium allows a biuret reaction to occur in which Cu^{2+} cations are reduced to Cu^{+} ions forming a coloured complex. This initial step forms a pale blue complex due to the chelation of copper with the protein. During the next step two molecules of the BCA react with the Cu^{+} ions formed initially, hence producing an intense purple-colour. This complex is water soluble and exhibits an absorbance at 562 nm. The lysates were then placed immediately on ice to avoid further colour development. The optical density was determined spectrophotometrically at a wavelength of 562 nm (DU 640 series spectrophotometer) and a standard curve of the BSA standard serial dilutions is produced. The protein concentrations of the cell lysates were calculated based upon the BSA standard curve generated by the spectrophotometer.

2.3 Western transfer analysis

2.3.1 Protein gel electrophoresis

For sodium dodecyl sulphate polyacrylamide gel electrophoresis, the separating gels prepared had 12% acrylamide and the stacking gels had 3% acrylamide. For the separating gel the acrylamide to bisacrylamide ratio was 200:1 (w/w) and consisted of 12% polyacrylamide (v/v), 0.5 M Tris-HCl pH 8.8, 0.1% (w/v) SDS, 0.05% (w/v) ammonium persulphate (APS) and 0.1% (v/v) N, N, N', N'-tetramethylethylenediamine (TEMED). The stacking gel's acrylamide to bisacrylamide ratio was 20:1 (w/w) and contained 3% polyacrylamide (v/v), 125 mM Tris-HCl pH 6.8, 0.1% (w/v) SDS, 0.1% (w/v) ammonium persulphate and 0.5% (v/v) TEMED.

The gels were cast in a Hoeffer mighty small 10 x 12 cm vertical gel apparatus. After the separating gel was added, it was overlayed with 200 µl of water saturated butan-2-ol (50% butan-2-ol and 50% SDW) in order to avoid meniscus formation, and the acrylamide was allowed to polymerise for 45 - 60 minutes. After the separating gel had set, water saturated butan-2-ol was poured off and the 15-well or 20-well lane combs were inserted to cast the stacking gel. This was then left for 30 minutes to allow complete polymerisation. Protein samples of 10 µg were prepared by mixing the lysates samples diluted in RIPA buffer with 10 µl of 2 x SDS mix containing 0.125 M Tris-HCl, 25 mM EDTA, 4% SDS, 20% glycerol, 0.01% bromophenol blue and 10% β-mercaptoethanol, pH 6.8 making up to a total volume of 20 µl. This sample mixture was vortexed and boiled for 10 minutes on a heat block at 95 ^{o}C. Samples were loaded into lanes within the stacking gel. Protein markers of full range known molecular mass (Rainbow marker, GE Life Sciences) were electrophoresed alongside the samples. The cassettes were placed and secured in electrophoresis chambers and were electrophoresed in running buffer containing 0.38 M glycine, 0.5 M Tris-HCl and 0.1% SDS at a constant current of 10 mA per gel.

2.3.2 Western transfer

Proteins were separated by polyacrylamide gel electrophoresis and were transferred to 0.45 µM nitrocellulose membranes (VWR International, UK). A semi-dry transfer apparatus (S&S CarboGlas, Peqlab, PerfectBlue) was used. The transfer sandwich comprised of 2 sheets of 3 mm Whatman chromatography paper soaked in 0.3 M Tris, and 20% methanol (anode buffer 1), one sheet soaked in 25 mM Tris and 20% methanol (anode buffer 2), a sheet of 0.45 µM nitrocellulose membrane pre-wet in SDW, and soaked in anode buffer 2, the polyacrylamide gel and 3 sheets of chromatography paper soaked in 25 mM Tris, 40 mM 6-amino-n-hexanoic acid pH 9.4 and 20% methanol (cathode buffer). The protein transfer from the polyacrylamide gel to the nitrocellulose membrane was at a constant current of 100 mA per gel for 45 - 60 minutes. Following transfer the membranes were left to dry overnight at room temperature.

2.3.3 Incubation with antibodies

The membranes were blocked in 5% (w/v) milk containing 20 mM Tris-HCl, 140 mM NaCl and 0.1% Tween 20 (TBS-Tween solution) for 1 hour at room temperature. Later the membranes were washed three times with TBS-Tween for 5 minutes each with gentle shaking. After the final wash, the membranes were incubated overnight at 4 ^{o}C with specific primary antibodies. The NKCC1 antibody was a rabbit monoclonal raised against a synthetic peptide corresponding to residues surrounding Arg80 of the human NKCC1 protein detected a broad protein band around 160 - 200 kDa (1:5000-1:20000) (#8351; Cell Signalling Technology, UK). The NHERF3 antibody was a rabbit polyclonal immunogen detected NHERF3 at an apparent molecular mass of about 66 kDa (1:5000-1:10000) (HPA006155; Atlas antibodies, UK). The ENaC-β antibody was a mouse monoclonal synthetic peptide raised against residues of 271-460 of human ENaC-β and detected a protein band at an apparent molecular mass of approximately 70 kDa (1:100-1:200) (sc25354; Santa Cruz Biotechnology, USA). The HRP-GAPDH, a rabbit polyclonal raised against amino acids 1-335 representing the full length of human GAPDH (1:10000-1:50000) (sc-25778;

Santa Cruz Biotechnology, USA) followed by horseradish peroxidase conjugated anti-rabbit or anti-mouse secondary antibodies (1:5000-1:20000) (7074S and 7076S respectively; Cell Signalling, UK) diluted in Tris buffered saline tween / 5% milk for 1 hour at 37 ^{o}C. After incubation with the secondary antibodies, the membranes were washed three times with TBS-Tween and once with TBS.

2.3.4 Development of filter

Proteins were visualised by enhanced chemiluminescence with SuperSignal West Dura Extended Duration Substrate (Thermo Scientific, UK). The chemiluminescent solutions Luminol/Enhancer and peroxide buffer were mixed at a 1:1 ratio. The membranes were incubated with the mix for 5 minutes at room temperature. They were exposed to X-ray films (Fujifilm, SuperRX) and developed using the developer machine.

2.3.5 Densitometric analysis

Following development, the X-ray films were digitally scanned and the intensity of the signal was quantified by densitometric analysis using Lab Works 4.0 software (Ultra Violet Products, UK). The background of the film was subtracted from the densitometry analysis. Data were normalised, by dividing the densitometry values of the protein of interest to the expression values of GAPDH. This would adjust for any variances in protein loading for each sample.

2.4 Immunofluorescence

2.4.1 Cell culture

Coverslips 20 mm x 20 mm (VWR International Ltd, UK) were sterilized in ethanol for a few minutes. Using a needle and forceps each of the coverslips were then left standing by the side of each well in a 6-well plate and left to dry in a laminar flow hood. Cells were seeded at the required density onto a 6-well plate and incubated for 24 hours for attachment.

2.4.2 Fixation of cells

Once the cells reached confluency, they were then washed with PBS once and fixed in methanol or ice-cold 4% paraformaldehyde at -20 ^{o}C or at room temperature, respectively. A fixative such as methanol dehydrates the cells, allowing easy access of antibodies to the protein of interest. But in some cases depending on the proteins analysed, dehydration might cause damage to cell morphology (Stadler *et al.*, 2010). Therefore methanol fixation is widely used for evaluating cytoskeletal proteins. In contrast, paraformaldehyde allows conservation of soluble proteins without causing much damage to internal cell structures. Hence paraformaldehyde is commonly used in the analysis of soluble proteins within the cell. After fixation the cells were washed with PBS three times with each wash lasting 20 minutes.

2.4.3 Blocking and permeabilisation of cells

After fixation, cells were blocked in blocking buffer consisting of 1x PBS, 5% goat serum and 0.3% Triton X-100 for 1 hour at room temperature. Triton X-100 of 0.3% was replaced with 0.2% Saponin depending on the primary antibody used. Triton is a mild detergent that causes irreversible permeabilisation of cellular membranes, whereas saponin preserves the membrane structures better and results in a reversible permeabilisation (Stadler *et al.*, 2010). This permeabilisation step is crucial to allow antibodies to gain access to the inside of the cell.

2.4.4 Incubation with antibodies

The blocking buffer was aspirated and the appropriate primary antibody was added at different dilutions from 1:100 to 1:2000 and incubated overnight at 4 ^{o}C. The next day the primary antibody was aspirated and the coverslips were washed 3 times with PBS. The appropriate secondary antibody, Alexa fluor 488 conjugated goat anti-rabbit IgG (A11034, Invitrogen, UK) or Alexa fluor 568 conjugated goat anti-mouse IgG (A11004, Invitrogen, UK) was added at a dilution of 1:1000 and the plates were covered with foil as the secondary antibody is sensitive to light. The cells were incubated for 1 - 2 hours at room

temperature. As mentioned previously, cells were washed 3 times on a shaker whilst covered in foil. Mounting media with DAPI (H-1200, Vector Laboratories, UK) was added to the glass slides prior to placing the coverslip on the glass slide. DAPI intercalates with DNA and produces a blue fluorescence when bound to DNA. In some experiments, prior to mounting the coverslip on a glass slide, phalloidin (Alexa fluor 555 conjugated phalloidin, #8953; Cell Signalling Technology, UK) was added at a dilution of 1:100 for 15 minutes at room temperature. This was to selectively label the F-actin filaments of cells. The slides were then examined under the laser scanning spectral confocal microscope (Leica TCS SP2) or on the fluorescent microscope (Leica DMR). The confocal images were taken with a 63x oil immersion objective and 1.3x numerical aperture. Images were collected from 10 to 15 sections and all slices were stacked together to produce the final image.

2.5 $^{86}Rb^{+}$ (K^{+}) influx measurement as a functional assay for NKCC1

2.5.1 Cell culture

MCF-7 and EFM-19 cells were seeded to sub-confluency at a density of 10,000 and 30,000 cells per well respectively, in 6-well plates (Corning, UK). Plates used for culturing MCF-7 cells in withdrawn media, were coated with rat-tail type 1 collagen (#11179179001, Roche Applied Science, Germany) at a concentration of 5 µg/cm^2 to enhance cell attachment. Cells were seeded at high density (1 – 2 million cells per filter) onto polycarbonate Transwell filter supports of pore size 0.4 µm, 12 mm diameter (#3401, Corning, UK) and at similar high density to collagen-coated polytetrafluoroethylene (PTFE) filter supports, pore size 0.4 µm, 12 mm diameter (#3493, Corning, UK). One milliliter of culture media was added to the upper compartment which is the inside of the transwell insert and 2 ml were added to the lower, plate well compartment. Media were changed daily.

2.5.2 Preparation of Krebs's solution

A modified Krebs's solution consisting of 137 mM NaCl, 5.4 mM KCl, 2.8 mM $CaCl_2$, 1.0 mM $MgSO_4$, 0.3 mM KH_2PO_4, 0.3 mM NaH_2PO_4, 10 mM Glucose and 10 mM HEPES was prepared. The pH was adjusted to pH 7.4 by addition of Tris.

2.5.3 Measurement of $^{86}Rb^+$ (K^+) influx

Radioactive Rubidium, $^{86}Rb^+$ provides an isotopic tracer of K^+ ion movement (Simmons, 1984). The $^{86}Rb^+$ (K^+) influx assay allows assessment of the K^+ influx through the Na^+/K^+ ATPase and NKCC1 in breast cancer cells. Since $^{42}K^+$ has a short half-life of 12 hours, $^{86}Rb^+$ with a half-life of approximately 19 days is used as a convenient alternative. The $^{86}Rb^+$ tracer was added at 0.1 µCi/ml to experimental solutions in modified Krebs's solution. Stock solutions of the inhibitors ouabain and furosemide were dissolved in distilled water at 10^{-3} M and 10^{-2} M respectively. Ouabain is a Na^+K^+ATPase inhibitor and used at a concentration of 10^{-5} M whereas furosemide is an NKCC1 inhibitor, used at a concentration of 10^{-4} M (Hannaert *et al.*, 2002; Hamann *et al.*, 2010). These two inhibitors are used alone and in combination. Cell monolayers were washed once with warm (37 ^oC) modified Krebs' solution. The cells were incubated in Krebs' solutions for different lengths of time to determine the optimum incubation time. Cell monolayers were then washed rapidly four times with ice cold Krebs' solution to remove any extracellular radioactive tracer. Cells were lysed by incubation in 1 ml of distilled water. The $^{86}Rb^+$ activity of the cell extracts was measured by counting its β-emissions in a liquid scintillation spectrometer in 2 ml of scintillation cocktail.

2.5.4 Determination of cell number and calculation of influx

A similar parallel plate of cells were treated with a trypsin solution (0.25% w/v) to form a cell suspension for determination of cell numbers per well.

The reading produced by the scintillation spectrometer is in counts per minute (CPM). Then the following equation was applied to convert measurements to molar terms.

$$Flux = \frac{(counts\ of\ sample - blanks) x\ n\ x\ 5.4}{(counts\ of radioactive\ isotope)\ x\ 5\ x\ (cell\ count)}$$

Where n=fraction of sample taken for counting and 5.4 is the K^+ concentration in mM. Blanks are counts from a plate containing no cells, treated in the same way as plates containing cells, in order to eliminate non-specific radioactivity from the culture plate and to define cell dependent uptake. The cell count per well is expressed in 10^6 cells. The influx measurements are then multiplied by 10^3 to be expressed in nanomoles/10^6 cells per 15 min.

2.6 Measurement of pH_i and regulation of Na^+/H^+ exchange

2.6.1 Cell culture

Different cell numbers ranging from 1000 – 10000 cells per well were seeded onto 96-well plates (#3598, Corning, UK) and left in an incubator. MCF-7 cells were cultured in steroid-depleted media and plated on collagen-coated 96-well plates to allow for better cell attachment. These plates were coated with rat-tail type 1 collagen (#11179179001, Roche Applied Science, Germany) at a concentration of 5 µg/cm^2.

2.6.2 Preparation of standards and bathing solution

The high K^+ buffers consisted of 110 mM K_2HPO_4 with 20 mM NaCl at pH 8.96 (Solution A), and 135 mM KH_2PO_4 with 20 mM NaCl at pH 4.45 (Solution B). Standard pH buffers of pH 6.0, 6.2, 6.6, 7.0, 7.4 and 7.8 were prepared by titrating Solution A with Solution B.

The bathing solution was Krebs's Henseleit HEPES-buffered (KHH) media at pH 6.0 and pH 7.4, consisting of 140 mM NaCl, 3 mM KCl, 1 mM $MgCl_2$, 1 mM $CaCl_2$, 20 mM HEPES and 10 mM Glucose. The pH was adjusted to pH 7.4 by addition of Tris, whereas pH 6.0 was adjusted by addition of MES hydrate.

2.6.3 Measurement of pH_i

2',7'-bis-(2-carboxyethyl)-5-(and-6)-carboxyfluorescein acetoxymethyl ester (BCECF-AM, Invitrogen, UK) is a pH-sensitive indicator with a pK_a of ~7.0. It has a dual excitation and single emission fluorescence. The excitation at ~490 nm is pH-dependent whereas, the excitation at its isosbestic point of ~440 nm is pH-independent. The isosbestic point is the wavelength at which the absorbance remains constant. Emission is at ~535 nm. BCECF-AM is cell-permeant thus enabling efficient measurement of changes in cytosolic pH. Intracellular esterases are involved in the hydrolytic conversion of non-fluorescent BCECF-AM to fluorescent pH-sensitive BCECF.

A stock solution of 1 mM BCECF-AM was prepared by dissolving BCECF-AM in anhydrous DMSO. Cells were washed with Krebs's Henseleit HEPES-buffered (KHH) solution. BCECF-AM was added to the cells at a concentration of 10 µM and incubated for 15-30 minutes in an incubator at 37 ^{o}C. Cells were washed with KHH solution and the different pH buffers standards ranging from pH 6.0, 6.2, 6.6, 7.0, 7.4, 7.8 containing 10 µM Nigericin (Invitrogen, UK) were added to the standard wells. Nigericin is a K^+/H^+ ionophore which transports K^+ and H^+ ions across the cell membrane to equilibrate the intracellular pH with the extracellular pH of the solution. This method is known as the high K^+/Nigericin technique. KHH solution was added to the experimental cells. Additionally a set of blanks, consisting of unloaded cells (i.e. non BCECF-AM added), were later replaced with the standard pH buffers for pH 6.0, 6.2, 6.6, 7.0, 7.4, 7.8 containing 10 µM Nigericin to allow for correction of fluorescent data cell autofluorescence.

The fluorescent intensity was measured with a FLUOstar Omega plate reader (BMG Labtech Ltd., UK). The plate reader had excitation filters for 485 nm ± 10 nm and 420 nm ± 10 nm and an emission filter for 520 nm ± 10 nm. A calibration curve was produced using the standards. This was linear over the given pH range. The pH of the experimental cells was determined from the fluorescence ratio of 485 nm / 420 nm of the standard curve. The ratio of fluorescent intensity was calculated using Microsoft Excel 2010 software. Calculations of the intracellular pH were performed by linear regression and

interpolating from the standard curve using the software GraphPad Prism version 6.0.

2.7 Statistics

The statistical significance of observed differences were tested using ANOVA generated by the software GraphPad Prism version 6.0. Error bars indicate standard errors of mean of replicates in each experiment. A p-value of <0.05 was considered to be statistically significant.

Chapter 3. *SLC12A2* (NKCC1)

3.1 Introduction

The study of the function of genes regulated by oestrogen is crucial in understanding the underlying causes of breast tumourigenesis. One of the oestrogen-regulated genes identified from expression analyses is *SLC12A2*. The expression of *SLC12A2* was found to be decreased by oestrogen in oestrogen-responsive breast cancer cells (Wright *et al.*, 2009). This gene encodes the protein NKCC1.

NKCC1 is a Na^+-K^+-Cl^- co-transporter, that has 12 α-helical transmembrane spanning domains (Xu *et al.*, 1994). It has three regions, an amino-terminal region, a central hydrophobic region and a carboxy-terminal. NKCC1 is located mainly in the basolateral membrane of many different epithelial cells including colon, salivary gland, testes and airway. NKCC1 transports the three types of ions with a stoichiometry of 1 Na^+: 1 K^+: 2 Cl^- (Geck *et al.*, 1980) and therefore is electroneutral. Ion transporters such as NKCC1 play an important role in the regulation of epithelial cell volume and in the maintenance of ion secretion. Ion transporters have functions in intercellular communication, secretion, migration and invasion. Alteration or defects in the structure and function of ion transporters contribute to a wide range of diseases including cancer (Li and Xiong, 2011). Such abnormalities in membrane ion transporters of tumour cells have been shown to be involved in promoting uncontrolled growth, proliferation and progression of cancer (Kunzelmann, 2005; Prevarskaya *et al.*, 2010).

Ion transporters have been implicated in promoting cell motility, however the exact process by which motility occurs is not understood fully. Cell motility is considered to involve movement of osmotically-active ions Na^+ and K^+ and changes in Ca^{2+} activities in the cytosol. NKCC1 maintains an ionic gradient across the cell membrane by allowing Na^+, K^+ and Cl^- ions into the cell. The net flux is dependent on the sum of the chemical activity gradients for Na^+, K^+ and Cl^- ions. NKCC1 plays a role in cell volume regulation and is activated in response to shrinkage of cells (Russell, 2000). The alteration of the net chemical gradient in response to an increased external osmolarity leads to an

accumulation of Na^+, K^+ and Cl^- ions intracellularly (Hebert *et al.*, 2004). Water follows into the cell osmotically allowing the cell to regain cell volume.

3.1.1 Aim

The aim of the experiments reported in this chapter is to investigate the expression, cellular localisation, regulation and function of NKCC1 in three oestrogen-responsive breast cancer cell lines MCF-7, EFM-19 and EFF-3.

3.2 Expression of NKCC1 in breast cancer cells

3.2.1 Expression of NKCC1 protein in breast cancer cell lines

The expression of NKCC1 protein in breast cancer cell lines was investigated by western transfer analysis. Protein extracts were prepared from T75 flasks of breast cancer cells cultured in DMEM containing 10 % FCS and 1 µg/ml insulin. Equal amounts of 20 µg of protein were separated by polyacrylamide gel electrophoresis and transferred to nitrocellulose membranes. The oestrogen responsive cell lines were MCF-7, EFM-19, EFF-3, BT-474, T47-D and ZR-75. The oestrogen unresponsive cells were MDA-MB-231, SKBR3, BT-20, Hs578T and HBL-100. A rabbit monoclonal antibody against NKCC1 detected NKCC1 protein at an apparent molecular mass of around 160 - 200 kDa. As shown in Figure 3.1, ZR-75 and Hs578T had the highest levels of NKCC1 protein expression, followed by BT-474, EFF-3 and EFM-19 cells. MCF-7, MDA-MB-231 and HBL-100 cells expressed similar amounts of NKCC1. Lower levels of NKCC1 protein were detected in SKBR3 and BT-20 cells. T47-D cells did not express any NKCC1 protein.

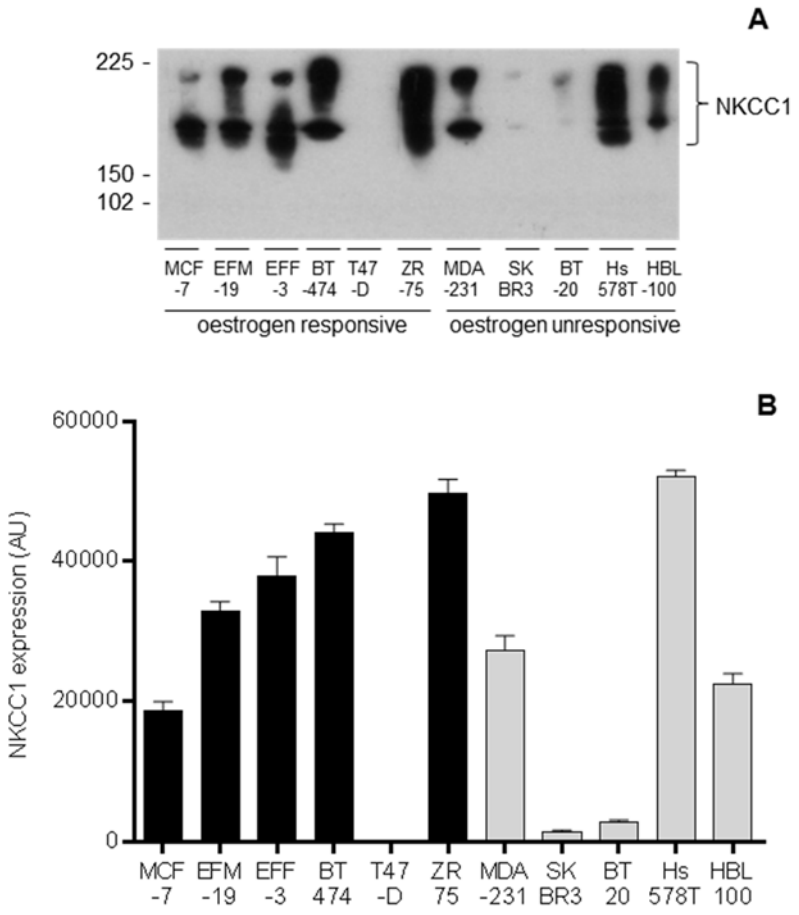

Figure 3.1 Expression of NKCC1 in breast cancer cells. Different breast cancer cell lines were cultured in routine culture medium in T75 flasks. Cells were lysed and protein extracts were prepared. Equal amounts of 20 µg of protein were separated by 12% polyacrylamide gel electrophoresis and then transferred to nitrocellulose membranes. The membranes were incubated with anti-NKCC1 antibody (1:10000 dilution) overnight at 4 ^{o}C, followed by horseradish peroxidase conjugated goat-anti-rabbit secondary antibody for 1 hour at 37 ^{o}C. Proteins were visualised by enhanced chemiluminescence with SuperSignal West Dura Extended Duration Substrate. **A.** The protein expression of NKCC1 was determined by Western transfer analysis in MCF-7, EFM-19, EFF-3, BT-474, T47-D, ZR-75, MDA-MB-231 (MDA-231), SKBR3, BT-20, Hs578T and HBL-100 cells. **B.** Densitometric quantification of NKCC1. The black bars (■) represent oestrogen-responsive cell lines, whereas the grey bars (□) indicate the oestrogen-unresponsive cell lines. Error bars indicate standard errors of the mean of triplicate measurements.

3.3 Cellular localisation of NKCC1 in breast cancer cells

The cellular localisation of NKCC1 in breast cancer cells was analysed by immunofluorescence.

3.3.1 Optimisation of conditions and the antibody concentration

Figure 3.2 shows the optimisation of different combinations of cell fixation and permeabilisation conditions prior to immunofluorescence to determine the ideal

condition for the NKCC1 antibody. MCF-7 cells were seeded onto 6-well plates containing coverslips and grown in maintenance medium. Cells were washed with PBS and fixed in methanol or 4% paraformaldehyde as detailed in the Materials and Methods section. Fixation was followed by blocking in 1x PBS, 5% goat serum and 0.3% triton X-100 or 0.2% saponin (blocking buffer) for 1 hour at room temperature. The cells were then incubated with the primary NKCC1 antibody at a dilution of 1:100 and incubated overnight at 4 ^{o}C.

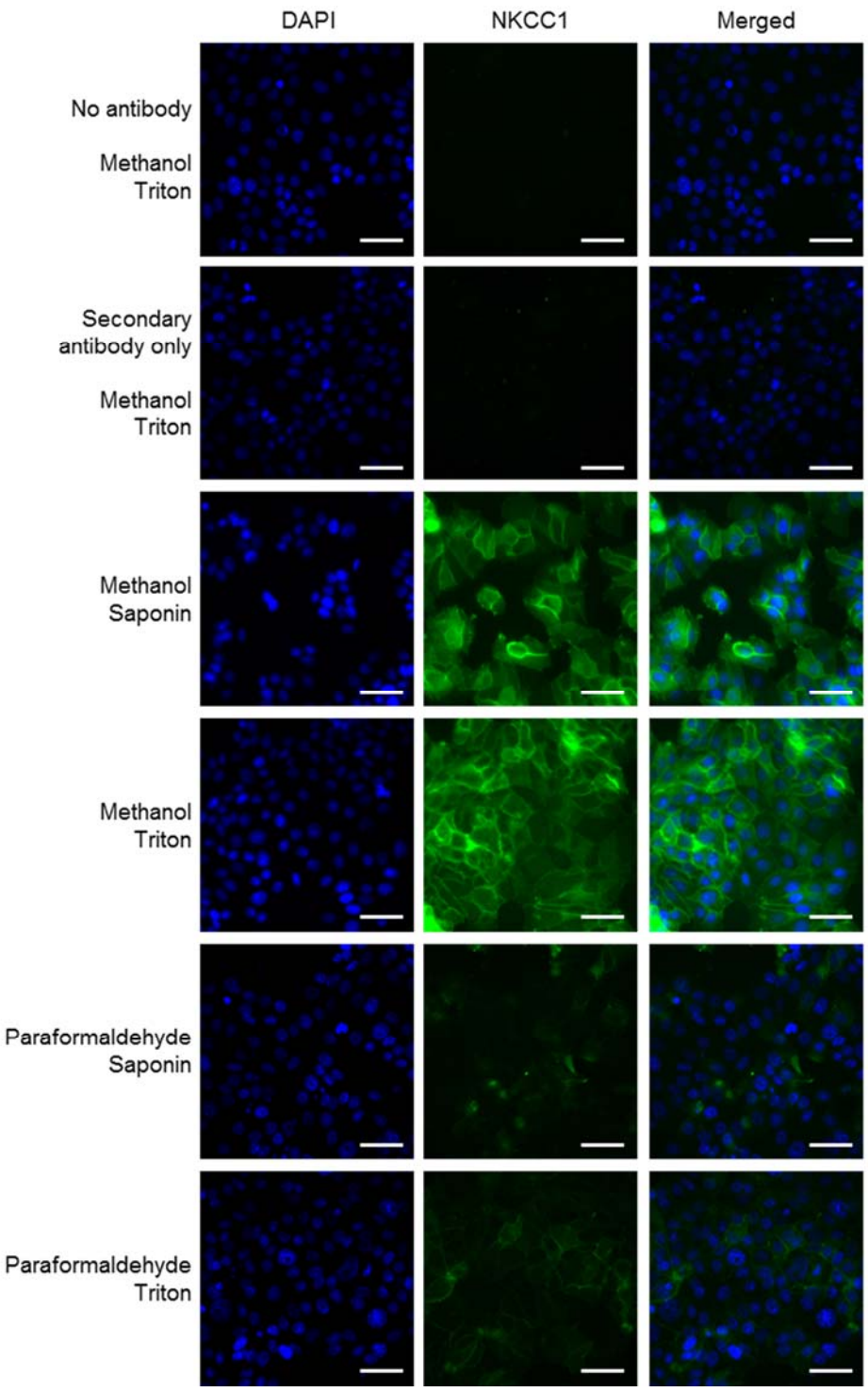

Figure 3.2 Optimisation of fixation and permeabilisation conditions for detection of NKCC1. MCF-7 cells were seeded at a density of $1x10^5$ cells onto 6-well plates and cultured in routine culture medium for 24 hours. The next day, cells were washed with PBS and fixed in either methanol at -20 ^oC or in 4 % paraformaldehyde at room temperature. After fixation, the cells were washed with PBS thrice with each wash lasting 20 minutes. Cells were then blocked in blocking buffer containing either triton or saponin for 1 hour at room temperature. The blocking buffer was aspirated and the primary antibody NKCC1 was added at 1:100 dilution and incubated overnight at 4 ^oC. The following day the primary antibody was aspirated and the cells were washed 3 times with PBS, 15 minutes each. The secondary antibody Alexa fluor 488 conjugated goat anti-rabbit were added at a dilution of 1:1000 and the coverslips were covered

in foil and the cells were incubated for 1 - 2 hours at room temperature. Cells were washed 3 times with PBS. DAPI mounting media was added to the glass slides prior to placing the coverslip on the slide and the cells were examined under the fluorescent microscope (Leica DMR) using a 40x objective. Results are shown for different treatment conditions of fixation and permeabilisation. Images on the column indicated with “DAPI” show nuclear staining, whereas the images indicated with “NKCC1” show the immunoreaction for NKCC1. The “Merged” images show both nuclear (blue) and NKCC1 (green) staining together. Scale bar = 45 µm.

Cells with either no NKCC1 antibody or probed with AF488 anti-rabbit (1:1000 dilution) secondary antibody only was used to determine whether there would be an indication of any non-specific signal. This showed that there was no autofluorescence from the cells itself and there was no background signal. Results showed that fixing cells with methanol was better than with paraformaldehyde. Permeabilisation with either Saponin or Triton produced similar intensities of fluorescence and NKCC1 was localised to the cellular membranes. Therefore in future experiments, cells were fixed with methanol and permeabilised with saponin.

3.3.2 Localisation of NKCC1 in MCF-7, EFM-19 and EFF-3 cells

The cellular localisation of NKCC1 in MCF-7, EFM-19 and EFF-3 cells was investigated by immunofluorescence. As stated previously, we plated cells onto coverslips in 6-well plates and incubated for 24 hours. The primary antibody NKCC1 diluted in PBS was added at a dilution of 1:100 and the secondary antibody Alexa fluor 488 conjugated goat anti-rabbit IgG was added at a dilution of 1:1000. The coverslips were mounted with DAPI mounting media and examined under the fluorescent microscope.

As illustrated in Figure 3.3, the immunofluorescence images A3, B3 and C3 show localisation of NKCC1 at the plasma membrane in all three cell lines. However, a few EFM-19 cells (B2) and EFF-3 cells (C2) show a stronger immunoreaction at some sites in the membrane. Also we can observe some NKCC1 expression of vesicular nature especially in EFF-3 cells.

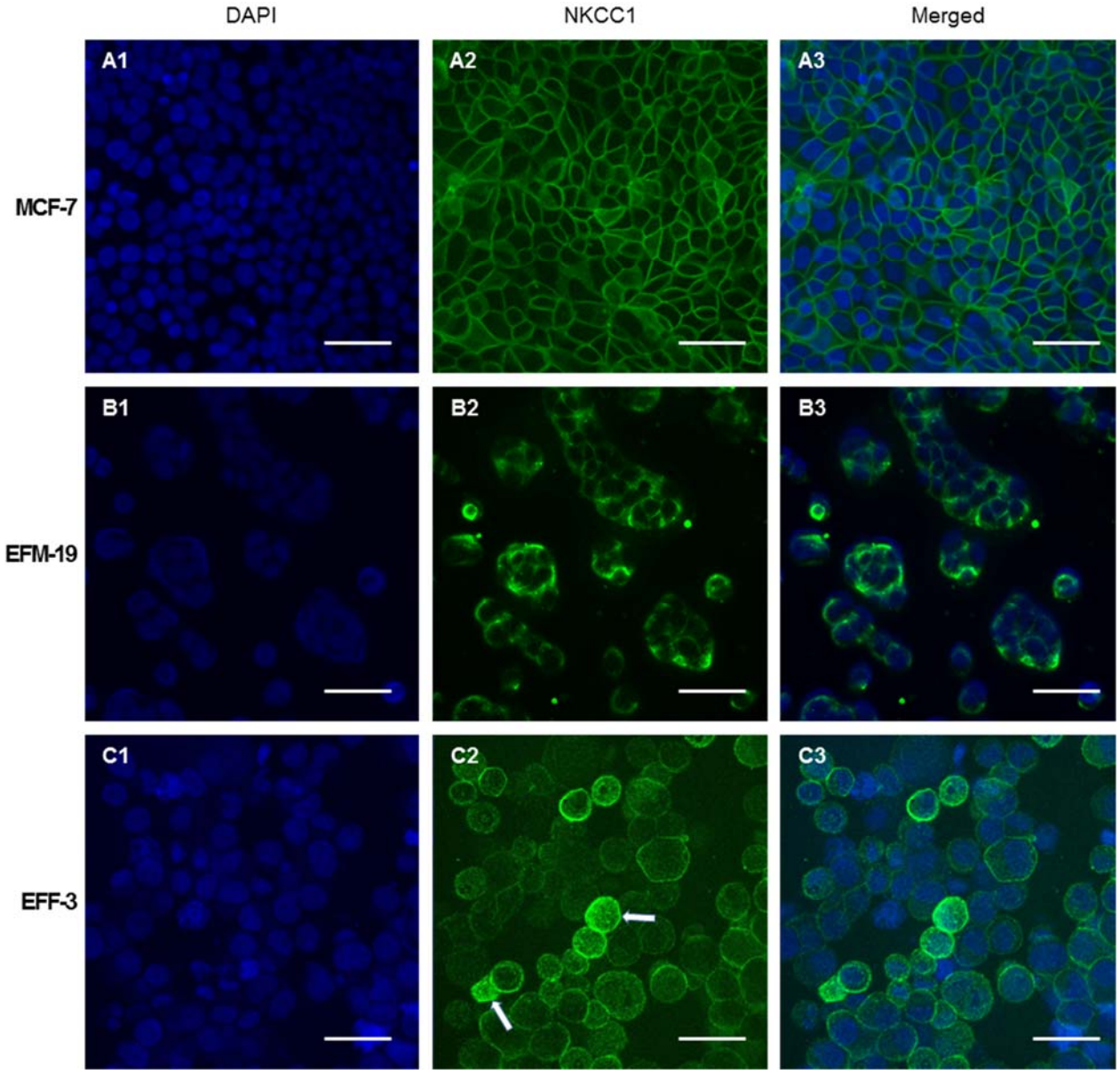

Figure 3.3 Localisation of NKCC1 in cell lines. MCF-7, EFM19 and EFF-3 cells were seeded onto 6-well plates and cultured in routine culture medium for 24 hours. Cells were washed with PBS and fixed in methanol at -20 ºC. After fixation, cells were washed with PBS three times for 15 minutes each. Cells were then blocked in blocking buffer containing saponin for 1 hour at room temperature. The blocking medium was aspirated and the primary antibody NKCC1 was added at 1:100 dilution and incubated overnight at 4 ºC. Cells were washed 3 times with PBS, 15 minutes each. The secondary antibody Alexa fluor 488 conjugated goat anti-rabbit were added at a dilution of 1:1000 and were covered in foil and the cells were incubated for 1 hour at room temperature. Cells were washed 3 times with PBS. DAPI mounting media was added to the glass slides prior to placing the coverslip on the slide and the cells were examined under the fluorescent microscope (Leica DMR) using a 40x objective. Images A1, B1 and C1 show the nuclear staining, whereas the images A2, B2 and C2 show the immunoreaction for NKCC1 in MCF-7, EFM-19 and EFF-3 cells, respectively. The merged images A3, B3 and C3 show DAPI (blue) and NKCC1 (green) staining combined together. Scale bar = 45 µm. The white arrow (⇨) indicate examples of clear vesicular expression.

3.4 Regulation of NKCC1 by oestrogen

3.4.1 Investigation of the regulation of NKCC1 expression by oestradiol in MCF-7 cells

MCF-7 cells were cultured in maintenance medium, and withdrawn from growth factors, by growing in phenol-red-free DMEM containing 10 % dextran-coated charcoal treated newborn calf serum and 1 µg/ml insulin for 5 days. Following the withdrawal, cells were cultured in the absence or presence of 10^{-9} M oestradiol for different lengths of time from 0 hours to 8 days.

The Figure 3.4 illustrates the effect of exposure to oestrogen on the morphology of MCF-7 cells. As indicated on the diagram “Day 1 - withdrawal”, which is the first day of media change from routine culture media to withdrawal media, the cells appear rounded and large in size. The cells are densely packed and lack any space between cells. When the cells have been cultured in withdrawal media for 5 days, their morphology was observed to change. The cells are less spherical and look elongated. An increase in intercellular space is noticeable. Cells start to form blister-like structures. These fluid-filled blisters contains small vesicles within them. When MCF-7 cells have been treated with 10^{-9} M oestradiol, the intercellular space disappears and the cells return to being more spherical.

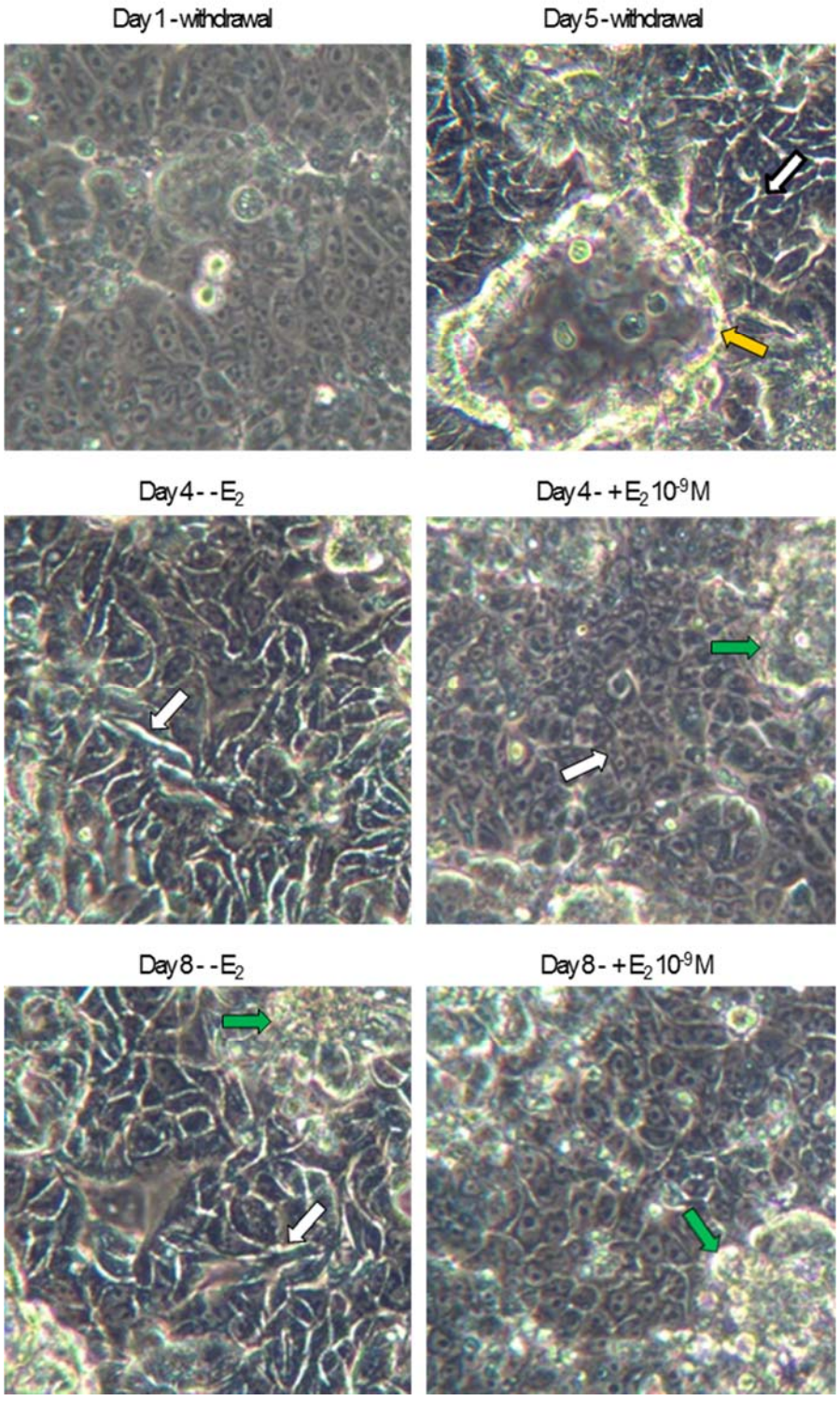

Figure 3.4 Morphological changes of MCF-7 cells in the absence and presence of oestrogen. MCF-7 cells were plated at density of 50,000 cells per well in a 24-well plate and cultured in withdrawal media for 5 days. Then cells were cultured in the absence and presence of 10^{-9} M oestradiol from 0 hours to 8 days. The photographs were taken at 20x magnification. The yellow arrow (⇨) indicate examples of a blister, the white arrow (⇨) indicates intercellular space and the green arrow (⇨) indicates piled cells.

This experiment was designed to determine the regulation of NKCC1 by oestrogen. MCF-7 cells were seeded onto 24-well plates at a density of 50,000 cells per well. They were grown in routine culture medium for 24 hours, and then withdrawn from growth factors, by culturing in withdrawal media for 5 days. Following withdrawal, cells were cultured in the absence or presence of 10^{-9} M oestradiol for varying time periods from 0 hours to 12 days.

As shown in Figure 3.5, the effect of 10^{-9} M oestradiol was noticeable from 4 days. The presence of oestradiol, in comparison with the absence of oestradiol, showed a marked decrease in the expression of NKCC1 protein. This significant decrease in protein expression was more noticeable at 8 days. There seems to be a reduction of NKCC1 expression with time in the untreated cells, therefore future experiments in MCF-7 cells were devised for treatments lasting for 8 days and not any further than that.

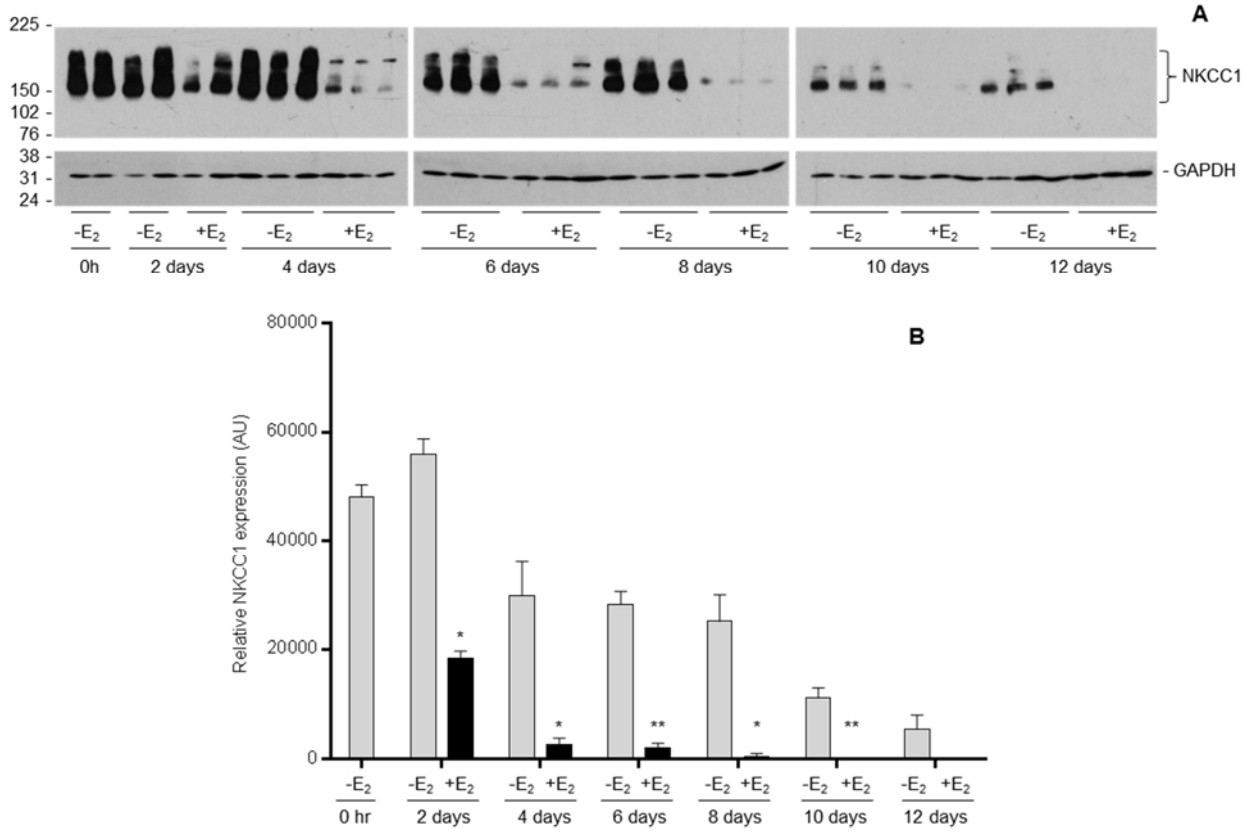

Figure 3.5 Effect of oestrogen on expression of NKCC1 in MCF-7 cells. Cells were steroid deprived by growing in phenol-red-free media containing 10% dextran-coated charcoal treated serum and 1 µg/ml insulin, for 5 days and then treated with 10^{-9} M of 17β-oestradiol for different lengths of time upto 12 days. Both the oestradiol-treated and untreated cells were lysed and protein extracts prepared. Protein aliquots of 20 µg were separated by 12% polyacrylamide gel

electrophoresis and then transferred to nitrocellulose membranes. The membranes were incubated with anti-NKCC1 antibody (dilution 1:10000) overnight at 4 ^{o}C, followed by horseradish peroxidase conjugated goat-anti-rabbit secondary antibody for 1 hour at 37 ^{o}C. Proteins were visualised by enhanced chemiluminescence with SuperSignal West Dura Extended Duration Substrate. **A.** The protein expression of NKCC1 in MCF-7 cells after oestrogen stimulation for a timecourse of 0 hours to 12 days, comparing serum withdrawn (-E_2 □) samples with oestrogen-stimulated (+E_2 ■) samples. **B.** Quantification of NKCC1 normalised against the corresponding GAPDH signal, *p < 0.05 and **p < 0.001 by ANOVA. Error bars indicate SEM of triplicate measurements.

3.4.2 Investigation of the regulation of NKCC1 expression by oestradiol in EFM-19 cells

A similar experiment investigated changes in NKCC1 protein expression with the duration of exposure to 10^{-9} M oestradiol in EFM-19 cells.

The changes in cellular morphology are shown in Figure 3.6. On the first day of media change from routine culture media, to withdrawal media, the cells are confluent and the intercellular space is smaller. After 5 days of culturing cells in withdrawal media, the increase is intercellular space is clearly visible. Cells cultured in withdrawal media tend to give rise to fluid-filled blisters as indicated in the diagram. When comparing the images of untreated and cells grown in the presence of oestrogen at 8 days after treatment, there is a noticeable increase in the number of cells.

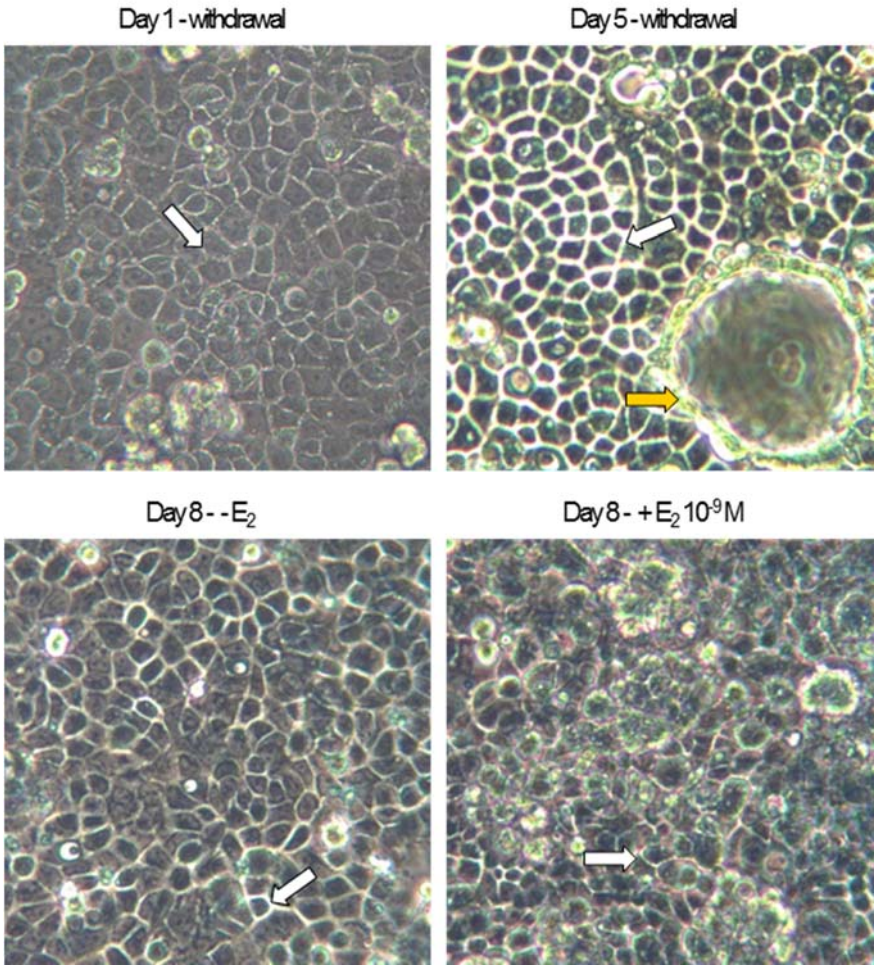

Figure 3.6 Morphological changes of EFM-19 cells in the absence and presence of oestrogen. EFM-19 cells were plated at density of 50,000 cells per well in a 24-well plate and cultured in withdrawal media for 5 days. Then cells were cultured in the absence and presence of 10^{-9} M oestradiol from 0 hours to 8 days. The photographs were taken at 20x magnification. The yellow arrow (⇨) indicate examples of a blister and the white arrow (⇨) indicates intercellular space.

Representative data from western transfer is shown in Figure 3.7. NKCC1 protein expression decreases with oestradiol treatment at 2 days. When comparing the expression of the treated cells with the untreated cells at 4 and 6 days, there is not much of a difference. The maximum effect of oestrogen on the reduction of NKCC1 was observed at 8 days treatment. After longer incubation, untreated cells expressed lower levels of NKCC1.

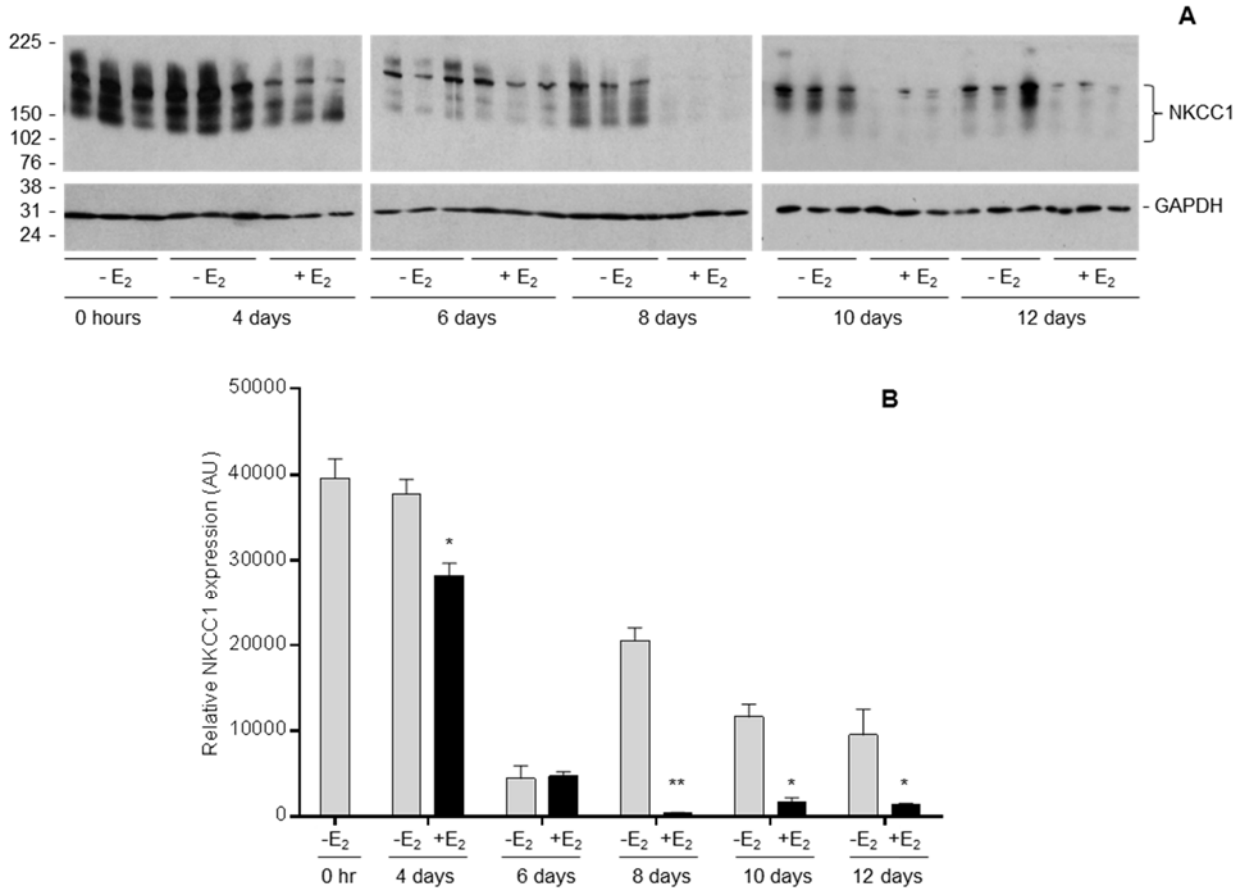

Figure 3.7 Effect of oestrogen on expression of NKCC1 in EFM-19 cells. Cells were steroid deprived by growing in phenol-red-free media containing 10% dextran-coated charcoal treated serum and 1 µg/ml insulin, for 5 days and then treated with 10^{-9} M of 17β-oestradiol for different lengths of time ranging from 0 hours to a maximum of 10 days. Both the oestradiol-treated and untreated cells were lysed and protein extracts prepared. Protein aliquots of 20 µg were separated by 12% polyacrylamide gel electrophoresis and then transferred to nitrocellulose membranes. The membranes were incubated with anti-NKCC1 antibody (dilution 1:10000) overnight at 4 °C, followed by horseradish peroxidase conjugated goat-anti-rabbit secondary antibody for 1 hour at 37 °C. Proteins were visualised by enhanced chemiluminescence with SuperSignal West Dura Extended Duration Substrate. **A.** The protein expression of NKCC1 in EFM-19 cells after oestrogen stimulation for a timecourse of 0 hours to 10 days, comparing serum withdrawn (-E_2 □) samples with oestrogen-stimulated (+E_2 ■) samples. **B.** Quantification of NKCC1 normalised against the corresponding GAPDH signal, *p < 0.05 and **p < 0.001 by ANOVA. Error bars indicate SEM of triplicate measurements.

3.4.3 Investigation of the regulation of NKCC1 expression by oestradiol in EFF-3 cells

The effect of oestrogen on the expression of NKCC1 in EFF-3 cells was tested. The results are shown in Figure 3.8. A decrease in expression is observed from 2 days onwards, but a significant decrease in the expression of NKCC1 in the presence of oestradiol is observed at longer exposures from 8 days to 10 days.

From 6 days onwards the strong diffused protein band somewhat disappears, and leaves a double band. The higher molecular weight band does not change much with exposure to oestradiol nor with time. However the lower molecular weight band decreases in the presence of oestradiol from 6th day onwards and disappears completely at 10 days.

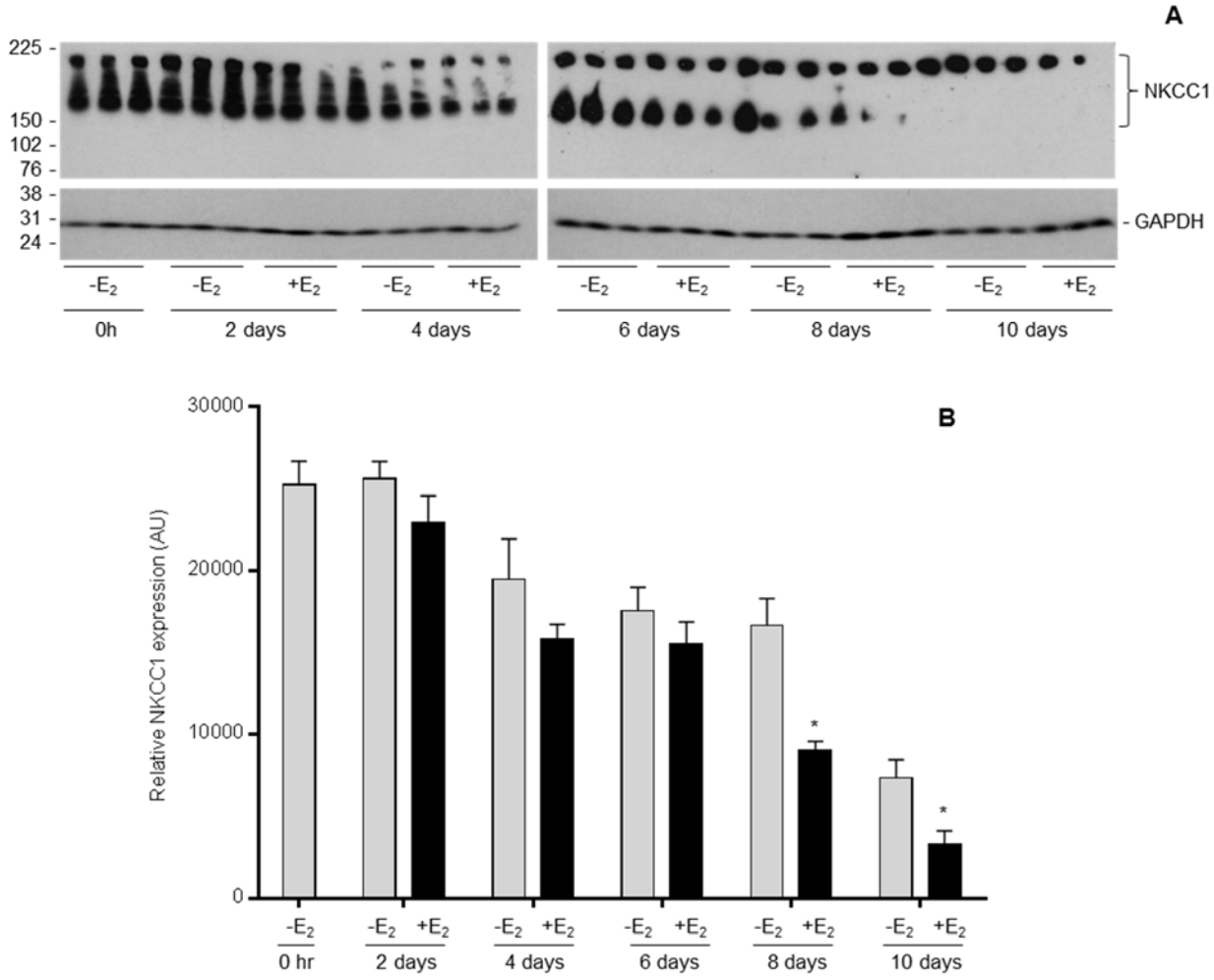

Figure 3.8 Effect of oestrogen on expression of NKCC1 in EFF-3 cells. EFF-3 cells were plated at a density of 100,000 cells per well onto a 24-well plate. Cells were steroid deprived by growing in phenol-red-free media containing 10% dextran-coated charcoal treated serum and 1 µg/ml insulin, for 5 days and then treated with 10^{-9} M of 17β-oestradiol for different lengths of time ranging from 0 hours to a maximum of 10 days. Both the oestradiol-treated and untreated cells were lysed and protein extracts prepared. Protein aliquots of 20 µg were separated by 12% polyacrylamide gel electrophoresis and then transferred to nitrocellulose membranes. The membranes were incubated with anti-NKCC1 antibody (dilution 1:10000) overnight at 4 ºC, followed by horseradish peroxidase conjugated goat-anti-rabbit secondary antibody for 1 hour at 37 ºC. Proteins were visualised by enhanced chemiluminescence with SuperSignal West Dura Extended Duration Substrate. **A.** The protein expression of NKCC1 in EFF-3 cells after oestrogen stimulation for a timecourse of 0 hours to 10 days, comparing serum withdrawn ($-E_2$ □) samples with oestrogen-stimulated ($+E_2$ ■) samples. **B.** Quantification of NKCC1 normalised against the corresponding GAPDH signal, *$p < 0.05$ by ANOVA. Error bars indicate SEM of triplicate measurements.

3.4.4 Effect of oestradiol on the expression of NKCC1 in MCF-7 cells by immunofluorescence

The aim of this experiment was to visualise the expression of NKCC1 in the absence and presence of 10^{-9} M oestradiol. MCF-7 cells were seeded onto coverslips in 12-well plates and cultured in withdrawal media for 5 days and then grown in the absence or presence of 10^{-9} M oestradiol for a further 8 days.

Cells were isolated at 0 hours, 4 days and 8 days and fixed with methanol at -20 ^{o}C for 20 minutes, as this is the optimum fixation condition detailed in section 3.3.1. Immunofluorescence procedure was followed as stated in Materials and Methods. MCF-7 cells were blocked in blocking buffer containing saponin. Following primary and secondary antibody incubations, DAPI mounting media was added and cells were observed under the laser scanning spectral confocal microscope (Leica TCS SP2). The fluorochrome settings were kept the same throughout the timecourse to minimise variations in intensities, thus allowing slight changes in expression to be visualised.

The results obtained are shown in Figure 3.9. NKCC1 is localised to the cell membrane. There is evidence of vesicular expression, which is more clearly evident in some cells. Similar to data from timecourse experiments, there is a marked reduction in the expression of NKCC1 in the presence of oestradiol.

Figure 3.10 illustrates the x-z cross-sections from the same experiment. The images were taken with a 63x oil immersion objective. NKCC1 protein is lateralised and MCF-7 cells cultured in the absence of oestrogen appear to be flattened in comparison to the oestrogen-treated cells. Upon oestrogen stimulation, there is a reduction in the NKCC1 expression in the lateral aspects of the cell. Also the increase in cell proliferation in the presence of oestradiol, is more visible at 8 days, as the cells are more dense and no longer in a monolayer. The depth of cells has increased.

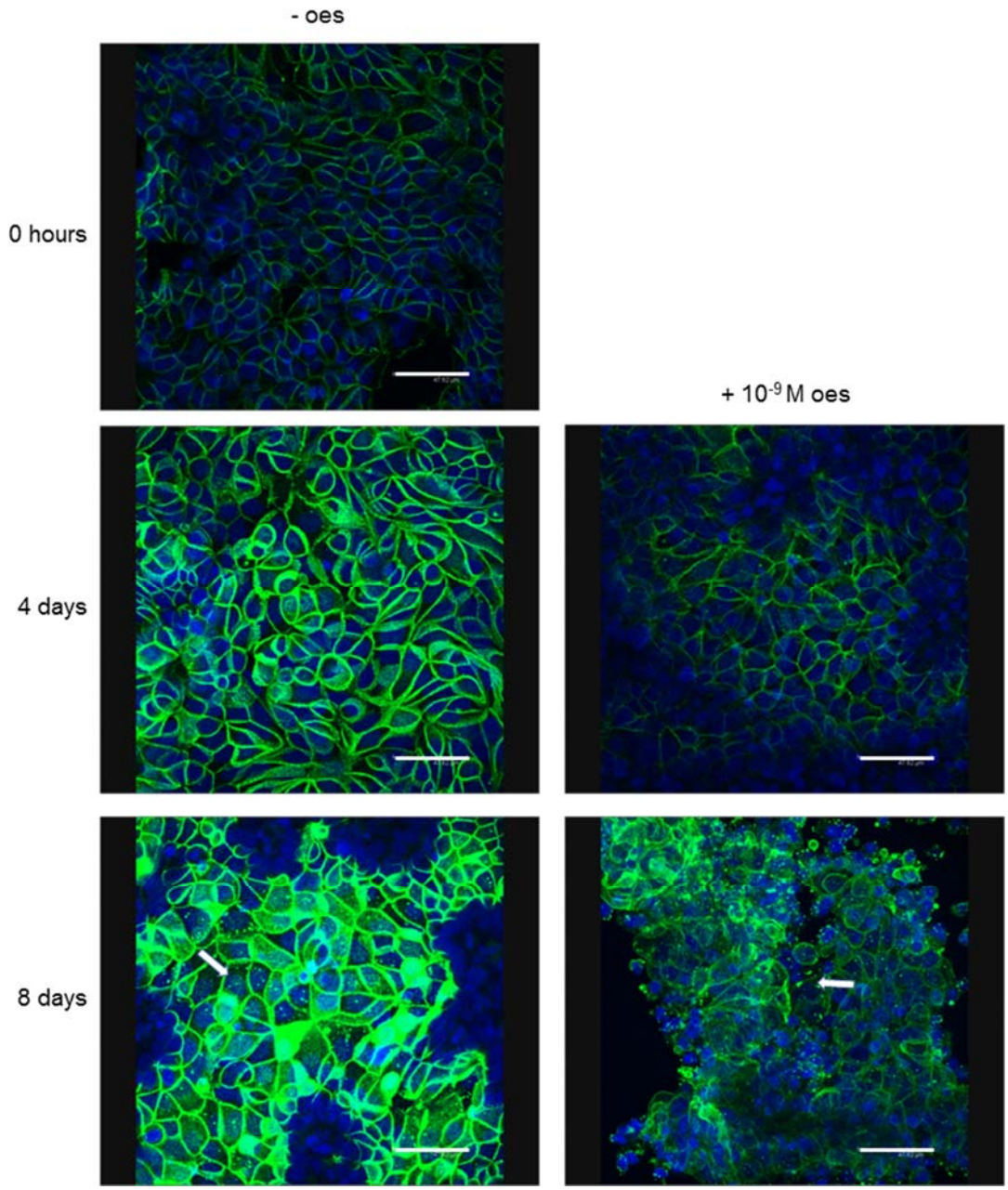

Figure 3.9 Effect of oestradiol on the expression and localisation of NKCC1 in MCF-7 cells. MCF-7 cells were seeded onto 12-well plates and cultured in routine culture medium for 24 hours. Cells were cultured in withdrawal media for 5 days and grown in the absence or presence of 10^{-9} M oestradiol for different time periods ranging from 0 hours to 8 days. Cells were washed with PBS and fixed in methanol at -20 ^{o}C. After fixation, cells were washed with PBS three times for 15 minutes each. Cells were then blocked in blocking buffer containing saponin for 1 hour at room temperature. The blocking medium was aspirated and the primary antibody NKCC1 was added at 1:100 dilution and incubated overnight at 4 ^{o}C. Cells were washed 3 times with PBS, 15 minutes each. The secondary antibody Alexa fluor 488 conjugated goat anti-rabbit were added at a dilution of 1:1000 and were covered in foil and the cells were incubated for 1 hour at room temperature. Cells were washed 3 times with PBS. DAPI mounting media was added to the glass slides prior to placing the coverslip on the slide and the cells were examined under the confocal microscope using a 63x objective (Oil, 1.63). X-Y images show DAPI (blue) and NKCC1 (green) staining at the times indicated on the left of the diagram. The images on the right show cells treated with 10^{-9} M of 17β-oestradiol. Scale bars = 47 µm. The white arrow (⇨) indicate examples of vesicular expression.

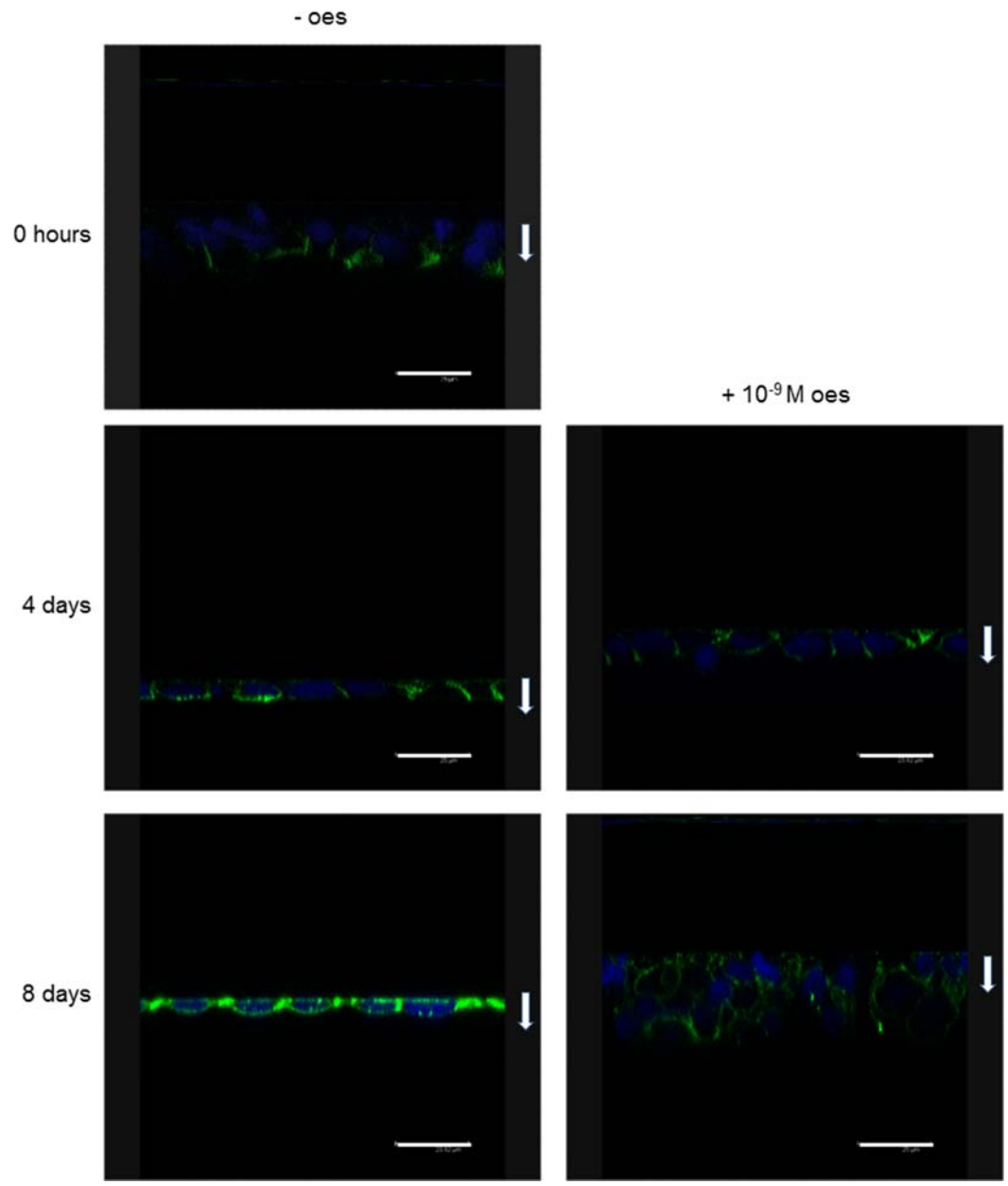

Figure 3.10 Cross-sectional images of the effect of oestradiol on the expression and localisation of NKCC1 in MCF-7 cells. MCF-7 cells were seeded onto 12-well plates and cultured in routine culture medium for 24 hours. Cells were cultured in withdrawal media for 5 days and grown in the absence or presence of 10^{-9} M oestradiol for different time periods ranging from 0 hours to 8 days. Cells were washed with PBS and fixed in methanol at -20 ^{o}C. After fixation, cells were washed with PBS three times for 15 minutes each. Cells were then blocked in blocking buffer containing saponin for 1 hour at room temperature. The blocking medium was aspirated and the primary antibody NKCC1 was added at 1:100 dilution and incubated overnight at 4 ^{o}C. Cells were washed 3 times with PBS, 15 minutes each. The secondary antibody Alexa fluor 488 conjugated goat anti-rabbit were added at a dilution of 1:1000 and were covered in foil and the cells were incubated for 1 hour at room temperature. Cells were washed 3 times with PBS. DAPI mounting media was added to the glass slides prior to placing the coverslip on the slide and the cells were examined under the confocal microscope using a 63x objective (Oil, 1.63). X-Z images show DAPI (blue) and NKCC1 (green) staining at the times indicated on the left of the diagram. The images on the right show cells treated with 10^{-9} M of 17β-oestradiol. Scale bars = 25 μm. The white arrow head (⇩) point towards the top of cell.

3.4.5 Effect of oestradiol on the expression of NKCC1 in EFM-19 cells by immunofluorescence

To study the effect on oestradiol, EFM-19 cells were seeded onto permeable Transwell filter supports at a high density of 1 million each. The filter supports were held in place in a 12-well plate. Cell culture media was changed from routine culture media to withdrawal media. The upper compartment containing cells and the lower compartments were carefully washed with PBS and replenished with withdrawal media. Further to withdrawal for 5 days, cells were cultured with or without 10^{-9} M oestradiol for 8 days. The cells were fixed with methanol and the filters were removed from the Transwell insert by carefully cutting around the membrane edges with a scalpel. The filters were then blocked in blocking buffer and permeabilised with saponin and processed accordingly.

The results are presented in Figure 3.11 below. As illustrated previously, NKCC1 has been localised to the cell membrane of EFM-19 cells. This experiment demonstrated the effect of oestradiol on the expression of NKCC1 by immunofluorescence. It clarified the reduction of NKCC1 protein in response to oestradiol treatment, as observed with western transfer too.

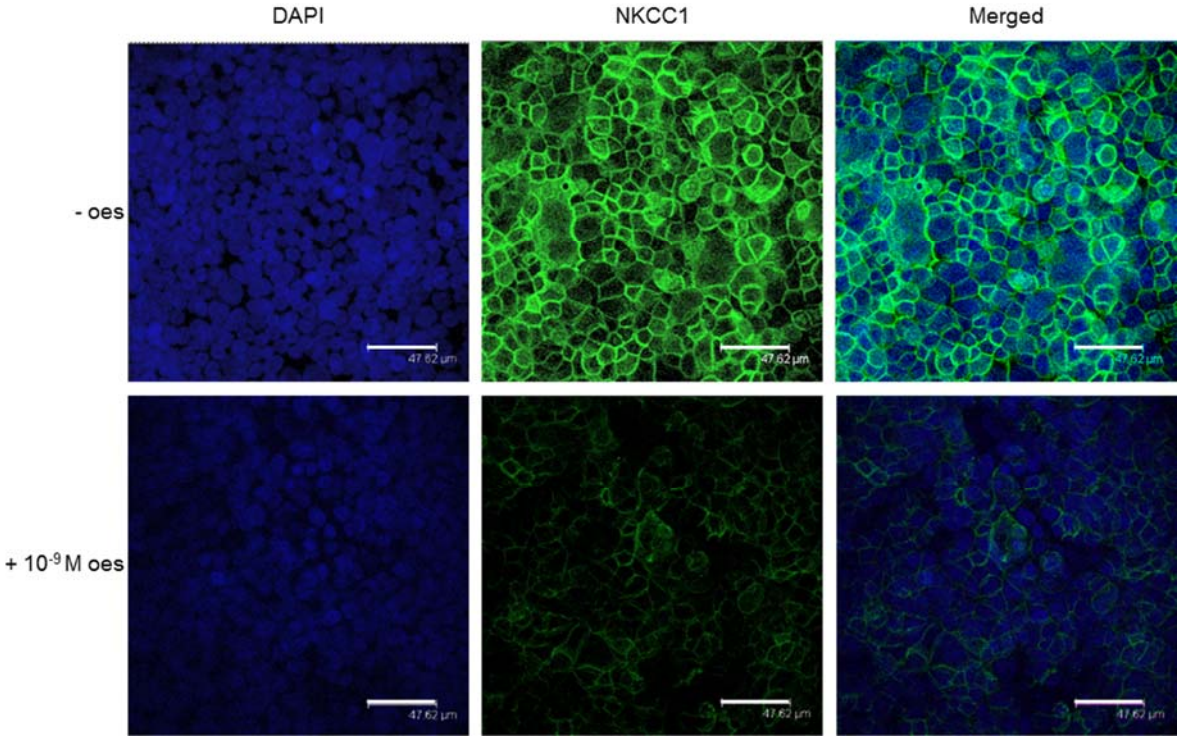

Figure 3.11 Effect of oestradiol on the expression and localisation of NKCC1 in EFM-19 cells. EFM-19 cells were seeded onto Transwell filter supports at a density of 1,000,000 cells per filter and cultured in routine culture medium for 24 hours. Cells were cultured in withdrawal media for 5 days and grown in the absence or presence of 10^{-9} M oestradiol for 8 days. Cells were washed with PBS and fixed in methanol at -20 ^{o}C. After fixation, cells were washed with PBS three times for 15 minutes each. Cells were then blocked in blocking buffer containing saponin for 1 hour at room temperature. The blocking medium was aspirated and the primary antibody NKCC1 was added at 1:100 dilution and incubated overnight at 4 ^{o}C. Cells were washed 3 times with PBS, 15 minutes each. The secondary antibody Alexa fluor 488 conjugated goat anti-rabbit were added at a dilution of 1:1000 and were covered in foil and the cells were incubated for 1 hour at room temperature. Cells were washed 3 times with PBS. DAPI mounting media was added to the glass slides prior to placing the coverslip on the slide and the cells were examined under the confocal microscope using a 63x objective (Oil, 1.63). X-Y images show DAPI (blue) and NKCC1 (green) staining at 8 days in the absence or presence of 10^{-9} M of 17β-oestradiol. The treatments conditions are indicated to the left of the diagram. Scale bars = 47 μm.

The X-Z sections shown in Figure 3.12, are indicative of basolateral staining of NKCC1. There is an increase in the number of cell layers in the presence of oestradiol, whereas in its absence, cells are in a monolayer. The reduction in the NKCC1 expression at the basolateral surface when treated with oestradiol is clearly evident.

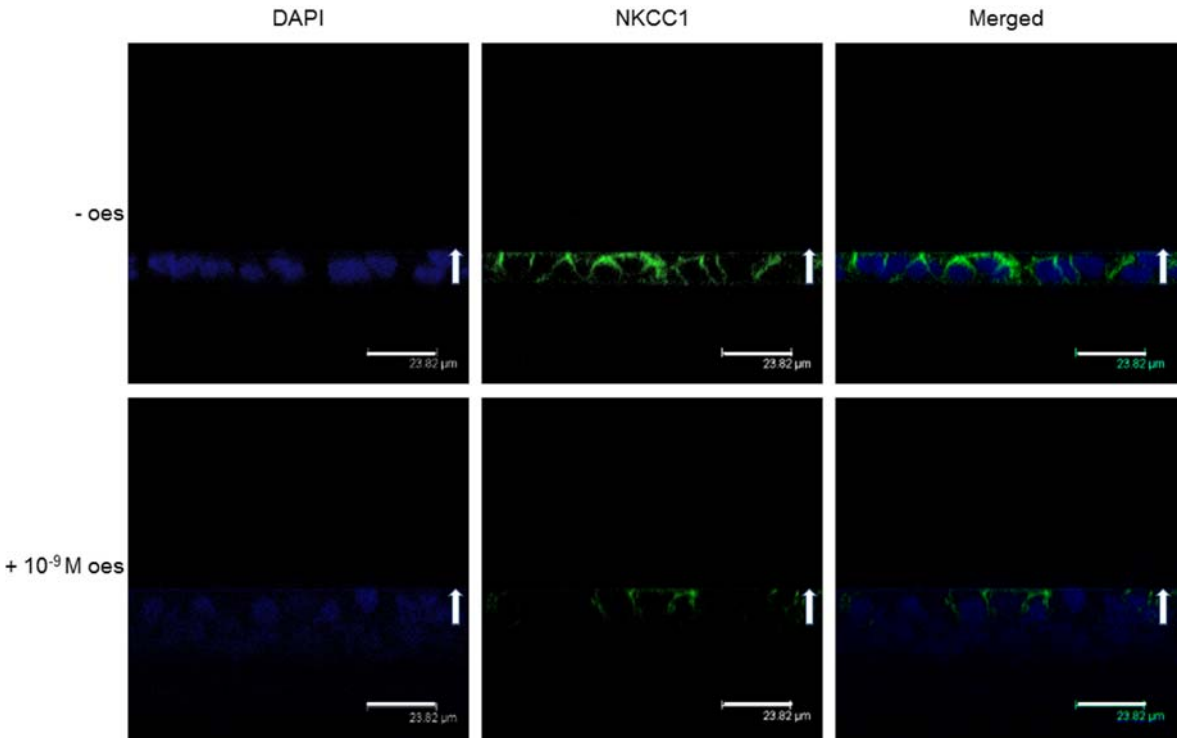

Figure 3.12 Effect of oestradiol on the expression and localisation of NKCC1 in EFM-19 cells. EFM-19 cells were seeded onto Transwell filter supports at a density of 1,000,000 cells per filter in routine culture medium for 24 hours. Cells were cultured in withdrawal media for 5 days and grown in the absence or presence of 10^{-9} M oestradiol for 8 days. Cells were washed with PBS and fixed in methanol at -20 ^{o}C. After fixation, cells were washed with PBS three times

for 15 minutes each. Cells were then blocked in blocking buffer containing saponin for 1 hour at room temperature. The blocking medium was aspirated and the primary antibody NKCC1 was added at 1:100 dilution and incubated overnight at 4 ^{o}C. Cells were washed 3 times with PBS, 15 minutes each. The secondary antibody Alexa fluor 488 conjugated goat anti-rabbit were added at a dilution of 1:1000 and were covered in foil and the cells were incubated for 1 hour at room temperature. Cells were washed 3 times with PBS. DAPI mounting media was added to the glass slides prior to placing the coverslip on the slide and the cells were examined under the confocal microscope using a 63x objective (Oil, 1.63). X-Z images show DAPI (blue) and NKCC1 (green) staining at 8 days in the absence or presence of 10^{-9} M of 17β-oestradiol. The treatments conditions are indicated to the left of the diagram. Scale bars = 23 μm. The white arrow head (⇧) point towards the top of cell.

3.5 The concentration dependence of the regulation of NKCC1 by oestrogen

3.5.1 Evaluation of concentration dependent effects of oestradiol on the regulation of NKCC1 protein expression in MCF-7, EFM-19 and EFF-3 cells

The aim of these experiments was to determine the effect of different concentrations of oestradiol ranging from 10^{-13} M to 10^{-7} M. A stock concentration of 10^{-4} M was prepared and serially diluted to obtain a range of concentrations 10^{-5} M, 10^{-6} M, 10^{-7} M, 10^{-8} M, 10^{-9} M and 10^{-10} M. Cells were withdrawn for 5 days, and then cultured in the presence of the different oestradiol concentrations given above. These stock concentrations were diluted 1:1000 times with withdrawal media to the required final concentrations.

Concentration dependent effect of oestradiol on the expression of NKCC1 in MCF-7 cells is shown in Figure 3.13. NKCC1 expression was maximal when cells were cultured in the absence of oestradiol. With increasing concentrations of oestradiol, the expression of NKCC1 decreases. The expression was minimal following the addition of 10^{-10} M oestradiol to the culture medium.

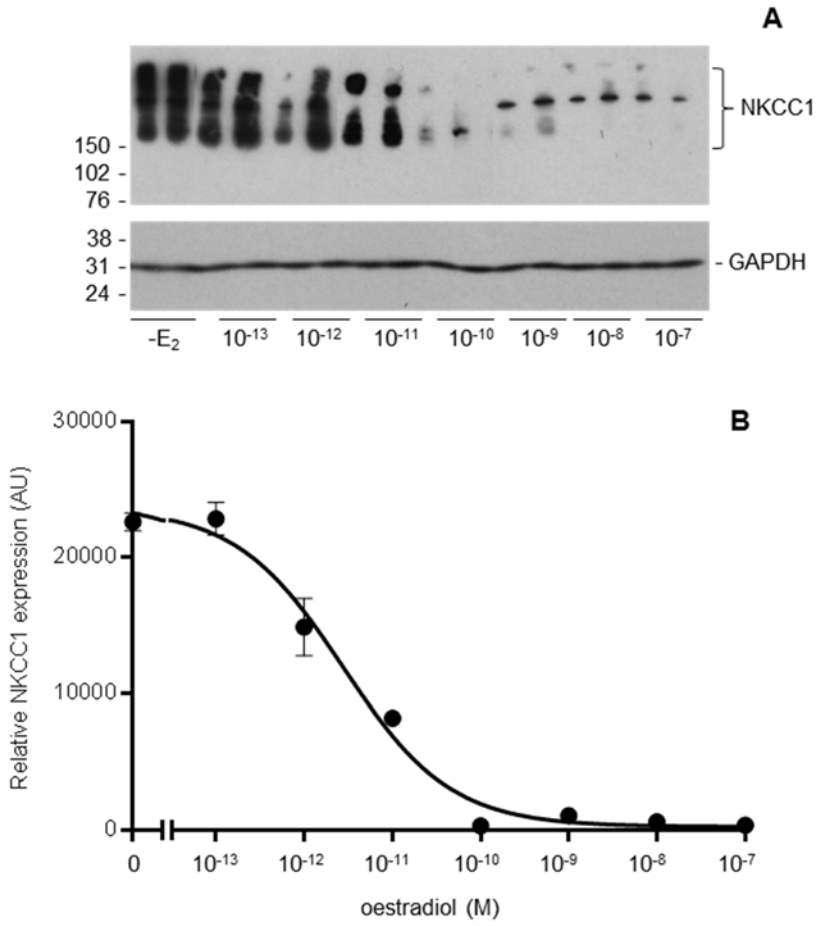

Figure 3.13 Effect of oestradiol on NKCC1 protein expression in MCF-7 cells. MCF-7 cells were seeded onto 24-well plates and withdrawn for 5 days and treated with different concentrations of oestradiol for a period of 8 days. Cells were lysed and protein extracts prepared. Protein aliquots of 10 µg were separated by 12% polyacrylamide gel electrophoresis and then transferred to nitrocellulose membranes. The membranes were incubated with anti-NKCC1 antibody (dilution 1:20000) overnight at 4 ^{o}C, followed by horseradish peroxidase conjugated goat-anti-rabbit secondary antibody for 1 hour at 37 ^{o}C. Proteins were visualised by enhanced chemiluminescence with SuperSignal West Dura Extended Duration Substrate. **A.** The protein expression of NKCC1 in MCF-7 cells treated with different concentrations of oestradiol for 8 days. Image shown are from a representative experiment which has been repeated three times. **B.** Densitometric quantification of NKCC1 with Labworks 4.0 software, normalised against the corresponding GAPDH signal. Error bars indicate SEM of duplicate measurements.

The concentration dependent effect of oestradiol on NKCC1 protein expression in EFM-19 cells is shown in Figure 3.14. Similar to the results for MCF-7 cells, the expression level decrease dramatically at 10^{-10} M oestradiol, and continues to stay low with further increasing concentrations of oestradiol.

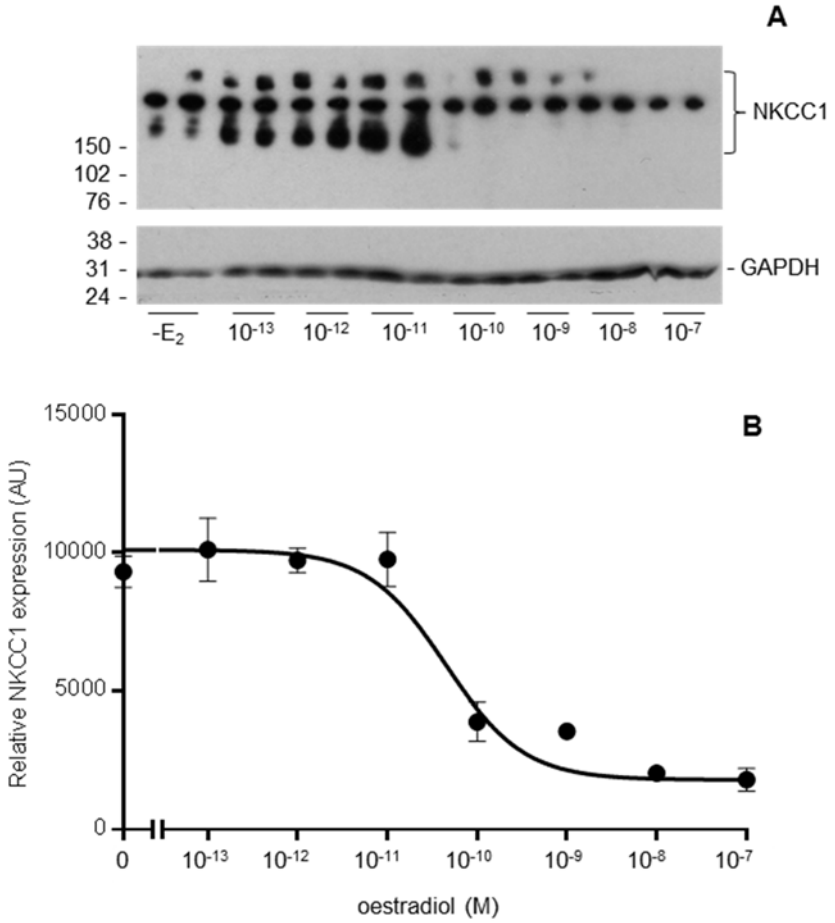

Figure 3.14 Effect of oestradiol on NKCC1 protein expression in EFM-19 cells. EFM-19 cells were seeded onto 24-well plates and withdrawn for 5 days and treated with different concentrations of oestradiol for a period of 8 days. Cells were lysed and protein extracts prepared. Protein aliquots of 10 µg were separated by 12% polyacrylamide gel electrophoresis and then transferred to nitrocellulose membranes. The membranes were incubated with anti-NKCC1 antibody (dilution 1:20000) overnight at 4 ^{o}C, followed by horseradish peroxidase conjugated goat-anti-rabbit secondary antibody for 1 hour at 37 ^{o}C. Proteins were visualised by enhanced chemiluminescence with SuperSignal West Dura Extended Duration Substrate. **A.** The protein expression of NKCC1 in EFM-19 cells treated with different concentrations of oestradiol for 8 days. Image shown are from a representative experiment which has been repeated three times. **B.** Densitometric quantification of NKCC1 with Labworks 4.0 software, normalised against the corresponding GAPDH signal. Error bars indicate SEM of duplicate measurements.

EFF-3 cells were plated onto 24-well tissue culture plates, and were withdrawn from steroids for 5 days followed by treatments with a range of oestradiol concentrations for a further 8 days. Untreated EFF-3 cells expressed higher amounts of NKCC1 protein, whereas cells treated with oestradiol showed a concentration dependent effect. A decline in protein content was observed with increasing concentrations of oestradiol from $2x10^{-10}$ M onwards. These results are indicated in Figure 3.15 given below.

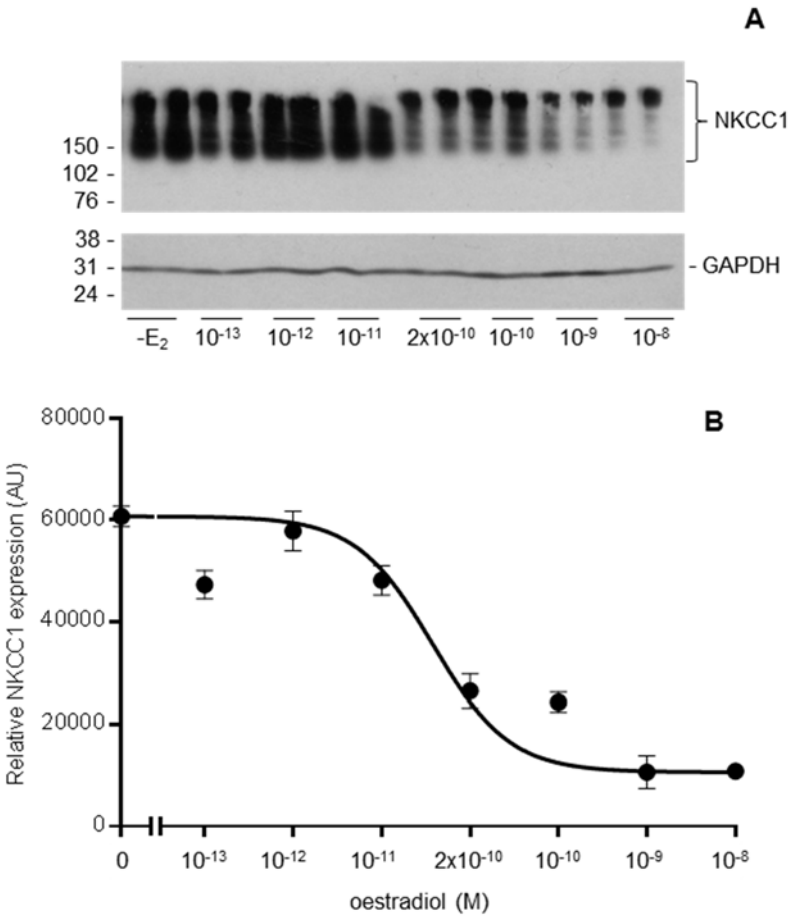

Figure 3.15 Effect of oestradiol on NKCC1 protein expression in EFF-3 cells. EFF-3 cells were seeded onto 24-well plates and withdrawn for 5 days and treated with different concentrations of oestradiol for a period of 8 days. Cells were lysed and protein extracts prepared. Protein aliquots of 10 µg were separated by 12% polyacrylamide gel electrophoresis and then transferred to nitrocellulose membranes. The membranes were incubated with anti-NKCC1 antibody (dilution 1:20000) overnight at 4 ^{o}C, followed by horseradish peroxidase conjugated goat-anti-rabbit secondary antibody for 1 hour at 37 ^{o}C. Proteins were visualised by enhanced chemiluminescence with SuperSignal West Dura Extended Duration Substrate. **A.** The protein expression of NKCC1 in EFF-3 cells treated with different concentrations of oestradiol for 8 days. Image shown are from a representative experiment which has been repeated three times. **B.** Densitometric quantification of NKCC1 with Labworks 4.0 software, normalised against the corresponding GAPDH signal. Error bars indicate SEM of duplicate measurements.

3.6 Functional activity of NKCC1 in breast cancer cells

This section investigates the activity of NKCC1 in oestrogen-responsive breast cancer cells MCF-7 and EFM-19. Radioactive Rubidium, $^{86}Rb^{+}$ provides an isotopic tracer for K^{+} ion movement. $^{86}Rb^{+}$ has a half-life of approximately 19 days.

3.6.1 $^{86}Rb^{+}$ (K^{+}) influx measurement and the effect of inhibitors furosemide and ouabain on MCF-7 and EFM-19 cells cultured in full medium

The initial experiment was designed to evaluate the time dependence of $^{86}Rb^{+}$ (K^{+}) influx in MCF-7 cells. Cells were incubated in the absence or presence of the inhibitors 10^{-4} M furosemide and 10^{-5} M ouabain. Furosemide is an NKCC1 inhibitor and ouabain is a $Na^{+}K^{+}$ATPase inhibitor. These inhibitor concentrations were well known to cause maximal inhibition of the transporters (Lamb *et al.*, 1981; Aiton and Simmons, 1984). The linearity of the uptake curve indicates that the optimal time is between 10-15 minutes as shown in Figure 3.16. During this period, the $^{86}Rb^{+}$ (K^{+}) influx into MCF-7 cells approximates 1st order kinetics. Hence, in subsequent experiments, cells were incubated for 15 minutes in Krebs's solutions containing $^{86}Rb^{+}$ (K^{+}) isotope along with the inhibitors.

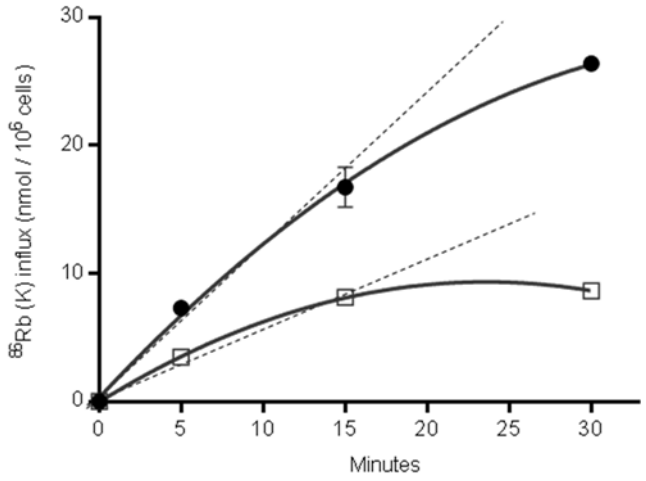

Figure 3.16 Time dependence of $^{86}Rb^{+}$ (K^{+}) uptake into MCF-7 cells. MCF-7 cells were cultured in routine culture medium in 6-well plates. Cells were washed with Krebs' solution and $^{86}Rb^{+}$ was added. Cells were washed 4 times and lysed in distilled water. Cell lysates were collected and $^{86}Rb^{+}$ activity was measured. The $^{86}Rb^{+}$ (K^{+}) influx of total MCF-7 cell samples in the absence of any inhibitors (total ●) and cell samples with furosemide at 10^{-4} M in the presence of ouabain at 10^{-5} M (F + O □). Data is normalised against the cell number. Error bars indicate standard error of the mean of three replicates per condition from one experiment.

The following experiment analysed $^{86}Rb^{+}$ (K^{+}) influx in MCF-7 cells grown in routine culture medium. MCF-7 cells were plated onto 6-well plates at a density of 50000 cells per well. They were cultured for 3 days in phenol-red DMEM, containing 10 % foetal calf serum and 1 µg/ml (0.17 µM) insulin. $^{86}Rb^{+}$ (K^{+}) influx in MCF-7 cells was measured.

The $^{86}Rb^{+}$ (K^{+}) influx measurements made in the absence and presence of furosemide and ouabain is shown in Figure 3.17A. “Total” indicates the complete $^{86}Rb^{+}$ (K^{+}) influx in MCF-7 cells in the absence of any inhibitors. The total influx comprises of three components. “Furosemide-sensitive” component is either, total minus furosemide or ouabain minus (furosemide + ouabain). “Ouabain-sensitive” component is either total minus ouabain or furosemide minus (furosemide + ouabain). The “residual” component is both furosemide-insensitive and ouabain-insensitive influx. The total influx was 13.28±0.71 nmol/10^{6} cells/15mins. In the presence of the NKCC1 inhibitor furosemide, there was no change in influx, which indicates that there is no significant furosemide-sensitive influx ($p = 0.9976$, ANOVA). However, in the presence of the $Na^{+}K^{+}$ATPase inhibitor ouabain, the influx decreased to 6.71±0.38 nmol/10^{6} cells/15mins which is about half the total value ($p = 0.0001$, ANOVA). In the presence of both NKCC1 and $Na^{+}K^{+}$ATPase inhibitors the influx was reduced further to 5.54±0.51 nmol/10^{6} cells/15mins ($p = 0.0001$, ANOVA) when comparing total influx with the influx in the presence of both inhibitors. This residual influx is due to the presence of other channels which may take up K^{+} ions in MCF-7 cells.

Figure 3.17B shows the calculated furosemide-sensitive influx and ouabain-sensitive influx in MCF-7 cells. The ouabain-sensitive influx of 7.93 nmol/10^{6} cells/15mins is considerably higher than the furosemide-sensitive influx of 1.17 nmol/10^{6} cells/15mins. Therefore, this suggests that K^{+} ion influx at the cell membrane occurs mostly through the $Na^{+}K^{+}$ATPase. The apparent lack of a significant furosemide-sensitive influx could be due to the activity of oestrogen present in foetal calf serum (FCS) in phenol-red DMEM (routine culture medium).

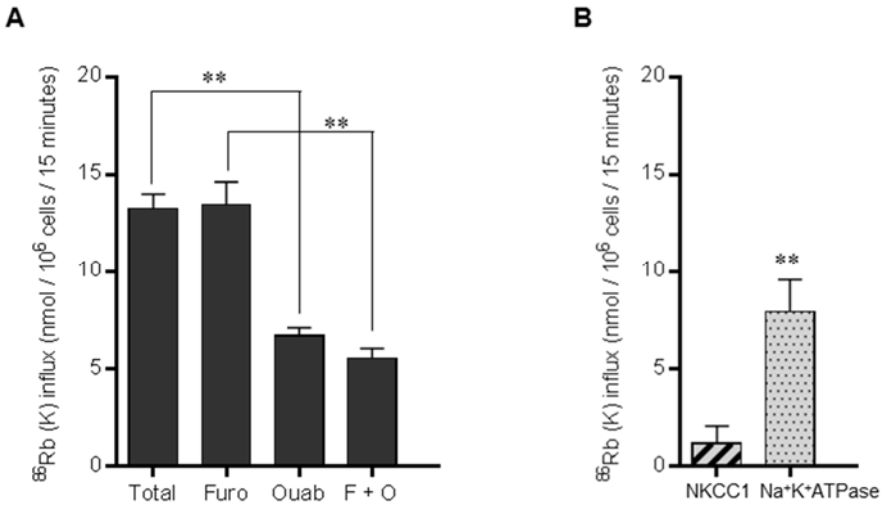

Figure 3.17 $^{86}Rb^{+}$ (K^{+}) influx in MCF-7 cells. MCF-7 cells were cultured in routine culture medium in 6-well plates for 3 days. Cells were washed with Krebs' solution and incubated in experimental solutions containing $^{86}Rb^{+}$ (K^{+}) isotope with the inhibitors alone and in combination for 15 minutes. Cells were washed 4 times with ice-cold Krebs' solution and lysed in distilled water. Cell extracts were collected and $^{86}Rb^{+}$ activity was measured. **A.** The $^{86}Rb^{+}$ (K^{+}) influx in the absence (Total) and presence of 10^{-4} M furosemide (Furo), 10^{-5} M ouabain (Ouab) and both furosemide and ouabain (F + O). Data is normalised against the cell number. **p < 0.0001 by ANOVA. Error bars indicate standard error of the mean of six replicates per condition from one experiment. **B.** An illustration of the furosemide-sensitive influx (NKCC1) and ouabain-sensitive influx ($Na^{+}K^{+}$ATPase) in MCF-7 cells. Furosemide-sensitive influx = (ouabain) - (furosemide + ouabain), Ouabain-sensitive influx = (furosemide) - (furosemide + ouabain).

The functional activity of NKCC1 was evaluated in EFM-19 cells (Figure 3.18A). The total $^{86}Rb^{+}$ (K^{+}) influx was 15.55±0.59 nmol/10^{6} cells/15mins and the influx decreased to 14.45±0.55 nmol/10^{6} cells/15mins in the presence of furosemide. This slight inhibition by furosemide was not significant (p = 0.3117, ANOVA). However in the presence of ouabain, the influx dropped even further to 3.80±0.26 nmol/10^{6} cells/15mins and was statistically significant (p = 0.0001 ANOVA).

Figure 3.18B shows a representative graph of the furosemide-sensitive influx and ouabain-sensitive influx from the same experiment. Similar to the MCF-7 cells there is a considerably higher ouabain-sensitive influx of 12.86 nmol/10^{6} cells/15mins and was significantly different (p = 0.0001 ANOVA). In contrast to MCF-7 cells, the lower furosemide-sensitive influx of 2.22 nmol/10^{6} cells/15mins was of statistical significance (p = 0.0091 ANOVA).

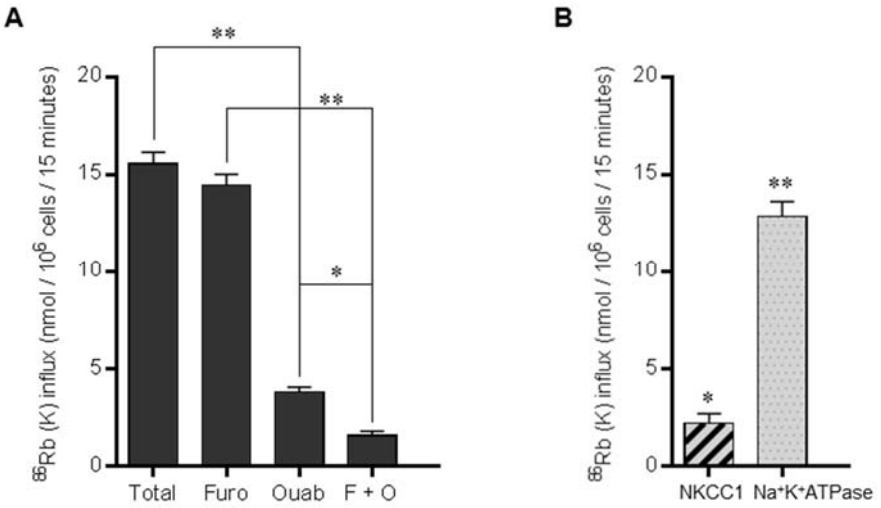

Figure 3.18 $^{86}Rb^+$ (K^+) influx in EFM-19 cells. EFM-19 cells were cultured in routine culture medium in 6-well plates for 3 days. Cells were washed with Krebs' solution and incubated in experimental solutions containing $^{86}Rb^+$ (K^+) isotope with the inhibitors alone and in combination for 15 minutes. Cells were washed 4 times with ice-cold Krebs' solution and lysed in distilled water. Cell lysates were collected and $^{86}Rb^+$ activity was measured. **A.** The $^{86}Rb^+$ (K^+) influx in the absence (Total) and presence of 10^{-4} M furosemide (Furo), 10^{-5} M ouabain (Ouab) and both furosemide and ouabain (F + O). Data is normalised against the cell number. *$p < 0.05$ and **$p < 0.0001$ by ANOVA. Error bars indicate standard error of the mean of six replicates per condition from one experiment. **B.** An illustration of the furosemide-sensitive influx (NKCC1) and ouabain-sensitive influx (Na^+K^+ATPase) in EFM-19 cells. Furosemide-sensitive influx = (ouabain) - (furosemide + ouabain), Ouabain-sensitive influx = (furosemide) - (furosemide + ouabain).

These data obtained from both cell lines MCF-7 and EFM-19 suggest that oestrogen present in foetal calf serum in the routine culture medium is responsible for mediating the lower furosemide-sensitive influx through the NKCC1 cotransporter at the cell membrane. The ouabain-sensitive Na^+K^+ATPase is shown to be the main driver facilitating K^+ ion influx in MCF-7 and EFM-19 cells.

3.6.2 $^{86}Rb^+$ (K^+) influx measurement under isosmotic and hypertonic conditions of MCF-7 cells grown in full media

The effect of hypertonicity on the $^{86}Rb^+$ (K^+) influx in MCF-7 cells cultured in full medium was evaluated. One of the main roles of NKCC1 is cell volume regulation. Cell shrinkage causes activation of NKCC1 (Russell, 2000). The intracellular accumulation of Cl^- ions leads to loss of water causing cells to shrink. The activation of NKCC1 is mediated through a cascade of protein

phosphorylation (Lytle and Forbush, 1992; Selvaraj *et al.*, 2000). Data presented previously showed that cells grown in full media had very low levels of furosemide-sensitive (NKCC1) influx. Therefore we postulated that NKCC1 present in the cell membrane or in recycling endosomes in close proximity to the plasma membrane, may be in a quiescent state. In order to reveal this inactive NKCC1, half the cells were treated with a hypertonic Krebs's solution containing 200 mM mannitol along with the inhibitors ouabain (10^{-5} M) and furosemide (10^{-4} M). In the presence of mannitol, cells are subject to hypertonic stress and the external osmolarity is raised. This increase in osmolarity causes cell shrinkage leading to the activation of NKCC1.

$^{86}Rb^{+}$ (K^{+}) influx measurements under isosmotic and hypertonic conditions are shown below in Figure 3.19A. Hypertonicity leads to an increase in the furosemide-sensitive influx as indicated in Figure 3.19B. Under isosmotic conditions the furosemide-sensitive influx was 32.49 nmol/10^6 cells/15mins, whereas in the presence of mannitol the furosemide-sensitive influx increased to 68.74 nmol/10^6 cells/15mins ($p = 0.9825$, ANOVA). The ouabain-sensitive influx remained approximately at 231.07 nmol/10^6 cells/15mins in both isosmotic and hypertonic conditions. However, in comparison with the axis in Figure 3.17B to that of Figure 3.19B, the effect of hypertonicity on the increased $^{86}Rb^{+}$ (K^{+}) influx is evident. These results suggests that hypertonic stimulation reveals the previously inactive NKCC1 present in the cell membrane.

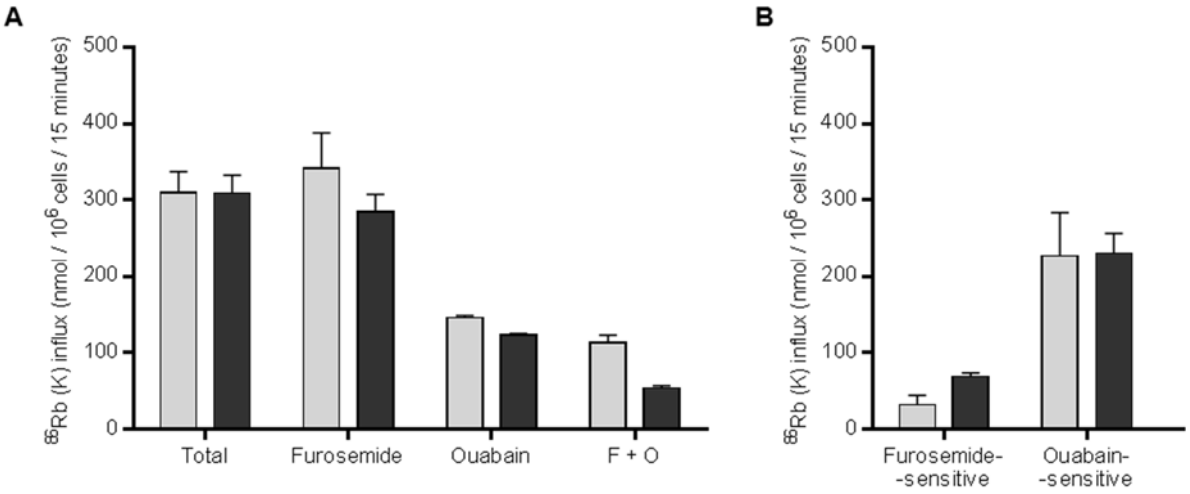

Figure 3.19 $^{86}Rb^{+}$ (K^{+}) influx in MCF-7 cells under isosmotic and hypertonic conditions. MCF-7 cells were cultured in routine culture medium in 6-well plates for 3 days. Cells were washed with Krebs' solution and incubated in experimental solutions containing $^{86}Rb^{+}$ (K^{+})

isotope with the inhibitors alone and in combination for 15 minutes. Cells were washed 4 times with ice-cold Krebs' solution and lysed in distilled water. Cell extracts were collected and $^{86}Rb^{+}$ activity was measured. **A.** The $^{86}Rb^{+}$ influx data of MCF-7 cells, comparing isosmotic (□) to hypertonic (■) conditions in the absence (Total) and presence of 10^{-4} M furosemide, 10^{-5} M ouabain and both furosemide and ouabain (F + O). Data is normalised against the cell number. *p < 0.05 and **p < 0.0001 by ANOVA. Error bars indicate standard error of the mean of four replicates per condition from one experiment. **B.** An illustration of the furosemide-sensitive (NKCC1) influx samples and ouabain-sensitive ($Na^{+}K^{+}$ATPase) influx in MCF-7 cells. Furosemide-sensitive influx = (ouabain) - (furosemide + ouabain), Ouabain-sensitive influx = (furosemide) - (furosemide + ouabain).

3.6.3 $^{86}Rb^{+}$ (K^{+}) influx measurement under isosmotic and hypertonic conditions of EFM-19 cells grown in full media

The results of assessing the effect of hypertonicity in EFM-19 cells is shown in Figure 3.20A. In the presence of furosemide under hypertonic conditions, the total $^{86}Rb^{+}$ (K^{+}) influx decreased significantly from 101.40±11.73 nmol/10^{6} cells/15mins to 70.47±3.52 nmol/10^{6} cells/15mins (p = 0.0233, ANOVA). Similarly when furosemide was added in the presence and absence of ouabain in hypertonic conditions, the $^{86}Rb^{+}$ (K^{+}) influx decreased further from 54.23±4.39 nmol/10^{6} cells/15mins to 5.89±0.31 nmol/10^{6} cells/15mins (p = 0.0001, ANOVA) and was statistically significant. The calculated furosemide-sensitive and ouabain-sensitive influx is shown in Figure 3.20B. When comparing the furosemide-sensitive influx between isosmotic and hypertonic conditions, the furosemide-sensitive influx increased from 10.44 nmol/10^{6} cells/15mins to 51.68 nmol/10^{6} cells/15mins and was statistically different (p = 0.0108, ANOVA). This activation of NKCC1 in response to decreased cell volume under hypertonic conditions further supports the well-known role of NKCC1 in the regulation of cell volume. There was no change in the ouabain-sensitive influx under both isosmotic and hypertonic conditions.

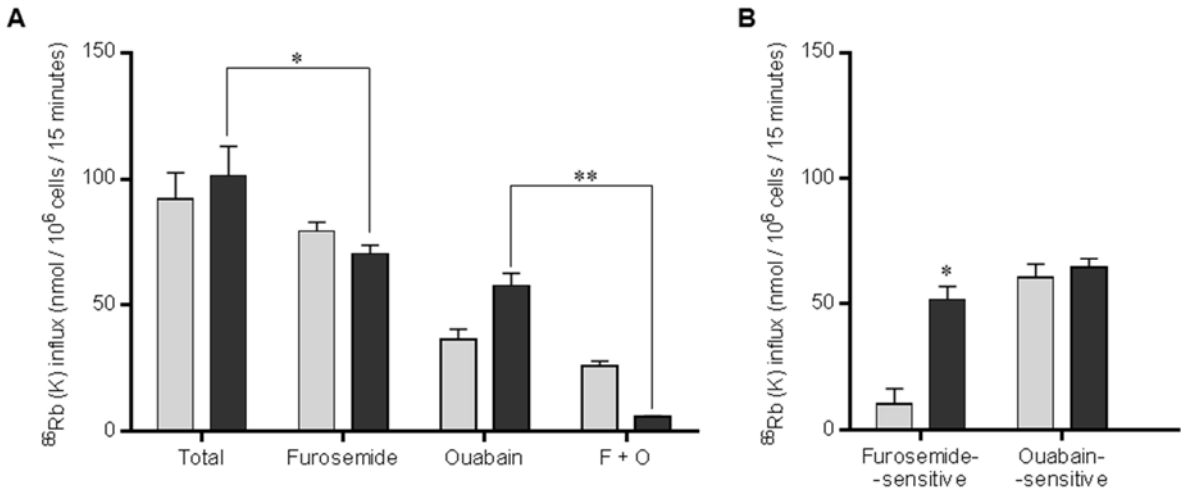

Figure 3.20 $^{86}Rb^{+}$ (K^{+}) influx in EFM-19 cells under isosmotic and hypertonic conditions. EFM-19 cells were cultured in routine culture medium in 6-well plates for 3 days. Cells were washed with Krebs' solution and incubated in experimental solutions containing $^{86}Rb^{+}$ (K^{+}) isotope with the inhibitors alone and in combination for 15 minutes. Cells were washed 4 times with ice-cold Krebs' solution and lysed in distilled water. Cell lysates were collected and $^{86}Rb^{+}$ activity was measured. **A.** The $^{86}Rb^{+}$ influx data of EFM-19 cells, comparing isosmotic (□) to hypertonic (■) conditions in the absence (Total) and presence of 10^{-4} M furosemide, 10^{-5} M ouabain and both furosemide and ouabain (F + O). Data is normalised against the cell number. *$p < 0.05$ and **$p < 0.0001$ by ANOVA. Error bars indicate standard error of the mean of four replicates per condition from one experiment. **B.** An illustration of the furosemide-sensitive (NKCC1) influx samples and ouabain-sensitive ($Na^{+}K^{+}$ATPase) influx in EFM-19 cells. Furosemide-sensitive influx = (ouabain) - (furosemide + ouabain), Ouabain-sensitive influx = (furosemide) - (furosemide + ouabain).

3.6.4 Action of oestradiol on $^{86}Rb^{+}$ (K^{+}) influx in MCF-7 cells

The effect of oestrogen on 86Rb+ (K+) influx in MCF-7 cells was assessed. It was noted that in the presence of oestrogen, MCF-7 cells were prone to detachment during the washes required to perform the 86Rb+ (K+) influx measurements. As a result of this cell detachment the results obtained were not consistent. Therefore to overcome this problem of detachment and to increase adherence, MCF-7 cells were seeded onto collagen-coated plates. The cells grown on collagen-coated plates were able to withstand the rapid washes with Krebs' solution subsequent to incubation.

The $^{86}Rb^{+}$ (K^{+}) influx of MCF-7 cells grown on collagen-coated plates is shown in Figure 3.21A. The influx of cells cultured in the absence of oestrogen were always higher than the influx of oestrogen-treated cells. In the presence of furosemide, there was a decrease in total influx from 59.04±8.27 nmol/10^{6}

cells/15mins to 51.54±2.25 nmol/10^6 cells/15mins in the absence of oestrogen (p = 0.9926, ANOVA), and from 50.96±2.36 nmol/10^6 cells/15mins to 38.66±4.87 nmol/10^6 cells/15mins in the presence of oestrogen (p = 0.5228, ANOVA). However, this comparison between the total influx in the absence and presence of oestrogen was not statistically significant (p = 0.9811, ANOVA).

As shown in Figure 3.21B the furosemide-sensitive influx reduced from 6.97 nmol/10^6 cells/15mins in the oestrogen withdrawn cells to 2.46 nmol/10^6 cells/15mins, in the oestrogen treated cells and this difference was not statistically significant (p = 0.9593, ANOVA). Similarly the ouabain-sensitive influx was 36.37 nmol/10^6 cells/15mins in oestrogen withdrawn cells and decreased to 26.93 nmol/10^6 cells/15mins in oestrogen treated cells. However this decrease was not statistically significant (p = 0.4743, ANOVA).

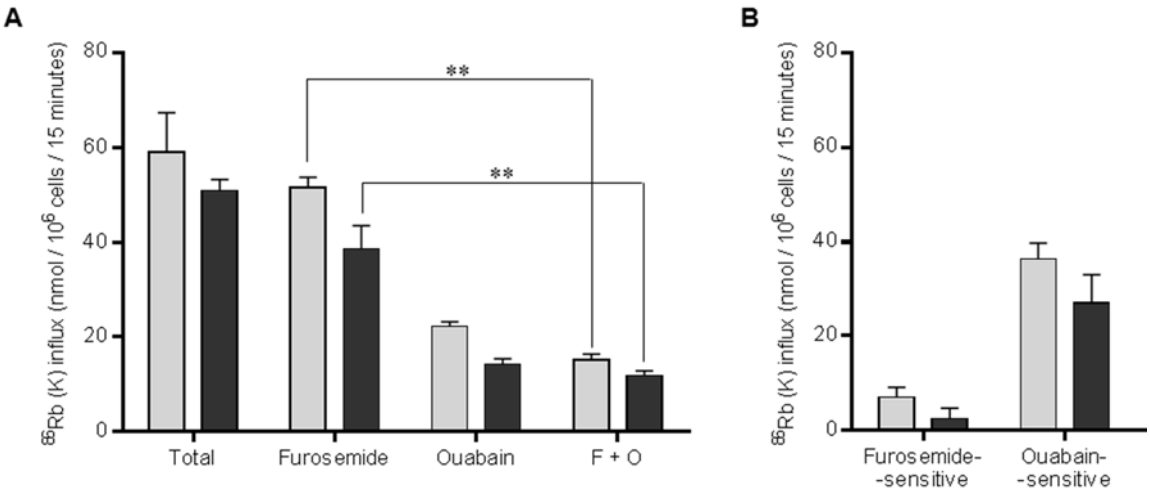

Figure 3.21 $^{86}Rb^+$ (K^+) influx in MCF-7 cells grown on collagen-coated plates in the absence and presence of oestrogen. MCF-7 cells were seeded at a density of 10,000 cells per well in a 6-well plate and cultured in phenol-red-free media alone or in the presence of 10^{-9} M of 17β-oestradiol for 8 days. The cells were cultured in steroid depleted media for 2 days prior to oestradiol treatment. Cells were washed with Krebs' solution and incubated in experimental solutions containing $^{86}Rb^+$ (K^+) isotope with the inhibitors alone and in combination for 15 minutes. Cells were washed 4 times with ice-cold Krebs' solution and lysed in distilled water. Cell lysates were collected and $^{86}Rb^+$ activity was measured. **A.** The $^{86}Rb^+$ influx data of MCF-7 cells after oestrogen stimulation for 8 days, comparing untreated (-E_2 □) cells to oestrogen stimulated (+E_2 ■) cells in the absence (Total) and presence of 10^{-4} M furosemide, 10^{-5} M ouabain and both furosemide and ouabain (F + O). Data is normalised against the cell number. **p < 0.0001 by ANOVA. Error bars indicate standard error of the mean of four replicates per condition from one experiment. **B.** An illustration of the furosemide-sensitive (NKCC1) influx samples and ouabain-sensitive (Na^+K^+ATPase) influx in MCF-7 cells. Furosemide-sensitive influx = (ouabain) - (furosemide + ouabain), Ouabain-sensitive influx = (furosemide) - (furosemide + ouabain).

3.6.5 Action of oestradiol on $^{86}Rb^{+}$ (K^{+}) influx in EFM-19 cells

Figure 3.22A displays the results from a similar experiment in EFM-19 cells. With the addition of furosemide, the influx in serum depleted cells dropped from 57.54±6.96 nmol/10^6 cells/15mins to 39.66±4.18 nmol/10^6 cells/15mins. This decrease was not statistically significant (p = 0.1067, ANOVA). But in response to the addition of furosemide in the oestrogen treated cells the total influx decreased significantly from 54.14±2.54 nmol/10^6 cells/15mins to 29.56±6.22 nmol/10^6 cells/15mins (p = 0.0056, ANOVA).

However as shown in Figure 3.22B, the furosemide-sensitive influx was not significant (p = 0.8884, ANOVA) when comparing the oestrogen withdrawn and oestrogen treated EFM-19 cells. Also a comparison between the ouabain-sensitive influx between oestrogen withdrawn and oestrogen treated cells was not statistically significant (p = 0.6783, ANOVA).

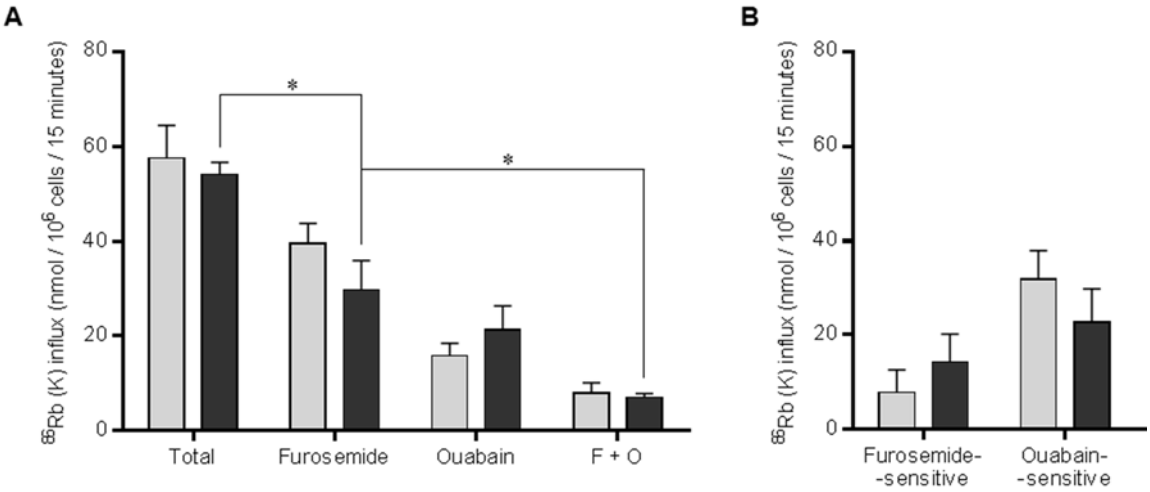

Figure 3.22 $^{86}Rb^{+}$ (K^{+}) influx in EFM-19 cells in the absence and presence of oestrogen. EFM-19 cells were cultured in phenol-red-free media alone or in the presence of 10^{-9} M of 17β-oestradiol for 8 days. The cells were cultured in steroid depleted media for 2 days prior to oestradiol treatment. Cells were washed with Krebs' solution and incubated in experimental solutions containing $^{86}Rb^{+}$ (K^{+}) isotope with the inhibitors alone and in combination for 15 minutes. Cells were washed 4 times with ice-cold Krebs' solution and lysed in distilled water. Cell extracts were collected and $^{86}Rb^{+}$ activity was measured. **A.** The $^{86}Rb^{+}$ influx data of EFM-19 cells after oestrogen stimulation for 6 days, comparing untreated (-E_2 □) cells to oestrogen stimulated (+E_2 ■) cells in the absence (Total) and presence of 10^{-4} M furosemide, 10^{-5} M ouabain and both furosemide and ouabain (F + O). Data is normalised against the cell number. *p < 0.05 and **p < 0.0001 by ANOVA. Error bars indicate standard error of the mean of four replicates per condition from one experiment. **B.** An illustration of the furosemide-sensitive (NKCC1) influx samples and ouabain-sensitive ($Na^{+}K^{+}$ATPase) influx in EFM-19 cells. Furosemide-sensitive influx = (ouabain) - (furosemide + ouabain), Ouabain-sensitive influx = (furosemide) - (furosemide + ouabain).

3.6.6 Effect of hypertonicity on $^{86}Rb^{+}$ (K^{+}) influx measurement of MCF-7 cells in the absence and presence of oestrogen

In section 3.6.2, it was shown that hypertonic stimulation by 200 mM mannitol activated the previously quiescent NKCC1 in cells grown in full media. Therefore it is now possible to investigate whether there is an alteration in the activity of NKCC1 between untreated and oestrogen-treated cells.

MCF-7 cells cultured on collagen-coated plates were withdrawn for 5 days and half the cells were treated with 10^{-9} M oestrogen for a period of 10 days before the $^{86}Rb^{+}$ (K^{+}) influx was measured.

Figure 3.23A shows the variation of $^{86}Rb^{+}$ (K^{+}) influx in the absence and presence of oestrogen when subject to hypertonic stress. In the presence of the $Na^{+}K^{+}$ATPase inhibitor ouabain there was a significant difference in influx between the serum withdrawn and oestrogen-treated cells ($p = 0.0001$, ANOVA). Similarly, under hypertonic conditions the influx in the presence of ouabain decreased from 102.13±8.74 nmol/10^6 cells/15mins to 59.39±6.72 nmol/10^6 cells/15mins which was of statistical significance ($p = 0.0360$, ANOVA). Nevertheless, there was almost no change in the bumetanide-sensitive influx between serum withdrawn and oestrogen treated cells and was not statistically significant under both isosmotic and hypertonic conditions ($p = 0.9999$, ANOVA) as shown in Figure 3.23B.

The effect of hypertonicity on NKCC1 sensitive influx is also shown in Figure 3.23B. NKCC1 is seen to be activated by the increase in the bumetanide-sensitive influx from 7.46 nmol/10^6 cells/15mins to 45.17 nmol/10^6 cells/15mins in the absence of oestrogen and from 9.50 nmol/10^6 cells/15mins to 37.54 nmol/10^6 cells/15mins in the presence of oestrogen. However both these increases did not reach statistical significance ($p = 0.2740$, ANOVA).

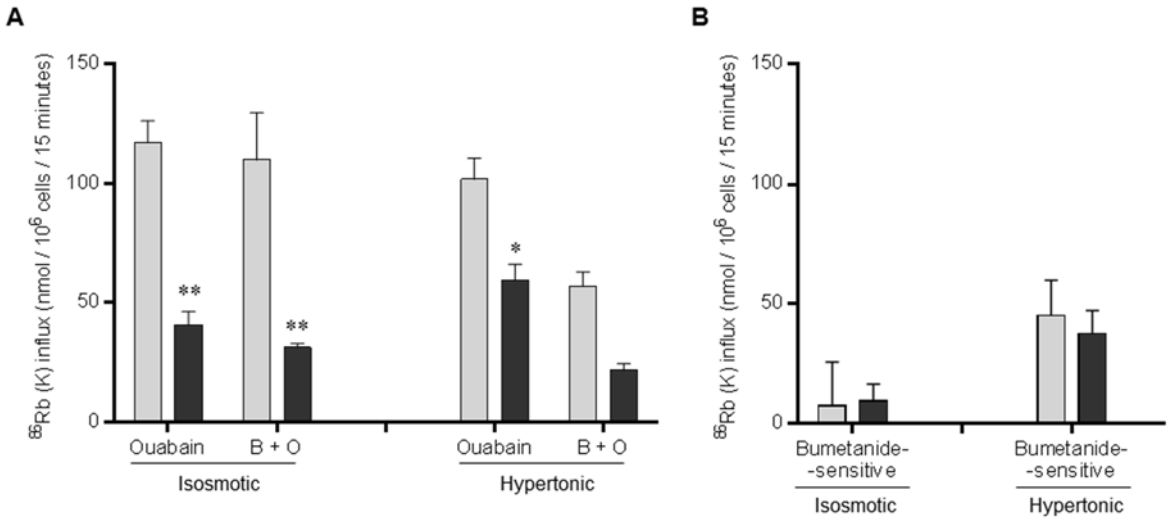

Figure 3.23 $^{86}Rb^+$ (K^+) influx in MCF-7 cells grown on collagen-coated plates in the absence and presence of oestrogen under isosmotic and hypertonic conditions. MCF-7 cells were cultured in phenol-red-free media alone or in the presence of 10^{-9} M of 17β-oestradiol for 10 days. The cells were cultured in steroid depleted media for 5 days prior to oestradiol treatment. Cells were washed with Krebs' solution and incubated in experimental solutions containing $^{86}Rb^+$ (K^+) isotope with the inhibitors alone and in combination for 15 minutes. Cells were washed 4 times with ice-cold Krebs' solution and lysed in distilled water. Cell extracts were collected and $^{86}Rb^+$ activity was measured. **A.** The $^{86}Rb^+$ influx data of MCF-7 cells after oestrogen stimulation for 10 days, comparing untreated (-E_2 □) cells to oestrogen stimulated (+E_2 ■) cells in the presence of 10^{-5} M ouabain alone and both 10^{-4} M bumetanide and ouabain (B + O) under isosmotic and hypertonic conditions. Data is normalised against the cell number. *p < 0.05 and **p < 0.0001 by ANOVA. Error bars indicate standard error of the mean of four replicates per condition from one experiment. **B.** An illustration of the bumetanide-sensitive (NKCC1) influx samples and ouabain-sensitive (Na^+K^+ATPase) influx in MCF-7 cells. Bumetanide-sensitive influx = (ouabain) - (bumetanide + ouabain).

3.6.7 Effect of hypertonicity on $^{86}Rb^+$ (K^+) influx measurement of EFM-19 cells in the absence and presence of oestrogen

Similarly the effect of hypertonicity on the activation of NKCC1 in oestrogen withdrawn and oestrogen stimulated EFM-19 cells was evaluated. The $^{86}Rb^+$ (K^+) influx data from this experiment is shown below.

From Figure 3.24A it is evident that the addition of ouabain under both isosmotic and hypertonic conditions caused a significant decrease (p = 0.0001, ANOVA) in influx when comparing between oestrogen withdrawn and oestrogen treated cells.

As indicated in Figure 3.24B, hypertonicity causes a dramatic increase in the bumetanide-sensitive influx in both serum withdrawn and oestrogen treated

cells. In cells grown in the absence of oestrogen, the bumetanide-sensitive influx increased significantly from 15.57 nmol/10^6 cells/15mins to 119.32 nmol/10^6 cells/15mins (p = 0.0001, ANOVA). Likewise, the bumetanide-sensitive influx in cells in the presence of oestrogen increased significantly from 4.37 nmol/10^6 cells/15mins to 52.02 nmol/10^6 cells/15mins (p = 0.0001, ANOVA). When comparing the bumetanide-sensitive influx between cells in the absence and presence of oestrogen, a slight non-significant decrease (p = 0.5559, ANOVA) was observed in isosmotic conditions. But under hypertonic conditions the bumetanide-sensitive influx decreased from 119.32 nmol/10^6 cells/15mins to 52.02 nmol/10^6 cells/15mins in the presence of oestrogen. This difference was of statistical significance (p = 0.0001, ANOVA).

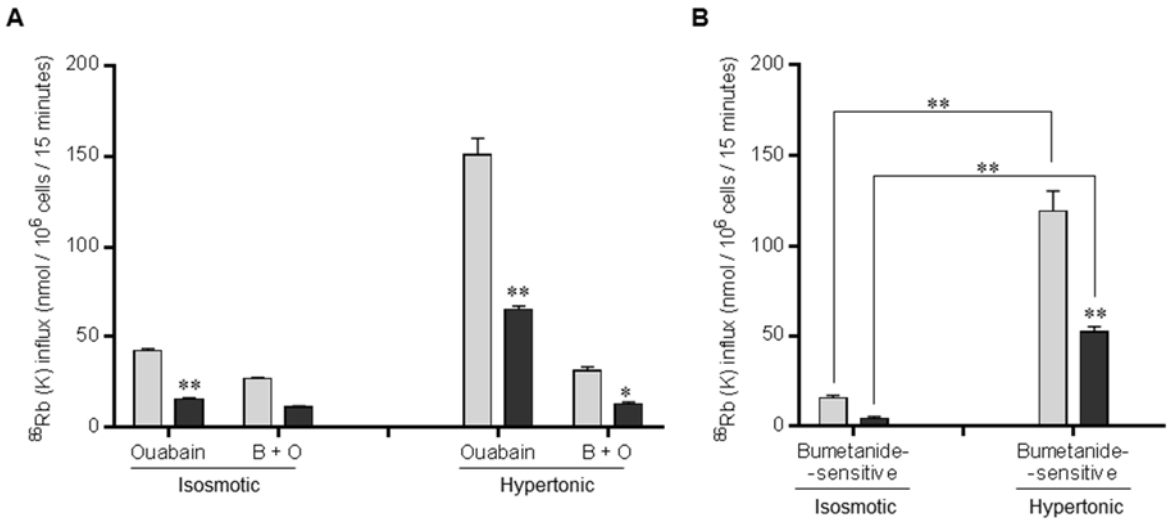

Figure 3.24 $^{86}Rb^+$ (K^+) influx in EFM-19 cells in the absence and presence of oestrogen under isosmotic and hypertonic conditions. EFM-19 cells were cultured in phenol-red-free media alone or in the presence of 10^{-9} M of 17β-oestradiol for 10 days. The cells were cultured in steroid depleted media for 5 days prior to oestradiol treatment. Cells were washed with Krebs' solution and incubated in experimental solutions containing $^{86}Rb^+$ (K^+) isotope with the inhibitors alone and in combination for 15 minutes. Cells were washed 4 times with ice-cold Krebs' solution and lysed in distilled water. Cell lysates were collected and $^{86}Rb^+$ activity was measured. **A.** The $^{86}Rb^+$ influx data of EFM-19 cells after oestrogen stimulation for 10 days, comparing untreated (-E_2 □) cells to oestrogen stimulated (+E_2 ■) cells in the presence of 10^{-5} M ouabain alone and both 10^{-4} M bumetanide and ouabain (B + O) under isosmotic and hypertonic conditions. Data is normalised against the cell number. *p < 0.05 and **p < 0.0001 by ANOVA. Error bars indicate standard error of the mean of four replicates per condition from one experiment. **B.** An illustration of the bumetanide-sensitive (NKCC1) influx samples and ouabain-sensitive (Na^+K^+ATPase) influx in EFM-19 cells. Bumetanide-sensitive influx = (ouabain) - (bumetanide + ouabain).

Collectively these results suggest that there is a possibility of inducing a loop-diuretic-sensitive influx by activating the previously quiescent NKCC1 under hypertonic conditions. The effect of oestrogen on hypertonically activated NKCC1 in EFM-19 cells seems promising as it significantly reduced the bumetanide-sensitive influx. In MCF-7 cells, there was almost no difference in the bumetanide-sensitive influx between oestrogen withdrawn and oestrogen treated cells under hypertonic conditions. However this requires further evaluation due to discrepancy in the data obtained.

3.7 Discussion

3.7.1 Expression and localization

Ion transporters have been implicated in many aspects of cancer pathogenesis and their stimulation may promote tumour cell migration and invasion. Microarrays using Affymetrix GeneChips identified a novel oestrogen-regulated gene *SLC12A2* which was downregulated in response to oestrogen in three oestrogen receptor α-positive cell lines: MCF-7, EFM-19 and EFF-3 (Wright *et al.*, 2009). The data presented in this chapter evaluated the expression and function of the NKCC1 protein which is encoded by the *SLC12A2* gene.

This is the first study that investigated the protein expression of NKCC1 in breast cancer cells. Western transfer analysis revealed the variability of glycosylated NKCC1 protein expression between different oestrogen-responsive and oestrogen-unresponsive cell lines. The highest level of expression was observed in the ZR-75 and Hs578T cells, whereas the lowest levels were in the cell lines SKBR3 and BT-20. BT-474, EFF-3 and EFM-19 cells had a higher NKCC1 expression in comparison to the cell lines MCF-7, MDA-MB-231 and HBL-100. Also there was no detectable NKCC1 expression in T47-D cells.

Experiments using immunofluorescence discovered the cellular localisation of NKCC1 in the three oestrogen-responsive breast cancer cell lines MCF-7, EFM-19 and EFF-3. Results showed that NKCC1 is localised to the plasma

membrane in all three cells lines. In EFF-3 cells, vesicle-like immunoreactions were observed in addition to the stronger immunoreaction at the plasma membrane. In virgin mouse mammary ductal epithelial cells, NKCC1 was localised to the basolateral membrane (Shillingford *et al.*, 2002).

3.7.2 Oestrogen regulation

The previously unrecognised regulation of *SLC12A2* gene and its protein NKCC1 by oestrogen was confirmed. In this study, the NKCC1 protein expression was clearly decreased in response to oestrogen treatment. After eight days of oestrogen treatment there was almost complete reduction of NKCC1 expression in all three cell lines. This result was consistent with the previous findings demonstrating the downregulation of the gene *SLC12A2* and the reduction in mRNA expression of NKCC1 by oestrogen (Wright *et al.*, 2009). In the current study, immunofluorescence images of MCF-7 and EFM-19 cells showed a honeycomb appearance, suggesting that NKCC1 is localised to the lateral aspects of the cell. The x-z images revealed that the oestrogen-stimulated cells do not show marked lateralisation of NKCC1 at the membrane, in comparison to the unstimulated cells. Also the oestrogen-treated cells form a multilayer, suggesting that oestrogen promotes cell proliferation. The reduction in NKCC1 protein expression was oestrogen concentration dependent. Together, these data support that NKCC1 is under direct regulation of oestrogen.

3.7.3 Functional activity

Radioactive Rubidium $^{86}Rb^{+}$ is an isotopic tracer that allows measurement of the movement of K^{+} ions. This $^{86}Rb^{+}$ (K^{+}) influx assay provides a measure of the activity of NKCC1 in breast cancer cells. Influx measurements were made in the presence of two types of inhibitors: a $Na^{+}K^{+}$ATPase inhibitor, ouabain, and the NKCC1 inhibitors, furosemide and bumetanide. The loop diuretic bumetanide is a more potent inhibitor of NKCC1 than furosemide.

Results indicated that MCF-7 and EFM-19 cells cultured in routine medium had higher ouabain-sensitive influx and a lower furosemide-sensitive influx,

suggesting that the functional activity of NKCC1 is low in these cells. The reason for this low activity of NKCC1 could perhaps be due to oestrogens in the foetal calf serum which suppresses the expression of *SLC12A2*. Any residual NKCC1 at the cell membrane exists presumably in a quiescent state under such conditions, giving rise to very low $^{86}Rb^{+}$ (K^{+}) influx measurements. Therefore the main mode of K^{+} ion influx is through $Na^{+}K^{+}$ATPase in MCF-7 and EFM-19 cells. Although these results formed a positive basis for determining the effects of oestrogen in the regulation of functional NKCC1, further experimentation was required to come to a firm conclusion.

The addition of 200 mM osmolyte mannitol to the experimental solutions introduced hypertonicity leading to a significant increase in the furosemide-sensitive influx which is representative of the activation of NKCC1. Similar hypertonicity-induced NKCC1 activation have been demonstrated in other studies (Glanville *et al.*, 2001; Delpire and Gagnon, 2011). The addition of mannitol increases the osmolarity, leading to loss of water from the cells, which in turn cause cell shrinkage. Data from the present study supports the known ability of NKCC1 to regulate cell volume and the activation of NKCC1 in response to cell shrinkage (Russell, 2000; Hebert *et al.*, 2004). These data demonstrated also that NKCC1 present at the cell membrane was previously inactive under isosmotic conditions. The activation of NKCC1 in response to hypertonic stress is mediated via phosphorylation and activation of the WNK signalling pathway. The phosphorylation of WNK leads to the phosphorylation of SPAK/OSR1, which then phosphorylates and activates NKCC1 (Smith *et al.*, 2008; Thastrup *et al.*, 2012). A decrease in intracellular concentration of Cl^{-} ions plays a major role in the regulatory volume increase by allowing the transport of Na^{+}, K^{+} and Cl^{-} ions through activation of NKCC1 (Lytle and McManus, 2002; Monette and Forbush, 2012).

There was a possibility that the high-confluency of cells cultured in 6-well plates limited the access of $^{86}Rb^{+}$ to the basal surface of cells, on which NKCC1 is located, therefore lower seeding densities were tested. This too proved impossible as cells especially MCF-7 cells detached from the plate during the

rapid washes. Therefore alternate methods of strengthening cell attachment to the 6-well plates, such as the use of collagen-coated plates were considered.

The effect of oestrogen on the functional regulation of NKCC1 was evaluated. The influx data indicated that there is a slight but statistically insignificant decrease in the loop-diuretic-sensitive influx in both MCF-7 and EFM-19 cells cultured in the presence of oestrogen, despite a significant decrease in NKCC1 protein expression in response to oestrogen. Further investigation of untreated and oestrogen treated EFM-19 cells showed a statistically significant decrease in the bumetanide-sensitive influx under hypertonic conditions in the presence of mannitol. However, this notable decrease in bumetanide-sensitive influx is not observed under isosmotic conditions. It is observed only under hypertonic conditions.

3.8 Conclusion

In summary, it was shown that NKCC1 is expressed in a variety of breast cancer cell lines, both ER-positive and ER-negative. Also data from western transfer and immunofluorescence showed positive results, as NKCC1 protein expression was decreased in oestrogen-stimulated cells in comparison to the unstimulated cells. These results confirmed the previously obtained microarray data in MCF-7, EFM-19 and EFF-3 cells. The functional studies showed that the NKCC1 present at the cell membrane is inactive under isotonic conditions. NKCC1 could be activated via induction of hypertonic stress. Results from this functional assay demonstrate the role of NKCC1 in the regulation of cell volume in oestrogen-responsive breast cancer cell lines MCF-7 and EFM-19. Although it is difficult to conclude firmly that oestrogen reduces the bumetanide-sensitive influx in MCF-7 and EFM-19 cells, there is a hint of such a reduction. Collectively, these results demonstrate that the total NKCC1 protein expression in these cells might have decreased in response to oestrogen, but the functional NKCC1 present in the cell membrane has not. Further investigation is required to elucidate the possible revelation of functional activity of NKCC1 at the cell membrane.

Chapter 4. *PDZK1* (NHERF3)

4.1 Introduction

The oestrogen-responsive gene *PDZK1*, located in chromosome 1, encodes the NHERF3 protein. The 519 amino acid protein NHERF3 is a Na^+ H^+ exchange regulatory co-factor. NHERF3 is a member of the NHERF family that has four members, NHERF1, NHERF2, NHERF3 and NHERF4. These proteins contain PDZ domains that have roles in many cellular functions such as cell proliferation, differentiation and ion transport. The expression of NHERF3 is limited to epithelial cells of breast, pancreas, gastrointestinal tract and proximal tubule of the kidney (Kocher *et al.*, 1998). NHERF1 and NHERF2 have two PDZ domains, while NHERF3 and NHERF4 have four PDZ domains. These PDZ family proteins are also known as adapter proteins, because they facilitate the organisation of proteins at the cell membrane. The PDZ domains can interact simultaneously with several membrane-associated proteins at the cell membrane.

NHERF3 has been reported to be overexpressed in cancers originating from epithelial cells (Kocher *et al.*, 1999). NHERF3 overexpression is more common in oestrogen receptor-positive breast cancers, than in oestrogen receptor-negative breast cancers. Several gene expression studies have identified *PDZK1* as an oestrogen-regulated gene that is increased in response to oestrogen (Ghosh *et al.*, 2000; Wright *et al.*, 2009).

4.1.1 Aim

The experiments described in this chapter, firstly aim to evaluate the expression and localisation of NHERF3 protein in MCF-7, EFM-19 and EFF-3 cells. Secondly, the effects of oestrogen and anti-oestrogens on the expression of NHERF3 were studied. The final section measures the internal pH of these oestrogen-responsive breast cancer cells, as a model designed to assess the functional role of NHERF3.

4.2 Expression of NHERF3 in breast cancer cells

4.2.1 Expression of NHERF3 in breast cancer cell lines

The expression of NHERF3 protein in several oestrogen-responsive and oestrogen-unresponsive cell lines was evaluated by western transfer analysis. Protein lysates were extracted from T75 flasks of breast cancer cells and equal amounts of 20 µg of protein were separated by gel electrophoresis. The results are shown below in Figure 4.1.

Strong immunoreactive protein bands were detected at 66 kDa, corresponding to the theoretical mass of the NHERF3 protein. The oestrogen responsive cell line ZR-75 had the highest level of protein expression, followed by MCF-7, T47-D and EFM-19. The high molecular mass band present in ZR-75 cells was a strong diffuse protein band. The rabbit polyclonal antibody detected also an additional protein band at around 46 kDa. This 46 kDa band was slightly more abundant than the 66 kDa band in MCF-7 and EFM-19 cells, whereas it was less abundant in T47-D and ZR-75 cell lines. However, EFF-3 and BT-474 cells had no detectable expression of the NHERF3 protein. None of the oestrogen unresponsive cell lines MDA-MB-231, SKBR3, BT-20, Hs578T and HBL-100 had detectable expression of the NHERF3 protein.

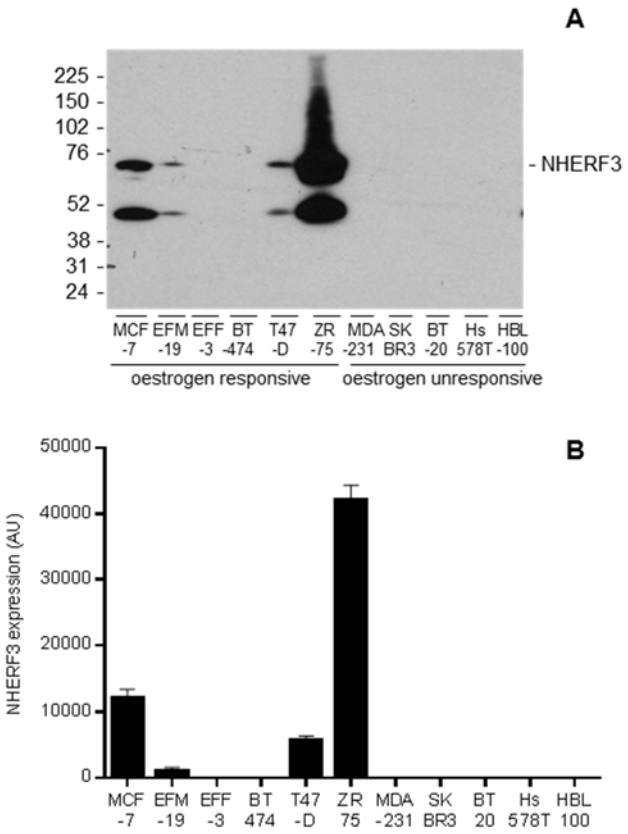

Figure 4.1 Expression of NHERF3 in breast cancer cells. Different breast cancer cell lines were cultured in routine culture medium in T75 flasks. Cells were lysed and protein extracts were prepared. Equal amounts of 20 µg of protein were separated by 12% polyacrylamide gel electrophoresis and then transferred to nitrocellulose membranes. The membranes were incubated with anti-NHERF3 antibody (1:10000 dilution) overnight at 4 ºC, followed by horseradish peroxidase conjugated goat-anti-rabbit secondary antibody for 1 hour at 37 ºC. Proteins were visualised by enhanced chemiluminescence with SuperSignal West Dura Extended Duration Substrate. **A.** The protein expression of NHERF3 was determined by Western transfer analysis in MCF-7, EFM-19, EFF-3, BT-474, T47-D, ZR-75, MDA-MB-231 (MDA-231), SKBR3, BT-20, Hs578T and HBL-100 cells. **B.** Densitometric quantification of the 66 kDa band for NHERF3. The black bars (■) represent oestrogen-responsive cell lines, whereas the grey bars (□) indicate the oestrogen-unresponsive cell lines. Error bars indicate standard errors of the mean of triplicate measurements.

4.3 Cellular localisation of NHERF3 in breast cancer cells

This section aims to identify the cellular localisation of NHERF3 in three oestrogen responsive breast cancer cells MCF-7, EFM-19 and EFF-3 by immunofluorescence.

4.3.1 Optimisation of conditions

One of the most important steps in immunofluorescence is the fixation and permeabilisation treatment. Typically several different combinations of

treatments have to be tested. The cell fixation and permeabilisation conditions were optimised to determine the best conditions for the NHERF3 antibody.

Cells were fixed in either methanol or 4% paraformaldehyde and permeabilised in either 0.3% triton X-100 or 0.2% saponin. Immunofluorescence procedure is as described in Materials and Methods.

The evaluation of the effects of different fixation and permeabilisation conditions are shown in Figure 4.2. When cells were fixed in methanol and permeabilised with blocking buffer containing triton, and then incubated with no primary NHERF3 antibody or only with the AF488 anti-rabbit (1:1000 dilution) secondary antibody, there was no signal. These results indicate that under these conditions there was no non-specific immunofluorescence. The results indicated that the optimum condition for detection of NHERF3 by immunofluorescence are cell fixation with 4% paraformaldehyde and permeabilisation with saponin.

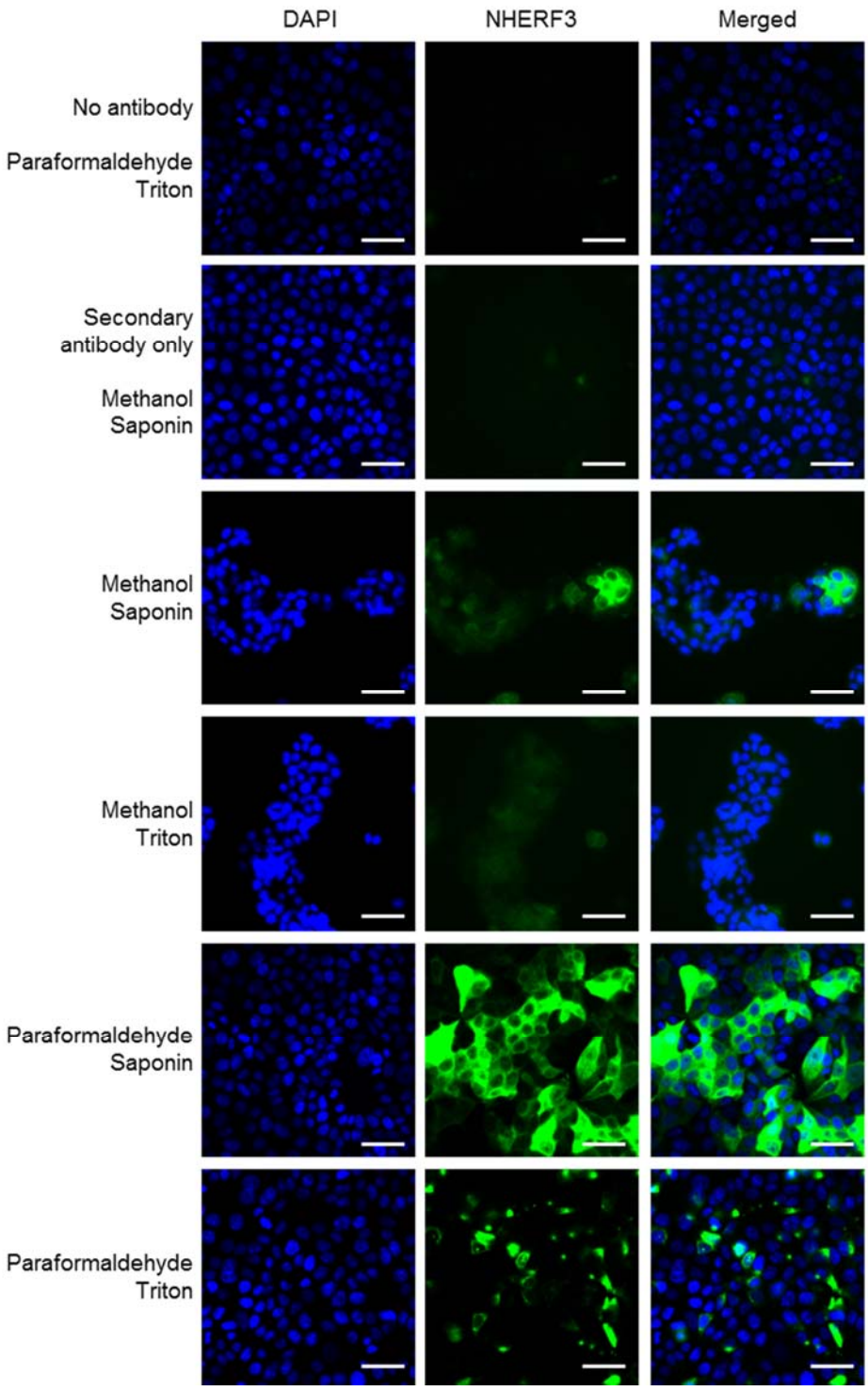

Figure 4.2 Optimisation of fixation and permeabilisation conditions for detection of NHERF3. MCF-7 cells were seeded at a density of $1x10^5$ cells onto 6-well plates and cultured in routine culture medium for 24 hours. The next day, cells were washed with PBS and fixed in either methanol at -20 ^oC or in 4 % paraformaldehyde at room temperature. After fixation, the cells were washed with PBS thrice with each wash lasting 20 minutes. Cells were then blocked in blocking buffer containing either triton or saponin for 1 hour at room temperature. The blocking buffer was aspirated and the primary antibody NHERF3 was added at 1:100 dilution and incubated overnight at 4 ^oC. The following day the primary antibody was aspirated and the cells were washed 3 times with PBS, 15 minutes each. The secondary antibody Alexa fluor 488 conjugated goat anti-rabbit were added at a dilution of 1:1000 and the coverslips were covered

in foil and the cells were incubated for 1 - 2 hours at room temperature. Cells were washed 3 times with PBS. DAPI mounting media was added to the glass slides prior to placing the coverslip on the slide and the cells were examined under the fluorescent microscope (Leica DMR) using a 40x objective. Results are shown for different treatment conditions of fixation and permeabilisation. Images on the column indicated with “DAPI” show nuclear staining, whereas the images indicated with “NHERF3” show the immunoreaction for NHERF3. The “Merged” images show both nuclear (blue) and NHERF3 (green) staining together. Scale bar = 45 µm.

4.3.2 Localisation of NHERF3 in oestrogen-responsive cell lines

After the fixation and permeabilisation conditions had been optimised, the next step was to analyse the cellular localisation of NHERF3 protein in the MCF-7, EFM-19 and EFF-3 cells.

The images A3, B3 and C3 of Figure 4.3 illustrate the localisation of NHERF3 in MCF-7, EFM-19 and EFF-3 cells, respectively. NHERF3 protein is observed to be localised to the cytoplasm. There is a variation in the expression between cells within each image. As observed in images A2 (MCF-7) and B2 (EFM-19) cells show a degree of heterogeneous immunoreaction between cells. In some cells, clear vesicular expression is noticeable as indicated by the white arrows. This vesicular nature is more frequently observed in EFF-3 cells.

Images presented in Figure 4.4 were collected with a 63x oil immersion objective of a confocal microscope and then the cross-sectional view was computed. Figure 4.4B clearly represents the vesicular expression of NHERF3 in MCF-7 cells. The red fluorescence is the AF555 conjugated phalloidin, which binds to the actin filaments of the cell and identifies the cytoskeleton. The white arrow in Figure 4.4C indicates phalloidin immunoreaction on the perijunctional ring. Also notice the stronger expression of actin at the surface where the cells attach to the coverslip. Pointed out by the yellow arrows in Figure 4.4D, are sites where NHERF3 is co-localised with actin.

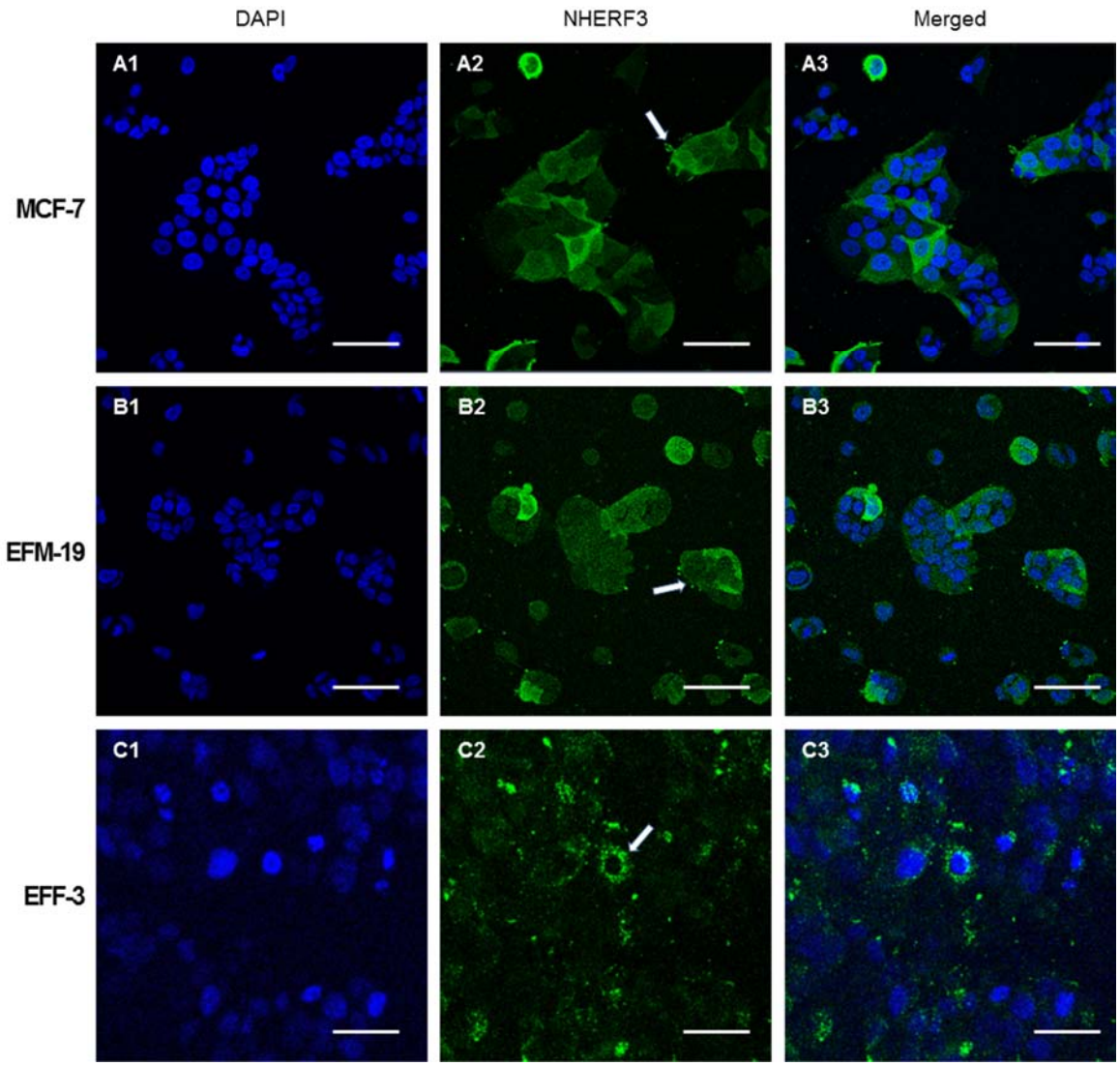

Figure 4.3 Localisation of NHERF3 in cell lines. MCF-7, EFM19 and EFF-3 cells were seeded onto coverslips in 6-well plates and cultured in routine culture medium for 24 hours. Cells were washed with PBS and fixed in 4% paraformaldehyde at room temperature. After fixation, cells were washed with PBS three times for 15 minutes each. Cells were then blocked in blocking buffer containing saponin for 1 hour at room temperature. The blocking medium was aspirated and the primary antibody NHERF3 was added at 1:100 dilution and incubated overnight at 4 ^{o}C. Cells were washed 3 times with PBS, 15 minutes each. The secondary antibody Alexa fluor 488 conjugated goat anti-rabbit were added at a dilution of 1:1000 and were covered in foil and the cells were incubated for 1 hour at room temperature. Cells were washed 3 times with PBS. DAPI mounting media was added to the glass slides prior to placing the coverslip on the slide and the cells were examined under the fluorescent microscope (Leica DMR) using a 40x objective. Images A1, B1 and C1 show the nuclear staining, whereas the images A2, B2 and C2 show the immunoreaction for NHERF3 in MCF-7, EFM-19 and EFF-3 cells, respectively. The merged images A3, B3 and C3 show both nuclear (blue) and NHERF3 (green) staining combined together. Scale bar = 45 µm. The white arrow (⇨) indicate examples of clear vesicular expression.

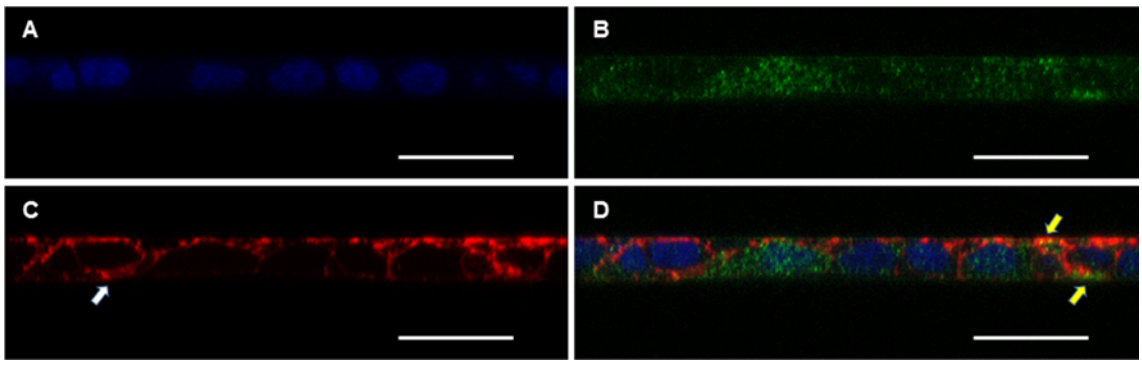

Figure 4.4 Cross-sectional images of the localisation of NHERF3 in MCF-7 cells. MCF-7 cells were seeded onto coverslips in 6-well plates and cultured in routine culture medium for 24 hours. Cells were washed with PBS and fixed in 4% paraformaldehyde at room temperature. After fixation, cells were washed with PBS three times for 15 minutes each. Cells were then blocked in blocking buffer containing saponin for 1 hour at room temperature. The blocking medium was aspirated and the primary antibody NHERF3 was added at 1:100 dilution and incubated overnight at 4 ºC. Cells were washed 3 times with PBS, 15 minutes each. The secondary antibody Alexa fluor 488 conjugated goat anti-rabbit were added at a dilution of 1:1000 and were covered in foil and the cells were incubated for 1 hour at room temperature. Cells were washed 3 times with PBS. Alexa fluor 555 conjugated phalloidin was added at a dilution of 1:100 and incubated for 15 minutes at room temperature. DAPI mounting media was added to the glass slides prior to placing the coverslip on the slide and the cells were examined under the confocal microscope using a 63x objective (Oil, 1.63). X-Z images A, B and C show nuclear (blue), NHERF3 (green) and phalloidin (red) staining, respectively. X-Z image D is an overlay of A, B and C. Scale bars = 25 µm. The white arrow (⇨) indicate a perijunctional ring and the yellow arrow (⇨) indicate examples of co-localisation of NHERF3 with actin.

4.4 Evaluation of the regulation of NHERF3 by oestrogen

4.4.1 Effect of oestradiol on NHERF3 protein expression in MCF-7 cells

The regulation of protein expression of NHERF3 by oestrogen was tested. The temporal response to oestrogen stimulation was studied by culturing MCF-7 cells in steroid depleted media for 5 days followed by addition of 10^{-9} M oestradiol for different lengths of time from 0 hours upto 10 days. A similar set of untreated cells for each timepoint were used for comparison. Cells were lysed and protein extracts were separated by gel electrophoresis. The results are shown in Figure 4.5.

In comparison to the expression measured in cells grown in routine culture medium (Figure 4.1A), after the cells have been withdrawn from growth factors for 5 days, the NHERF3 expression diminishes completely as observed at the 0 hours timepoint. This observation suggests that oestrogen present in the FCS of full DMEM medium is responsible for the induction of NHERF3 expression.

When MCF-7 cells are cultured in the presence of oestrogen, there is a significant stimulation of NHERF3 protein expression starting from 2 days onwards. This stimulation is maximal at 6 days and persists with time.

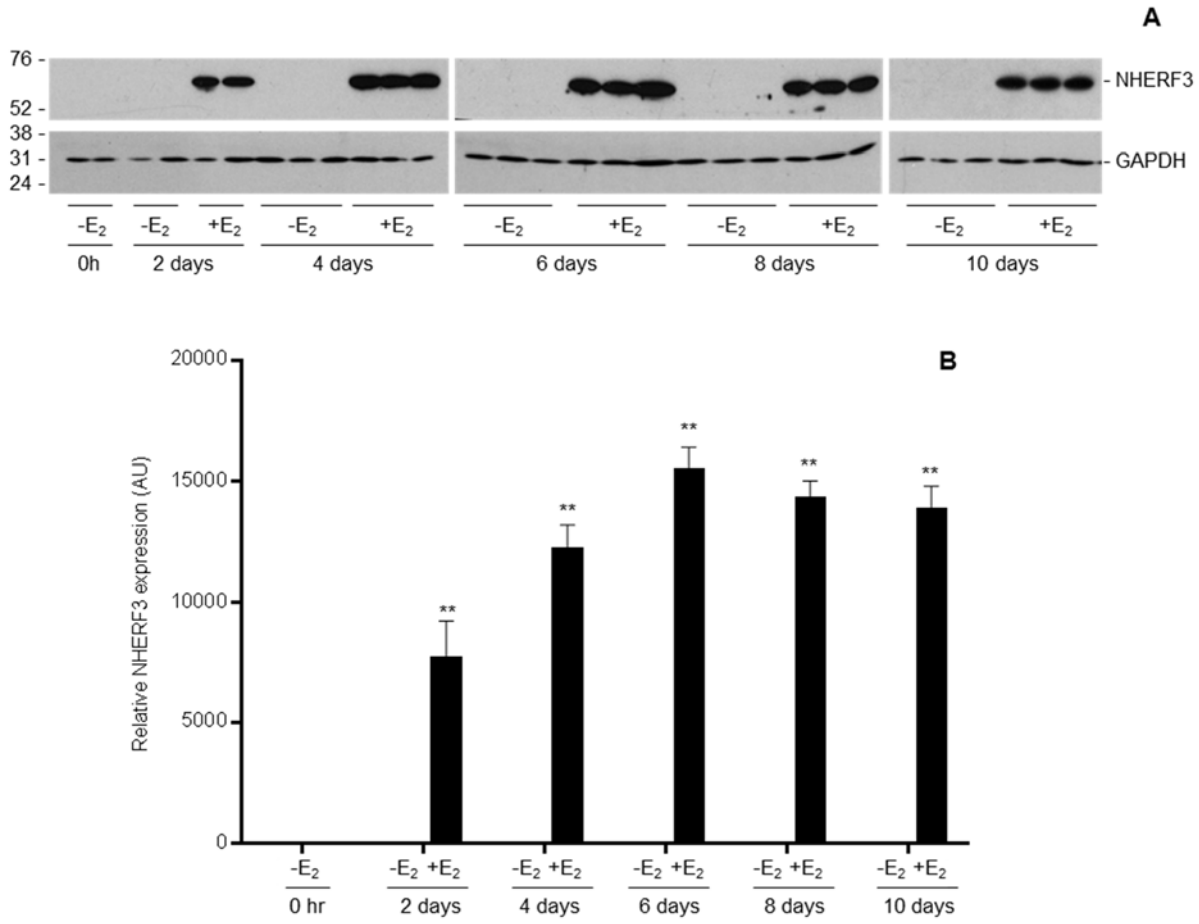

Figure 4.5 Effect of oestrogen on expression of NHERF3 in MCF-7 cells. Cells were steroid deprived by growing in phenol-red-free media containing 10% dextran-coated charcoal treated serum and 1 µg/ml insulin, for 5 days and then treated with 10^{-9} M of 17β-oestradiol for different lengths of time upto 10 days. Both the oestradiol-treated and untreated cells were lysed and protein extracts prepared. Protein aliquots of 20 µg were separated by 12% polyacrylamide gel electrophoresis and then transferred to nitrocellulose membranes. The membranes were incubated with anti-NHERF3 antibody (dilution 1:5000) overnight at 4 °C, followed by horseradish peroxidase conjugated goat-anti-rabbit secondary antibody for 1 hour at 37 °C. Proteins were visualised by enhanced chemiluminescence with SuperSignal West Dura Extended Duration Substrate. **A.** The protein expression of NHERF3 in MCF-7 cells after oestrogen stimulation for a timecourse of 0 hours to 10 days, comparing serum withdrawn ($-E_2$ □) samples with oestrogen-stimulated ($+E_2$ ■) samples. Images shown are representative of results from experiments which have been replicated thrice. **B.** Quantification of NHERF3 normalised against the corresponding GAPDH signal, **p < 0.001 by ANOVA. Error bars indicate SEM of triplicate measurements.

4.4.2 Effect of oestradiol on NHERF3 protein expression in EFM-19 cells

The regulation of expression of NHERF3 protein by oestrogen in EFM-19 cells was investigated. The addition of oestrogen to cells resulted in an increase in NHERF3 protein expression. After 2 days of treatment, there was a slight induction, which increased gradually with longer incubation times. The stimulation of NHERF3 expression was highest at day 8, but detected a lower level of induction at 10 days. (Figure 4.6)

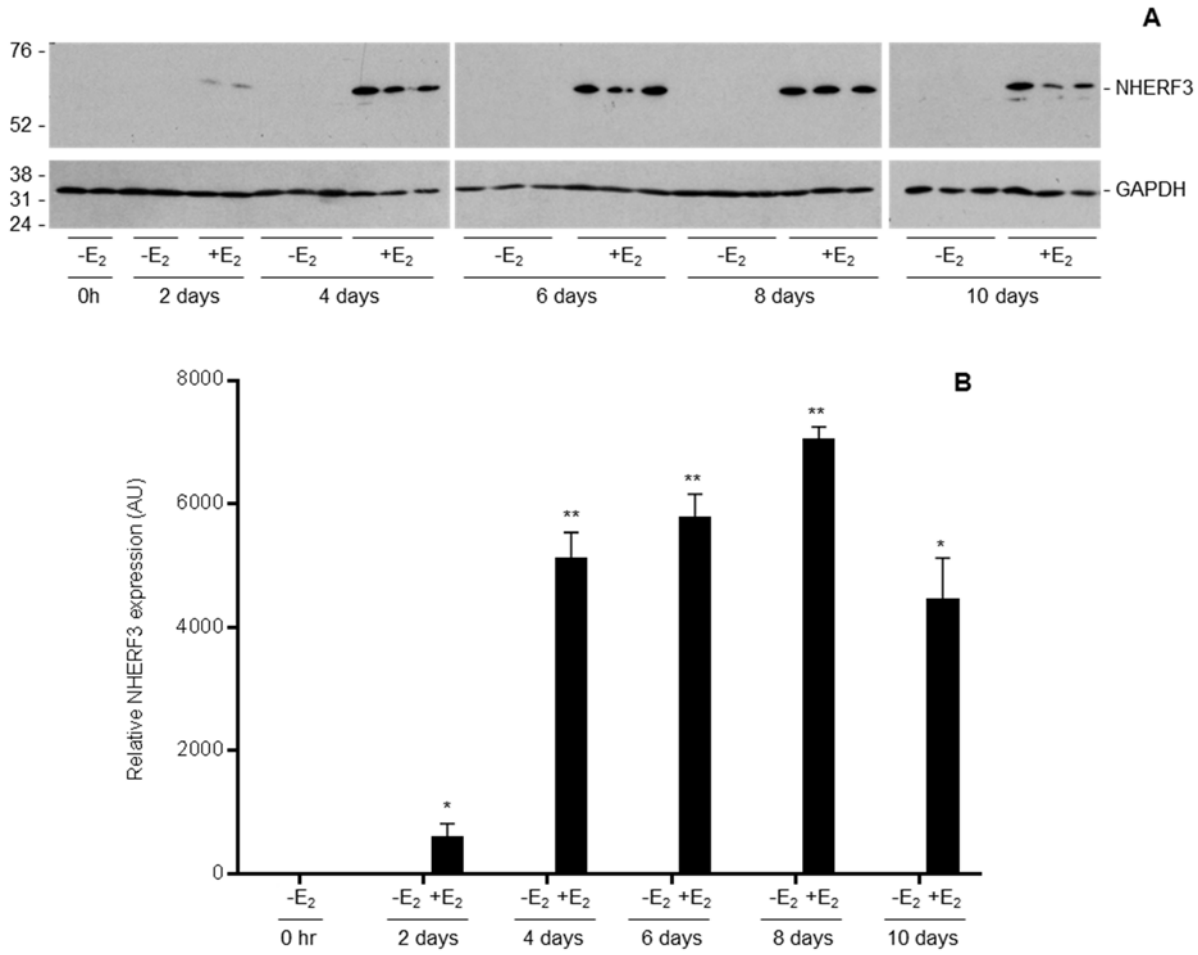

Figure 4.6 Effect of oestrogen on expression of NHERF3 in EFM-19 cells. Cells were steroid deprived by growing in phenol-red-free media containing 10% dextran-coated charcoal treated serum and 1 µg/ml insulin, for 5 days and then treated with 10^{-9} M of 17β-oestradiol for different lengths of time upto 10 days. Both the oestradiol-treated and untreated cells were lysed and protein extracts prepared. Protein aliquots of 20 µg were separated by 12% polyacrylamide gel electrophoresis and then transferred to nitrocellulose membranes. The membranes were incubated with anti-NHERF3 antibody (dilution 1:5000) overnight at 4 °C, followed by horseradish peroxidase conjugated goat-anti-rabbit secondary antibody for 1 hour at 37 °C. Proteins were visualised by enhanced chemiluminescence with SuperSignal West Dura Extended Duration Substrate. **A.** The protein expression of NHERF3 in EFM-19 cells after oestrogen stimulation for a timecourse of 0 hours to 10 days, comparing serum withdrawn (-E_2 □) samples with oestrogen-stimulated (+E_2 ■) samples. Images shown are representative of

results from experiments which have been replicated thrice. **B.** Quantification of NHERF3 normalised against the corresponding GAPDH signal, *p<0.05 and **p < 0.001 by ANOVA. Error bars indicate SEM of triplicate measurements.

4.4.3 Effect of oestradiol on NHERF3 protein expression in EFF-3 cells

Although there was no expression of NHERF3 protein detected in EFF-3 cells cultured in full medium, we evaluated the effects of oestrogen on NHERF3 expression after different times of treatment. Results from this experiment are illustrated in Figure 4.7. There was no induction of NHERF3 during the first 4 days. However, very little expression was detected after 6 days of oestradiol treatment. Interestingly, there was a more prominent induction at 8 and 10 days.

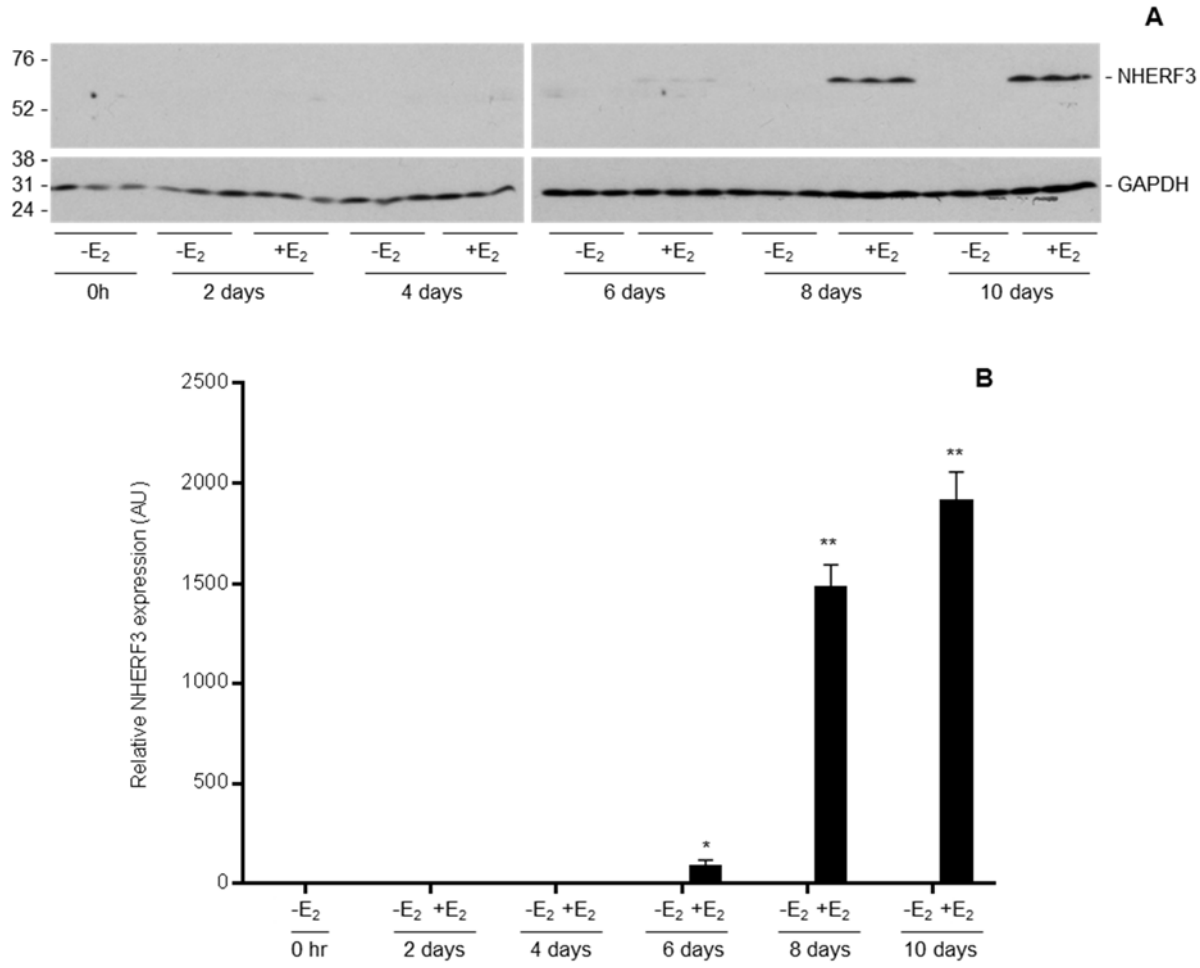

Figure 4.7 Effect of oestrogen on expression of NHERF3 in EFF-3 cells. EFF-3 cells were plated at a density of 150,000 cells per well onto a 24-well plate. Cells were steroid deprived by growing in phenol-red-free media containing 10% dextran-coated charcoal treated serum and 1 µg/ml insulin, for 5 days and then treated with 10^{-9} M of 17β-oestradiol for different lengths of time upto 10 days. Both the oestradiol-treated and untreated cells were lysed and protein extracts prepared. Protein aliquots of 20 µg were separated by 12% polyacrylamide gel

electrophoresis and then transferred to nitrocellulose membranes. The membranes were incubated with anti-NHERF3 antibody (dilution 1:5000) overnight at 4 ^{o}C, followed by horseradish peroxidase conjugated goat-anti-rabbit secondary antibody for 1 hour at 37 ^{o}C. Proteins were visualised by enhanced chemiluminescence with SuperSignal West Dura Extended Duration Substrate. **A.** The protein expression of NHERF3 in EFF-3 cells after oestrogen stimulation for a timecourse of 0 hours to 10 days, comparing serum withdrawn (-E_2 □) samples with oestrogen-stimulated (+E_2 ■) samples. Images shown are representative of results from experiments which have been replicated twice. **B.** Quantification of NHERF3 normalised against the corresponding GAPDH signal, *$p<0.05$ and **$p < 0.001$ by ANOVA. Error bars indicate SEM of triplicate measurements.

4.4.4 Regulatory effect of oestradiol on the expression of NHERF3 in MCF-7 cells by immunofluorescence

The regulation of NHERF3 protein expression with time in the absence or presence of oestrogen was tested by immunofluorescence. This method enables clear observation of the localisation of NHERF3.

MCF-7 cells were plated onto 13 mm coverslips in 12-well plates and withdrawn from growth factors for 5 days. Cells were then treated with 10^{-9} M oestradiol for various times. Cells were isolated at 0, 2, 4, 6 and 8 days and fixed in 4 % paraformaldehyde as described in Materials and Methods section. The confocal microscope settings for the different fluorochromes were unchanged throughout the duration of the timecourse experiment, to facilitate objective visualisation of changes in protein expression.

The cytoplasmic and vesicular expression of NHERF3 (green) is clearly visible in the MCF-7 cells treated with oestrogen (Figure 4.8). There is agreement between data obtained from the western transfer (Figure 4.5), in which, oestrogen causes an increase in the expression of NHERF3 protein.

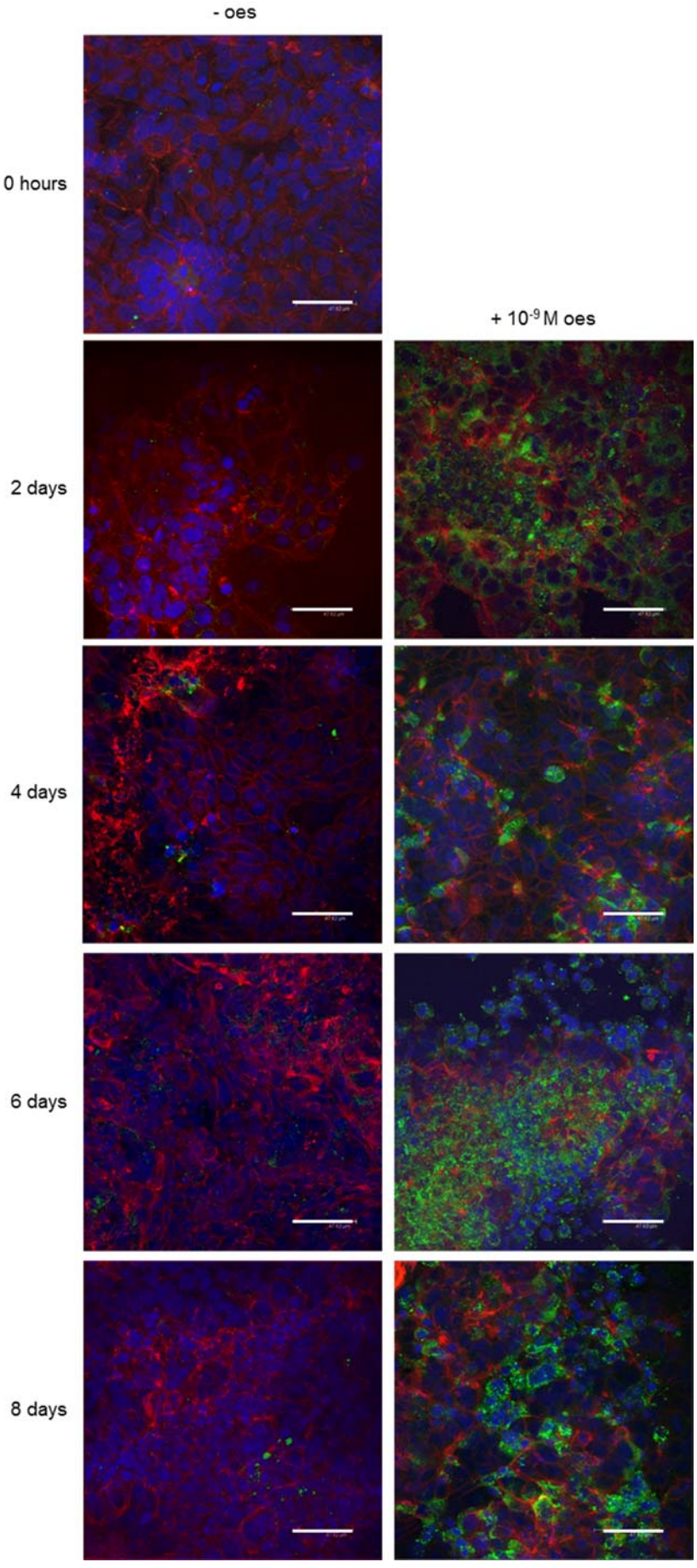
- oes
+ 10^{-9} M oes
0 hours
2 days
4 days
6 days
8 days

Figure 4.8 Effect of oestradiol on the expression and localisation of NHERF3 in MCF-7 cells. MCF-7 cells were seeded onto coverslips in 12-well plates and cultured in routine culture medium for 24 hours. Cells were cultured in withdrawal media for 5 days and grown in the absence or presence of 10^{-9} M oestradiol for different time periods ranging from 0 hours to 8 days. Cells were washed with PBS and fixed in 4% paraformaldehyde at room temperature. After fixation, cells were washed with PBS three times for 15 minutes each. Cells were then blocked in blocking buffer containing saponin for 1 hour at room temperature. The blocking medium was aspirated and the primary antibody NHERF3 was added at 1:100 dilution and incubated overnight at 4 ^{o}C. Cells were washed 3 times with PBS, 15 minutes each. The secondary antibody Alexa fluor 488 conjugated goat anti-rabbit were added at a dilution of 1:1000 and were covered in foil and the cells were incubated for 1 hour at room temperature. Cells were washed 3 times with PBS. Alexa fluor 555 conjugated phalloidin was added at a dilution of 1:200 and incubated for 15 minutes at room temperature. DAPI mounting media was added to the glass slides prior to placing the coverslip on the slide and the cells were examined under the confocal microscope using a 63x objective (Oil, 1.63). Images show DAPI (blue), NHERF3 (green) and phalloidin (red) staining at the times indicated to the left of the diagram. The panels on the left are untreated cells and the panel on the right are cells treated with 10^{-9} M oestradiol for the indicated duration. Scale bars = 47 µm.

Illustrated in Figure 4.9 below, are the x-z cross sectional images from the same experiment. The effect of oestrogen on cell proliferation is visible, as there is an increase in the depth of the cell layer. NHERF3 (green) is mostly confined intracellularly, but the distribution is variable between cells. Phalloidin (red) stains the actin cytoskeleton. The stimulation of NHERF3 protein expression increases with time in the presence of oestrogen.

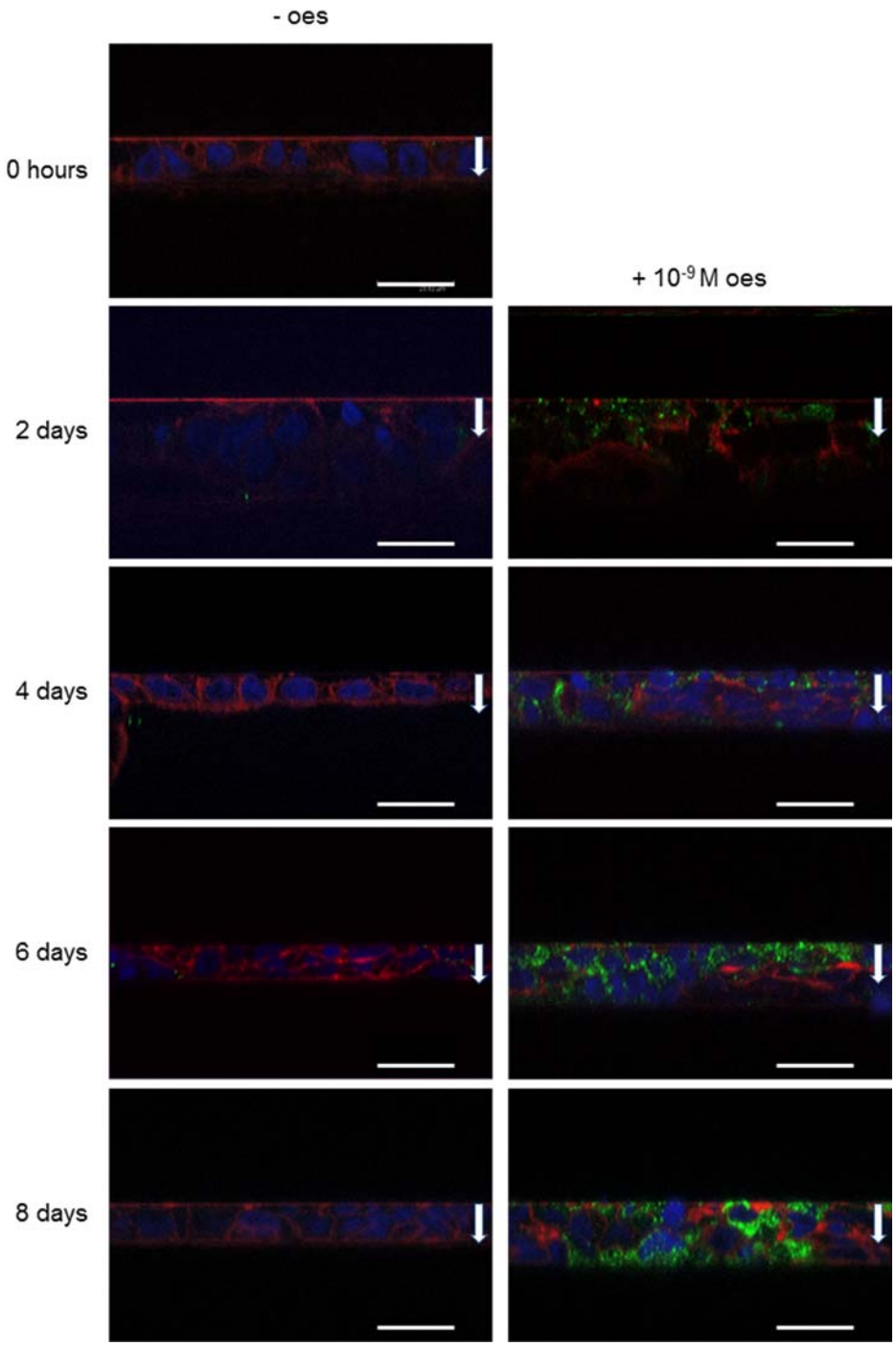

Figure 4.9 Cross-sectional images of the effect of oestradiol on the expression and localisation of NHERF3 in MCF-7 cells. MCF-7 cells were seeded onto coverslips in 12-well plates and cultured in routine culture medium for 24 hours. Cells were cultured in withdrawal media for 5 days and grown in the absence or presence of 10^{-9} M oestradiol for different time periods ranging from 0 hours to 8 days. Cells were washed with PBS and fixed in 4% paraformaldehyde at room temperature. After fixation, cells were washed with PBS three times for 15 minutes each. Cells were then blocked in blocking buffer containing saponin for 1 hour at room temperature. The blocking medium was aspirated and the primary antibody NHERF3 was added at 1:100 dilution and incubated overnight at 4 ºC. Cells were washed 3 times with PBS, 15 minutes each. The secondary antibody Alexa fluor 488 conjugated goat anti-rabbit were added at a dilution of 1:1000 and were covered in foil and the cells were incubated for 1 hour at room temperature. Cells were washed 3 times with PBS. Alexa fluor 555 conjugated phalloidin was added at a dilution of 1:200 and incubated for 15 minutes at room temperature. DAPI

mounting media was added to the glass slides prior to placing the coverslip on the slide and the cells were examined under the confocal microscope using a 63x objective (Oil, 1.63). Images show DAPI (blue), NHERF3 (green) and phalloidin (red) staining at the times indicated to the left of the diagram. The panels on the left are untreated cells and the panel on the right are cells treated with 10^{-9} M oestradiol for the indicated duration. Scale bars = 23 µm.

4.5 The regulation of NHERF3 by oestrogen in a concentration dependent manner

4.5.1 Concentration dependent effects of oestradiol on NHERF3 in oestrogen responsive cells

The following experiments were designed to test the concentration dependent effects of oestradiol on the regulation of expression of NHERF3 protein. Cells were cultured in the absence or presence of a range of concentrations of oestradiol varying from 10^{-13} M to 10^{-7} M for a period of 8 days.

The results obtained for the three oestrogen responsive cell lines; MCF-7, EFM-19 and EFF-3 are depicted in Figure 4.10. All cell lines exhibit a concentration dependent effect. In MCF-7 cells (A), NHERF3 is expressed at concentrations of oestradiol between $2x10^{-10}$ M and 10^{-8} M, with the maximal induction at 10^{-9} M. However, in EFM-19 cells (B), NHERF3 protein is detected at oestradiol concentrations above 10^{-9} M. The expression of NHERF3 in EFF-3 cells (C) was similar to that of MCF-7 cells, as protein was detected at oestradiol concentrations from $2x10^{-10}$ M to 10^{-8} M, with the highest expression measured at 10^{-9} M.

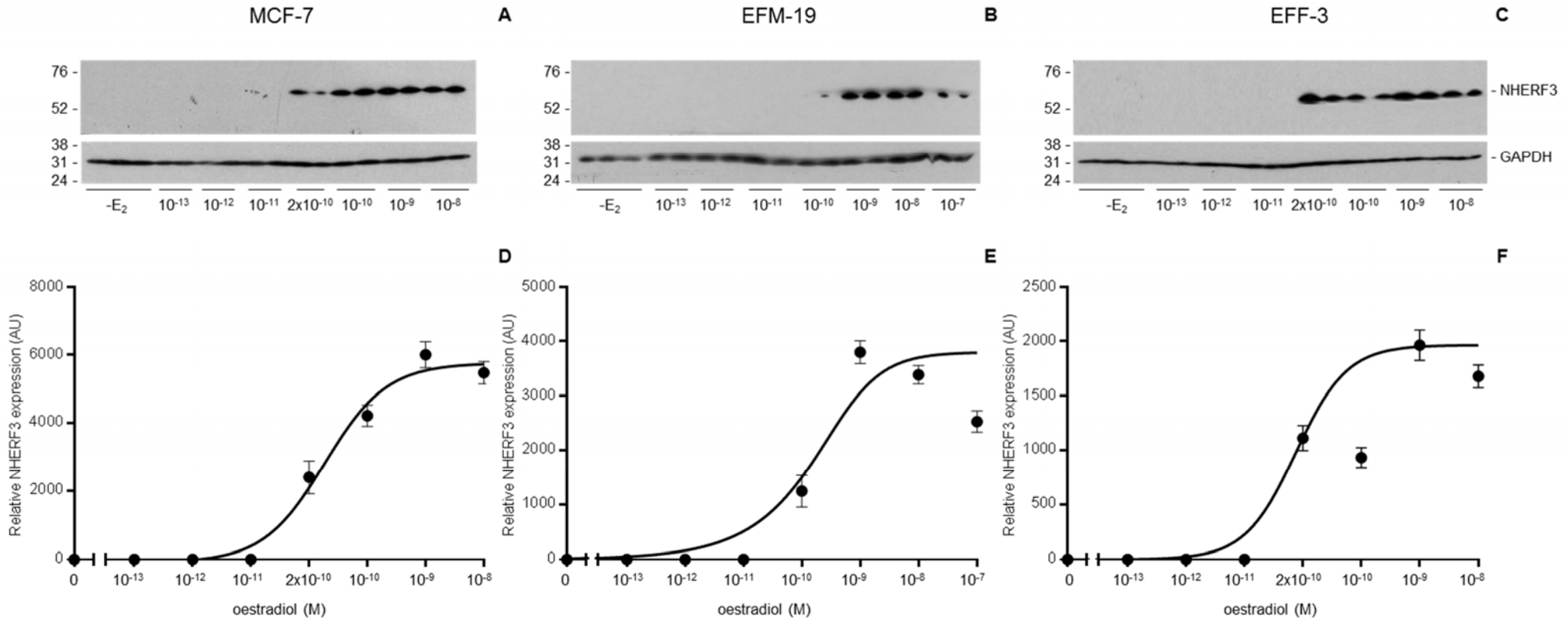

Figure 4.10 Concentration dependent effects of oestradiol on NHERF3 protein expression in MCF-7, EFM-19 and EFF-3 cells. Cells were seeded onto 24-well plates and withdrawn for 5 days and treated with different concentrations of oestradiol for 8 days. Protein aliquots of 10 µg were separated by 12% polyacrylamide gel electrophoresis and transferred to nitrocellulose membranes. Membranes were incubated with anti-NHERF3 antibody (dilution 1:10000) overnight at 4 ^{o}C, followed by horseradish peroxidase conjugated goat-anti-rabbit secondary antibody for 1 hour at 37 ^{o}C. Proteins were visualised by enhanced chemiluminescence with SuperSignal West Dura Extended Duration Substrate. **A, B, C.** The protein expression of NHERF3 in MCF-7, EFM-19 and EFF-3 cells treated with different concentrations of oestradiol for 8 days. Images shown are from representative experiments which have been repeated three times. **D, E, F.** Densitometric quantification of NHERF3 with Labworks 4.0 software, normalised against the corresponding GAPDH signal in MCF-7, EFM-19 and EFF-3 cells, respectively. Error bars indicate SEM of duplicate measurements.

4.6 Measurement of pH_i in breast cancer cells

The expression of NHERF3 protein has been shown to be regulated by oestrogen as depicted in the previous sections within this chapter. This section aims to assess the functional activity of NHERF3. It is well known that NHERF3 acts as a scaffolding protein for Na^+/H^+ exchangers (NHE) allowing the attachment and organisation of such proteins at or in close proximity to the plasma membrane of epithelial cells (Thomson *et al.*, 2005; Zachos *et al.*, 2009).

Na^+/H^+ exchangers are responsible for balancing and regulating intracellular pH. These NHE are called antiporters because they transport Na^+ ions into and H^+ ions out of the cell. We hypothesised that an increase in the expression of NHERF3 in response to oestrogen would enhance the capacity of Na^+/H^+ exchange at the cell membrane. Therefore we measured the intracellular pH (pH_i) of cells grown in full media, oestrogen-withdrawn media and in cells stimulated with oestrogen.

A pH indicator dye, BCECF-AM allows measurement of the intracellular pH of breast cancer cells. BCECF-AM has single emission fluorescence at ~535 nm and dual-excitation at ~490 nm and ~440 nm. The pH_i was determined on the basis of the pH-dependent ratio of excitation intensity using the high K^+/Nigericin calibration technique as described in Materials and Methods section 2.6.3.

4.6.1 Optimisation of conditions

The optimum BCECF-AM concentrations and incubation times were evaluated. Cells were plated at a density of 10,000 cells per well onto 96-well plates. Cells were incubated for 2 days in routine culture medium. The culture media was removed by aspiration and cells were washed with Krebs's Henseleit HEPES-buffered (KHH) solution. Subsequently 1 µM, 5 µM and 10 µM of BCECF-AM in KHH were added to cells. Cells that do not contain any BCECF-AM were included in parallel. Cells were incubated for 15 min, 30 min and 60 min in a 37^{o}C incubator. It is important to cover the 96-well plates in foil, as the BCECF-AM dye is sensitive to light. Cells were then washed with KHH solution. The

fluorescence intensity was measured with a FLUOstar Omega plate reader at 485 nm and 420 nm.

Results obtained are shown in Figure 4.11. The calibration curve was linear over the pH range from 6.0 to 7.8 (Figure 4.11A). Cells were incubated with different concentrations of BCECF-AM at 1 μM, 5 μM and 10 μM to determine the optimum concentration to be loaded into cells. Cells that do not contain any BCECF-AM are indicated as 0 μM. The fluorescent intensity ratio increased with increasing concentrations of BCECF-AM, with 10 μM producing the highest ratio. Figure 4.11B shows that the ideal incubation time would be 15 minutes. Therefore in subsequent experiments cells were incubated with 10 μM BCECF-AM for 15 mins.

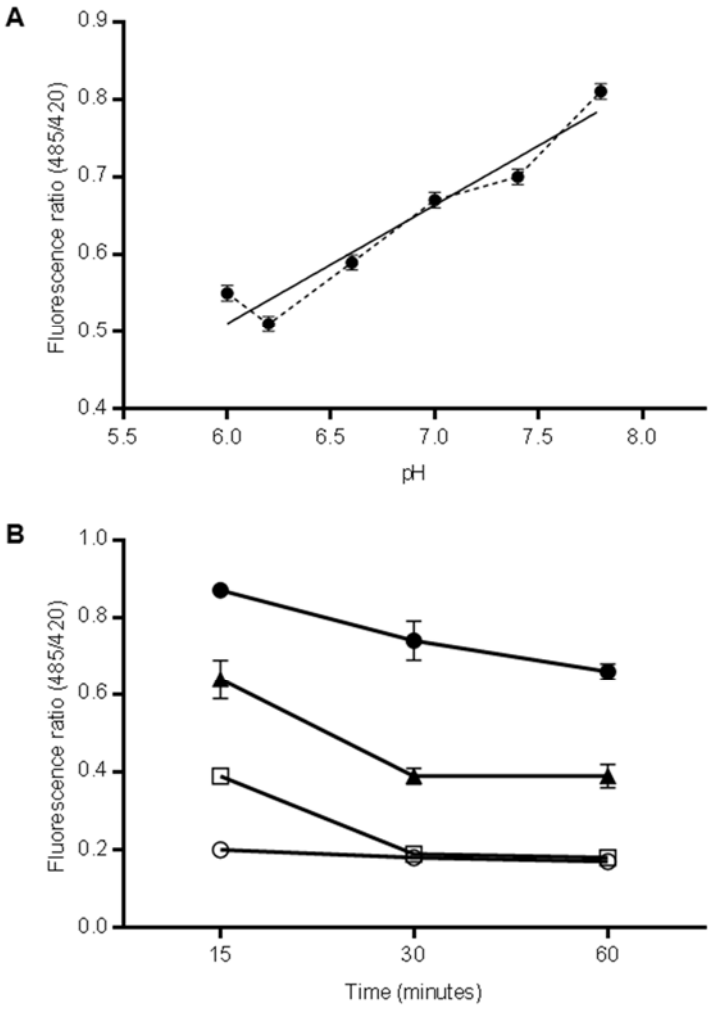

Figure 4.11 Optimisation of BCECF-AM concentrations and incubation times. EFM-19 cells were seeded at a density of 10,000 cells per well in 96-well plates in routine culture medium. Cells were washed with KHH solution once and incubated with 0 μM, 1 μM, 5 μM and 10 μM BCECF-AM. Cells were incubated for 15 mins, 30 mins and 60 mins at 37°C. Cells were

then washed once with KHH solution. **A.** The calibration curve was constructed from cells resuspended in high K^+ buffers of known pH ranging from 6.0 to 7.8. These buffers contained 10 μM nigericin to equilibrate the internal and external pH of cells. Fluorescence intensities at 485 nm and 420 nm were determined using the FLUOstar Omega plate reader. The ratio of absorbance at 485 nm and 420 nm was calculated and calibration curves of the fluorescence ratios against pH were produced. **B.** Calculated fluorescence ratio 485/420nm measurements in EFM-19 cells incubated with BCECF-AM at 0 μM (○), 1 μM (□), 5 μM (▲) and 10 μM (●) for 15, 30 and 60 mins in at 37ºC. The pH_i of the cells was estimated from the reference curves. Error bars indicate standard errors of the mean of four replicates per condition from one experiment.

4.6.2 pH_i measurement in MCF-7 and EFM-19 cells cultured in full medium

The aim of this experiment was to determine the resting pH_i of MCF-7 and EFM-19 cells. Cells were seeded onto 96-well plates at a density of 5000 cells per well and were grown in routine culture medium for 3 days. Cells were then incubated with KHH solution containing 10 μM BCECF-AM for 15 minutes. KHH solutions were prepared at two different pH. One was at pH 6.0, whereas the other was at pH 7.4. KHH solution at pH 6.0, would allow determination of the ability of cells to regulate pH_i.

Following incubation, cells were washed with KHH and half of the cells were incubated with a KHH solution at pH 6.0, whereas the other half of cells was incubated with pH 7.4 KHH solution. The fluorescent intensity readings were obtained and the steady-state (resting) pH_i of MCF-7 and EFM-19 cells was determined (Figure 4.12).

In a KHH solution at the physiological pH of 7.4, the steady-state pH_i was 7.43 and 7.35 in MCF-7 and EFM-19 cells, respectively. In an acidic pH 6.0, the resting pH_i of MCF-7 cells was 6.73 and was 6.63 in EFM-19 cells. This suggests that in the presence of a more acidic extracellular pH, cells attempt to adjust and regulate its internal pH to the baseline resting pH. Intracellular buffering and pH_i regulatory mechanisms prevent the pH_i from equilibrating with the external acidic pH. The Na^+/H^+ exchangers function at a stoichiometry of 1:1, and allows the extrusion of H^+ ions only when the gradient is less than the inverse Na^+ ion gradient. Therefore at an external pH 6.0, the Na^+/H^+ exchangers are not completely effective at maintaining the pH_i at physiological values.

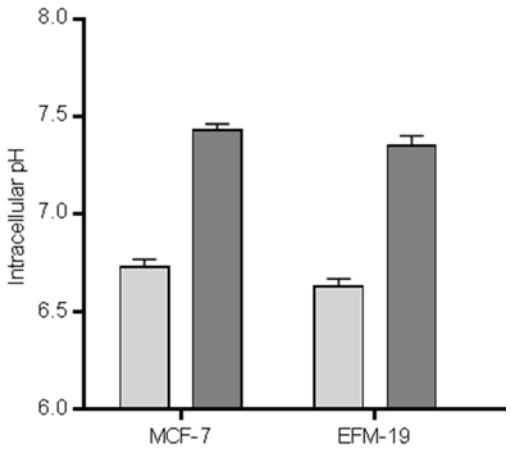

Figure 4.12 Measurement of pH_i in MCF-7 and EFM-19 cells. MCF-7 and EFM-19 cells were seeded at a density of 5,000 cells per well in 96-well plates in routine culture medium. Cells were washed with KHH solution once and incubated with 10 µM BCECF-AM for 15 mins. Cells were then washed once with KHH solution and a KHH solution of pH 6.0 (□) was added to half the cells, whereas a KHH solution of pH 7.4 (■) was added to the other half. Fluorescence intensities at 485 nm and 420 nm were determined using the FLUOstar Omega plate reader. The ratio of absorbance at 485 nm and 420 nm was calculated and the pH_i was estimated from the calibration curve. Error bars indicate standard errors of the mean, where n=20 for MCF-7 cells and n=25 for EFM-19 cells.

4.6.3 Effect of oestrogen on pH_i measurements of MCF-7 and EFM-19 cells

To study the effect of oestrogen on the regulation of pH_i, MCF-7 and EFM-19 cells were withdrawn from growth factors for 5 days. Cells were then cultured in the absence or presence of 10^{-9} M oestradiol for 5 days.

In MCF-7 cells (Figure 4.13A), oestrogen causes a significant decrease in pH_i in KHH solution at pH 6.0, where the pH_i decreases from 6.78±0.06 to 6.38±0.05 ($p=0.0047$, ANOVA). In the KHH solution at pH 7.4, the pH_i changes slightly from 7.48±0.16 to 7.40±0.12 ($p=0.5268$, ANOVA). This result was not expected, as we anticipated that in the presence of oestrogen, cells would have the capacity to increase their pH_i, since we have previously confirmed that there is an induction of NHERF3 protein expression. However, the results obtained for MCF-7 cells at an external pH 6.0 show a decreased capacity whilst at pH 7.4 the cells do not indicate a change in set-point. The set-point is the pH at which there is minimal transporter activity.

In contrast to MCF-7 cells, the EFM-19 cells show a significant increase in pH_i in both KHH solutions at pH 6.0 and pH 7.4 in response to the oestrogen

stimulus. At pH 6.0, the pH_i increased from 6.73±0.05 to 6.99±0.09 (p=0.0049, ANOVA), whereas at pH 7.4 the pH_i increased significantly from 7.28±0.09 to 7.60±0.10 (p=0.0042, ANOVA). These results suggest that there is a shift in the set-point and that oestrogen-treated EFM-19 cells have an increased capacity to regulate pH_i.

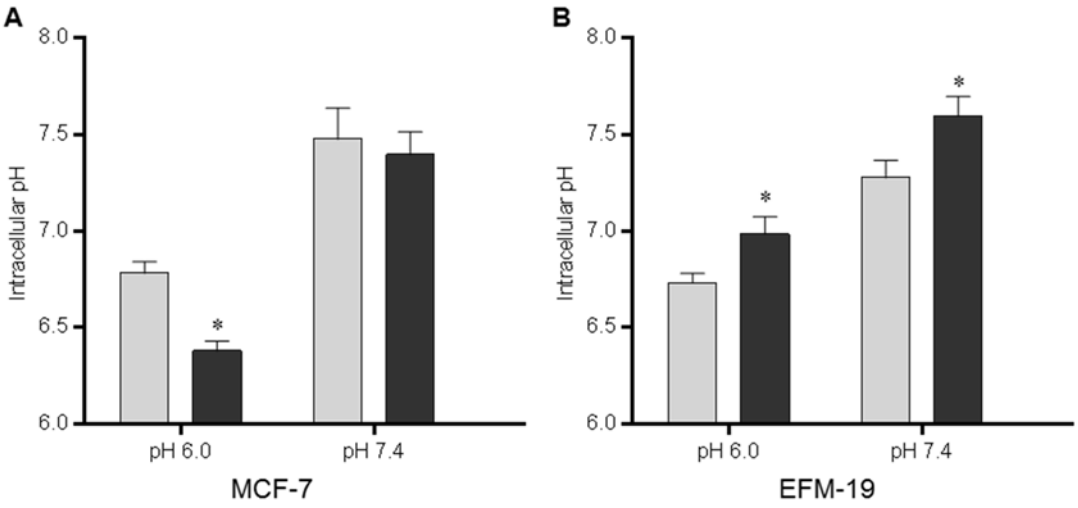

Figure 4.13 Effect of oestrogen on pH_i of MCF-7 and EFM-19 cells. MCF-7 and EFM-19 cells were seeded at a density of 5,000 cells per well in collagen-coated 96-well plates. Cells were cultured in steroid depleted media for 5 days. For a further 5 days, cells were grown in phenol-red-free media alone or in the presence of 10^{-9} M of 17β-oestradiol. Cells were washed with KHH solution once and incubated with 10 μM BCECF-AM for 15 mins. Cells were then washed once incubated with either a KHH solution at pH 6.0 or at pH 7.4. Fluorescence intensities at 485 nm and 420 nm were determined using the FLUOstar Omega plate reader. The ratio of absorbance at 485 nm and 420 nm was calculated and the pH_i was estimated from the calibration curve. **A.** the intracellular pH of MCF-7 cells and **B.** EFM-19 cells, comparing untreated ($-E_2$ □) and oestrogen stimulated ($+E_2$ ■) cells. *p < 0.05 by ANOVA. Error bars indicate standard errors of the mean of four replicates per condition from 4 separate experiments.

4.6.4 Effect of hypertonicity on pH_i of MCF-7 and EFM-19 cells cultured in full media

Cells subject to hyperosmotic conditions by incubation with mannitol undergo cell shrinkage. This cell shrinkage should result in activation of Na^+/H^+ exchangers, which allows to increase the entry of Na^+ ions into the cell. This increased intracellular Na^+ subsequently leads to cell swelling due to the

osmotic uptake of water. The process of swelling of cells following hyperosmotic stress is referred to as regulatory volume increase (RVI).

Mannitol was added to KHH solutions at concentrations of 80, 100, 150 and 200 mM to study its effects in activation of Na^+/H^+ exchangers in MCF-7 and EFM-19 cells cultured in full medium.

The steady-state intracellular pH of MCF-7 cells was 6.50 when exposed to an external pH 6.0 KHH solution. As shown in Figure 4.14A, the pH_i increased dramatically to 7.40, 7.33, 7.30, 7.19, in the presence of 80 mM, 100 mM, 150 mM and 200 mM mannitol, respectively. The shows that stimulation of Na^+/H^+ exchangers is greatly enhanced when subject to hypertonicity. The baseline pH_i when exposed to a KHH solution of pH 7.4 was 7.61. A reduction in pH_i to 7.45, 7.31, 7.32, and 7.24 is observed in the presence of increasing concentrations of mannitol.

In EFM-19 cells, the steady-state pH in the absence of mannitol was 6.25 at external pH 6.0. With the addition of 80 mM, 100 mM, 150 mM and 200 mM mannitol, there was alkalisation of pH to 6.54, 6.47, 6.44 and 6.49. Similar to the effect of mannitol in MCF-7 cells, a decrease in pH_i was observed with the addition of mannitol to KHH solution at pH 7.4. The baseline pH decreased from 7.35 to 7.00, 6.97, 6.94, and 6.91 with increasing concentrations of mannitol. These results are shown in Figure 4.14B.

These results indicate that when cells are exposed to an external pH of 6.0 in the presence of mannitol, alkalisation occurs. In contrast, the pH_i acidifies when the external pH is 7.4 in the presence of mannitol. Therefore these observations suggest that at an acidic external pH, the cells alkalinise by extruding H^+ ions through Na^+/H^+ exchangers. The hypertonic effect of mannitol causes activation of NHE, allowing for movement of H^+ ions out of the cell. Conversely, at an external pH of 7.4, the pH_i acidifies even in the presence of mannitol, signifying a reversal effect of NHE by the accumulation of H^+ ions within the cell. The decrease in pH may well be mediated by other transporters such as sodium-driven Cl^-/HCO_3^- exchanger. In both cells lines at pH 7.4, the set-point shifts towards a more acidic pH. As shown in the previous chapter, the $Na^+/K^+/Cl^-$ co-

transporter, NKCC1 is also activated under hypertonic conditions resulting in an influx of Cl^- ions. Therefore in the presence of mannitol the sodium-driven Cl^-/HCO_3^- exchanger might be activated in order to regulate pH as well as to extrude the increased Cl^- ion concentration.

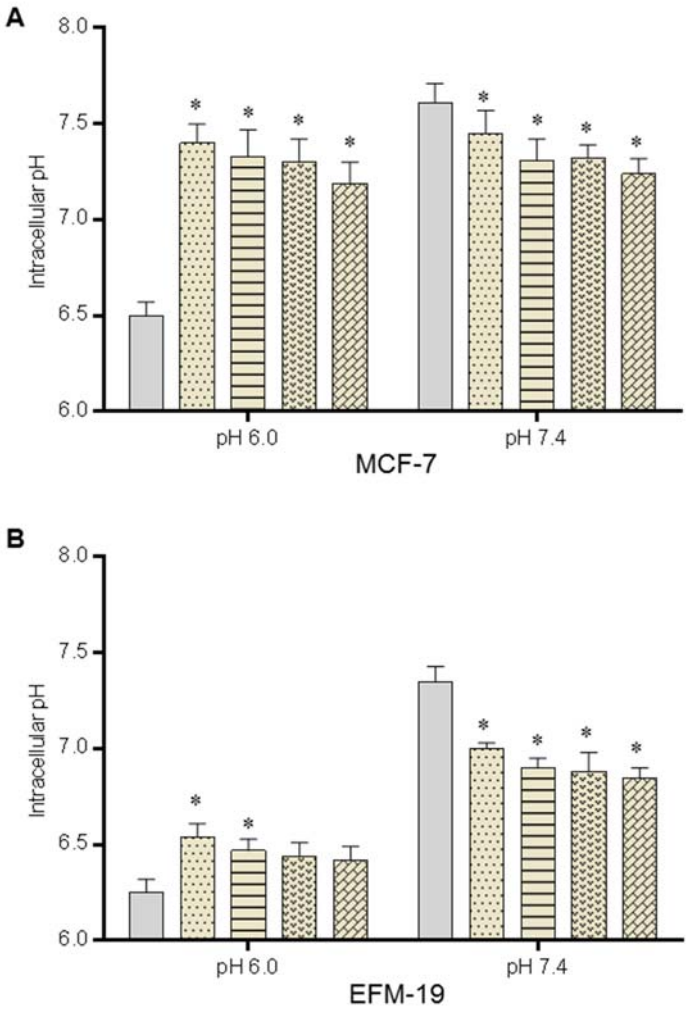

Figure 4.14 Effect of mannitol on pH_i of MCF-7 and EFM-19 cells. MCF-7 and EFM-19 cells were seeded at a density of 5,000 cells per well in 96-well plates in routine culture medium. Cells were washed with KHH solution once and incubated with 10 µM BCECF-AM for 15 mins. Cells were then washed once with KHH solution and incubated with either a KHH solution of pH 6.0 or a KHH solution of pH 7.4. Fluorescence intensities at 485 nm and 420 nm were determined using the FLUOstar Omega plate reader. After the initial fluorescent readings were taken, cells were incubated with one of the following; 80, 100, 150 or 200 µM mannitol. The ratio of absorbance at 485 nm and 420 nm was calculated and the pH_i was estimated from the calibration curve. **A.** The effect of mannitol on intracellular pH of MCF-7 cells and **B.** EFM-19 cells, comparing baseline pH_i (□) to the effect of 80, 100, 150 and 200 µM mannitol (from left to right) at an external pH of 6.0 (left panel) or pH 7.4 (right panel). *$p < 0.05$ by ANOVA. Error bars indicate standard errors of the mean of four replicates per condition from 3 separate experiments.

4.6.5 Effect of hypertonicity on pH_i of MCF-7 cells in the absence and presence of oestrogen

The effect of hypertonicity on pH_i of withdrawn and oestrogen stimulated MCF-7 cells was tested. Cells were grown on collagen-coated 96-well plates and withdrawn for 5 days and then cultured in the presence or absence of 10^{-9} M oestradiol for 5 days before measuring the pH_i. Once the initial steady-state pH_i was measured, cells were subject to hypertonic stress by the addition of mannitol to KHH solutions of pH 6.0 or 7.4. Mannitol was added at either 80 mM or 200 mM.

Results are shown in Figure 4.15. When cells were incubated with KHH at pH 6.0, the pH_i was 6.66±0.03 in withdrawn cells and 6.29±0.04 in the oestrogen treated cells. This difference was statistically significant (p=0.0001, ANOVA). In the presence of 80 and 200 mM mannitol, a significant decrease in pH_i was observed when comparing the untreated and oestrogen-treated cells. In the presence of 80 and 200 mM mannitol, the pH_i decreased from 6.69±0.06 to 6.30±0.02 (p=0.0001, ANOVA) and from 6.41±0.03 to 6.03±0.04 (p=0.0001, ANOVA), respectively. However this was not the case for cells in a KHH solution of pH 7.4, as there was no significant difference observed between withdrawn and oestrogen-treated cells. The effect of oestrogen was only noticeable in cells incubated with 80 mM mannitol, as there was a statistically significant decrease from 6.98±0.03 to 6.82±0.02 (p=0.0137, ANOVA).

From our previous observations of the effect of mannitol in full media (Figure 4.14A), we expected the cells treated with oestrogen to alkalise when incubated with KHH at pH 6.0 and acidify when exposed to an external pH of 7.4 in the presence of 80 or 200 mM mannitol. However, this effect of mannitol was noticeable when cells were exposed to KHH solution at pH 7.4 in the presence of 80 mM mannitol. Acidification was observed in both withdrawn and oestrogen-treated cells. But exposure to 200 mM mannitol in KHH of pH 7.4 had no effect on the pH_i. At an external pH 6.0, our previous findings showed an increase in pH_i in response to addition of mannitol. However in comparison to cells in full media, oestrogen-treated cells show a significant difference, but in the opposite direction, as it should alkalise instead of acidify. These results

suggest that untreated MCF-7 cells do not have an increase in Na^+/H^+ exchange capacity to maintain pH_i when exposed to an external pH 6.0. This effect could possibly due to that lack / reduction in organisation of NHE at the plasma membrane, since untreated cells do not express NHERF3 protein.

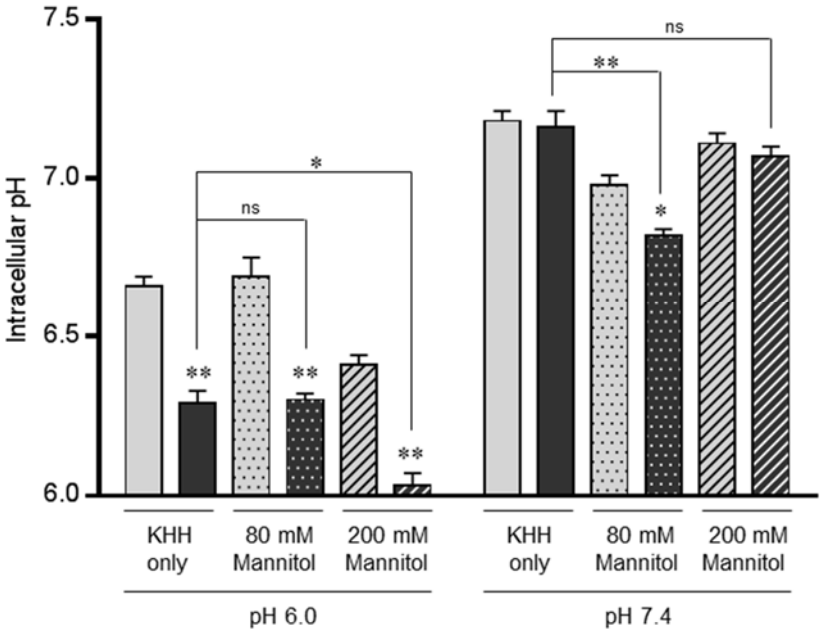

Figure 4.15 Effect of mannitol on pH_i of MCF-7 cells in the absence and presence of oestrogen. MCF-7 cells were seeded at a density of 5,000 cells per well in collagen-coated 96-well plates in routine culture medium. Cells were cultured in steroid depleted media for 5 days. For a further 5 days, cells were grown in phenol-red-free media alone or in the presence of 10^{-9} M of 17β-oestradiol. Cells were washed with KHH solution once and incubated with 10 μM BCECF-AM for 15 mins. Cells were then washed once with KHH solution and incubated with either a KHH solution of pH 6.0 or a KHH solution of pH 7.4. Fluorescence intensities at 485 nm and 420 nm were determined using the FLUOstar Omega plate reader. After the initial fluorescent readings were taken, cells were incubated with either 80 or 200 μM mannitol. The ratio of absorbance at 485 nm and 420 nm was calculated and the pH_i was estimated from the calibration curve. The intracellular pH of MCF-7 cells, comparing untreated ($-E_2$ □) and oestrogen stimulated ($+E_2$ ■) cells incubated with 80 or 200 μM mannitol as indicated. *$p < 0.05$ and **$p < 0.0001$ by ANOVA, ns- not significant. Error bars indicate standard errors of the mean of 4 replicates per condition from 3 separate experiments.

4.6.6 Effect of hypertonicity on pH_i of EFM-19 cells in the absence and presence of oestrogen

Figure 4.16 displays the results obtained from a similar experiment investigating the effect of hypertonicity in unstimulated and oestrogen-stimulated EFM-19 cells. Consistent with our previous findings shown in Figure 4.14B in EFM-19 cells, there was a significant difference observed between untreated and

oestrogen-treated cells in all conditions, except in the presence of 80 mM mannitol at an external pH 6.0. In contrast to MCF-7 cells, the pH_i of oestrogen-treated cells was more alkaline with respect to that of the withdrawn untreated cells. At an external pH of 6.0, the pH_i of withdrawn cells was 6.81±0.05, whereas that of oestrogen-treated cells was 6.97±0.04 (p=0.0368, ANOVA). The pH_i increased from 7.13±0.05 to 7.35±0.06, when comparing the withdrawn cells to the oestrogen-treated cells at an external pH of 7.4 (p=0.0098, ANOVA).

Similar to MCF-7 cells, the oestrogen-treated cells did not alkalise when exposed to hypertonic mannitol at an external pH 6.0. However, oestrogen-treated cells incubated with KHH solution of pH 7.4 in the presence of mannitol acidified, as anticipated. The initial pH_i was 7.35±0.06. The pH_i then reduced to 7.03±0.05 and 7.13±0.04 in the presence of 80 and 200 mM mannitol, respectively. The oestrogen-treated cells behave in a similar manner to the cells cultured in routine culture media, as the foetal calf serum contains oestrogen. The cells stimulated with oestrogen show increased pH_i regulatory capacity in comparison to the withdrawn cells. However, it is unclear as to why the addition of mannitol causes an acidification when oestrogen-treated cells are incubated with KHH solution at pH 6.0.

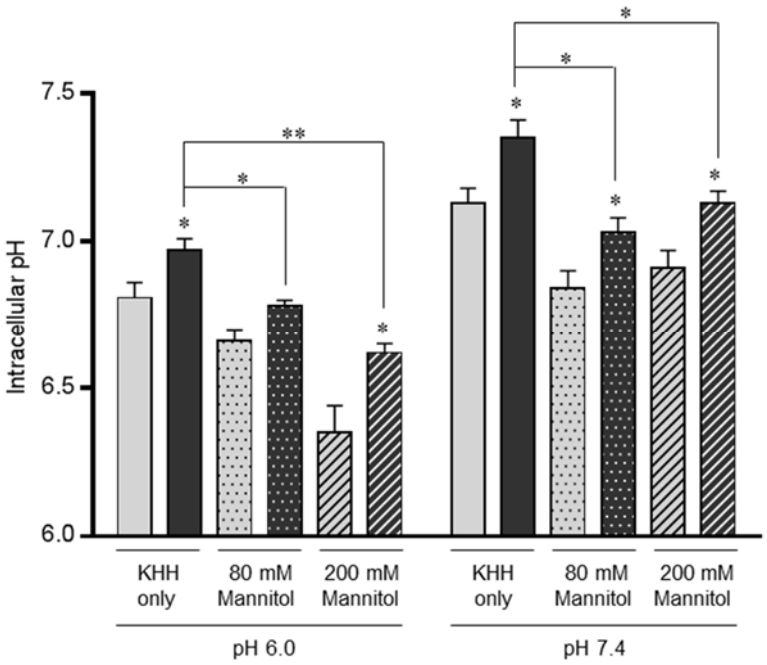

Figure 4.16 Effect of mannitol on pH_i of EFM-19 cells in the absence and presence of oestrogen. EFM-19 cells were seeded at a density of 5,000 cells per well in 96-well plates in routine culture medium. Cells were cultured in steroid depleted media for 5 days. For a further 5

days, cells were grown in phenol-red-free media alone or in the presence of 10^{-9} M of 17β-oestradiol. Cells were washed with KHH solution once and incubated with 10 μM BCECF-AM for 15 mins. Cells were then washed once with KHH solution and incubated with either a KHH solution of pH 6.0 or a KHH solution of pH 7.4. Fluorescence intensities at 485 nm and 420 nm were determined using the FLUOstar Omega plate reader. After the initial fluorescent readings were taken, cells were incubated with either 80 or 200 μM mannitol. The ratio of absorbance at 485 nm and 420 nm was calculated and the pH_i was estimated from the calibration curve. The intracellular pH of EFM-19 cells, comparing untreated (-E_2 □) and oestrogen stimulated (+E_2 ■) cells incubated with 80 or 200 μM mannitol as indicated. *$p < 0.05$ and **$p < 0.0001$ by ANOVA. Error bars indicate standard errors of the mean of 4 replicates per condition from 3 separate experiments.

4.6.7 Effect of NH_4Cl on pH_i of MCF-7 and EFM-19 cells cultured in full media

The addition of NH_4Cl leads to alkalisation of the intracellular pH of cells. This alkalisation occurs due to the passive entry of NH_3 into the cell. NH_3 binds to H^+ ions present within the cell. Alkalisation tends to cease once the intracellular NH_3 concentration equilibrates with the extracellular concentration of NH_3. The slow influx of NH_4^+ ions into the cell causes a decrease in pH_i. This slow acidification is a result of the dissociation of NH_4^+ into NH_3 and H^+ ions. The removal of NH_4Cl causes the pH_i to decrease further than the initial baseline levels as intracellular NH_3 diffuses out from the cell resulting in an acid load. The NH_4^+ ions within the cell then dissociate into NH_3 and H^+ ions in order to maintain equilibrium. The additional H^+ ions are then extruded by active transport, thus allowing cells to maintain their baseline pH.

Cells were cultured in full media for 3 days and incubated with BCECF-AM. The initial fluorescence reading was obtained and cells were then subjected to an acid load by the addition of KHH solution containing 40 mM NH_4Cl. The addition of NH_4Cl allows to test the acid extrusion capability. Cells were exposed to NH_4Cl for 10 minutes, and then incubated with KHH solution immediately. Fluorescent intensity readings were measured every 10 minutes for a period of 1 hour. The results show the pH_i recovery from an acid load in both MCF-7 (Figure 4.17A) and EFM-19 cells (Figure 4.17B).

In MCF-7 cells incubated with KHH of pH 7.4, the pH_i raised rapidly from 7.58±0.02 to 8.14±0.09 with the addition of 40 mM NH_4Cl. The removal of NH_4Cl leads to a rapid decline in pH_i, even below the initial steady-state pH.

Further addition of KHH did not change the pH_i. This indicates that the pH_i recovery due to Na^+/H^+ exchange is substantially slower. Also the final pH_i of 7.14±0.04 was lower than the initial steady-state pH_i. Conversely, the addition and removal of NH_4Cl did not have much of an effect on pH_i in cells exposed to an external pH 6.0.

Shown in Figure 4.17B are the results from EFM-19 cells. The baseline pH_i for cells incubated with KHH solution of pH 7.4 was 7.52±0.07, which then increased to 7.86±0.13 with the addition of 40 mM NH_4Cl. Then there was a dramatic decrease to 6.49±0.10 with the rapid removal of NH_4Cl. With the re-addition of KHH solution there was a slight increase in pH_i to a final value of upto 6.65±0.07, although it still did not reach the initial values of steady-state pH_i. The recovery of pH_i in EFM-19 cells was quicker than that of MCF-7 cells. In contrast to MCF-7 cells, the EFM-19 cells exposed to KHH of pH 6.0 showed a gradual overall decline in pH_i. The initial pH_i was 6.78±0.03, whereas the final pH_i was 5.99±0.03. The cells are unable to recover their pH_i as the ability of the Na^+/H^+ exchangers are limited at pH 6.0 since the chemical gradient for H^+ ions out to in is higher than the Na^+ ion gradient.

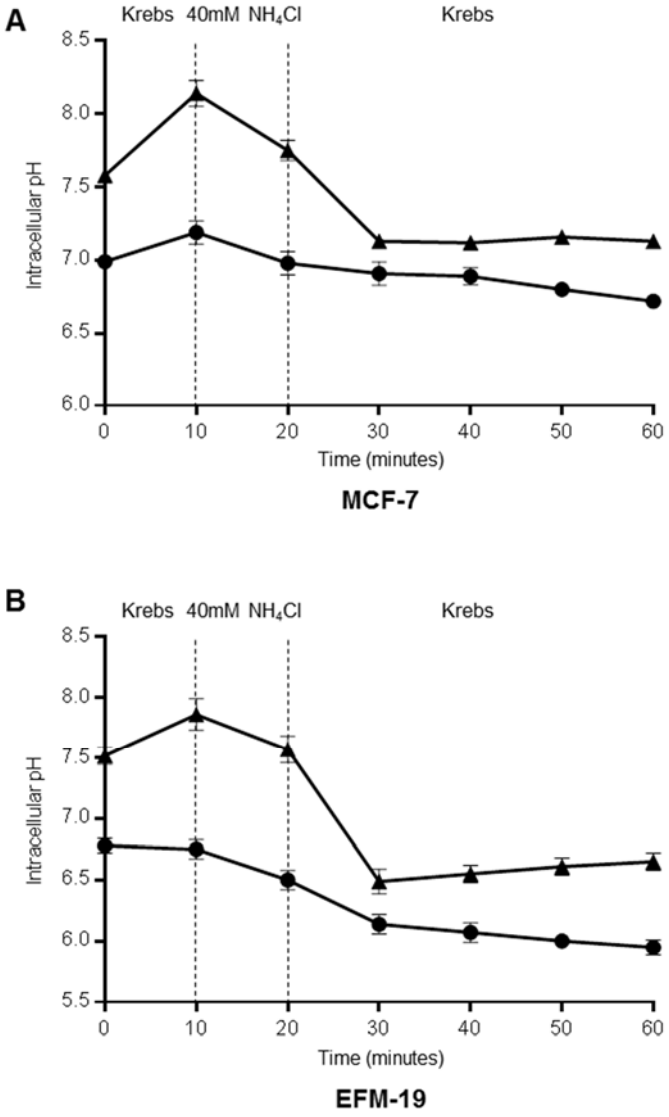

Figure 4.17 Effect of 40 mM NH_4Cl on pH_i of MCF-7 and EFM-19 cells. MCF-7 and EFM-19 cells were seeded at a density of 5,000 cells per well in 96-well plates in routine culture medium. Cells were washed with KHH solution once and incubated with 10 µM BCECF-AM for 15 mins. Cells were then washed once with KHH solution and incubated with either a KHH solution of pH 6.0 or a KHH solution of pH 7.4. Fluorescence intensities at 485 nm and 420 nm were determined using the FLUOstar Omega plate reader. After the initial fluorescent readings were taken, cells were incubated with 40 mM NH_4Cl for 10 mins. Then NH_4Cl was aspirated and KHH solutions of pH 6.0 and pH 7.4 were added to the appropriate cells. Fluorescence intensity readings were measured at 10 min intervals for a period of 60 mins in total. The ratio of absorbance at 485 nm and 420 nm was calculated and the pH_i was estimated from the calibration curve. **A.** The effect of 40 mM NH_4Cl on intracellular pH of MCF-7 cells and **B.** EFM-19 cells, at an external pH of 6.0 (●) or pH 7.4 (▲). The images shown are representative of experiments which have been replicated three times. Error bars indicate standard errors of the mean of four replicates per condition.

4.6.8 Effect of NH_4Cl on pH_i of MCF-7 cells in the absence and presence of oestrogen

Since we have investigated the effect of NH_4Cl in cells grown in routine media, it was important to study the effect of an acid load in withdrawn and cells that have been oestrogen-stimulated. MCF-7 cells were withdrawn for 5 days and cultured in the absence or presence of oestrogen for 5 days. The following result shown in Figure 4.18 is from such an experiment in MCF-7 cells.

When both withdrawn and oestrogen-treated cells were incubated with a KHH solution of pH 7.4, there was hardly any difference in pH_i throughout the experiment (Figure 4.18B). The addition of NH_4Cl caused an alkalisation, while the removal of NH_4Cl caused acidification in both untreated and oestrogen-treated cells. With the re-addition of KHH solution, the pH_i recovery was faster in the withdrawn cells than that of oestrogen stimulated cells, although neither reached the initial baseline pH_i. In the case of cells incubated with a pH 6.0 KHH solution, the oestrogen-treated cells had a more acidic initial steady-state pH_i in comparison to withdrawn cells (Figure 4.18A). These results are contradictory to what we expected, as this suggests that withdrawn cells have more Na^+/H^+ exchange than oestrogen-treated cells. Yet, results from protein expression indicate a clear upregulation of the scaffolding protein NHERF3 in response to oestrogen.

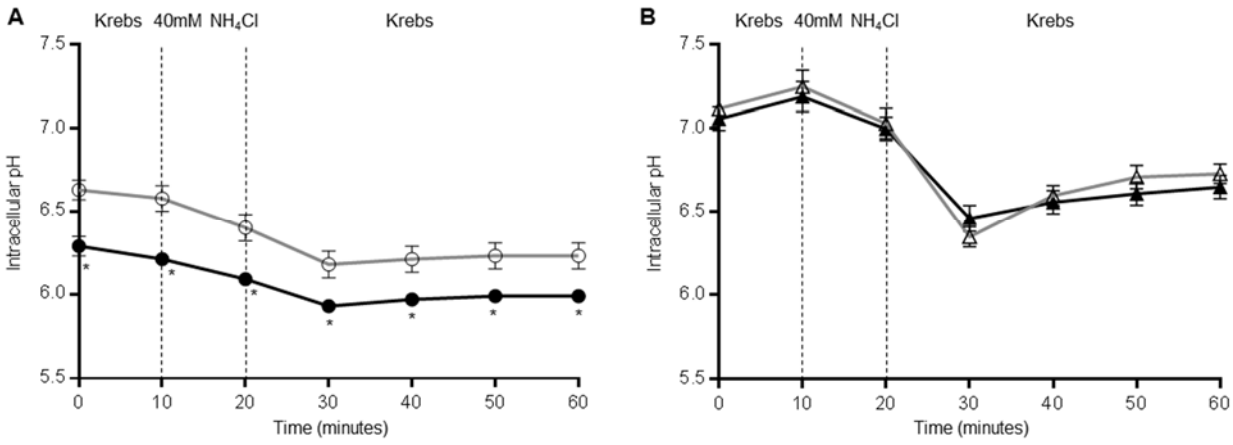

Figure 4.18 Effect of 40 mM NH_4Cl on pH_i of MCF-7 cells in the absence and presence of oestrogen. MCF-7 were seeded at a density of 5,000 cells per well in collagen-coated 96-well plates in routine culture medium. Cells were cultured in steroid depleted media for 5 days. For a further 5 days, cells were grown in phenol-red-free media alone or in the presence of 10^{-9} M of 17β-oestradiol. Cells were washed with KHH solution once and incubated with 10 μM BCECF-

AM for 15 mins. Cells were then washed once with KHH solution and incubated with either a KHH solution of pH 6.0 or a KHH solution of pH 7.4. Fluorescence intensities at 485 nm and 420 nm were determined using the FLUOstar Omega plate reader. After the initial fluorescent readings were taken, cells were incubated with 40 mM NH_4Cl for 10 mins. Then NH_4Cl was aspirated and KHH solutions of pH 6.0 and pH 7.4 were added to the appropriate cells. Fluorescence intensity readings were measured at 10 min intervals for a period of 60 mins in total. The ratio of absorbance at 485 nm and 420 nm was calculated and the pH_i was estimated from the calibration curve. **A.** The effect of 40 mM NH_4Cl on intracellular pH of MCF-7 cells, comparing untreated cells ($-E_2$ ○) with oestrogen stimulated cells ($+E_2$ ●) at an external pH of 6.0. and **B.** comparing untreated cells ($-E_2$ △) with oestrogen stimulated cells ($+E_2$ ▲) at an external pH of 7.4. The image shown is representative of an experiment which has been replicated three times. *$p < 0.05$ by ANOVA. Error bars indicate standard errors of the mean of four replicates per condition.

4.6.9 Effect of NH_4Cl on pH_i of EFM-19 cells in the absence and presence of oestrogen

Results obtained from a similar experiment in EFM-19 cells are shown in Figure 4.19. Consistent with our previous findings, the oestrogen stimulated cells had a more alkaline pH_i with respect to that of untreated cells, under both external pH of 6.0 and 7.4. With the addition of 40 mM NH_4Cl, both withdrawn and oestrogen-treated cells incubated in a KHH solution at the external pH 7.4, showed a rapid increase in pH_i. There was a significant difference between the pH_i values of untreated and oestrogen-treated cells initially as well as during the first 10-20 minutes. Also the removal of NH_4Cl caused an even faster decline in pH_i. Although the recovery from 30-60 minutes appeared to be slightly faster in oestrogen stimulated cells, than in withdrawn cells (Figure 4.19B), there was no statistically significant difference observed during the recovery phases. When both withdrawn and oestrogen-treated cells were incubated in a KHH solution of pH 6.0, the pH_i continued to decrease when NH_4Cl was added. Also the removal of NH_4Cl lead to a further decrease in pH_i (Figure 4.19A). A similar effect was observed in EFM-19 cells cultured in full DMEM media when incubated with pH 6.0 KHH (Figure 4.17B). These cells do not seem to be able to increase its pH_i and reach its initial baseline pH_i. The difference in pH_i between untreated and oestrogen-treated cells was significant at 30 minutes ($p=0.0493$, ANOVA) and at 40 minutes ($p=0.0243$, ANOVA).

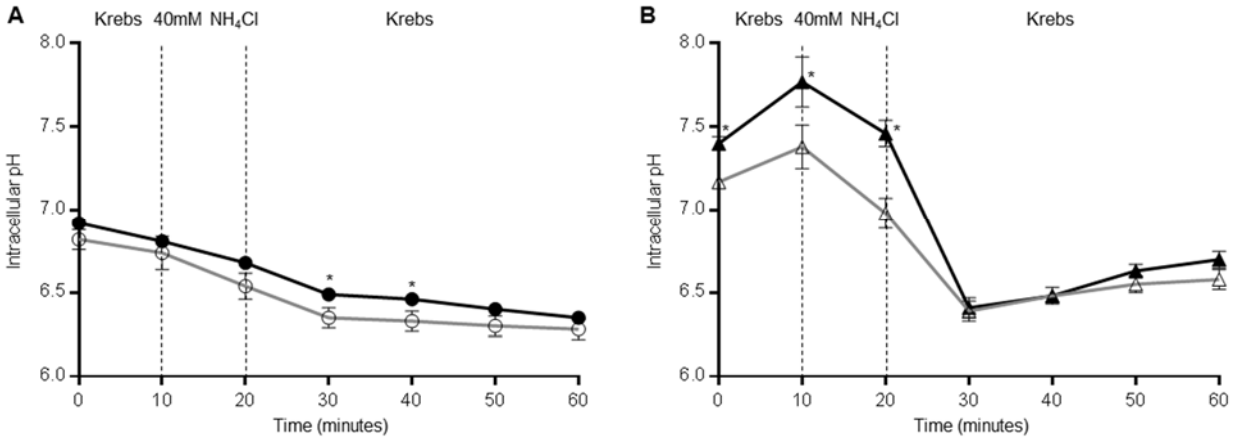

Figure 4.19 Effect of 40 mM NH_4Cl on pH_i of EFM-19 cells in the absence and presence of oestrogen. EFM-19 were seeded at a density of 5,000 cells per well in 96-well plates in routine culture medium. Cells were cultured in steroid depleted media for 5 days. For a further 5 days, cells were grown in phenol-red-free media alone or in the presence of 10^{-9} M of 17β-oestradiol. Cells were washed with KHH solution once and incubated with 10 μM BCECF-AM for 15 mins. Cells were then washed once with KHH solution and incubated with either a KHH solution of pH 6.0 or a KHH solution of pH 7.4. Fluorescence intensities at 485 nm and 420 nm were determined using the FLUOstar Omega plate reader. After the initial fluorescent readings were taken, cells were incubated with 40 mM NH_4Cl for 10 mins. Then NH_4Cl was aspirated and KHH solutions of pH 6.0 and pH 7.4 were added to the appropriate cells. Fluorescence intensity readings were measured at 10 min intervals for a period of 60 mins in total. The ratio of absorbance at 485 nm and 420 nm was calculated and the pH_i was estimated from the calibration curve. **A.** The effect of 40 mM NH_4Cl on intracellular pH of EFM-19 cells, comparing untreated cells ($-E_2$ ○) with oestrogen stimulated cells ($+E_2$ ●) at an external pH of 6.0. and **B.** comparing untreated cells ($-E_2$ △) with oestrogen stimulated cells ($+E_2$ ▲) at an external pH of 7.4. The image shown is representative of an experiment which has been replicated three times. *$p < 0.05$ by ANOVA. Error bars indicate standard errors of the mean of four replicates per condition.

4.7 Discussion

4.7.1 Expression and localisation

Previous studies have shown that the *PDZK1* gene is regulated by oestrogen in breast and ovarian cancer (Ghosh *et al.*, 2000; Walker *et al.*, 2007; Wright *et al.*, 2009). In this chapter, the expression of the NHERF3 protein encoded by *PDZK1* and the oestrogen regulation of *PDZK1* in three oestrogen-responsive cell lines was investigated. Western transfer analysis detected the expression of NHERF3 protein in four out of six oestrogen-responsive cell lines studied. The NHERF3 antibody detected two protein bands, one with an approximate molecular mass of 66 kDa and the other of 46 kDa in cells cultured in routine culture medium. The 66 kDa protein band is likely full length NHERF3, as it has a close approximation to the theoretical molecular mass of the NHERF3 protein.

None of the oestrogen-unresponsive cell lines expressed NHERF3. Amongst the oestrogen-responsive cell lines, ZR-75 expressed the highest levels of NHERF3, followed by MCF-7, T47-D and EFM-19. Amongst the oestrogen-responsive cell lines, the NHERF3 protein expression in MCF-7 cells, and not T47-D cells was consistent with the findings of O'Leary PC *et al.* (2013). The authors showed that T47-D cells expressed the most amount of NHERF3 protein. Similar to the observations in this chapter, these authors did not detect any NHERF3 expression in the oestrogen-unresponsive cell lines.

The cytoplasmic localisation of NHERF3 was confirmed by immunofluorescence in all three cell lines MCF-7, EFM-19 and EFF-3. Similarly, previous studies have demonstrated localisation of NHERF3 to the cytoplasm and sub-apical regions in opossum kidney (OK) cells and in colorectal adenocarcinoma-brush border expressing Caco2-BBE cells (Pribanic *et al.*, 2003; Zachos *et al.*, 2009).

4.7.2 Oestrogen regulation

The effect of oestrogen on the expression of NHERF3 protein was demonstrated in this study. Cells cultured in steroid-depleted media in the absence of oestradiol showed no expression of NHERF3, whereas cells grown in the presence of 10^{-9} M oestradiol expressed significant levels of NHERF3 protein. The 46 kDa protein band detected in cells grown in full media was not detected in cells cultured either in steroid withdrawn media or in oestrogen treated media. Although there was no detectable expression of NHERF3 in EFF-3 cells cultured in routine culture medium, very low levels of NHERF3 protein were detected in oestrogen-treated EFF-3 cells. These results suggest that oestrogen induces NHERF3 protein expression fairly rapidly in MCF-7 and EFM-19 cells. However, in EFF-3 cells the induction of NHERF3 by oestrogen occurs late that is after 6 days of oestradiol treatment.

During this study, Kim *et al.* (2013) published their work in which they claim that there was no correlation between the expression of ERα and *PDZK1* despite no data actually being shown. These authors also reported that there was a significant correlation between PDZK1 and IGF1R expression, and that the activity of IGF1R directly mediates *PDZK1* via the stimulation of ERα. However,

they came to this conclusion of an association between induction of PDZK1 and IGF1R, based on the immunohistochemical analysis of thirty two breast cancer cases. Previously, results from our group indicated that IGF1R was expressed in all ERα-positive and also in all ERα-negative cell lines (Davison *et al.*, 2011). Results from this chapter indicate that all oestrogen-responsive cells with the exception of BT-474 and none of the oestrogen-unresponsive cells express NHERF3 further confirming its regulation via oestrogen. It is also important to note that the addition of 1 µg/ml insulin to the phenol-red free DMEM in the current study, could be accountable to the differences in the results observed between the present study and the results from Kim *et al.* (2013) as they have not added insulin to the media. Insulin can bind to IGF1R with low affinity. Similarly, the ligand IGF-1 can also bind to the insulin receptor (IR) with a lower affinity than to IGF1R. Additionally, data from this chapter clearly suggest that NHERF3 expression is regulated by oestradiol, as cells grown in withdrawal media in the absence of oestrogen do not express any NHERF3 protein at all, despite insulin being present in the media. Therefore it is difficult to come to a definite conclusion that NHERF3 is indirectly regulated by IGF1R ligands. Often, findings from Kim *et al.* (2013) study were consistent with data from the present study. In MCF-7 cells, the NHERF3 protein expression was increased after 36 hours of oestrogen treatment, which agree with the demonstration in this study that the expression of NHERF3 increased from 2 days and lasted for up to 10 days. In addition, the Kim *et al.* (2013) study reported that oestrogen induced mainly the expression of NHERF3 located in the cytoplasm with some partial nuclear localisation.

4.7.3 Regulation of Na^+/H^+ exchange

NHERF3 is responsible for organisation of multiprotein complexes in the proximity of the plasma membrane of epithelial cells. NHERF3 anchors and regulates proteins and transporters such as the Na^+/H^+ exchangers that are responsible for the maintenance of intracellular pH (Thomson *et al.*, 2005). The current study demonstrated that the expression of NHERF3 is regulated by oestrogen. Hence the involvement of NHERF3 in the regulation of the cellular distribution of Na^+/H^+ exchangers in MCF-7 and EFM-19 cells was tested. An

established pH-sensitive fluorophore, BCECF-AM was used in the measurement of intracellular pH.

Initially, the steady-state pH_i of MCF-7 and EFM-19 cells cultured in routine culture medium was measured. Findings indicated that the pH_i of both MCF-7 and EFM-19 cells is closely similar to the external physiological pH of 7.4. The resting pH_i of MCF-7 breast cancer cells from previous studies were similar to the values obtained in the present study (Turturro *et al.*, 2004; Friday *et al.*, 2007). When the external pH is highly acidic at 6.0, the cells' internal pH_i becomes acidic. Although the pH_i is acidic, it is prevented from reaching equilibrium with the external pH, by pH regulatory mechanisms. Na^+/H^+ exchangers are ATP-independent and can only function using the driving force of the electrochemical Na^+ gradient which is directed inwards. The Na^+/H^+ exchangers exchange one Na^+ ion in for one H^+ ion out. Therefore in these breast cancers cells exposed to acidic external pH, the Na^+/H^+ exchangers are partially effective and the pH_i is not maintained at physiological values. Results from the pH_i measurements made in MCF-7 cells, either withdrawn or oestrogen-treated, indicated that at pH 7.4, there is no change in Na^+/H^+ exchange, whereas at pH 6.0, there is a decreased capacity of the Na^+/H^+ exchangers to regulate pH. Alternatively in comparison to withdrawn cells, oestrogen-treated EFM-19 cells demonstrated an increase in buffering capacity when exposed to KHH solutions at both pH 6.0 and pH 7.4.

MCF-7 and EFM-19 cells grown in full media were subject to volume regulatory stress with the addition of mannitol. In acidic external pH, both cell lines responded by increasing pH_i, thus representing hypertonic activation of the Na^+/H^+ exchangers. Results from the experiments testing the effect of mannitol in withdrawn and oestrogen-treated MCF-7 cells, depicted that at external pH 6.0, the withdrawn cells do not have the capacity to regulate pH_i. In contrast to the findings from MCF-7 cells grown in full media, the oestrogen-treated MCF- 7 cells show a further decrease in the ability to maintain pH_i. MCF-7 cells grown in the absence or presence of oestrogen did not respond well to hypertonicity. In EFM-19 cells that were withdrawn from growth factors and steroids, the addition of mannitol did not hypertonically activate Na^+/H^+ exchangers. However

oestrogen-treated EFM19 cells show an increase in activity in comparison to the withdrawn cells. The effect of mannitol in EFM-19 cells is not consistent with the results obtained from cells grown in full medium.

The addition of NH_4Cl causes an immediate cellular alkalisation followed by a slow pH_i recovery in response to cellular acidosis. The passive entry of NH_3 causes pH_i alkalisation initially, which then ceases as the intracellular and extracellular NH_3 concentrations reach equilibrium. The removal of external NH_4Cl, leads to acidification of the cytosol. Therefore cells recover their internal pH via Na^+/H^+ exchange or Cl^-/HCO_3^- exchange. Results obtained from this study indicate that in both MCF-7 and EFM-19 cells at external pH 7.4, the addition of NH_4Cl alkalinises pH_i and the removal of NH_4Cl leads to acidification of pH_i. The slow recovery of pH_i is due to regulation by Na^+/H^+ exchangers. Other studies have demonstrated that MCF-7 cells express Na^+/H^+ exchangers particularly NHE1 and NHE3 (Turturro *et al.*, 2004; Mehdawi *et al.*, 2012; Amith *et al.*, 2015; Wang *et al.*, 2015). When the cells are exposed to an external pH of 6.0, the pH_i does not vary much after being exposed to NH_4Cl. This is because the Na^+/H^+ exchangers are limited in their ability to extrude H^+ ions against the electrochemical gradient. Furthermore, data from MCF-7 cells cultured in withdrawal media and in oestrogen-supplemented media do not show a difference in the expected direction in response to recovery of pH_i after acidification. In oestrogen-stimulated EFM-19 cells at external pH 7.4, although there was a slight increase in recovery in comparison to oestrogen-depleted cells, it did not reach statistical significance.

4.8 Conclusion

Together, results from this chapter show that NHERF3 expression is limited to oestrogen-responsive cells and that its expression is regulated by oestradiol. The increase in NHERF3 protein expression is consistent with the results obtained from microarray analysis and confirms that oestrogen is an important regulator of *PDZK1* gene expression. The pH_i measurements provide evidence for the presence of Na^+/H^+ exchange in breast cancer cells MCF-7 and EFM-19. Despite the increase in NHERF3 protein expression in oestrogen-stimulated

cells there was no considerable difference in the ability of cells to recover pH_i. Therefore, it is still questionable whether NHERF3 provides an enhancement in pH_i regulatory capacity via activation of Na^+/H^+ exchangers at the plasma membrane.

Chapter 5. *SCNN1B* (ENaC-β)

5.1 Introduction

The *SCNN1B* gene encodes the epithelial sodium channel β subunit (ENaC-β). The epithelial sodium channel consists of three subunits namely ENaC-α, ENaC-β and ENaC-γ. A fourth subunit ENaC-δ has also been identified more recently in human epithelial cells (Yamamura *et al.*, 2008). The three subunits α, β and γ form heterotrimeric transmembrane segments and span the apical membrane of epithelial cells. Proteolytic cleavage and post-translational modifications are important for the regulation of activity and expression of ENaC.

The epithelial sodium channel is located in the apical surface of many epithelial cells types, including the lung, kidney, breast, salivary ducts and colon (Garty and Palmer, 1997; Gambling *et al.*, 2004; Quesnell *et al.*, 2007a). Correct function of ENaC is crucial for the maintenance of sodium homeostasis of cells. ENaC plays a role in the regulation of blood pressure and blood volume (Rossier *et al.*, 2002). ENaC is involved in cell migration. Cells that have migrated through narrow spaces activate ENaC in response to shrinkage to allow them to regain their cell volume (Cuddapah and Sontheimer, 2011). Studies have shown that knockdown of ENaC prevents cell migration (Kapoor *et al.*, 2009). Gain of function or loss of function mutations that result in increased or decreased activity of ENaC cause several diseases such as Liddle's syndrome, cystic fibrosis and type 1 pseudohypoaldosteronism (Knight *et al.*, 2006; Donaldson and Boucher, 2007).

The activity of ENaC is regulated by several hormones such as oestrogen, aldosterone, insulin and vasopressin (Nicco *et al.*, 2001; Liang *et al.*, 2010). These hormones activate ENaC, whereas bradykinin, epidermal growth factor (EGF) and endothelin inhibit ENaC activity (Gilmore *et al.*, 2001; Mamenko *et al.*, 2012). Drugs such as amiloride and benzamil are ENaC blockers that are used widely in studies to assess ENaC activity.

5.1.1 Aim

Previous data from microarray studies have identified the *SCNN1B* gene to be upregulated by oestrogen. This chapter aims to investigate the expression of ENaC-β protein in oestrogen-responsive breast cancer cell lines. The effect of 17β-oestradiol on the regulation of ENaC-β protein will be studied in MCF-7, EFM-19 and EFF-3 cells.

5.2 Expression of ENaC-β in breast cancer cells

5.2.1 Expression of ENaC-β in breast cancer cell lines

The protein expression of ENaC-β in different oestrogen-responsive and oestrogen-unresponsive cell lines was evaluated by western transfer analysis. Cells were cultured in full medium, lysed and proteins extracted and analysed by western transfer. Results are shown in Figure 5.1. Immunoreactive bands corresponding to a molecular mass of 72 kDa were detected in four oestrogen responsive, and three oestrogen unresponsive cell lines. Since the theoretical molecular mass of ENaC-β is 72 kDa coinciding with the observed band, we concluded that it is ENaC-β. We quantified this 72 kDa band only to produce the histogram (Figure 5.1B). Bands were also detected at approximately 30 kDa and 25 kDa in some cell lines. The highest expression of ENaC-β was detected in EFF-3 cells, followed by BT-474 and SKBR-3 expressing similar amounts. EFM-19, MDA-MB-231, Hs578T and MCF-7 expressed lower amounts of ENaC-β protein.

A band at 30 kDa was detected in the BT-20 cell line only. For the BT-20 cell line, there was no expression detected apart from the protein band of 30 kDa. The protein band at an apparent molecular mass of 25 kDa is more abundant than the 75 kDa band in SKBR-3 cells, whereas in EFF-3 and BT-474 cells, the 30 kDa band is much less abundant in comparison to the ENaC-β protein band at 72 kDa. There was no expression of ENaC-β in the oestrogen-responsive cell lines T47-D, ZR-75 and the oestrogen-unresponsive HBL-100 cells.

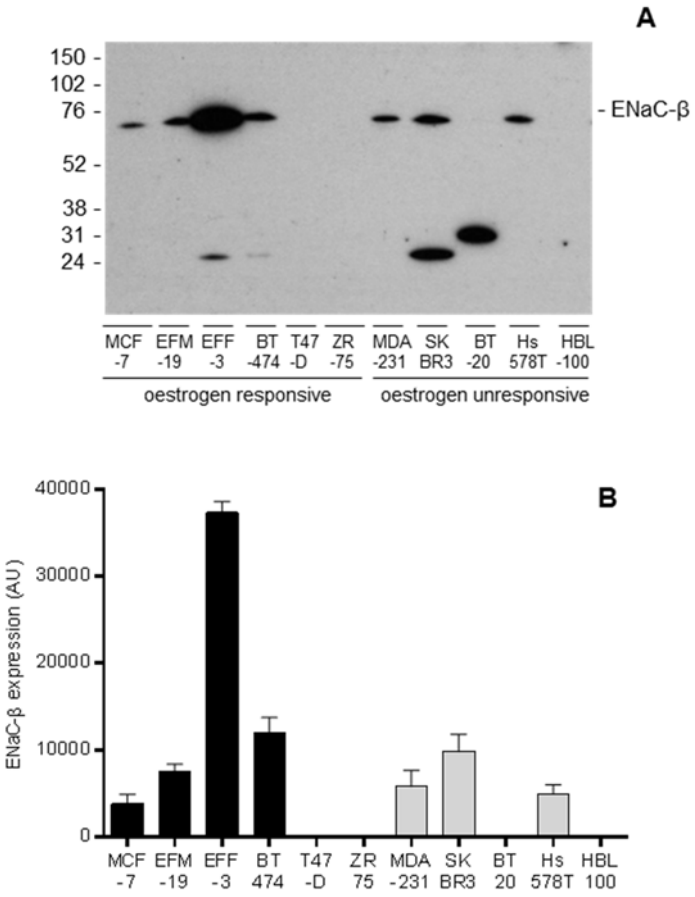

Figure 5.1 Expression of ENaC-β in breast cancer cells. Different breast cancer cell lines were cultured in routine culture medium in T75 flasks. Cells were lysed and protein extracts were prepared. Equal amounts of 20 µg of protein were separated by 12% polyacrylamide gel electrophoresis and then transferred to nitrocellulose membranes. The membranes were incubated with anti-ENaC-β antibody (1:100 dilution) overnight at 4 ºC, followed by horseradish peroxidase conjugated horse-anti-mouse secondary antibody for 1 hour at 37 ºC. Proteins were visualised by enhanced chemiluminescence with SuperSignal West Dura Extended Duration Substrate. **A.** The protein expression of ENaC-β was determined by Western transfer analysis in MCF-7, EFM-19, EFF-3, BT-474, T47-D, ZR-75, MDA-MB-231 (MDA-231), SKBR3, BT-20, Hs578T and HBL-100 cells. **B.** Densitometric quantification of ENaC-β. The black bars (■) represent oestrogen-responsive cell lines, whereas the grey bars (□) indicate the oestrogen-unresponsive cell lines. Error bars indicate standard errors of the mean of triplicate measurements.

5.3 Cellular localisation of ENaC-β in breast cancer cells

5.3.1 Localisation of ENaC-β in MCF-7, EFM-19 and EFF-3 cells

The localisation of ENaC-β in the three cell lines was evaluated. Cells were cultured in full media on coverslips in 6-well plates. Cells were fixed in 4% paraformaldehyde and permeabilised with saponin.

As illustrated in Figure 5.2, MCF-7 (A2) and EFM-19 (B2) cells showed immunoreaction within the nucleus and cytoplasm. For the EFF-3 (C2) cell line, we detected immunoreactions in the cytoplasm. There was also some expression of vesicular nature. There was no clear indication of any localisation to the cell membrane.

We found that different fixation and permeabilisation combinations gave rise to immunoreactions at different locations within the cell (data not shown). Mostly fixation with either methanol or 4% paraformaldehyde and permeabilisation with either triton or saponin showed immunofluorescence reactions within the nucleus. However, in one instance only, fixation with 4% paraformaldehyde and permeabilisation with saponin showed some localisation at the cell membrane. Also there were variations in localisation amongst the three different cell lines. These data were not consistent. It may well be that the fixation and permeabilisation conditions allowed the antibody to access through the cell membrane and bind to non-specific sites within the cell. Since this antibody gave rise to several immunoreactive bands for western analysis too, it might suggest there is some binding of non-specific nature. Alternatively, the antibody might be recognising cleaved forms of ENaC, hence explaining the vesicular and cytoplasmic localisation. The reason for these mixed results is unclear, therefore this antibody was not investigated any further for immunofluorescence.

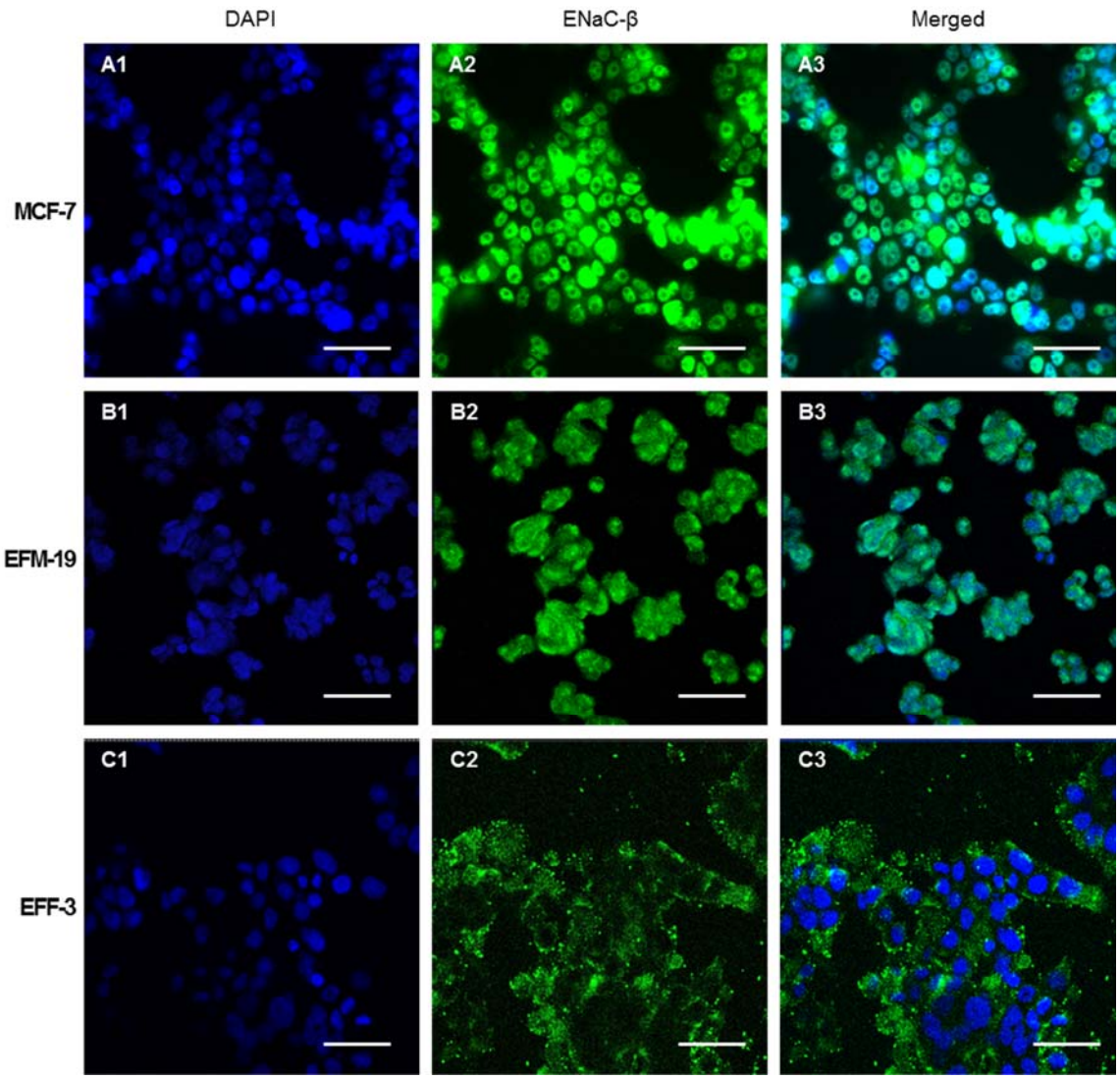

Figure 5.2 Localisation of ENaC-β in cell lines. MCF-7, EFM19 and EFF-3 cells were seeded onto coverslips in 6-well plates and cultured in routine culture medium for 24 hours. Cells were washed with PBS and fixed in 4% paraformaldehyde at room temperature. After fixation, cells were washed with PBS three times for 15 minutes each. Cells were then blocked in blocking buffer containing saponin for 1 hour at room temperature. The blocking medium was aspirated and the primary antibody ENaC-β was added at 1:50 dilution and incubated overnight at 4 ^{o}C. Cells were washed 3 times with PBS, 15 minutes each. The secondary antibody Alexa fluor 488 conjugated goat anti-mouse were added at a dilution of 1:1000 and were covered in foil and the cells were incubated for 1 hour at room temperature. Cells were washed 3 times with PBS. DAPI mounting media was added to the glass slides prior to placing the coverslip on the slide and the cells were examined under the fluorescent microscope (Leica DMR) using a 40x objective. Images A1, B1 and C1 show the nuclear staining, whereas the images A2, B2 and C2 show the immunoreaction for ENaC-β in MCF-7, EFM-19 and EFF-3 cells, respectively. The merged images A3, B3 and C3 show both nuclear (blue) and ENaC-β (green) staining combined together. Scale bar = 45 μm.

5.4 Clarification of the role of oestrogen in the regulation of ENaC-β

5.4.1 Regulation of ENaC-β protein expression by oestradiol in MCF-7 cells

The aim of these experiments was to determine the effects of oestrogen on the expression on ENaC-β. Cells were seeded onto 12-well plates and cultured in full media for 24 hours. Cells were then grown in withdrawal media for 5 days. Oestradiol was added to half the cells for a period ranging from 0 to 10 days.

The results shown in Figure 5.3 indicate a strong immunoreaction at 72 kDa that correspond to ENaC-β. Faint bands are observed at 50 kDa. ENaC-β is regulated by oestradiol after treatment for 6 days or longer. In comparison to untreated cells, there is a significant increase in protein expression when cells were grown in the presence of oestrogen.

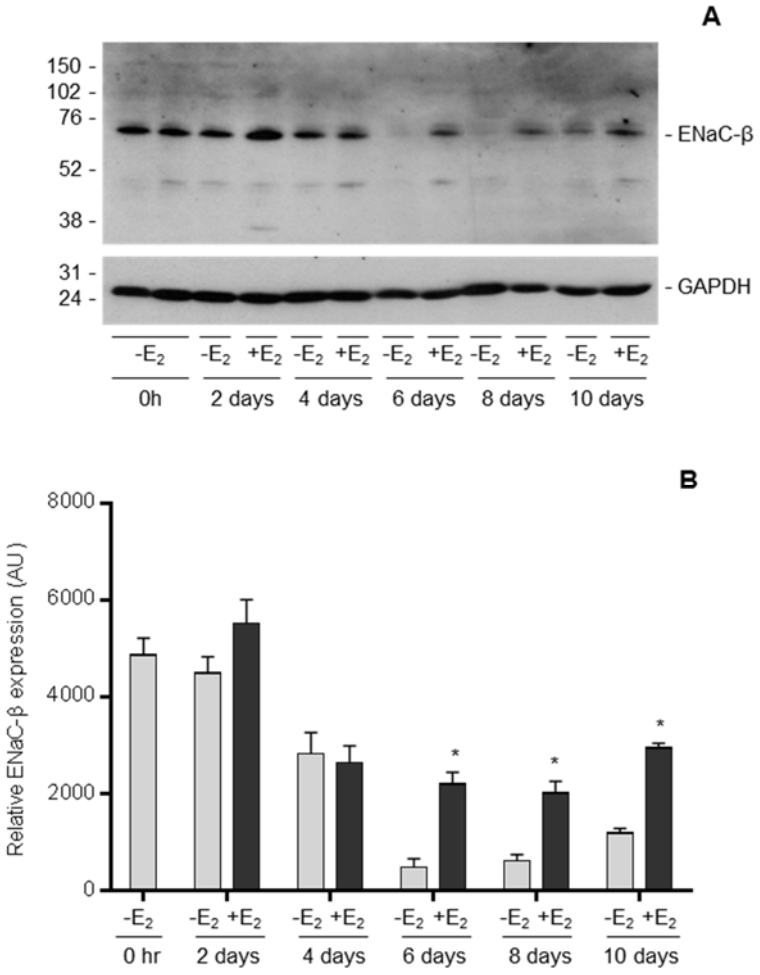

Figure 5.3 Regulation of ENaC-β protein expression in MCF-7 cells. Cells were steroid deprived by growing in phenol-red-free media containing 10% dextran-coated charcoal treated

serum and 1 µg/ml insulin, for 5 days and then treated with 10^{-9} M of 17β-oestradiol for different lengths of time upto 10 days. Both the oestradiol-treated and untreated cells were lysed and protein extracts prepared. Protein aliquots of 20 µg were separated by 12% polyacrylamide gel electrophoresis and then transferred to nitrocellulose membranes. The membranes were incubated with anti-ENaC-β antibody (dilution 1:100) overnight at 4 °C, followed by horseradish peroxidase conjugated horse-anti-mouse secondary antibody for 1 hour at 37 °C. Proteins were visualised by enhanced chemiluminescence with SuperSignal West Dura Extended Duration Substrate. **A.** The protein expression of ENaC-β in MCF-7 cells after oestrogen stimulation for a timecourse of 0 hours to 10 days, comparing serum withdrawn ($-E_2$ □) samples with oestrogen-stimulated ($+E_2$ ■) samples. Images shown are representative of results from experiments which have been replicated twice. **B.** Quantification of ENaC-β normalised against the corresponding GAPDH signal, *$p < 0.001$ by ANOVA. Error bars indicate SEM of triplicate measurements.

5.4.2 Regulation of ENaC-β protein expression by oestradiol in EFM-19 cells

Results from a similar experiment in EFM-19 cells are shown in Figure 5.4. In contrast to MCF-7 cells, only 72 kDa bands were observed. There was no additional band at detected around 50 kDa. The protein expression of untreated cells gradually declined with time. There was a marked increase in ENaC-β expression in the cells treated with oestrogen for 6 days or more. The stimulation of expression by oestrogen was greatest at 8 days, but decreased slightly at 10 days. Therefore we continued to treat cells for 8 days in future experiments.

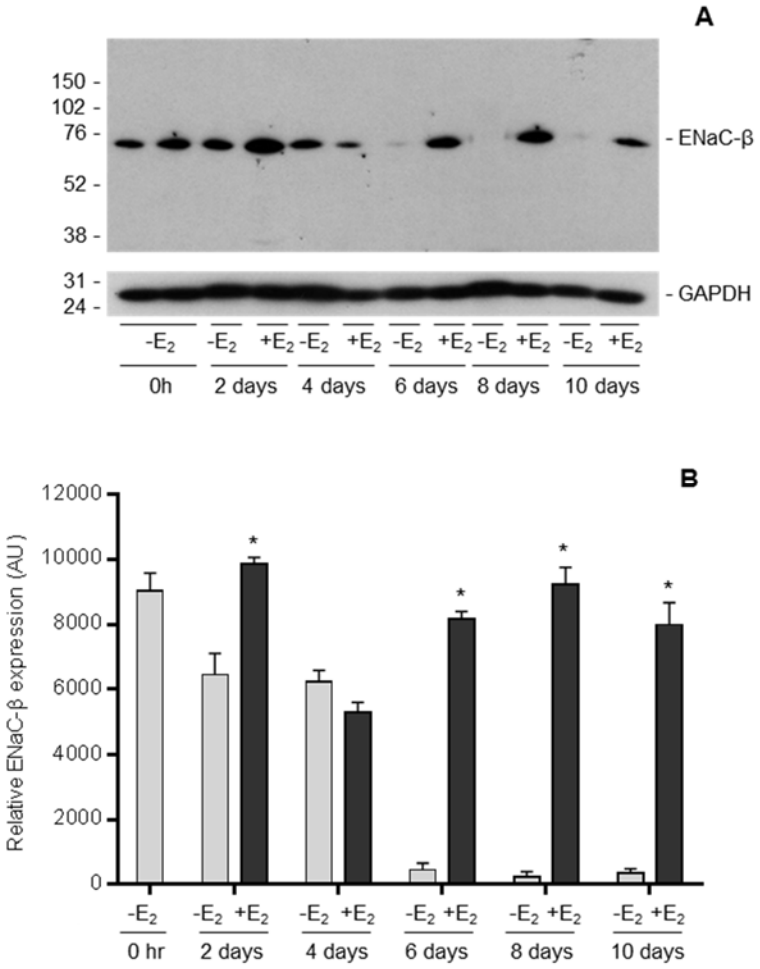

Figure 5.4 Regulation of ENaC-β protein expression in EFM-19 cells. Cells were steroid deprived by growing in phenol-red-free media containing 10% dextran-coated charcoal treated serum and 1 µg/ml insulin, for 5 days and then treated with 10^{-9} M of 17β-oestradiol for different lengths of time upto 10 days. Both the oestradiol-treated and untreated cells were lysed and protein extracts prepared. Protein aliquots of 20 µg were separated by 12% polyacrylamide gel electrophoresis and then transferred to nitrocellulose membranes. The membranes were incubated with anti-ENaC-β antibody (dilution 1:100) overnight at 4 ^{o}C, followed by horseradish peroxidase conjugated horse-anti-mouse secondary antibody for 1 hour at 37 ^{o}C. Proteins were visualised by enhanced chemiluminescence with SuperSignal West Dura Extended Duration Substrate. **A.** The protein expression of ENaC-β in EFM-19 cells after oestrogen stimulation for a timecourse of 0 hours to 10 days, comparing serum withdrawn (-E_2 □) samples with oestrogen-stimulated (+E_2 ■) samples. Images shown are representative of results from experiments which have been replicated twice. **B.** Quantification of ENaC-β normalised against the corresponding GAPDH signal, *p < 0.001 by ANOVA. Error bars indicate SEM of triplicate measurements.

5.4.3 Regulation of ENaC-β protein expression by oestradiol in EFF-3 cells

The effect of oestrogen treatment over time is shown in Figure 5.5. There is some background signal, but stronger immunoreactions are observed at 72 kDa and 50 kDa. In cells cultured in full media the 72 kDa band corresponding to

ENaC-β has a much greater expression than the withdrawn or oestrogen-treated cells. However, the diffused 50 kDa band expression is lower in cells in full media, in comparison to the withdrawn or oestrogen treated cells. ENaC-β expression was observed to increase in response to oestradiol. The differences were very small from 2 to 6 days, but there was a significant increase in ENaC-β expression at 8 and 10 days.

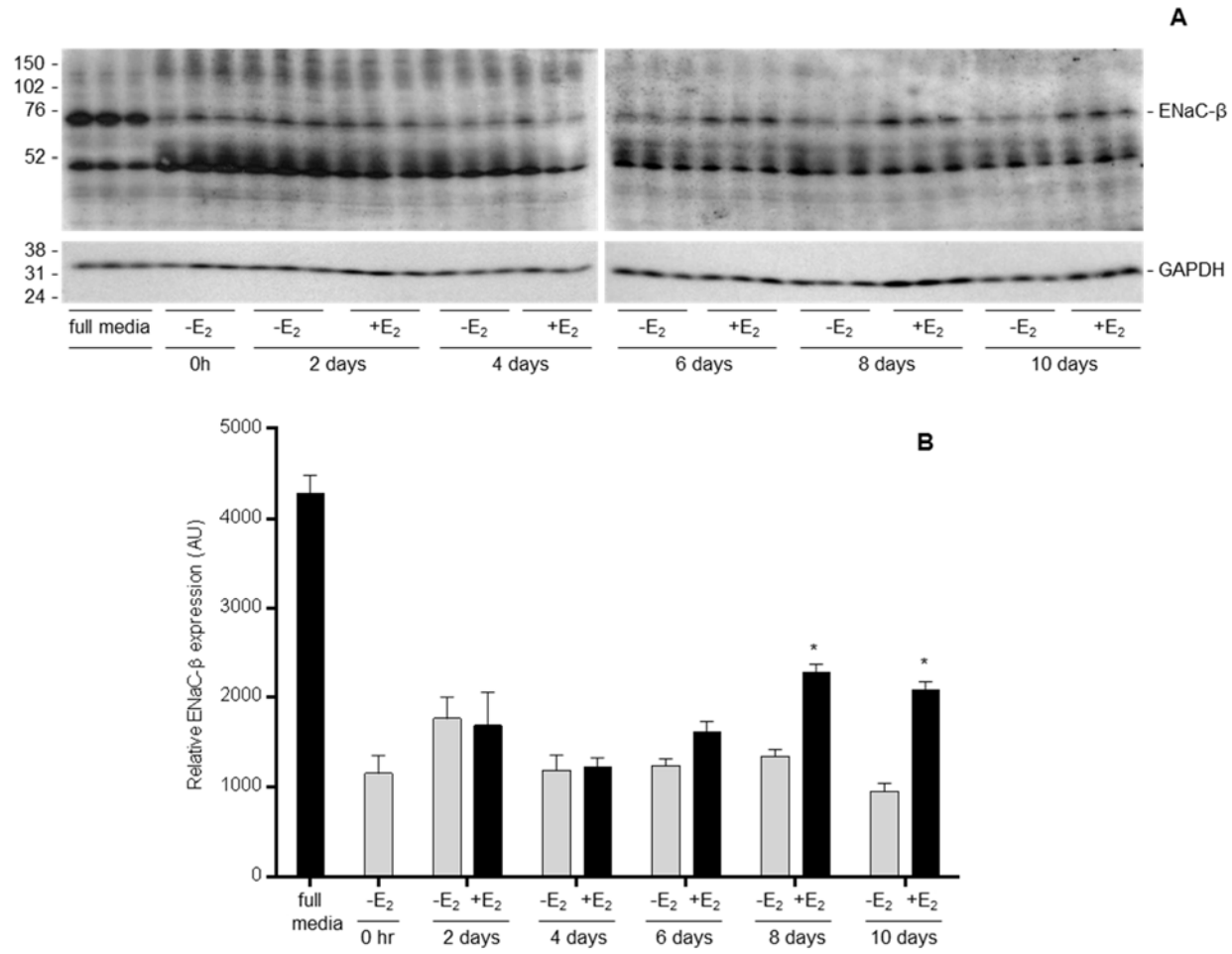

Figure 5.5 Regulation of ENaC-β protein expression in EFF-3 cells. Cells were steroid deprived by growing in phenol-red-free media containing 10% dextran-coated charcoal treated serum and 1 µg/ml insulin, for 5 days and then treated with 10^{-9} M of 17β-oestradiol for different lengths of time upto 10 days. Both the oestradiol-treated and untreated cells were lysed and protein extracts prepared. Protein aliquots of 20 µg were separated by 12% polyacrylamide gel electrophoresis and then transferred to nitrocellulose membranes. The membranes were incubated with anti-ENaC-β antibody (dilution 1:100) overnight at 4 °C, followed by horseradish peroxidase conjugated horse-anti-mouse secondary antibody for 1 hour at 37 °C. Proteins were visualised by enhanced chemiluminescence with SuperSignal West Dura Extended Duration Substrate. **A.** The protein expression of ENaC-β in EFF-3 cells after oestrogen stimulation for a timecourse of 0 hours to 10 days, comparing serum withdrawn ($-E_2$ □) samples with oestrogen-stimulated ($+E_2$ ■) samples. Images shown are representative of results from experiments which have been replicated twice. **B.** Quantification of ENaC-β normalised against the corresponding GAPDH signal, *p < 0.001 by ANOVA. Error bars indicate SEM of triplicate measurements.

5.5 Concentration dependent effects of oestradiol on the regulation of ENaC-β by oestrogen

5.5.1 Concentration dependent effects of oestradiol in MCF-7 cells

We investigated the concentration dependent effects of oestrogen on the expression of ENaC-β in MCF-7 cells. Cells were withdrawn from growth factors for 5 days and oestrogen treated with different concentrations of 17-β oestradiol ranging from 10^{-8} M to 10^{-13} M. As expected from our previous data, we observed immunoreactive bands at 72 and 50 kDa. Both bands were expressed in a concentration dependent manner. There was a dramatic increase from 10^{-12} M to 10^{-11} M, with the highest expression of the 72 kDa band (ENaC-β) at 10^{-10} M (Figure 5.6).

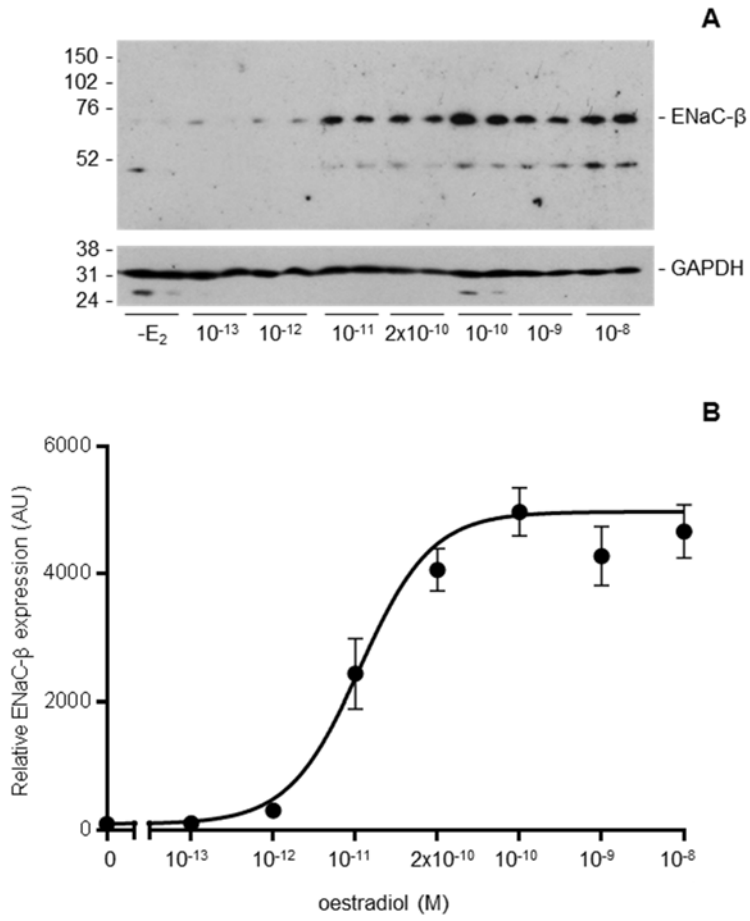

Figure 5.6 Effect of oestradiol on ENaC-β protein expression in MCF-7 cells. MCF-7 cells were seeded onto 24-well plates and withdrawn for 5 days and treated with different concentrations of oestradiol for a period of 8 days. Cells were lysed and protein extracts prepared. Protein aliquots of 10 µg were separated by 12% polyacrylamide gel electrophoresis and then transferred to nitrocellulose membranes. The membranes were incubated with anti-ENaC-β antibody (dilution 1:100) overnight at 4 ^{o}C, followed by horseradish peroxidase conjugated horse-anti-mouse secondary antibody for 1 hour at 37 ^{o}C. Proteins were visualised

by enhanced chemiluminescence with SuperSignal West Dura Extended Duration Substrate. **A.** The protein expression of ENaC-β in MCF-7 cells treated with different concentrations of oestradiol for 8 days. Image shown are from a representative experiment which has been repeated three times. **B.** Densitometric quantification of ENaC-β with Labworks 4.0 software, normalised against the corresponding GAPDH signal. Error bars indicate SEM of duplicate measurements.

5.5.2 Concentration dependent effects of oestradiol in EFM-19 cells

Results from a similar concentration dependent experiment in EFM-19 cells are shown in Figure 5.7. The untreated cells have very low expression of ENaC-β. In comparison to MCF-7 cells, there was a marked increase in ENaC-β expression when EFM-19 cells were treated with an oestradiol concentration of 10^{-11} M. Also the maximal effect was observed to be at $2x10^{-10}$ M. In contrast to MCF-7 cells, there was no band detected at 50 kDa. The absence of the 50 kDa band was consistent with our previous findings.

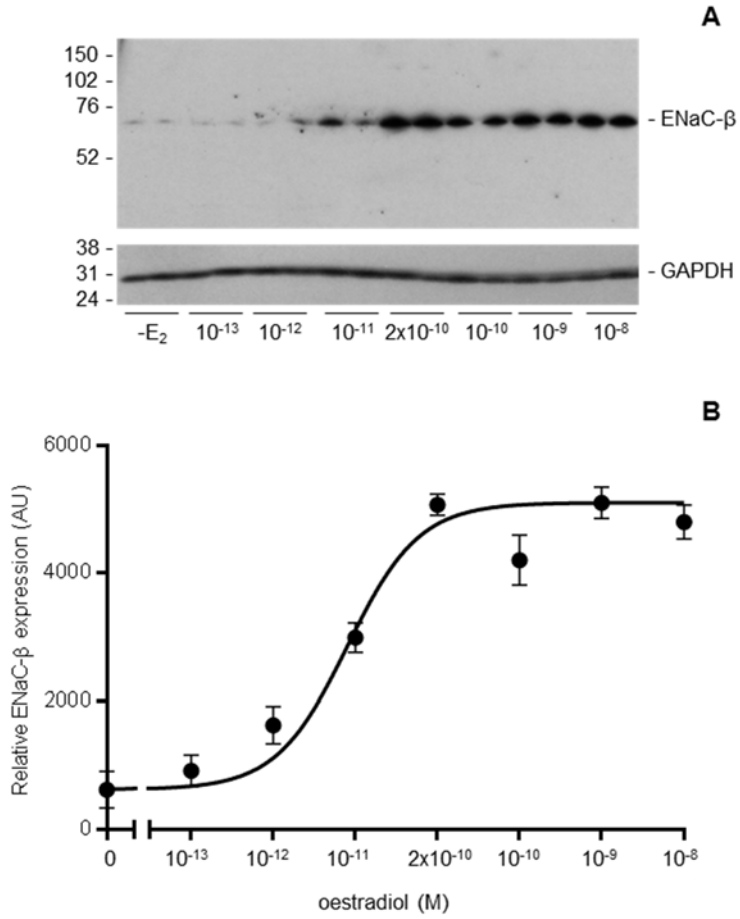

Figure 5.7 Effect of oestradiol on ENaC-β protein expression in EFM-19 cells. EFM-19 cells were seeded onto 24-well plates and withdrawn for 5 days and treated with different concentrations of oestradiol for a period of 8 days. Cells were lysed and protein extracts

prepared. Protein aliquots of 10 µg were separated by 12% polyacrylamide gel electrophoresis and then transferred to nitrocellulose membranes. The membranes were incubated with anti-ENaC-β antibody (dilution 1:100) overnight at 4 ^{o}C, followed by horseradish peroxidase conjugated horse-anti-mouse secondary antibody for 1 hour at 37 ^{o}C. Proteins were visualised by enhanced chemiluminescence with SuperSignal West Dura Extended Duration Substrate. **A.** The protein expression of ENaC-β in EFM-19 cells treated with different concentrations of oestradiol for 8 days. Image shown are from a representative experiment which has been repeated three times. **B.** Densitometric quantification of ENaC-β with Labworks 4.0 software, normalised against the corresponding GAPDH signal. Error bars indicate SEM of duplicate measurements.

5.5.3 Concentration dependent effects of oestradiol in EFF-3 cells

The effect of different concentrations of oestradiol on the expression of ENaC-β protein in EFF-3 cells was assessed. As shown in Figure 5.8, bands were detected at 72 kDa and a lower expression of the 50 kDa band too. The expression of ENaC-β remained unchanged in the untreated and oestrogen treated cells upto 10^{-11} M. A significant increase in expression was observed thereafter from increasing concentrations of $2x10^{-10}$ M upto 10^{-8} M.

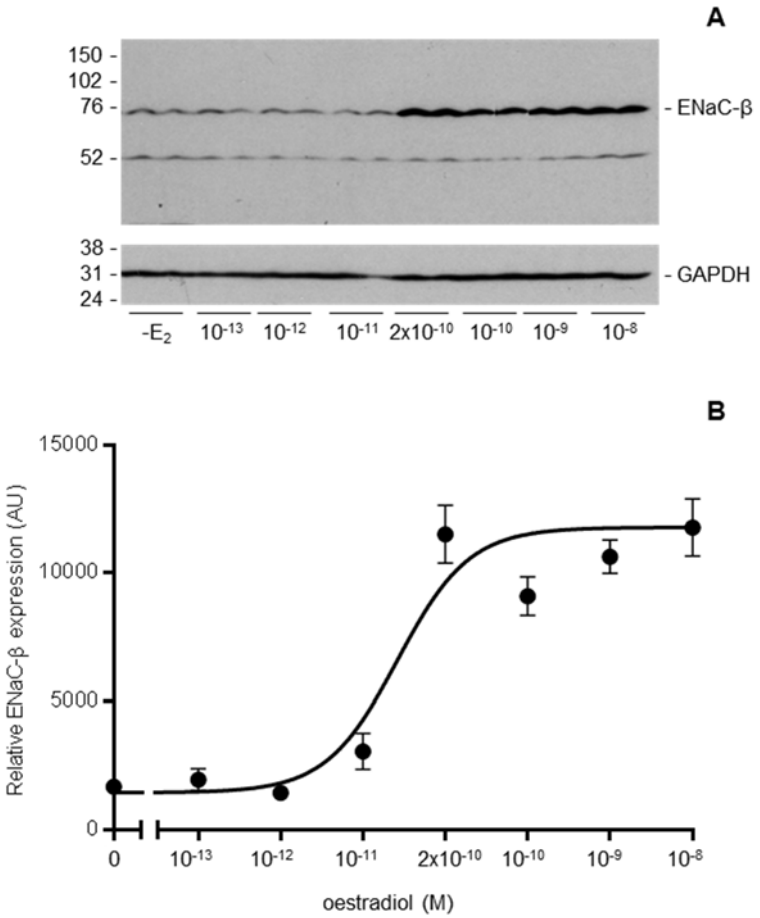

Figure 5.8 Effect of oestradiol on ENaC-β protein expression in EFF-3 cells. EFF-3 cells were seeded onto 24-well plates and withdrawn for 5 days and treated with different concentrations of oestradiol for a period of 8 days. Cells were lysed and protein extracts prepared. Protein aliquots of 10 µg were separated by 12% polyacrylamide gel electrophoresis and then transferred to nitrocellulose membranes. The membranes were incubated with anti-ENaC-β antibody (dilution 1:100) overnight at 4 ^{o}C, followed by horseradish peroxidase conjugated horse-anti-mouse secondary antibody for 1 hour at 37 ^{o}C. Proteins were visualised by enhanced chemiluminescence with SuperSignal West Dura Extended Duration Substrate. **A.** The protein expression of ENaC-β in EFF-3 cells treated with different concentrations of oestradiol for 8 days. Image shown are from a representative experiment which has been repeated three times. **B.** Densitometric quantification of ENaC-β with Labworks 4.0 software, normalised against the corresponding GAPDH signal. Error bars indicate SEM of duplicate measurements.

5.6 Discussion

5.6.1 Expression and localisation

The expression, localisation and the effect of oestrogen on the regulation of ENaC-β protein was studied in detail in this chapter. ENaC-β protein was detected in the oestrogen-responsive cell lines MCF-7, EFM-19, EFF-3 and BT-474 with the highest expression being in EFF-3 cells. Out of the five oestrogen-unresponsive cell lines, only three cell lines MDA-MB-231, SKBR-3 and Hs578T expressed ENaC-β protein. The cell lines T47-D, ZR-75, BT-20 and HBL-100 did not express any ENaC-β. Two other studies have also reported the expression of ENaC-β mRNA and protein in the normal breast epithelial cell line MCF-10A and cancerous breast cell lines MCF-7 and T47-D (Boyd and Naray-Fejes-Toth, 2007; Wang and Schultz, 2014). Although Boyd and Naray-Fejes-Toth (2007) showed that T47-D cells express ENaC-β mRNA, the current study did not detect any ENaC-β protein in T47-D cells. A possible explanation for this inconsistency may be that ENaC-β mRNA is not translated into protein. However, this study did not investigate the mRNA expression of ENaC-β in breast cancer cells lines; therefore it is difficult to come to a definite conclusion.

The localisation of ENaC-β in oestrogen-responsive cell lines was determined by immunofluorescence. However the antibody did not detect ENaC-β at the cell membrane, instead immunoreactions were observed intracellularly, either in the nuclei or cytoplasm of these cells. There was also some evidence of vesicular expression. These results were in agreement with studies in a mouse collecting duct cell line (Dooley *et al.*, 2013) and also in the renal collecting

system of rats (Hager *et al.*, 2001; Sauter *et al.*, 2006), in which ENaC-β was detected in the cytoplasm. It is difficult to interpret this result of the lack of ENaC-β expression in the plasma membrane, but it could be related to vesicular trafficking of ENaC to the cell membrane. Nevertheless, discrepancies in the data obtained, led to the conclusion that this antibody was unsuitable for immunofluorescence. Therefore this antibody was not investigated any further to study the localisation of ENaC-β.

5.6.2 Oestrogen regulation

One of the main objectives was to evaluate the effects of oestrogen on the regulation of ENaC-β expression. Other studies have investigated the regulation of ENaC by steroidal and non-steroidal hormones; aldosterone, dexamethasone, vasopressin, oestrogen and progesterone (Gambling *et al.*, 2004; Boyd and Naray-Fejes-Toth, 2007; Liang *et al.*, 2010; Frindt and Palmer, 2012; Qi *et al.*, 2014; Yusef *et al.*, 2014). The effect of oestrogen on the expression of ENaC-β is controversial as some studies have shown that oestrogen increases the expression of ENaC-β (Gambling *et al.*, 2004; Riazi *et al.*, 2006; Chinigarzadeh *et al.*, 2015), whereas other studies have reported conflicting results. Yusef *et al.* (2014) showed that the total protein expression of ENaC-β was unchanged in a mouse collecting duct cell line treated with oestrogen for 30 minutes. Laube *et al.* (2011) reported that oestrogen alone does not increase the ENaC-β mRNA expression, instead the presence of both oestrogen and progesterone is required to induce expression of ENaC-β. Results from this chapter showed that there is an increase in the expression of ENaC-β in response to oestrogen in the breast cancer cells MCF-7, EFM-19 and EFF-3. The induction of ENaC-β protein was clearly evident and a significant difference was observed after 6 days of treatment with oestradiol in MCF-7 and EFM-19 cells and after 8 days in EFF-3 cells. This is the first study that investigates the role of oestrogen in regulation of ENaC-β expression in breast cancer cells. The present study showed that ENaC-β protein expression increased in an oestrogen concentration dependent manner in all three cell lines.

5.7 Conclusion

In conclusion, the results described in this chapter has shown that ENaC-β is expressed in a wide range of oestrogen-responsive and oestrogen-unresponsive breast cancer cell lines. The effect of oestrogen on ENaC-β protein expression was studied in detail. The expression of ENaC-β has been shown to increase in MCF-7, EFM-19 and EFF-3 cells stimulated with oestrogen. The EFF-3 cells were slower to respond in comparison to the other two cell lines.

Chapter 6. Role of anti-oestrogens

6.1 Introduction

Oestrogen receptor positive breast cancers are commonly treated with endocrine receptor-based therapies. Inhibition of the action of oestrogen by endocrine therapy has resulted in a decrease in mortality rates (Early Breast Cancer Trialists' Collaborative *et al.*, 2011b). Approximately two-thirds of breast cancers are hormone-responsive and respond to endocrine therapy. However, many patients either do not respond to endocrine therapy or acquire resistance with time.

Anti-oestrogens such as tamoxifen are often administered to patients with oestrogen receptor positive disease and have prolonged the survival of these patients (Osborne, 1998; Pritchard, 2005). 4-hydroxytamoxifen is a more potent active metabolite of tamoxifen which was detected in plasma and tumour extracts (Robinson and Jordan, 1988). Fulvestrant is a pure ER antagonist and has been shown to have no oestrogen agonist activity (DeFriend *et al.*, 1994b). Anti-oestrogens such as raloxifene, bazedoxifene and lasofoxifene used in the prevention and treatment of osteoporosis have also been beneficial in the treatment of breast cancer.

The concentrations of anti-oestrogens were chosen according to their binding affinities for the oestrogen receptor (Blair *et al.*, 2000; Li *et al.*, 2012). Previous studies have shown that tamoxifen alone is effective at 10^{-7} M, while a concentration of $5x10^{-6}$ M provides a more effective inhibition of the actions of oestrogens when tamoxifen is competing with oestrogen (Johnson *et al.*, 1989; Molloy *et al.*, 2000). 4-hydroxytamoxifen has a stronger ER binding affinity than tamoxifen (Favoni and de Cupis, 1998). Raloxifene and bazedoxifene are similar in structure and their binding affinities for ER were similar to each other. All three anti-oestrogens tamoxifen, raloxifene and lasofoxifene have a similar mechanism of action. They bind to the ligand binding domain of the ER and induce a change in conformation in which helix 12 is repositioned to occupy the AF-2. The blockage of the AF-2 prevents the binding of coactivators to its surface (Brzozowski *et al.*, 1997; Vajdos *et al.*, 2007). Toremifene is a tamoxifen

analogue, with comparable binding affinities for the ER. Therefore toremifene was added to the culture medium at 10^{-7} M. Fulvestrant was previously shown to be effective at 10^{-8} M (Molloy *et al.*, 2000), and the anti-oestrogen lasofoxifene had a similar ER binding affinity to that of fulvestrant, therefore lasofoxifene was added at a concentration of 10^{-8} M (Gennari *et al.*, 2006).

Anti-oestrogen	**Binding affinity for ER**	**Concentration**
Tamoxifen	5.55 x 10^{-8} M	10^{-7} M 5x10^{-6} M
4-Hydroxytamoxifen	5.13 x 10^{-10} M	10^{-8} M
Fulvestrant	2.40 x 10^{-9} M	10^{-8} M
Bazedoxifene	2.60 x 10^{-8} M	10^{-7} M
Toremifene	6.50 x 10^{-8} M	10^{-7} M
Raloxifene	7.58 x 10^{-8} M	10^{-7} M
Lasofoxifene	1.50 x 10^{-9} M	10^{-8} M

Table 6.1 Binding affinities of anti-oestrogens. Anti-oestrogens and their binding affinities for the oestrogen receptor.

Previous chapters have confirmed the repression of NKCC1 and induction of NHERF3 and ENaC-β in response to oestrogen. The experiments described in this chapter were designed to determine the agonist and oestrogen antagonist effects of anti-oestrogens on the protein expression of NKCC1, NHERF3 and ENaC-β.

6.2 Role of anti-oestrogens on NKCC1 expression

6.2.1 Characterisation of the agonist activity of anti-oestrogens on NKCC1 expression

The agonist effects of tamoxifen were tested at concentrations 10^{-7} M and $5x10^{-6}$ M, and the agonist effects of 4-hydroxytamoxifen and fulvestrant were tested at 10^{-8} M concentration. Cells were grown in steroid-withdrawn media for 5 days, followed by treatments with anti-oestrogens for 8 days.

The results for MCF-7, EFM-19 and EFF-3 cells are shown in Figure 6.1A, B and C, respectively. The protein expression of NKCC1 in MCF-7 and EFM-19 cells treated with the different anti-oestrogens were not significantly different from the NKCC1 expression in untreated cells. These results indicate that the anti-oestrogens tamoxifen, 4-hydroxytamoxifen and fulvestrant do not show agonist activity. At concentrations of 10^{-9} M oestradiol, expression of NKCC1 was decreased completely in MCF-7 cells. In comparison to untreated EFM-19 cells, a 9-fold reduction in NKCC1 expression was observed in the presence of 10^{-9} M oestradiol.

In EFF-3 cells, treatments with anti-oestrogens alone showed no oestrogen-like activity. The expression of NKCC1 was significantly higher in cells treated with 4-hydroxytamoxifen and fulvestrant with respect to the NKCC1 expression of untreated EFF-3 cells. The expression of NKCC1 decreased significantly when EFF-3 cells were treated with $2x10^{-10}$ M oestradiol.

Collectively, the anti-oestrogens tamoxifen, 4-hydroxytamoxifen and fulvestrant displayed no agonism in all three cell lines.

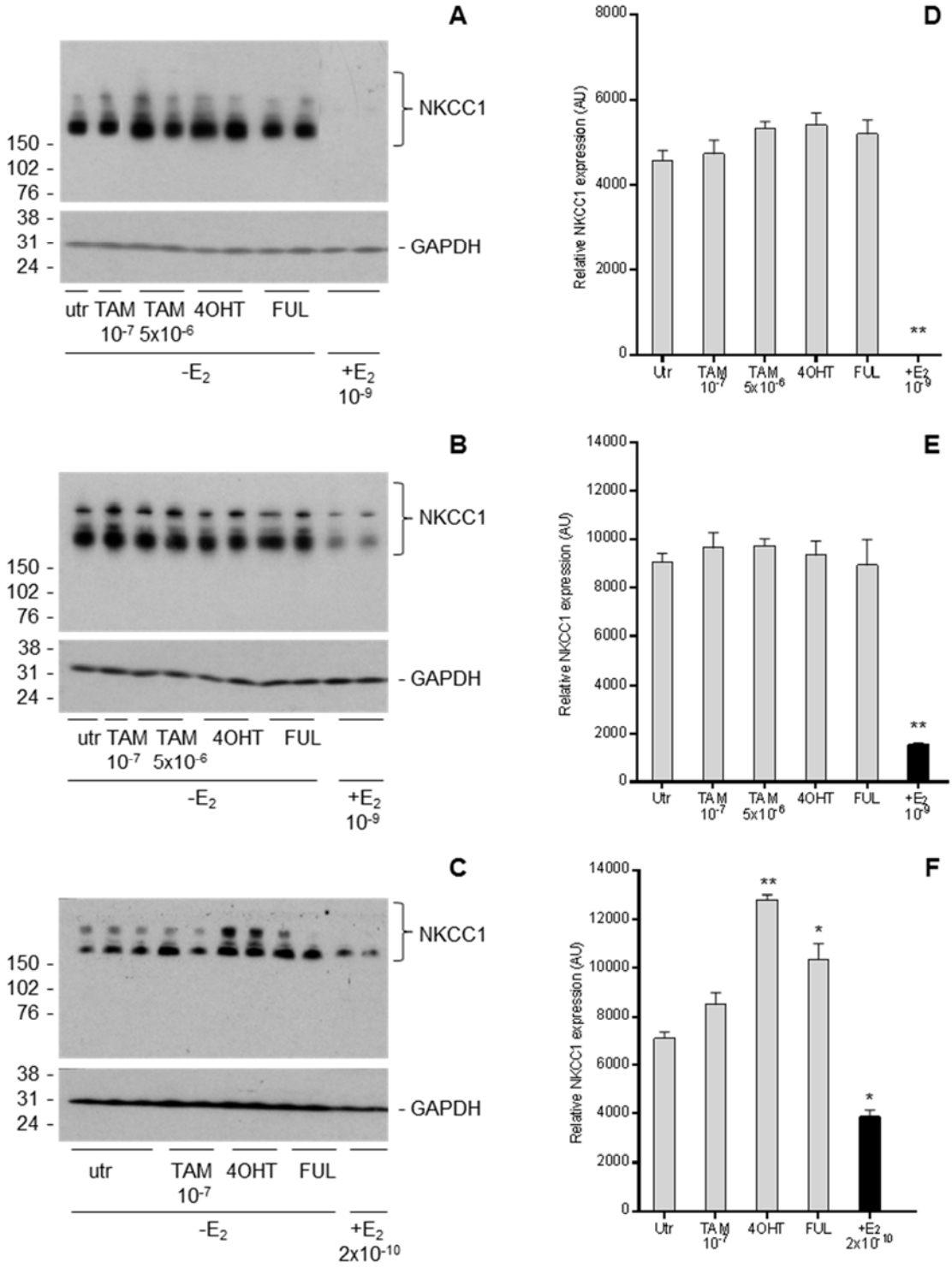

Figure 6.1 Agonist activity of anti-oestrogens on NKCC1 expression. MCF-7, EFM-19 (50,000 per well) and EFF-3 (100,000 per well) cells were plated onto a 24-well plate. Cells were steroid deprived by growth in phenol-red-free media containing 10% dextran-coated charcoal treated serum and 1 µg/ml insulin, for 5 days and then cultured in withdrawal medium alone (utr) or treated with either 10^{-7} M or $5x10^{-6}$ M tamoxifen (TAM), 10^{-8} M 4-hydroxytamoxifen (4OHT), 10^{-8} M Fulvestrant (FUL) and 10^{-9} M 17β-oestradiol alone for 8 days. Cells were lysed and protein extracts were prepared. Protein aliquots of 10 µg were separated by 12% polyacrylamide gel electrophoresis and then transferred to nitrocellulose membranes. The membranes were incubated with anti-NKCC1 antibody (dilution 1:10000) overnight at 4 ^{o}C,

followed by horseradish peroxidase conjugated goat-anti-rabbit secondary antibody for 1 hour at 37 ºC. Proteins were visualised by enhanced chemiluminescence with SuperSignal West Dura Extended Duration Substrate. **A, B, C.** The protein expression of NKCC1 in MCF-7, EFM-19 and EFF-3 cells treated with anti-oestrogens, comparing serum withdrawn (-E_2 □) samples with oestrogen-stimulated (+E_2 ■) samples. The images shown are representative of an experiment which has been replicated three times in MCF-7 and EFM-19 cells and twice in EFF-3 cells. **D, E, F.** Quantification of NKCC1 normalised against the corresponding GAPDH signal, *$p < 0.05$ and **$p < 0.001$ by ANOVA, compared with the untreated (utr) cells. Error bars indicate SEM of duplicate measurements.

The following experiments were designed to study the agonist effect of the anti-oestrogens bazedoxifene, toremifene, raloxifene and lasofoxifene on expression of NKCC1. Bazedoxifene, toremifene, and raloxifene were added at a concentration of 10^{-7} M, whereas lasofoxifene was added at 10^{-8} M. The results are shown in Figure 6.2.

The NKCC1 protein expression of MCF-7 cells treated with the different anti-oestrogens were similar to the NKCC1 expression in untreated cells. In the presence of 10^{-9} M oestradiol, a statistically significant decrease was observed.

In contrast to the results obtained from MCF-7 cells, bazedoxifene displays weak agonistic effects than toremifene, raloxifene and lasofoxifene in EFM-19 cells (Figure 6.2B). A 2.2-fold decrease in expression was observed in cells treated with bazedoxifene in comparison to untreated cells. This decrease was statistically significant.

In comparison to the untreated cells, the expression of NKCC1 did not vary much when EFF-3 cells were treated with bazedoxifene, toremifene, raloxifene and lasofoxifene alone. In the presence of oestradiol, the amount of NKCC1 protein detected was approximately 5.6-fold lower than that of untreated cells.

These results suggest that all four anti-oestrogens bazedoxifene, toremifene, raloxifene and lasofoxifene do not exert any agonist activity in MCF-7 and EFF-3 cells. However, bazedoxifene was obeserved to be weakly agonistic in EFM-19 cells.

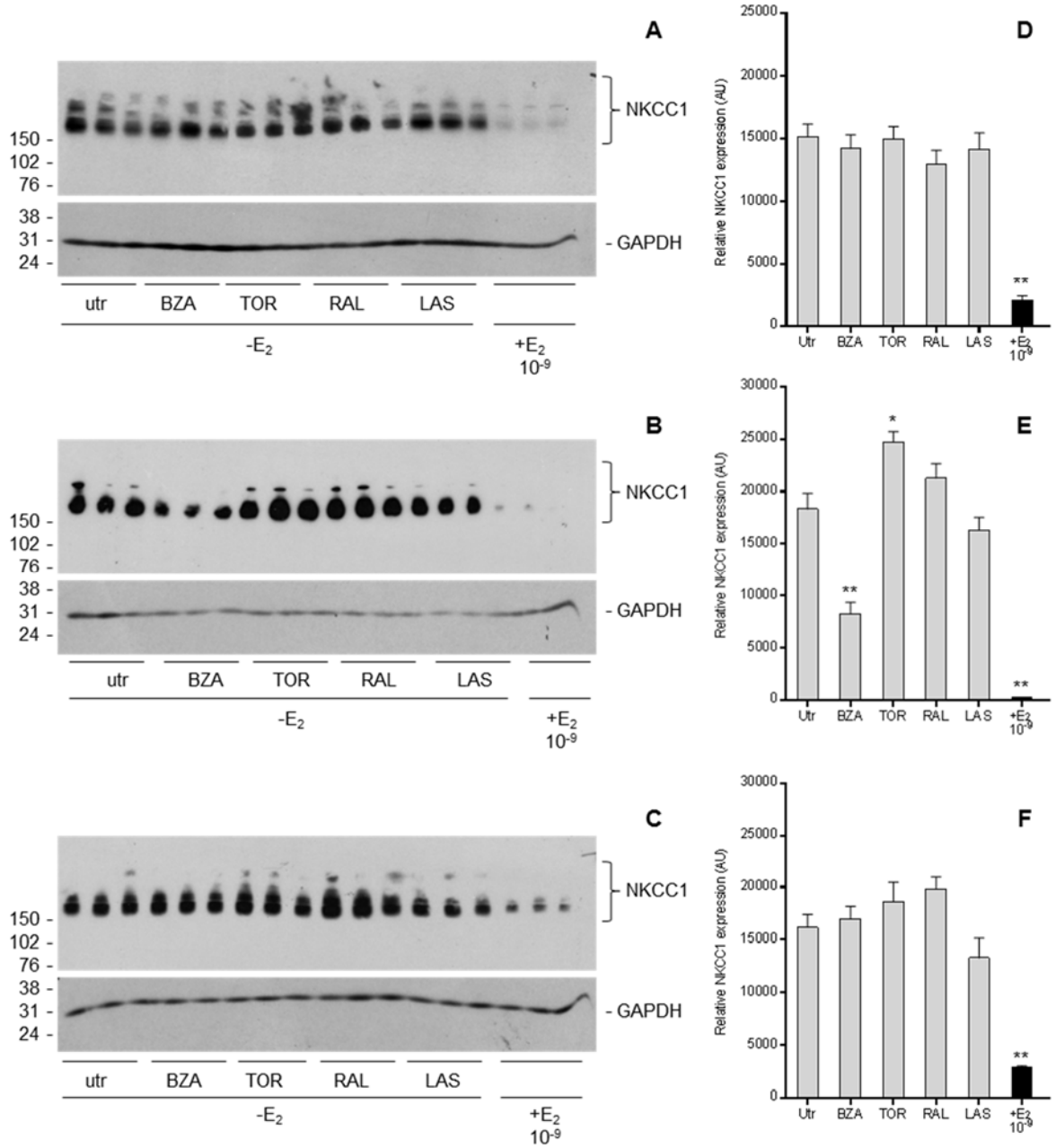

Figure 6.2 Agonist effect of anti-oestrogens BZA, TOR, RAL, LAS on NKCC1 expression. MCF-7, EFM-19 (50,000 per well) and EFF-3 (100,000 per well) cells were plated onto a 24-well plate. Cells were steroid deprived by growth in phenol-red-free media containing 10% dextran-coated charcoal treated serum and 1 µg/ml insulin, for 5 days and then cultured in withdrawal medium alone (utr) or treated with either 10^{-7} M Bazedoxifene (BZA), 10^{-7} M Toremifene (TOR), 10^{-7} M Raloxifene (RAL), 10^{-8} M Lasofoxifene (LAS) and 10^{-9} M 17β-oestradiol alone for 8 days. Cells were lysed and protein extracts were prepared. Protein aliquots of 10 µg were separated by 12% polyacrylamide gel electrophoresis and then transferred to nitrocellulose membranes. The membranes were incubated with anti-NKCC1 antibody (dilution 1:10000) overnight at 4 ºC, followed by horseradish peroxidase conjugated goat-anti-rabbit secondary antibody for 1 hour at 37 ºC. Proteins were visualised by enhanced chemiluminescence with SuperSignal West Dura Extended Duration Substrate. **A, B, C.** The protein expression of NKCC1 in MCF-7, EFM-19 and EFF-3 cells treated with anti-oestrogens, comparing serum withdrawn ($-E_2$ □) samples with oestrogen-stimulated ($+E_2$ ■) samples. The images shown are representative of an experiment which has been replicated twice. **D, E, F.** Quantification of NKCC1 normalised against the corresponding GAPDH signal, *$p < 0.05$ and **$p < 0.001$ by ANOVA, compared with the untreated (utr) cells. Error bars indicate SEM of triplicate measurements.

6.2.2 Characterisation of the antagonist activity of anti-oestrogens on NKCC1 expression

Cells were treated with $5x10^{-6}$ M tamoxifen, 10^{-8} M 4-hydroxytamoxifen and 10^{-8} M fulvestrant in combination with $2x10^{-10}$ M oestradiol to assess the antagonistic effects of the anti-oestrogens.

In MCF-7 cells (Figure 6.3A), tamoxifen $5x10^{-6}$ M in the presence of $2x10^{-10}$ M oestradiol had the most antagonist effect on NKCC1 expression. The effect of oestradiol was largely reversed and NKCC1 expression was increased 15-fold. However, 4-hydroxytamoxifen and fulvestrant in the presence of oestradiol exerted partial antagonist activity. 4-hydroxytamoxifen increased the expression of NKCC1 by approximately 2-fold in comparison to $2x10^{-10}$ M oestradiol treated cells.

When EFM-19 cells were treated with 10^{-9} M and $2x10^{-10}$ M oestradiol, the expression of NKCC1 decreased dramatically. The anti-oestrogens in the presence of $2x10^{-10}$ M oestradiol, did not inhibit the effects of oestrogen.

A decrease in NKCC1 expression was observed in EFF-3 cells treated with $2x10^{-10}$ M oestradiol. 4-hydroxytamoxifen in the presence of $2x10^{-10}$ M oestradiol were partially antagonistic. Compared to the expression of NKCC1 in the presence of $2x10^{-10}$ M oestradiol alone, tamoxifen and fulvestrant demonstrated antagonistic properties.

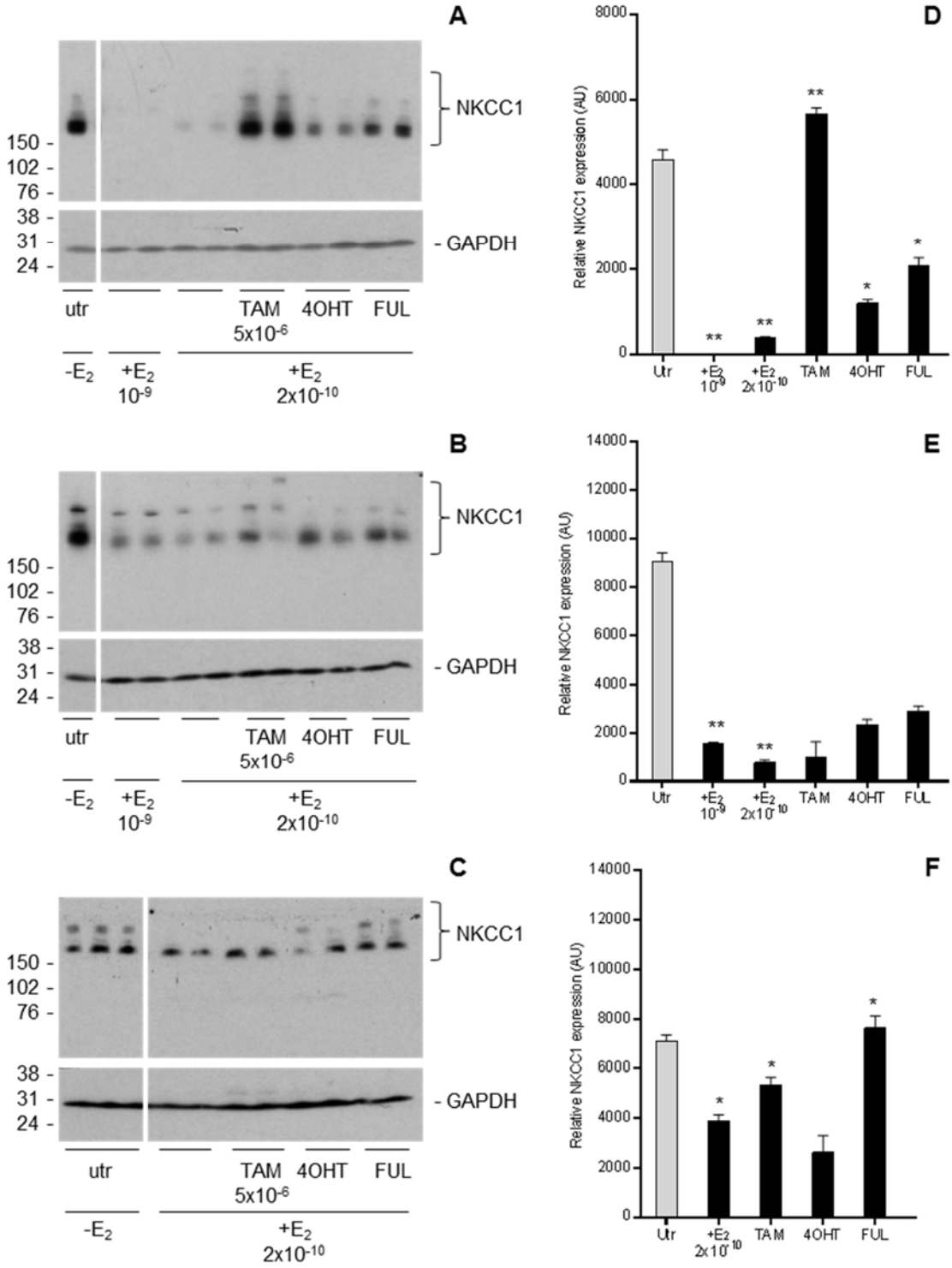

Figure 6.3 Antagonist activity of anti-oestrogens on NKCC1 expression. MCF-7, EFM-19 (50,000 per well) and EFF-3 (100,000 per well) cells were plated onto a 24-well plate. Cells were steroid deprived by growth in phenol-red-free media containing 10% dextran-coated charcoal treated serum and 1 µg/ml insulin, for 5 days and then cultured in withdrawal medium alone (utr) or treated with 10^{-9} M, $2x10^{-10}$ M 17β-oestradiol alone, or $5x10^{-6}$ M tamoxifen (TAM), 10^{-8} M 4-hydroxytamoxifen (4OHT), 10^{-8} M Fulvestrant (FUL) in combination with $2x10^{-10}$ M 17β-oestradiol for 8 days. Cells were lysed and protein extracts were prepared. Protein aliquots of 10 µg were separated by 12% polyacrylamide gel electrophoresis and then transferred to nitrocellulose membranes. The membranes were incubated with anti-NKCC1 antibody (dilution 1:10000) overnight at 4 °C, followed by horseradish peroxidase conjugated goat-anti-rabbit

secondary antibody for 1 hour at 37 °C. Proteins were visualised by enhanced chemiluminescence with SuperSignal West Dura Extended Duration Substrate. **A, B, C.** The protein expression of NKCC1 in MCF-7, EFM-19 and EFF-3 cells treated with anti-oestrogens, comparing serum withdrawn (-E_2 □) samples with oestrogen-stimulated (+E_2 ■) samples. The images shown are representative of an experiment which has been replicated three times in MCF-7 and EFM-19 cells and twice in EFF-3 cells. **D, E, F.** Quantification of NKCC1 normalised against the corresponding GAPDH signal, *$p < 0.05$ and **$p < 0.001$ by ANOVA, compared with $2x10^{-10}$ M oestradiol treated cells. Error bars indicate SEM of duplicate measurements.

The oestrogen antagonist activities of bazedoxifene, toremifene, raloxifene and lasofoxifene are shown in Figure 6.4.

In MCF-7 cells treated with these anti-oestrogens in the presence of $2x10^{-10}$ M oestradiol, toremifene showed partial antagonism with decreased NKCC1 expression levels similar to that of cells treated with $2x10^{-10}$ M oestradiol alone. Bazedoxifene, raloxifene and lasofoxifene displayed completely antagonistic properties.

Bazedoxifene and raloxifene exerts the most anti-estrogenic effect on the expression of NKCC1 in EFM-19 cells, by largely antagonising the effects of oestradiol. However, the partial antagonist activity of toremifene on the expression of NKCC1 is similar to the results observed in MCF-7 cells.

In EFF-3 cells, all four anti-oestrogens in the presence of $2x10^{-10}$ M oestradiol contributed to antagonising the effects of oestradiol, resulting in a dramatic increase in the expression of NKCC1. Out of these anti-oestrogens raloxifene was the most anti-oestrogenic, followed by toremifene, bazedoxifene and lasofoxifene respectively.

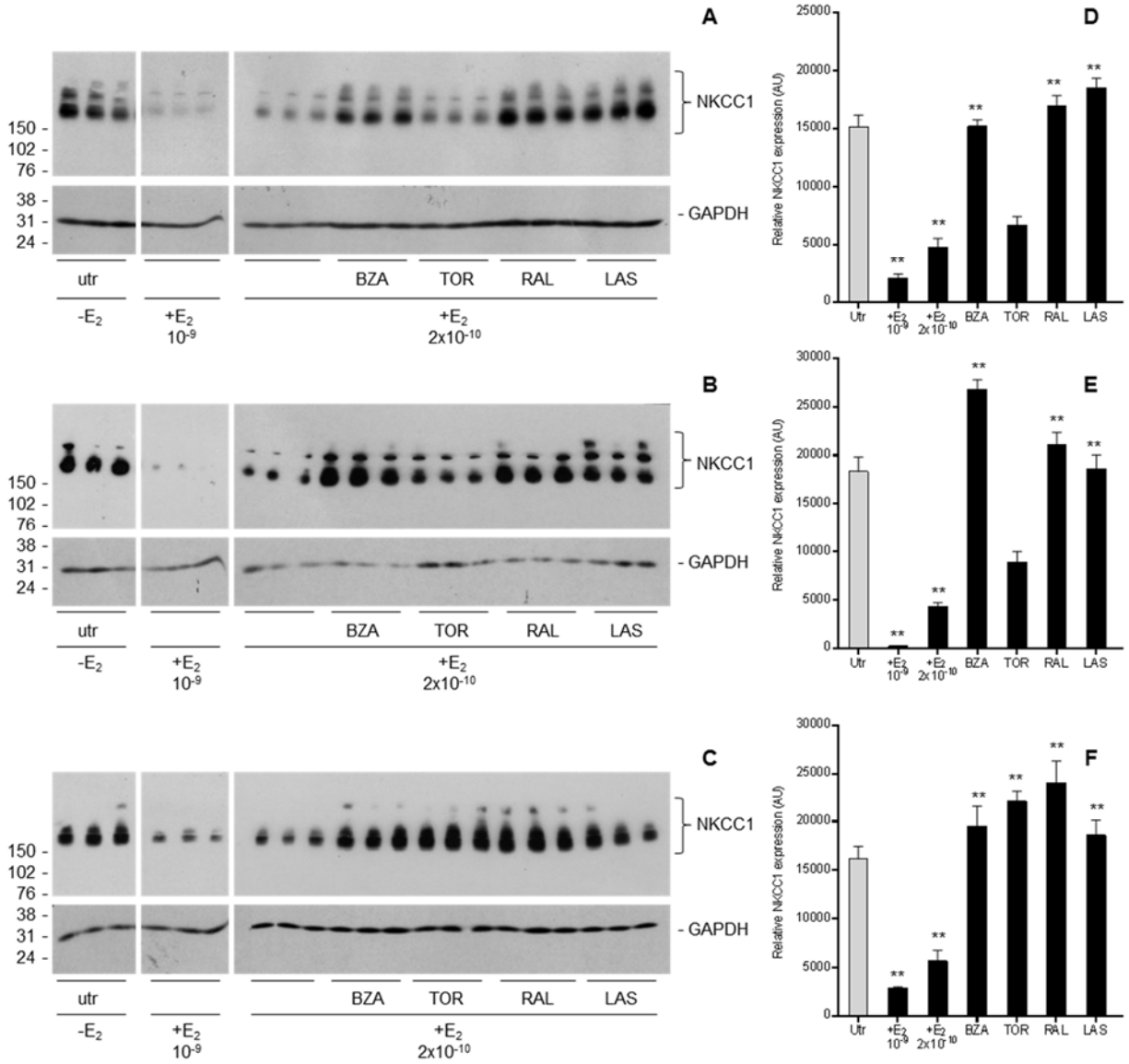

Figure 6.4 Antagonist activity of anti-oestrogens BZA, TOR, RAL, LAS on NKCC1 expression. MCF-7, EFM-19 (50,000 per well) and EFF-3 (100,000 per well) cells were plated onto a 24-well plate. Cells were steroid deprived by growth in phenol-red-free media containing 10% dextran-coated charcoal treated serum and 1 µg/ml insulin, for 5 days and then cultured in withdrawal medium alone (utr) or treated with 10^{-9} M, $2x10^{-10}$ M 17β-oestradiol alone, or 10^{-7} M Bazedoxifene (BZA), 10^{-7} M Toremifene (TOR), 10^{-7} M Raloxifene (RAL), 10^{-8} M Lasofoxifene (LAS) in combination with $2x10^{-10}$ M 17β-oestradiol for 8 days. Cells were lysed and protein extracts were prepared. Protein aliquots of 10 µg were separated by 12% polyacrylamide gel electrophoresis and then transferred to nitrocellulose membranes. The membranes were incubated with anti-NKCC1 antibody (dilution 1:10000) overnight at 4 ºC, followed by horseradish peroxidase conjugated goat-anti-rabbit secondary antibody for 1 hour at 37 ºC. Proteins were visualised by enhanced chemiluminescence with SuperSignal West Dura Extended Duration Substrate. **A, B, C.** The protein expression of NKCC1 in MCF-7, EFM-19 and EFF-3 cells treated with anti-oestrogens, comparing serum withdrawn ($-E_2$ □) samples with oestrogen-stimulated ($+E_2$ ■) samples. The images shown are representative of an experiment which has been replicated twice. **D, E, F.** Quantification of NKCC1 normalised against the corresponding GAPDH signal, *$p < 0.05$ and **$p < 0.001$ by ANOVA, compared with $2x10^{-10}$ M oestradiol treated cells. Error bars indicate SEM of triplicate measurements.

6.3 Action of anti-oestrogens on the protein expression of NHERF3

6.3.1 Analysis of the agonist activity of anti-oestrogens on the regulation of NHERF3 protein

This section investigated the agonist effects of different anti-oestrogens on the expression of the protein NHERF3. The anti-oestrogens tamoxifen, 4-hydroxytamoxifen and fulvestrant were tested at concentrations described in the previous section 6.1.

Figure 6.5 compares the agonist effects of anti-oestrogens in MCF-7, EFM-19 and EFF-3 cells. In MCF-7 cells, there was no expression of NHERF3 protein in the untreated cells, whereas cells treated with 10^{-9} M oestradiol had the most induction of NHERF3 expression. Tamoxifen at $5x10^{-6}$ M alone exerted a low oestrogen-like activity, in contrast to the other two anti-oestrogens 4-hydroxytamoxifen and fulvestrant.

EFM-19 cells treated with the different anti-oestrogens alone did not detect any NHERF3 protein expression and was similar to untreated EFM-19 cells (Figure 6.5B). These results indicate that none of the anti-oestrogens have agonist activity. Oestradiol treatment significantly increased NHERF3 protein expression.

Results obtained from western analysis of EFF-3 cells treated with anti-oestrogens in the absence of oestradiol is shown in Figure 6.5C. Tamoxifen and 4-hydroxytamoxifen on their own showed partial agonistic effects on the expression of NHERF3. The expression of NHERF3 was 1.5-fold higher in EFF-3 cells treated with 4-hydroxytamoxifen in comparison to the NHERF3 expression in cells with tamoxifen alone. In contrast to tamoxifen and 4-hydroxytamoxifen, fulvestrant did not have any detectable agonist activity. In the presence of $2x10^{-10}$ M oestradiol, the expression of NHERF3 was increased.

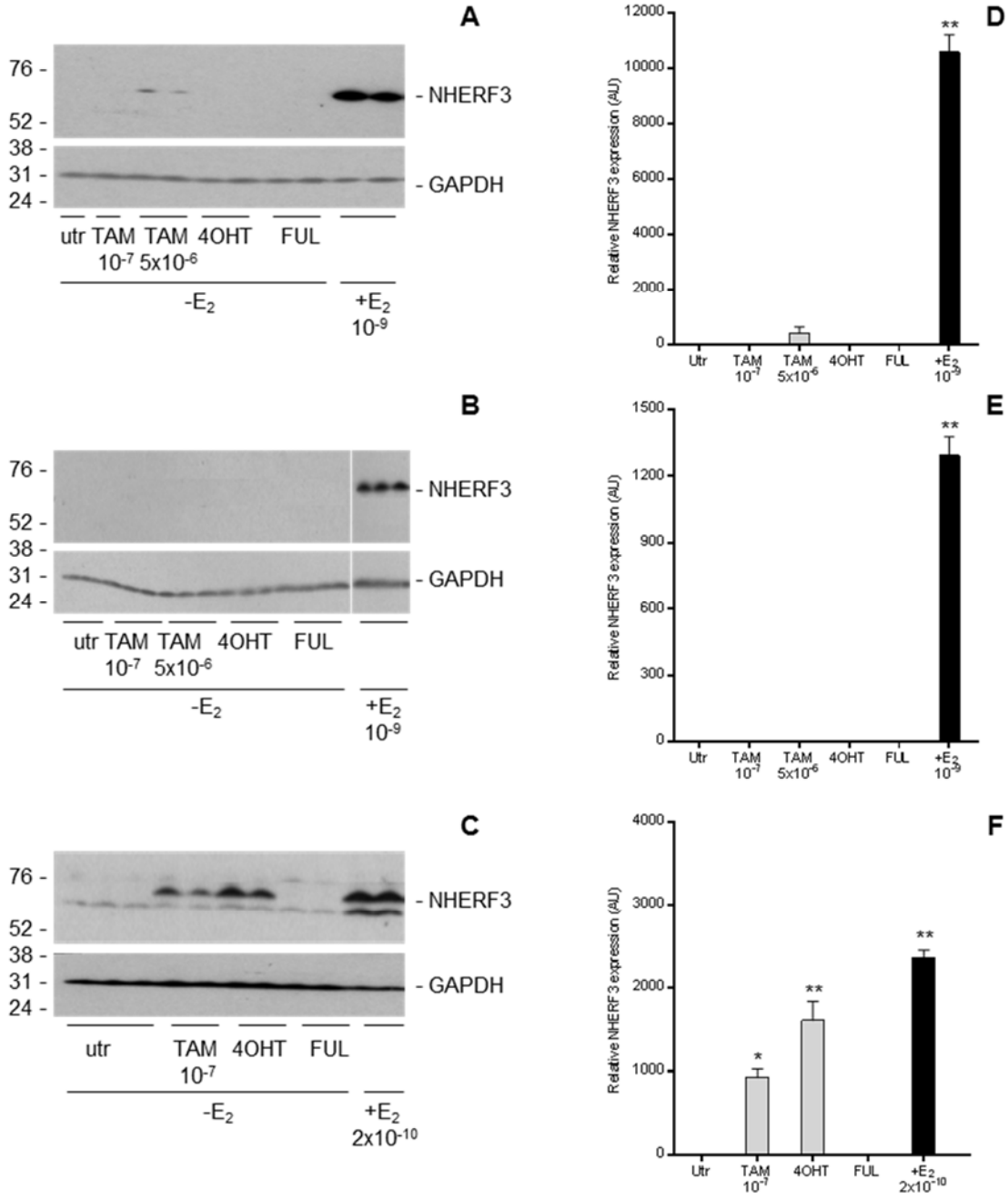

Figure 6.5 Agonist effects of anti-oestrogens on NHERF3 expression. MCF-7, EFM-19 (50,000 per well) and EFF-3 (100,000 per well) cells were plated onto a 24-well plate. Cells were steroid deprived by culturing in phenol-red-free media containing 10% dextran-coated charcoal treated serum and 1 µg/ml insulin, for 5 days and then cultured in withdrawal medium alone (utr) or treated with either 10^{-7} M or $5x10^{-6}$ M tamoxifen (TAM), 10^{-8} M 4-hydroxytamoxifen (4OHT), 10^{-8} M fulvestrant (FUL) and 10^{-9} M 17β-oestradiol alone for 8 days. Cells were lysed and protein extracts were prepared. Protein aliquots of 10 µg were separated by 12% polyacrylamide gel electrophoresis and then transferred to nitrocellulose membranes. The membranes were incubated with anti-NHERF3 antibody (dilution 1:10000) overnight at 4 ºC, followed by horseradish peroxidase conjugated goat-anti-rabbit secondary antibody for 1 hour at 37 ºC. Proteins were visualised by enhanced chemiluminescence with SuperSignal West Dura Extended Duration Substrate. **A, B, C.** The protein expression of NHERF3 in MCF-7, EFM-19 and EFF-3 cells treated with anti-oestrogens, comparing serum withdrawn (-E_2 □) samples with oestrogen-stimulated (+E_2 ■) samples. The image shown is representative of an experiment which has been replicated three times in MCF-7 and EFM-19 cells and twice in EFF-3 cells. **D,**

E, F. Quantification of NHERF3 normalised against the corresponding GAPDH signal, *p < 0.05 and **p < 0.001 by ANOVA, compared with the untreated (utr) cells. Error bars indicate SEM of duplicate measurements.

The agonist effects of the anti-oestrogens bazedoxifene, toremifene, raloxifene and lasofoxifene were explored (Figure 6.6).

A slight increase in NHERF3 expression was observed in MCF-7 cells treated with toremifene and lasofoxifene, which indicates weak partial agonist activity. There was no detectable induction of NHERF3 expression in cells grown in the presence of bazedoxifene and raloxifene alone. Treatment with 10^{-9} M oestradiol resulted in a marked increase in NHERF3 expression.

Figure 6.6B shows the effects of anti-oestrogens bazedoxifene, toremifene, raloxifene and lasofoxifene on the expression of NHERF3 protein in EFM-19 cells. There was no NHERF3 protein detected suggesting that all four of these anti-oestrogens alone exerted no oestrogen-like activity.

The agonistic properties of the four anti-oestrogens in EFF-3 cells was tested. The results were similar to that observed in EFM-19 cell as all four anti-oestrogens displayed no agonism. Treatment with oestradiol induced expression of NHERF3.

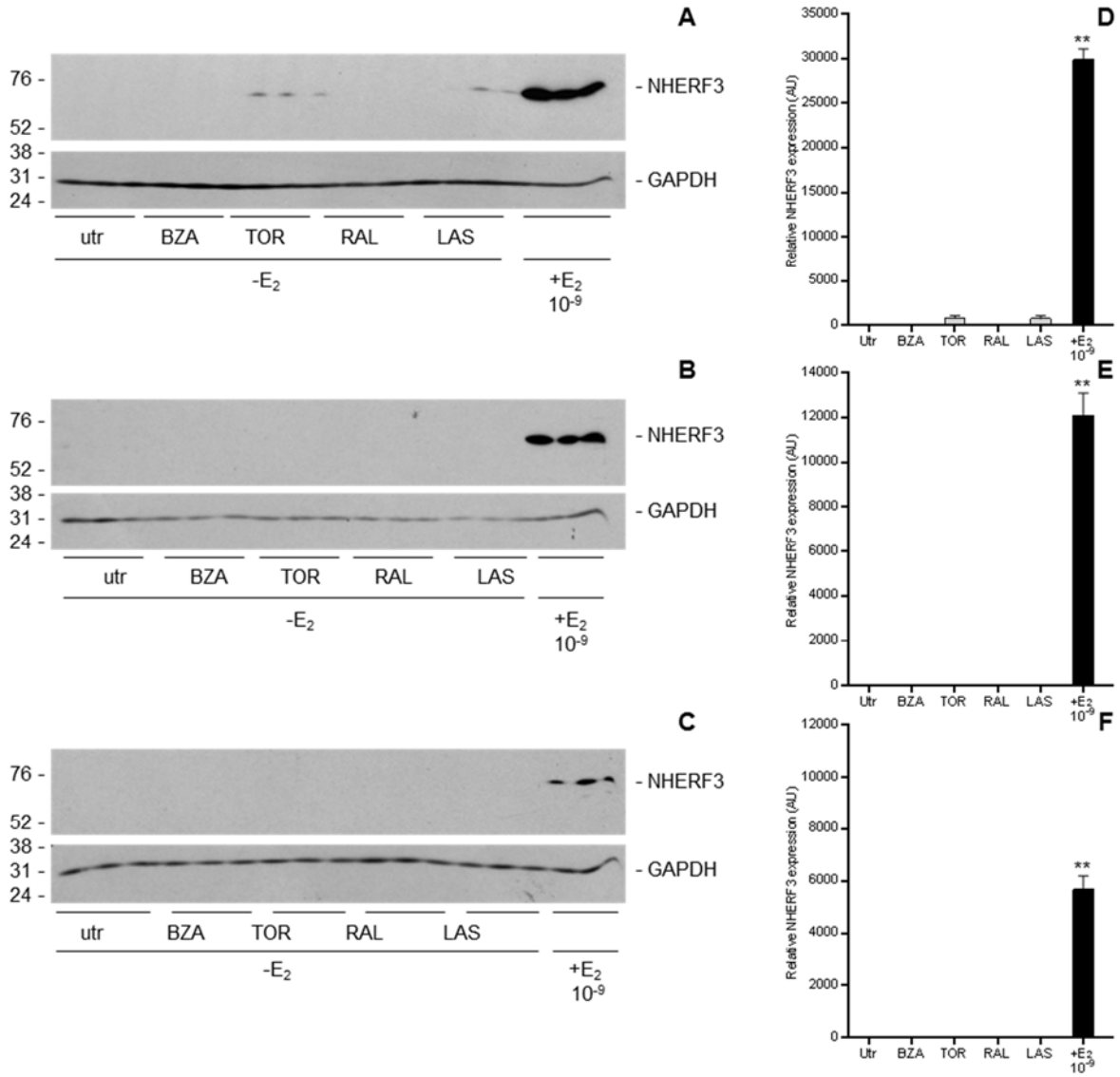

Figure 6.6 Agonist effects of anti-oestrogens BZA, TOR, RAL, LAS on NHERF3 expression. MCF-7, EFM-19 (50,000 per well) and EFF-3 (100,000 per well) cells were plated onto a 24-well plate. Cells were steroid deprived by culturing in phenol-red-free media containing 10% dextran-coated charcoal treated serum and 1 µg/ml insulin, for 5 days and then cultured in withdrawal medium alone (utr) or treated with either 10^{-7} M Bazedoxifene (BZA), 10^{-7} M Toremifene (TOR), 10^{-7} M Raloxifene (RAL), 10^{-8} M Lasofoxifene (LAS) and 10^{-9} M 17β-oestradiol alone for 8 days. Cells were lysed and protein extracts were prepared. Protein aliquots of 10 µg were separated by 12% polyacrylamide gel electrophoresis and then transferred to nitrocellulose membranes. The membranes were incubated with anti-NHERF3 antibody (dilution 1:10000) overnight at 4 °C, followed by horseradish peroxidase conjugated goat-anti-rabbit secondary antibody for 1 hour at 37 °C. Proteins were visualised by enhanced chemiluminescence with SuperSignal West Dura Extended Duration Substrate. **A, B, C.** The protein expression of NHERF3 in MCF-7, EFM-19 and EFF-3 cells treated with anti-oestrogens, comparing serum withdrawn ($-E_2$ □) samples with oestrogen-stimulated ($+E_2$ ■) samples. The image shown is representative of an experiment which has been replicated twice. **D, E, F.** Quantification of NHERF3 normalised against the corresponding GAPDH signal, *$p < 0.05$ and **$p < 0.001$ by ANOVA, compared with the untreated (utr) cells. Error bars indicate SEM of triplicate measurements.

6.3.2 Analysis of the antagonist activity of anti-oestrogens on the regulation of NHERF3 protein

The antagonist effects of tamoxifen, 4-hydroxytamoxifen and fulvestrant was evaluated in the three cell lines (Figure 6.7).

Treatment of MCF-7 cells with tamoxifen $5x10^{-6}$ M and 4-hydroxytamoxifen 10^{-8} M in the presence of $2x10^{-10}$ M oestradiol, resulted in an increase in NHERF3 expression. These results indicate that tamoxifen and 4-hydroxytamoxifen displayed partial antagonistic properties. However fulvestrant 10^{-8} M inhibited completely the effect of $2x10^{-10}$ M oestradiol.

While tamoxifen $5x10^{-6}$ M and 4-hydroxytamoxifen 10^{-8} M in the presence of oestradiol caused partial antagonism in MCF-7 cells, a similar observation was not made in EFM-19 cells. The anti-oestrogens tamoxifen, 4-hydroxytamoxifen and fulvestrant completely blocked the actions of oestrogen on NHERF3 protein expression (Figure 6.7).

Treatment of EFF-3 cells with $2x10^{-10}$ M oestradiol, stimulated expression of NHERF3. Tamoxifen and 4-hydroxtamoxifen did not inhibit the effect of oestrogen, whereas fulvestrant inhibited completely the effect of oestrogen on NHERF3 expression.

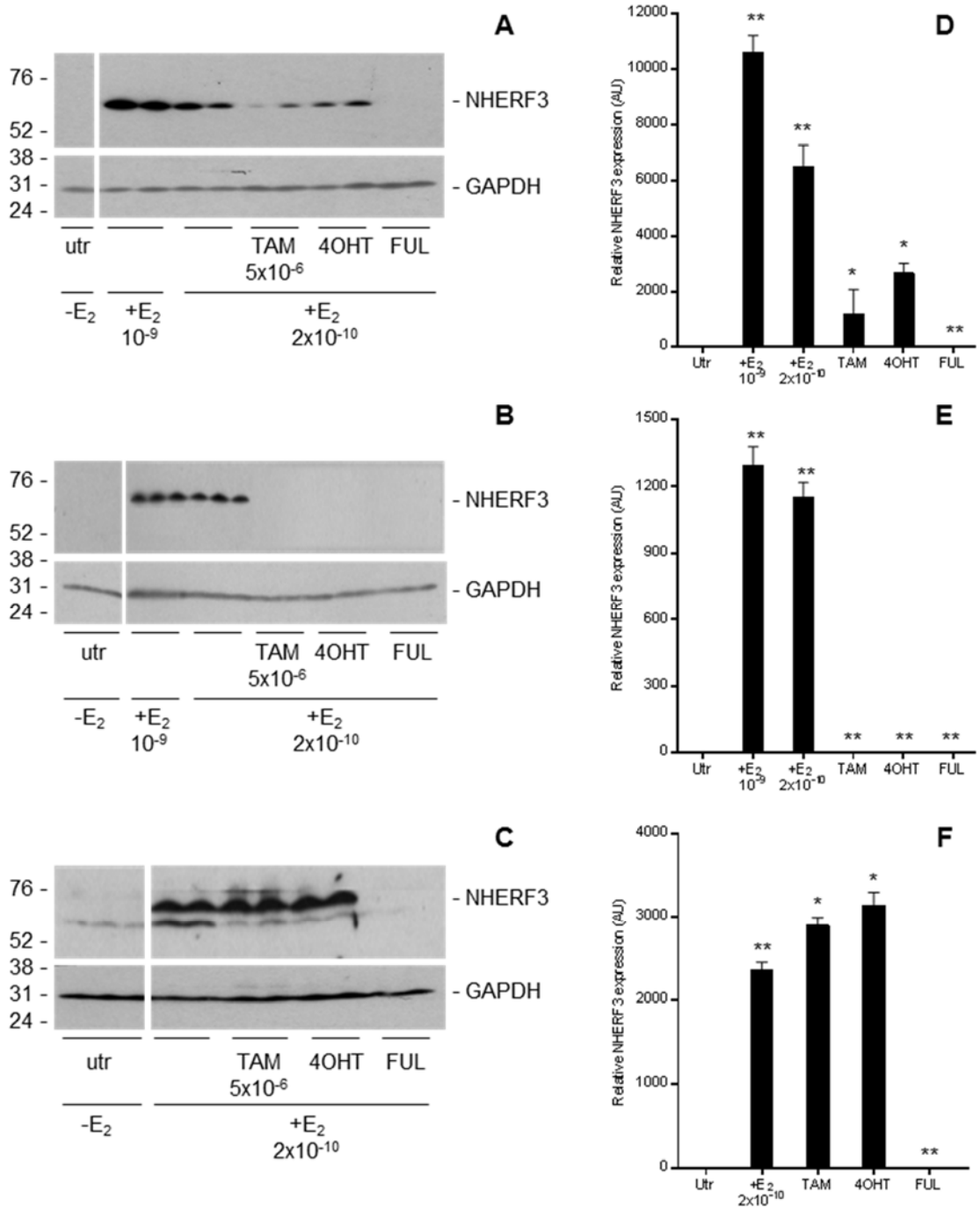

Figure 6.7 Antagonist effects of anti-oestrogens on NHERF3 expression. MCF-7, EFM-19 (50,000 per well) and EFF-3 (100,000 per well) cells were plated onto a 24-well plate. Cells were steroid deprived by culturing in phenol-red-free media containing 10% dextran-coated charcoal treated serum and 1 µg/ml insulin, for 5 days and then cultured in withdrawal medium alone (utr) or treated with 10^{-9} M, $2x10^{-10}$ M 17β-oestradiol alone, or $5x10^{-6}$ M tamoxifen (TAM), 10^{-8} M 4-hydroxytamoxifen (4OHT), 10^{-8} M Fulvestrant (FUL) in combination with $2x10^{-10}$ M 17β-oestradiol for 8 days. Cells were lysed and protein extracts were prepared. Protein aliquots of 10 µg were separated by 12% polyacrylamide gel electrophoresis and then transferred to nitrocellulose membranes. The membranes were incubated with anti-NHERF3 antibody (dilution 1:10000) overnight at 4 °C, followed by horseradish peroxidase conjugated goat-anti-rabbit secondary antibody for 1 hour at 37 °C. Proteins were visualised by enhanced chemiluminescence with SuperSignal West Dura Extended Duration Substrate. **A, B, C.** The protein expression of NHERF3 in MCF-7, EFM-19 and EFF-3 cells treated with anti-oestrogens,

comparing serum withdrawn (-E_2 □) samples with oestrogen-stimulated (+E_2 ■) samples. The image shown is representative of an experiment which has been replicated three times in MCF-7 and EFM-19 cells and twice in EFF-3 cells. **D, E, F.** Quantification of NHERF3 normalised against the corresponding GAPDH signal, *$p < 0.05$ and **$p < 0.001$ by ANOVA, compared with $2x10^{-10}$ M oestradiol treated cells. Error bars indicate SEM of duplicate measurements.

Figure 6.8 shows the oestrogen antagonist effects of bazedoxifene, toremifene, raloxifene and lasofoxifene.

In MCF-7 cells, treatment with 10^{-9} M and $2x10^{-10}$ M oestradiol resulted in a marked increase in NHERF3 expression. Toremifene did not completely antagonise the stimulatory effects of oestrogen, instead showed partial antagonism. There was almost a two-fold reduction in NHERF3 expression in comparison to the effect of oestrogen alone. In contrast to the effects of toremifene, the other three anti-oestrogens bazedoxifene, raloxifene and lasofoxifene exerted opposing effects. No expression of NHERF3 was detected as these anti-oestrogens completely antagonised the effects of oestrogen.

An induction in NHERF3 protein expression was observed in EFM-19 cells treated with toremifene 10^{-7} M in the presence of $2x10^{10}$ M oestradiol. This stimulation of NHERF3 expression was approximately 1.3-fold higher than that of $2x10^{10}$ M oestradiol alone. It is evident that toremifene is unable to inhibit the effects of oestrogen. The effects of bazedoxifene, raloxifene and lasofoxifene on the expression of NHERF3 differ from that of toremifene, as they completely opposed the effects of oestradiol and displayed complete antagonism.

The antagonistic effect of toremifene on the expression of NHERF3 in EFF-3 cells is comparable to that of EFM-19 cells. The expression of NHERF3 is about 2-fold higher when cells were treated with toremifene in the presence of oestradiol than in oestradiol alone. This suggests that toremifene was unable to antagonise the effects of oestrogen. Bazedoxifene and raloxifene completely blocked the effects of oestrogen. Interestingly, lasofoxifene showed no antagonistic effects, as there was almost no difference in NHERF3 expression, between cells treated with $2x10^{-10}$ M oestradiol and cells treated with lasofoxifene plus oestradiol.

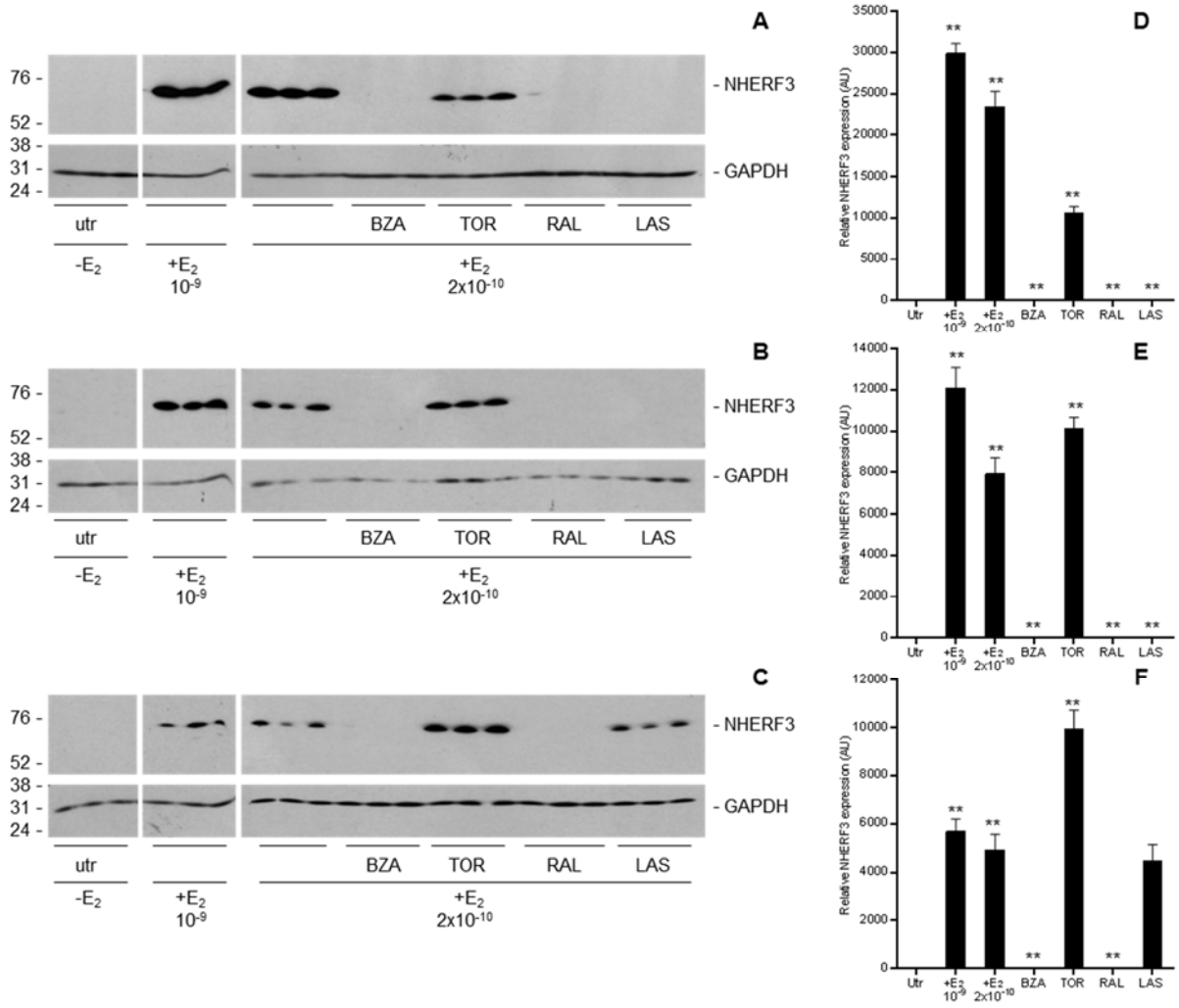

Figure 6.8 Antagonist effects of anti-oestrogens BZA, TOR, RAL, LAS on NHERF3 expression. MCF-7, EFM-19 (50,000 per well) and EFF-3 (100,000 per well) cells were plated onto a 24-well plate. Cells were steroid deprived by culturing in phenol-red-free media containing 10% dextran-coated charcoal treated serum and 1 µg/ml insulin, for 5 days and then cultured in withdrawal medium alone (utr) or treated with 10^{-9} M, $2x10^{-10}$ M 17β-oestradiol alone, or 10^{-7} M Bazedoxifene (BZA), 10^{-7} M Toremifene (TOR), 10^{-7} M Raloxifene (RAL), 10^{-8} M Lasofoxifene (LAS) in combination with $2x10^{-10}$ M 17β-oestradiol for 8 days. Cells were lysed and protein extracts were prepared. Protein aliquots of 10 µg were separated by 12% polyacrylamide gel electrophoresis and then transferred to nitrocellulose membranes. The membranes were incubated with anti-NHERF3 antibody (dilution 1:10000) overnight at 4 ºC, followed by horseradish peroxidase conjugated goat-anti-rabbit secondary antibody for 1 hour at 37 ºC. Proteins were visualised by enhanced chemiluminescence with SuperSignal West Dura Extended Duration Substrate. **A, B, C.** The protein expression of NHERF3 in MCF-7, EFM-19 and EFF-3 cells treated with anti-oestrogens, comparing serum withdrawn ($-E_2$ □) samples with oestrogen-stimulated ($+E_2$ ■) samples. The image shown is representative of an experiment which has been replicated twice. **D, E, F.** Quantification of NHERF3 normalised against the corresponding GAPDH signal, *$p < 0.05$ and **$p < 0.001$ by ANOVA, compared with $2x10^{-10}$ M oestradiol treated cells. Error bars indicate SEM of triplicate measurements.

Furthermore, the concentration-dependent agonist and antagonist activity of toremifene was investigated. Previously we showed that in the presence of oestradiol, toremifene induced NHERF3 expression above the level induced by oestradiol. Therefore this experiment would further test the concentration-dependent effects of toremifene on NHERF3 protein expression.

EFF-3 cells were cultured in steroid depleted media for 5 days and treated with concentrations of toremifene ranging from 10^{-10} M to 10^{-6} M in the absence or presence of $2x10^{-10}$ M oestradiol for 8 days. Results shown in Figure 6.9 indicate that there are two immunoreactive bands detected. The higher molecular weight band was quantified, as it matched more closely the molecular mass of NHERF3 protein. This protein band was not detected in cells treated with toremifene alone, which was consistent with our previous findings. There was a degree of variability in NHERF3 expression between different concentrations of toremifene in the presence of oestrogen. As for 10^{-7} M toremifene in the presence of oestrogen, the result was not similar to the previous experiment (Figure 6.8C), as NHERF3 expression was not induced to levels above that of oestradiol alone.

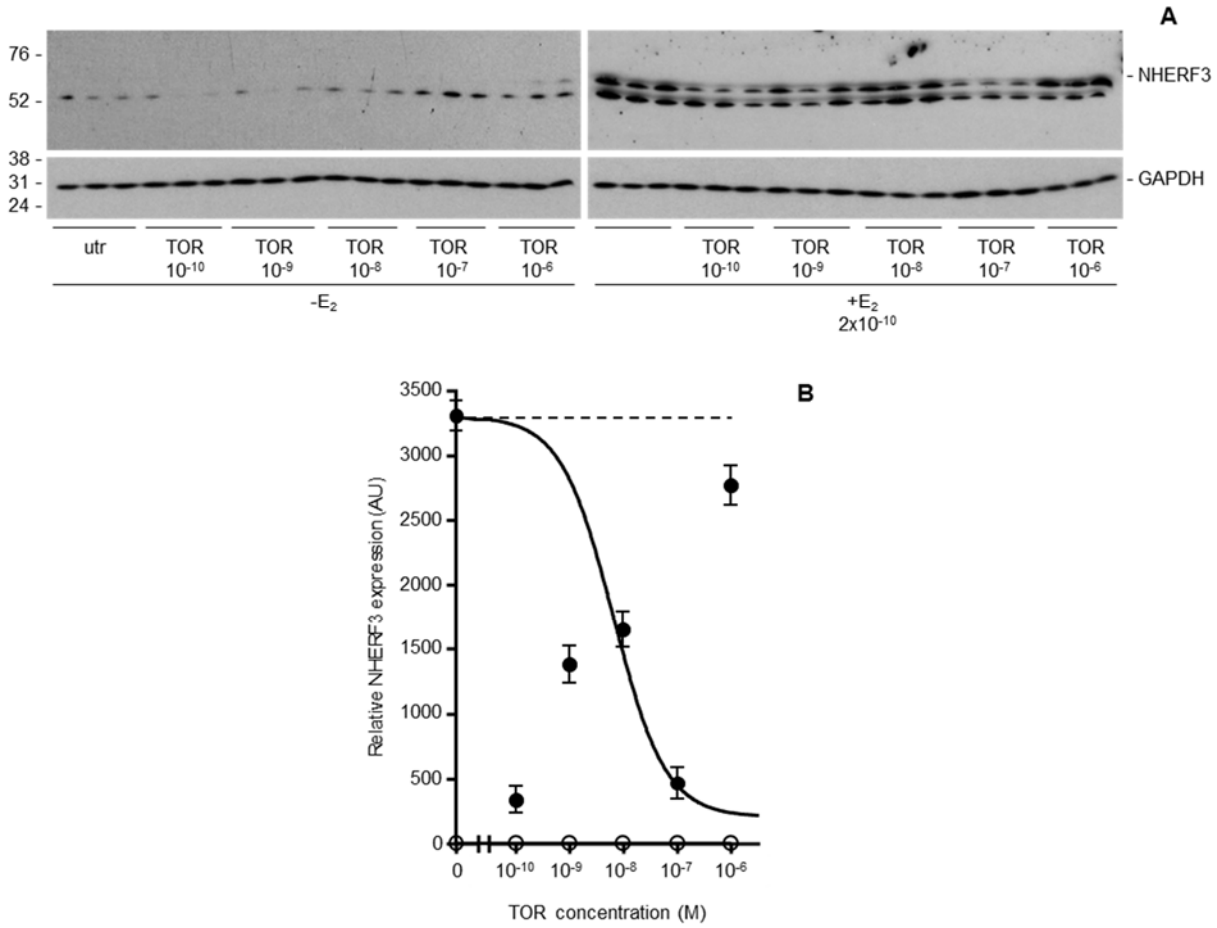

Figure 6.9 Effect of TOR on NHERF3 expression in EFF-3 cells. EFF-3 cells were plated at a density of 100,000 cells per well onto a collagen-coated 24-well plate. Cells were steroid deprived by culturing in phenol-red-free media containing 10% dextran-coated charcoal treated serum and 1 µg/ml insulin, for 5 days and then cultured in withdrawal medium alone (utr) or treated with toremifene (TOR) concentrations varying from 10^{-10} M to 10^{-6} M, alone or in combination with $2x10^{-10}$ M 17β-oestradiol for 8 days. Cells were lysed and protein extracts were prepared. Protein aliquots of 10 µg were separated by 12% polyacrylamide gel electrophoresis and then transferred to nitrocellulose membranes. The membranes were incubated with anti-NHERF3 antibody (dilution 1:10000) overnight at 4 ºC, followed by horseradish peroxidase conjugated goat-anti-rabbit secondary antibody for 1 hour at 37 ºC. Proteins were visualised by enhanced chemiluminescence with SuperSignal West Dura Extended Duration Substrate. **A.** The protein expression of NHERF3 in EFF-3 cells treated with anti-oestrogen toremifene, comparing serum withdrawn ($-E_2$ ○) samples with oestrogen-stimulated ($+E_2$ ●) samples. **B.** Quantification of NHERF3 normalised against the corresponding GAPDH signal. The dashed line indicates the level on NHERF3 protein expression in cells treated with $2x10^{-10}$ M 17β-oestradiol alone. Error bars indicate SEM of triplicate measurements.

6.4 Regulation of ENaC-β by anti-oestrogens

6.4.1 Investigation of the agonist activity of anti-oestrogens on the regulation of ENaC-β expression

The purpose of these experiments was to study the agonist effects of a range of anti-oestrogens on the expression of ENaC-β protein in oestrogen-responsive cell lines.

In the following experiments, cells were cultured in withdrawal media for 5 days. Treatments with different anti-oestrogens tamoxifen, 4-hydroxytamoxifen and fulvestrant lasted for 8 days.

Results for MCF-7 cells are presented in Figure 6.10A. Immunoreactive bands were detected at 70 kDa and around 50 kDa. For the purpose of this experiment the corresponding ENaC-β band at 70 kDa was quantified. Tamoxifen did not show agonism whilst, 4-hydroxytamoxifen and fulvestrant demonstrated substantial oestrogen-like effects. There is a clear indication of a significant increase in ENaC-β protein expression in cells treated with 10^{-9} M oestradiol.

Results from an experiment evaluating the effects of anti-oestrogens tamoxifen, 4-hydroxytamoxifen and fulvestrant in EFM-19 cells are shown in Figure 6.10B. Tamoxifen 10^{-7} M had oestrogen-like activity and increased ENaC-β protein expression to levels similar to that of oestradiol alone. Tamoxifen at $5x10^{-6}$ M, 4-hydroxytamoxifen and fulvestrant showed no agonist activity.

The action of anti-oestrogens on the expression of ENaC-β was tested in EFF-3 cells. As shown in Figure 6.10C, the anti-oestrogens had no significant effect on ENaC-β expression and did not show any agonist activity. Oestrogen induced the ENaC-β expression by approximately 2.5-fold.

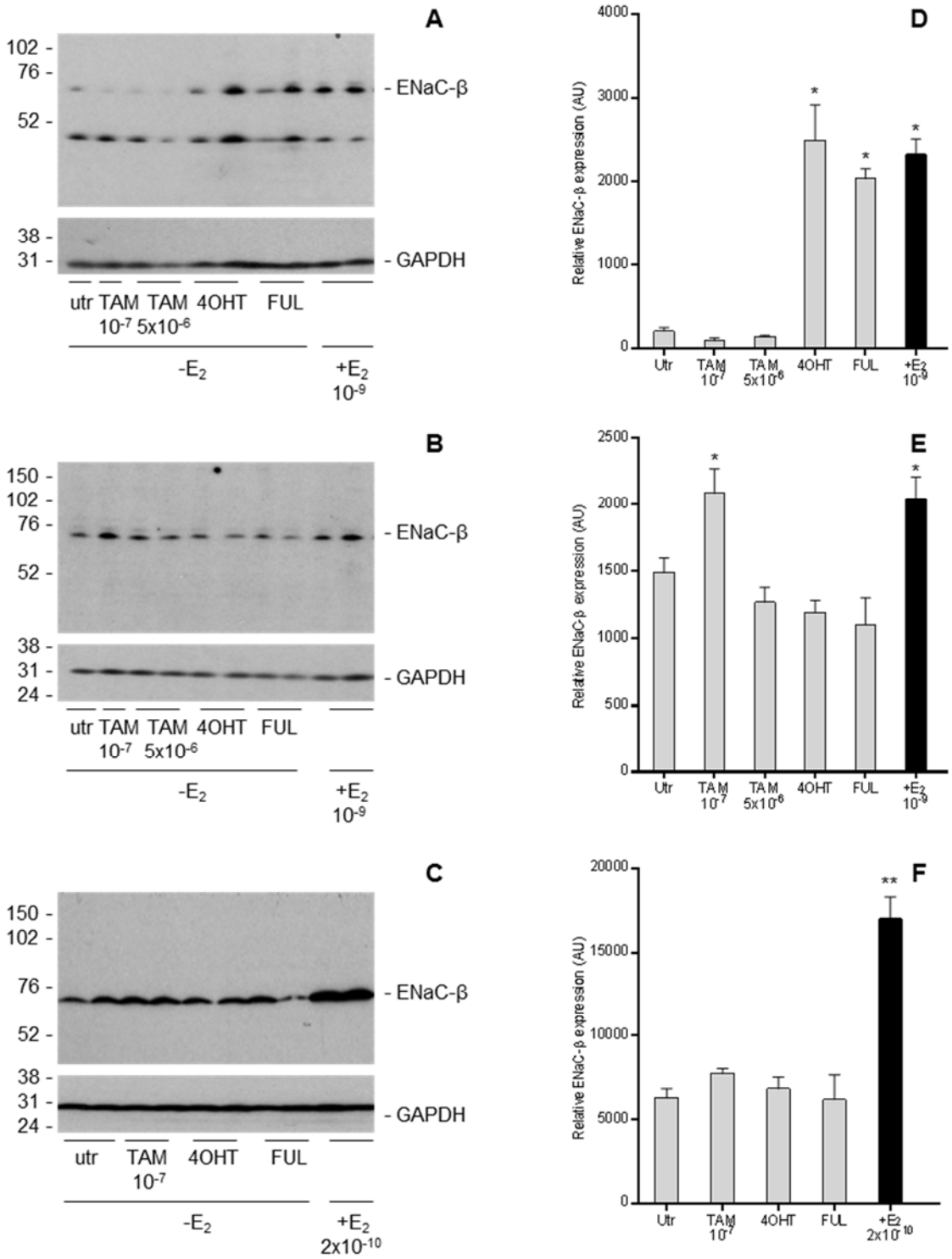

Figure 6.10 Agonist activity of anti-oestrogens on ENaC-β expression. MCF-7, EFM-19 (50,000 per well) and EFF-3 (100,000 per well) cells were plated onto a 24-well plate. Cells were steroid deprived by culturing in phenol-red-free media containing 10% dextran-coated charcoal treated serum and 1 μg/ml insulin, for 5 days and then cultured in withdrawal medium alone (utr) or treated with either 10^{-7} M or $5x10^{-6}$ M tamoxifen (TAM), 10^{-8} M 4-hydroxytamoxifen (4OHT), 10^{-8} M fulvestrant (FUL) and 10^{-9} M 17β-oestradiol alone for 8 days. Cells were lysed and protein extracts were prepared. Protein aliquots of 10 μg were separated by 12% polyacrylamide gel electrophoresis and then transferred to nitrocellulose membranes. The membranes were incubated with anti-ENaC-β antibody (dilution 1:100) overnight at 4 ºC, followed by horseradish peroxidase conjugated horse-anti-mouse secondary antibody for 1 hour

at 37 °C. Proteins were visualised by enhanced chemiluminescence with SuperSignal West Dura Extended Duration Substrate. **A, B, C.** The protein expression of ENaC-β in MCF-7, EFM-19 and EFF-3 cells treated with anti-oestrogens, comparing serum withdrawn (-E_2 □) samples with oestrogen-stimulated (+E_2 ■) samples. The image shown is representative of an experiment which has been replicated three times in MCF-7 and EFM-19 cells and twice in EFF-3 cells. **D, E, F.** Quantification of ENaC-β normalised against the corresponding GAPDH signal, *$p < 0.05$ and **$p < 0.001$ by ANOVA, compared with the untreated (utr) cells. Error bars indicate SEM of duplicate measurements.

The agonist activity of anti-oestrogens bazedoxifene, toremifene, raloxifene and lasofoxifene was tested.

As shown in Figure 6.11A, there was no difference in ENaC-β expression observed between the untreated MCF-7 cells and the cells treated with the different anti-oestrogens. However, cells treated with oestradiol showed approximately 1.5-fold increase in the expression of ENaC-β protein.

In EFM-19 cells, the ENaC-β expression was insensitive to bazedoxifene, toremifene, raloxifene and lasofoxifene. All four anti-oestrogens alone did not show any agonist activity. Oestradiol alone increased the expression of ENaC-β protein by about 2-fold. The results obtained in MCF-7 cells were comparable to the results in EFM-19 cells.

The agonist effects of bazedoxifene, toremifene, raloxifene and lasofoxifene on ENaC-β protein expression in EFF-3 cells is shown in Figure 6.11C. Surprisingly, there was no induction of ENaC-β expression by oestrogen. All four anti-oestrogens alone reduced the levels of ENaC-β expression by about half of that detected in untreated cells.

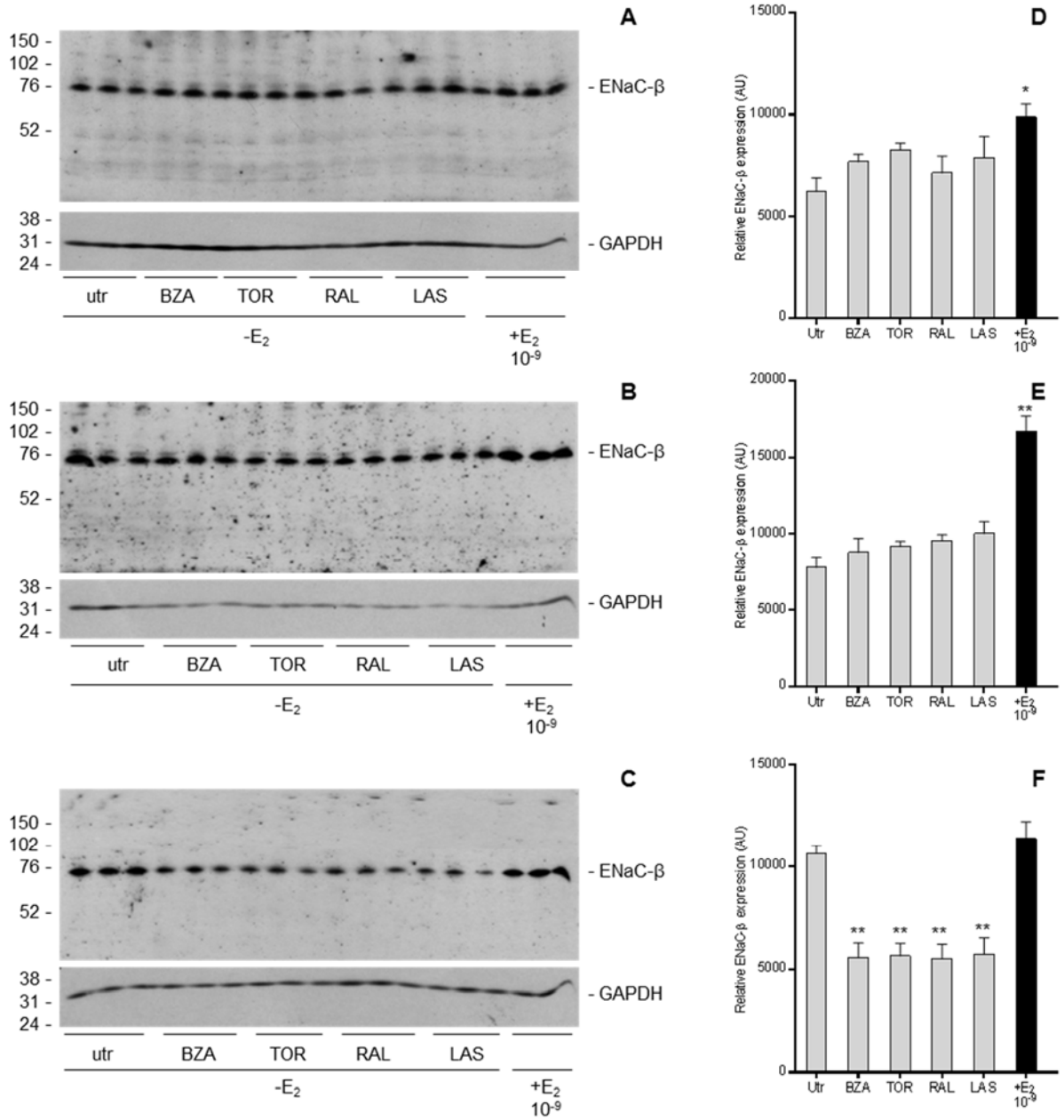

Figure 6.11 Agonist activity of anti-oestrogens BZA, TOR, RAL, LAS on ENaC-β expression. MCF-7, EFM-19 (50,000 per well) and EFF-3 (100,000 per well) cells were plated onto a 24-well plate. Cells were steroid deprived by culturing in phenol-red-free media containing 10% dextran-coated charcoal treated serum and 1 µg/ml insulin, for 5 days and then cultured in withdrawal medium alone (utr) or treated with either 10^{-7} M Bazedoxifene (BZA), 10^{-7} M Toremifene (TOR), 10^{-7} M Raloxifene (RAL), 10^{-8} M Lasofoxifene (LAS) and 10^{-9} M 17β-oestradiol alone for 8 days. Cells were lysed and protein extracts were prepared. Protein aliquots of 10 µg were separated by 12% polyacrylamide gel electrophoresis and then transferred to nitrocellulose membranes. The membranes were incubated with anti-ENaC-β antibody (dilution 1:100) overnight at 4 °C, followed by horseradish peroxidase conjugated horse-anti-mouse secondary antibody for 1 hour at 37 °C. Proteins were visualised by enhanced chemiluminescence with SuperSignal West Dura Extended Duration Substrate. **A, B, C.** The protein expression of ENaC-β in MCF-7, EFM-19 and EFF-3 cells treated with anti-oestrogens, comparing serum withdrawn (-E_2 □) samples with oestrogen-stimulated (+E_2 ■) samples. The image shown is representative of an experiment which has been replicated twice. **D, E, F.** Quantification of ENaC-β normalised against the corresponding GAPDH signal, *$p < 0.05$ and **$p < 0.001$ by ANOVA, compared with the untreated (utr) cells. Error bars indicate SEM of triplicate measurements.

6.4.2 Investigation of the antagonist activity of anti-oestrogens on the regulation of ENaC-β expression

The antagonist activity of tamoxifen, 4-hydroxytamoxifen and fulvestrant on the expression of ENaC-β was evaluated.

As shown in Figure 6.12A, tamoxifen was a partial antagonist in MCF-7 cells, and caused a 3.2-fold reduction in the oestrogen-stimulated ENaC-β protein expression. In contrast, 4-hydroxytamoxifen and fulvestrant showed the opposite effect of tamoxifen, as they increased ENaC-β expression by 2-fold and 1.5-fold, respectively. 4-hydroxytamoxifen and fulvestrant did not inhibit the effects of oestrogen, instead they caused an additive effect to that of oestrogen alone.

In EFM-19 cells, oestrogen induced ENaC-β expression. However, the three anti-oestrogens tamoxifen, 4-hydroxytamoxifen and fulvestrant in the presence of oestrogen, were weak antagonists.

Results from an experiment investigating the antagonist activity of anti-oestrogens in EFF-3 cells are shown in Figure 6.12C. All three anti-oestrogens were capable of significantly reducing the ENaC-β expression, largely reversing the induction by oestradiol.

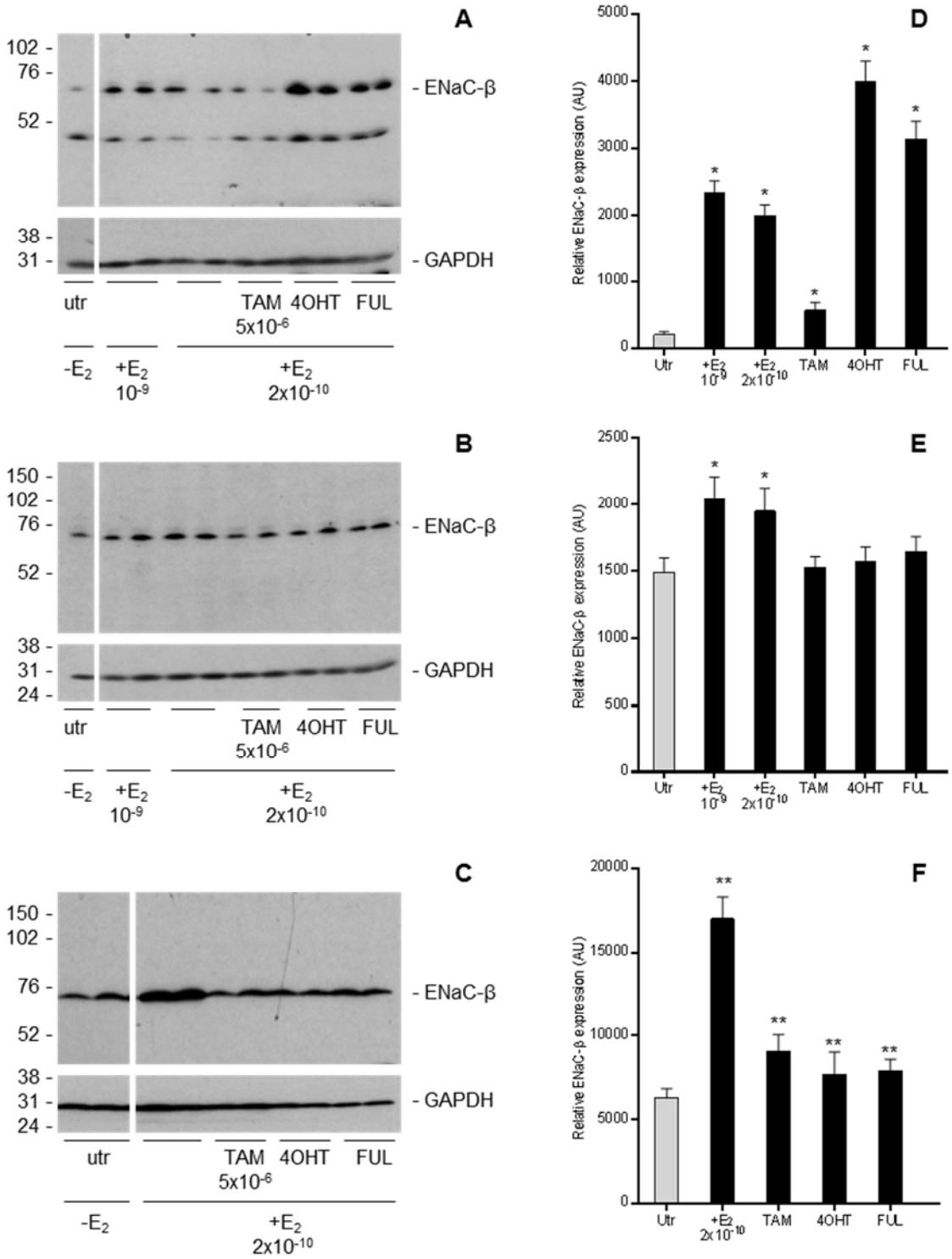

Figure 6.12 Antagonist activity of anti-oestrogens on ENaC-β expression. MCF-7, EFM-19 (50,000 per well) and EFF-3 (100,000 per well) cells were plated onto a 24-well plate. Cells were steroid deprived by culturing in phenol-red-free media containing 10% dextran-coated charcoal treated serum and 1 μg/ml insulin, for 5 days and then then cultured in withdrawal medium alone (utr) or treated with 10^{-9} M, $2x10^{-10}$ M 17β-oestradiol alone, or $5x10^{-6}$ M tamoxifen (TAM), 10^{-8} M 4-hydroxytamoxifen (4OHT), 10^{-8} M Fulvestrant (FUL) in combination with $2x10^{-10}$ M 17β-oestradiol for 8 days. Cells were lysed and protein extracts were prepared. Protein aliquots of 10 μg were separated by 12% polyacrylamide gel electrophoresis and then transferred to nitrocellulose membranes. The membranes were incubated with anti-ENaC-β antibody (dilution 1:100) overnight at 4 ^{o}C, followed by horseradish peroxidase conjugated

horse-anti-mouse secondary antibody for 1 hour at 37 ^{o}C. Proteins were visualised by enhanced chemiluminescence with SuperSignal West Dura Extended Duration Substrate. **A, B, C.** The protein expression of ENaC-β in MCF-7, EFM-19 and EFF-3 cells treated with anti-oestrogens, comparing serum withdrawn (-E_2 □) samples with oestrogen-stimulated (+E_2 ■) samples. The image shown is representative of an experiment which has been replicated three times in MCF-7 and EFM-19 cells and twice in EFF-3 cells. **D, E, F.** Quantification of ENaC-β normalised against the corresponding GAPDH signal, *$p < 0.05$ and **$p < 0.001$ by ANOVA, compared with $2x10^{-10}$ M oestradiol treated cells. Error bars indicate SEM of duplicate measurements.

Figure 6.13 shows the antagonist activity of bazedoxifene, toremifene, raloxifene and lasofoxifene in MCF-7, EFM-19 and EFF-3 cells.

In MCF-7 cells, bazedoxifene and lasofoxifene in the presence of oestradiol reduced the expression of ENaC-β to levels almost below that of untreated cells, suggesting that they were antagonistic to the effects of oestrogen. In the presence of oestrogen, toremifene and raloxifene increased the expression of ENaC-β to levels higher than that of oestrogen alone.

In the presence of oestradiol, toremifene demonstrated a considerable increase in ENaC-β expression and did not block the effects of oestrogen in EFM-19 cells (Figure 6.13B). Nevertheless, bazedoxifene, raloxifene and lasofoxifene largely antagonised the effects of oestrogen. Raloxifene was the most antagonistic as it decreased the oestrogen-induced ENaC-β expression by about 2.5-times that of oestrogen alone.

In EFF-3 cells, there was no significant difference in ENaC-β expression between untreated and oestrogen-treated cells, therefore it was difficult to test the antagonistic effects of these anti-oestrogens. This experiment requires further validation.

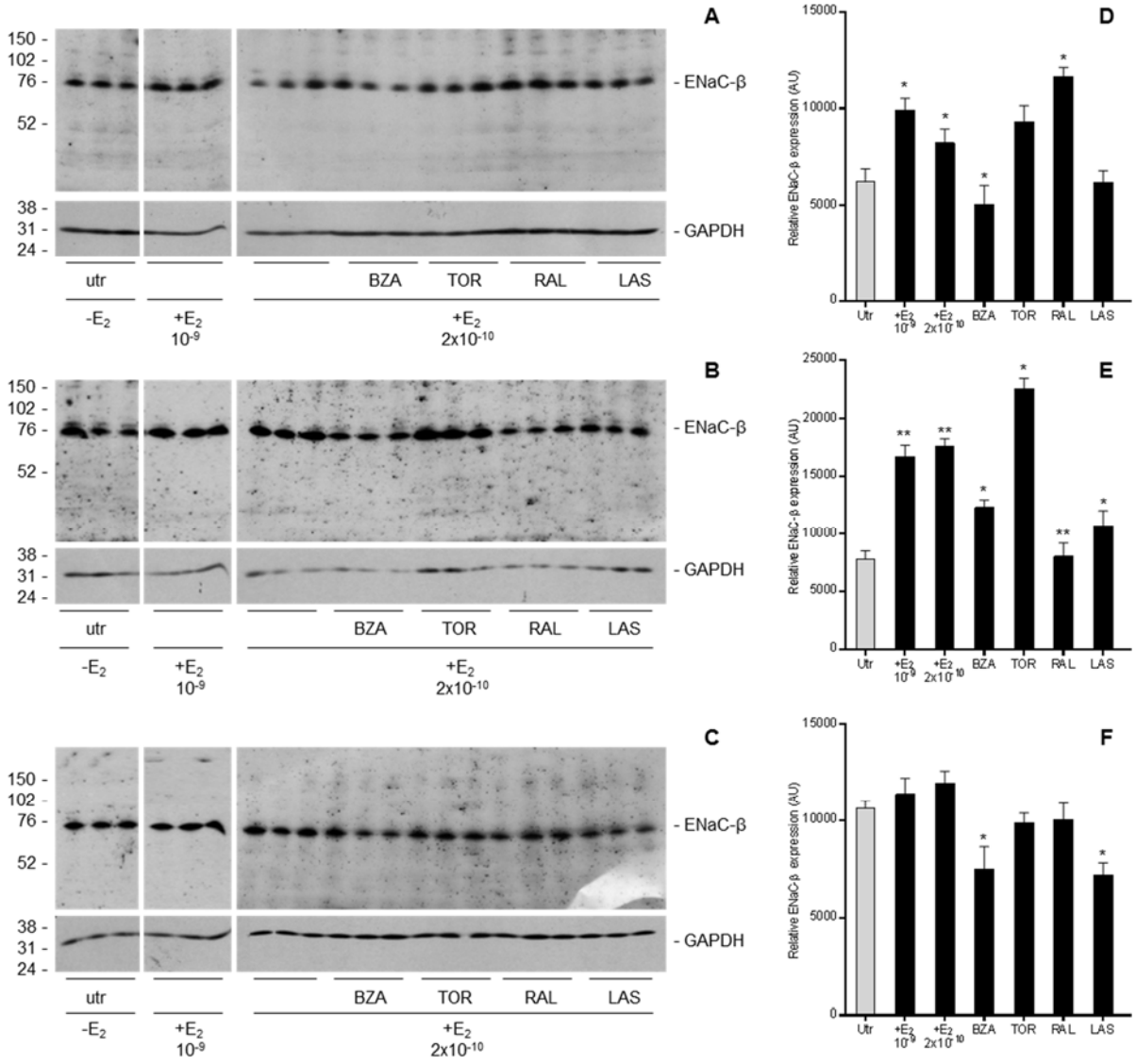

Figure 6.13 Antagonist activity of anti-oestrogens BZA, TOR, RAL, LAS on ENaC-β expression. MCF-7, EFM-19 (50,000 per well) and EFF-3 (100,000 per well) cells were plated onto a 24-well plate. Cells were steroid deprived by culturing in phenol-red-free media containing 10% dextran-coated charcoal treated serum and 1 µg/ml insulin, for 5 days and then cultured in withdrawal medium alone (utr) or treated with 10^{-9} M, $2x10^{-10}$ M 17β-oestradiol alone, or 10^{-7} M Bazedoxifene (BZA), 10^{-7} M Toremifene (TOR), 10^{-7} M Raloxifene (RAL), 10^{-8} M Lasofoxifene (LAS) in combination with $2x10^{-10}$ M 17β-oestradiol for 8 days. Cells were lysed and protein extracts were prepared. Protein aliquots of 10 µg were separated by 12% polyacrylamide gel electrophoresis and then transferred to nitrocellulose membranes. The membranes were incubated with anti-ENaC-β antibody (dilution 1:100) overnight at 4 ºC, followed by horseradish peroxidase conjugated horse-anti-mouse secondary antibody for 1 hour at 37 ºC. Proteins were visualised by enhanced chemiluminescence with SuperSignal West Dura Extended Duration Substrate. **A, B, C.** The protein expression of ENaC-β in MCF-7, EFM-19 and EFF-3 cells treated with anti-oestrogens, comparing serum withdrawn ($-E_2$ □) samples with oestrogen-stimulated ($+E_2$ ■) samples. The image shown is representative of an experiment which has been replicated twice. **D, E, F.** Quantification of ENaC-β normalised against the corresponding GAPDH signal, *p < 0.05 and **p < 0.001 by ANOVA, compared with $2x10^{-10}$ M oestradiol treated cells. Error bars indicate SEM of triplicate measurements.

6.5 Discussion

The effects of seven anti-oestrogens on the expression levels of the proteins NKCC1, NHERF3 and ENaC-β was studied. These proteins are encoded by the oestrogen-regulated genes *SLC12A2*, *PDZK1* and *SCNN1B*, respectively. The agonist activity of the anti-oestrogens tamoxifen, 4-hydroxytamoxifen, fulvestrant, bazedoxifene, toremifene, raloxifene and lasofoxifene were tested in the absence of oestrogen. The antagonistic properties of the different anti-oestrogens were investigated in the presence of 17β-oestradiol.

6.5.1 Effect of anti-oestrogens on NKCC1 expression

The anti-oestrogens tamoxifen, 4-hydroxytamoxifen, fulvestrant, toremifene, raloxifene and lasofoxifene in the absence of oestradiol did not exert any oestrogen-like agonistic effects on the expression of NKCC1 protein in any of the cell lines. Bazedoxifene on its own displayed very weak agonism in EFM-19 cells only. In MCF-7 and EFF-3 cells, bazedoxifene alone showed no agonism.

In the presence of oestrogen, tamoxifen completely reversed the negative effect of oestrogen on NKCC1 expression in MCF-7 and EFF-3 cells, but not in EFM-19 cells. 4-hydroxytamoxifen acted as a partial antagonist of oestrogen in all three cell lines. The fully antagonistic activity of tamoxifen and the partial antagonistic activity of fulvestrant in MCF-7 cells are interesting as generally tamoxifen and fulvestrant are known to be partially and fully anti-oestrogenic, respectively. Bazedoxifene, raloxifene and lasofoxifene antagonised fully the effect of oestrogen in all three cell lines. The structurally similar anti-oestrogens bazedoxifene and raloxifene behaved in a similar manner; they both inhibited the reduction of NKCC1 expression by oestrogen. The inhibition of the effect of oestrogen on the protein expression of NKCC1 by the anti-oestrogen toremifene varied between cell lines. In MCF-7 and EFM-19 cells, partial inhibition was detected, whereas in EFF-3 cells there was complete inhibition. These results indicated that, although tamoxifen, 4-hydroxytamoxifen and toremifene are similar in structure, their functional ability to block the effects of oestrogen on NKCC1 expression is dissimilar.

6.5.2 Effect of anti-oestrogens on NHERF3 expression

Tamoxifen alone at 10^{-7} M showed no agonism in MCF-7 and EFM-19 cells, but was a weak agonist for the expression of NHERF3 protein in EFF-3 cells. However, tamoxifen at a higher concentration of $5x10^{-6}$ M, was a weak agonist in MCF-7 cells but not in EFM-19 cells. In MCF-7 and EFM-19 cells, the tamoxifen derivative, 4-hydroxytamoxifen, did not have any oestrogen-like activity on the expression of NHERF3, with the exception of EFF-3 cells, where it showed partial agonist activity by inducing NHERF3 expression to levels higher than those of tamoxifen alone. The pure anti-oestrogen fulvestrant and two anti-oestrogens bazedoxifene and raloxifene showed no agonism in all three cell lines. Data from the current study are consistent with those of Englert *et al.* (2011) who showed that *PDKZ1* mRNA expression in MCF-7 cells is not increased by treatment with raloxifene. However, in long-term oestrogen exposed (LTEE) MCF-7 cells, *PDZK1* expression was increased by 7.8-fold and this induction was also shown to be abolished by exposure to raloxifene (Englert *et al.*, 2011). As observed in this chapter, similarities in the effects of bazedoxifene and raloxifene on the expression of NHERF3 protein could possibly be explained by their structural and functional similarities. In contrast, toremifene and lasofoxifene exerted a weak agonistic activity on NHERF3 expression in MCF-7 cells, but not in the other two cell lines EFM-19 and EFF-3.

Both tamoxifen and 4-hydroxytamoxifen inhibited completely the oestrogen-induced NHERF3 expression in EFM-19 cells, whereas in MCF-7 cells they only partially blocked the effects of oestrogen. Similar results have been reported previously in MCF-7 cells by Ghosh *et al.* (2000) who indicated by northern transfer analysis that tamoxifen inhibited the oestradiol-induced expression of *PDZK1*. However, in the present study, these two anti-oestrogens tamoxifen and 4-hydroxytamoxifen were unable to oppose the effects of oestrogen on the protein expression of NHERF3 in EFF-3 cells. Complete antagonism against the oestrogen-induced NHERF3 expression was achieved by fulvestrant, bazedoxifene and raloxifene. Although lasofoxifene completely inhibited the effects of oestrogen on NHERF3 expression in both MCF-7 and EFM-19 cells, it did not block the oestrogenic effects in EFF-3 cells. Toremifene has a

pharmacological profile similar to that of tamoxifen and has been shown to inhibit growth and proliferation of breast cancer cells (Robinson and Jordan, 1989; Grenman *et al.*, 1991). In the current study, the oestrogen antagonist property of toremifene varied between the three cell lines. In MCF-7 cells, it was weakly antagonistic, whereas in EFM-19 and EFF-3 cells toremifene increased the expression of NHERF3 above the level induced by oestrogen alone. The mechanism by which this effect occurs is not understood well, but studies have suggested the possible existence of oestrogen receptor heteroligand dimer complexes, in which oestradiol can bind to one ER monomer of the dimer subunit whilst the anti-oestrogen binds to the other monomer (Liu *et al.*, 2013). Therefore it is likely that in EFM-19 and EFF-3 cells, dimer complexes that contain both oestradiol and toremifene could cooperatively enhance the expression of NHERF3.

6.5.3 Effect of anti-oestrogens on ENaC-β expression

The effects of the different anti-oestrogens on the expression of ENaC-β were variable between the three cell lines as shown in section 6.4 of this chapter.

Tamoxifen at a concentration of 10^{-7} M and $5x10^{-6}$ M did not show any agonist behaviour in MCF-7 and EFF-3 cells. However, 10^{-7} M tamoxifen in EFM-19 cells showed oestrogen-like effects. Both 4-hydroxytamoxifen and fulvestrant were full agonists in MCF-7 cells, but not in EFM-19 and EFF-3 cells. In MCF-7 and EFM-19 cells, none of the anti-oestrogens bazedoxifene, toremifene, raloxifene and lasofoxifene had any oestrogen-like activity on ENaC-β expression. The levels of ENaC-β expression were less affected by the anti-oestrogens. Conversely, the treatment of EFF-3 cells with these four anti-oestrogens alone resulted in a significant decline in ENaC-β protein expression in comparison to the untreated cells. The results for tamoxifen and its active metabolite 4-hydroxytamoxifen are inconsistent. The mechanism of action is similar in both tamoxifen and 4-hydroxytamoxifen (Coezy *et al.*, 1982; DeFriend *et al.*, 1994a; Kiyotani *et al.*, 2012) therefore it is not clear why 4-hydroxytamoxifen induced the expression of ENaC-β whereas tamoxifen did not. The agonist activity of fulvestrant in MCF-7 cells is surprising, as it is considered

to be a pure anti-oestrogen. Agonist activity of fulvestrant has been reported in oestrogen-responsive breast cancer cells. Hutcheson *et al.* (2011) and Morrison *et al.* (2013) demonstrated that fulvestrant induces protein expression of members of the epidermal growth factor receptor (EGFR) family, ErbB3 and ErbB4. Hutcheson *et al.* (2011) showed that despite cell growth inhibition by fulvestrant, it stimulated expression of proteins involved in cell proliferation and survival, through posttranslational modifications hence allowing tumour cells to develop resistance.

When the antagonistic properties of tamoxifen was tested, results indicated that it was partially anti-oestrogenic in MCF-7 and EFF-3 cells and very weakly antagonistic in EFM-19 cells. The induction of ENaC-β protein expression by both 4-hydroxytamoxifen and fulvestrant was greater than that of oestradiol alone in MCF-7 cells only. In EFM-19 cells, 4-hydroxytamoxifen and fulvestrant were very weak antagonists, whilst in EFF-3 cells they effectively inhibited the oestrogen-induced ENaC-β expression. Bazedoxifene and lasofoxifene were antagonistic to the effects of oestrogen in both MCF-7 and EFM-19 cells, whereas raloxifene increased ENaC-β expression to levels higher than that of oestrogen in MCF-7 cells only. The level of induction of the expression of ENaC-β by toremifene was considerably higher than oestrogen alone in EFM-19 cells.

6.6 Conclusion

The oestrogenicity of the anti-oestrogens for the repression of NKCC1 or induction of NHERF3 and ENaC-β were specific for each protein and were variable between the three cell lines. Notably, the antagonistic effects of toremifene for NHERF3 and ENaC-β expression were somewhat similar, as it induced protein expression to higher levels than oestradiol alone. Tamoxifen, bazedoxifene, raloxifene and lasofoxifene completely inhibited the effects of oestrogen on NKCC1 expression.

This chapter has shown successfully the complexity of the differential effects anti-oestrogens might have on various genes regulated by oestrogen. These results could potentially be translated into the clinics because such valuable

biomarkers might provide means for predicting or monitoring a patient's response to endocrine therapy. It will be important to take into consideration the agonist activity of anti-oestrogens which might cause a limitation in their inhibitory anti-oestrogenic role and potentially lead to development of resistance or enhanced tumour progression.

Chapter 7. General Discussion

7.1 Discussion and Future work

Breast cancer is currently the most commonly diagnosed cancer in the UK and has the second highest incidence throughout the world. Despite early detection screening and advances in treatment procedures, a large proportion of women die from breast cancer every year. In the UK, the number of deaths caused by breast cancer in females is second only to lung cancer. Therefore there is a necessity to identify prognostic biomarkers which may aid in an effective diagnosis. Also it would be clinically beneficial to patients because such predictive biomarkers would enable accurate forecasting of the response to individual therapies. Additionally potential therapeutic targets could be identified in order to maximise the rate of response as well as to overcome the problems associated with resistance to drugs.

During recent years, ion transporters have been implicated in many characteristic features of cancer pathogenesis such as uncontrolled growth, migration, invasion and metastasis (Kunzelmann, 2005; Prevarskaya *et al.*, 2010; Li and Xiong, 2011). Therefore ion transporters are being identified as possible additional targets for combined therapies in cancer. Oestrogen is well known to play a major role in the progression and development of breast cancer. Previously, numerous genes that are regulated by oestrogen have been identified by our group (Westley and May, 2006; Wright *et al.*, 2009). The recognition of genes involved in exocytosis and vesicle transport thought to be associated with breast tumorigenesis, has led to the discovery of new avenues for further investigation. Understanding the role of oestrogen in altering the secretory phenotype and mediating polarised ion transport is of vital importance. Out of the many genes identified, the roles of three oestrogen-regulated genes *SLC12A2*, *PDZK1* and *SCNN1B* were studied in detail in this study. The regulation of the genes *SLC12A2* and *SCNN1B* by oestrogen was novel, whereas *PDZK1* was previously recognised as an oestrogen-regulated gene in breast cancer cells.

The expression of the proteins NKCC1, NHERF3 and ENaC-β which are encoded by the genes *SLC12A2*, *PDZK1* and *SCNN1B* were measured. The expression of these proteins was investigated initially in a panel of oestrogen-responsive and oestrogen-unresponsive breast cancer cell lines. The expression of NKCC1 varied between cell lines and the highest expression was in the oestrogen-responsive ZR-75 cells and the oestrogen-unresponsive in Hs578T cells. All other cell lines investigated, with the exception of SKBR3, BT-20 and T47-D, expressed moderate amounts of NKCC1 protein. The total protein expression of NHERF3 was highest in ZR-75 cells, but MCF-7, EFM-19 and T47-D cells also expressed NHERF3. It is important to note that there was no expression of NHERF3 in any of the oestrogen-unresponsive cell lines. Similar to NKCC1, some oestrogen-responsive and some oestrogen-unresponsive cell lines expressed ENaC-β protein. Out of the oestrogen-responsive cell lines, EFF-3 cells expressed highest levels of ENaC-β followed by BT-474, EFM-19 and MCF-7 cells. In the oestrogen-unresponsive cell lines, SKBR3, MDA-MB-231 and Hs578T cells expressed ENaC-β protein. The regulation of these proteins by oestradiol in three oestrogen-responsive breast cancer cell lines MCF-7, EFM-19 and EFF-3 was studied. Results obtained were consistent with the gene expression analysis, as NKCC1 expression was shown to decrease in response to oestradiol, whereas the expression of the proteins NHERF3 and ENaC-β were increased when stimulated with oestradiol. Furthermore, investigations showed that the regulation of these proteins by oestradiol was concentration dependent. The cellular localisation of these proteins was also evaluated by immunofluorescence and evidence showed that NKCC1 was clearly expressed in the cell membranes, whereas NHERF3 and ENaC-β were detected mainly in the cytoplasm. Investigation of the effects of oestrogen on the protein expression of NKCC1 showed a marked decrease whilst the expression of NHERF3 increased. These immunofluorescence results were consistent with the results from western transfer analysis. There was no expression of ENaC-β at the cell membrane therefore we were not so confident about the reliability of this immunofluorescent detection of ENaC-β. Future immunofluorescence experiments could include testing different commercially available antibodies against ENaC-β to identify its localisation within the cell. It

will be interesting to investigate any possible relocation of ENaC-β to the cell membrane through vesicular transport and also to explore and evaluate any changes in expression or localisation of ENaC-β in response to oestrogen stimulation.

NKCC1 and ENaC-β protein was expressed in oestrogen-unresponsive cell lines which lack the oestrogen receptor. Therefore it would be desirable to extend a similar study to other breast cancer cell lines, particularly the oestrogen-unresponsive cell lines, in order to determine whether there are any additional mechanisms of regulation of genes and their proteins such as NKCC1 and ENaC-β other than through the oestrogen receptor. The regulation of NHERF3 expression by oestrogen in ZR-75 cells could also be explored, because ZR-75 expressed high amounts of NHERF3 protein.

The functional activity of NKCC1 was assessed in the current study. Experiments with the ^{86}Rb (K^+) influx assay revealed lower activity of NKCC1 in comparison to Na^+/K^+ ATPase in both MCF-7 and EFM-19 cells cultured in full medium as the ouabain-sensitive influx was much greater than the loop-diuretic sensitive influx. Future work could include investigation of the expression and oestrogen regulation of Na^+/K^+ ATPase in the three breast cancer cell lines. In the present study, further experimentation in MCF-7 and EFM-19 cells grown in full media confirmed that NKCC1 is activated in response to cell shrinkage as induced by hypertonic mannitol and that NKCC1 is involved in the regulation of cell volume (Russell, 2000; Hebert *et al.*, 2004). Although the effect of oestrogen on NKCC1 protein expression clearly demonstrated a significant decrease, the results from the influx assay do not show such a dramatic reduction on the functional activity of NKCC1. We also determined that NKCC1 was activated in response to hypertonic stimulation by mannitol in both steroid withdrawn and in oestrogen stimulated cells. However, EFM-19 cells were significantly more responsive than MCF-7 cells, to both the effect of hypertonicity and also to the effect of oestrogen. This variability in the effects between the two cell lines is not understood and requires further clarification. Moreover, it would be useful to explore and compare the functional roles of NKCC1 present in cells that are treated with anti-oestrogens in the absence and

presence of oestrogen, to determine if the functional activity corresponds with the changes in expression induced by the anti-oestrogens shown in the current study.

In the present study, the intracellular pH of breast cancer cells was measured as means of investigating the activity of Na^+/H^+ exchangers, whose organisation and anchorage at the surface of the plasma membrane is determined by the oestrogen-regulated NHERF3. Results showed that MCF-7 and EFM-19 cells are subject to pH_i perturbations when exposed to highly acidic external pH. Since the inverse Na^+ ion gradient is higher than the gradient of H^+ ions, the Na^+/H^+ exchangers are unable to pump H^+ ions out, therefore the pH_i is not maintained at physiological values when the external pH is 6.0. The oestrogen-stimulated EFM-19 cells were shown to have an increased buffering capacity in comparison to the unstimulated cells, as the pH_i increased in response to oestrogen. This increase in buffering capacity coincides with the increase in NHERF3 protein. We have shown evidence for activation of Na^+/H^+ exchangers by the induction of hypertonicity with mannitol in both these breast cancer cell lines grown in full media. The effect of hypertonicity on untreated and oestrogen-treated cells was not consistent with the results from cells cultured in full media. At an external pH 6.0, the untreated MCF-7 and EFM-19 cells were unable to maintain pH_i under hypertonic conditions, which was even worsened in oestrogen-stimulated MCF-7 cells. However, oestrogen-treated EFM-19 cells show increased capacity to regulate pH_i. The ability of breast cancer cells to recover a physiological internal pH following an acidic pulse with the addition of NH_4Cl was explored. At external pH 7.4, the removal of NH_4Cl causes cytosolic acidification which then recovers slowly by the activity of Na^+/H^+ exchangers, but in an external pH 6.0, cells do not have the capacity to aid in recovering pH_i. Another study in MCF-7 cells has investigated the involvement of NHE1 in the recovery of pH_i in response to an acid pulse (Friday *et al.*, 2007). We hypothesised that, in comparison to the untreated cells, oestrogen-stimulated cells would have an enhancement in their rate of recovery by Na^+/H^+ exchange because NHERF3 protein expression is increased in cells treated with oestrogen. Nevertheless, current data showed no such enhancement in the pH_i regulatory capacity in oestrogen-treated MCF-7 and EFM-19 cells. To the best

of our knowledge this is the first study to demonstrate pH_i regulation in EFM-19 cells. Future experimentation could potentially involve siRNA knockdown of *PDZK1* in breast cancer cell lines which would enable understanding of the role played by NHERF3 in modulating the linkage and regulation of Na^+/H^+ exchangers associated with pH_i regulation. This study could be extended to measure the protein expression and the oestrogen-regulation of the different Na^+/H^+ exchangers in MCF-7, EFM-19 and EFF-3 breast cancer cells. The data obtained from the present study encourage further experimentation with the BCECF-AM assay, as it would be beneficial to include inhibitors of Na^+/H^+ exchangers such as ethyl-isopropyl-amiloride (EIPA) to evaluate the effects of oestrogen in mediating ion transport through upregulation of *PDZK1*.

The effects of anti-oestrogens on the expression of NKCC1, NHERF3 and ENaC-β protein was evaluated. It was evident that the agonistic and antagonistic effects of different anti-oestrogens on each of the three proteins were complex and there was variability between cell lines. Overall, none of the anti-oestrogens displayed oestrogen-like activity towards the expression of NKCC1, apart from bazedoxifene in EFM-19 cells. Tamoxifen, 4-hydroxytamoxifen, toremifene and lasofoxifene were partially agonistic to varying degrees for the expression of NHERF3 protein in MCF-7 and EFF-3 cells. The agonist effect of fulvestrant on increased expression of ENaC-β in MCF-7 cells was particularly surprising because this pure anti-oestrogen is a selective downregulator of the oestrogen receptor. In the three cell lines, all anti-oestrogens either partially or completely antagonised the effects of oestrogen for the expression of NKCC1 protein. The effect of oestrogen on the expression of NHERF3 was also reversed partially or completely by most of the anti-oestrogens, excluding toremifene in EFM-19 cells. In EFF-3 cells treated with tamoxifen, 4-hydroxytamoxifen, toremifene and lasofoxifene in the presence of oestrogen, no inhibition of the effect of oestrogen was observed. The antagonistic properties of the anti-oestrogens for the expression of ENaC-β were very variable between cell lines. In MCF-7 cells, 4-hydroxytamoxifen, fulvestrant, toremifene and raloxifene were unable to block the effects of oestrogen, whereas in EFM-19 cells toremifene was unable to inhibit the increased expression induced by oestrogen. The oestrogen-induced protein

expression of ENaC-β was almost completely inhibited by tamoxifen, 4-hydroxytamoxifen and fulvestrant in the EFF-3 cell line.

Differences in response of genes to anti-oestrogens could perhaps be accounted for by differences in genetic mutations between the cell lines. Analysis from the Catalogue Of Somatic Mutations In Cancer database, highlighted mutations in *PIK3CA* in both MCF-7 and EFM-19 cell lines (COSMIC). The mutation in *PIK3CA* in MCF-7 cells is a heterozygous, missense substitution, whereas in EFM-19 cells it is a homozygous missense substitution. It has been reported that oestradiol blocks apoptosis and promotes survival through activation of the PI3K and MAPK pathways (Fernando and Wimalasena, 2004). Activation of the PI3K/AKT pathway and the MAPK/ERK pathway have been reported to contribute to the development of resistance to endocrine therapy (Zhang *et al.*, 2011). In collecting duct cells, the regulation of ENaC activity by hormones such as oestrogen, aldosterone and insulin is mediated via a PI3K dependent mechanism which includes phosphorylation of SGK1 (Wang *et al.*, 2008; Baines, 2013). Moreover, in cortical collecting duct cells, the inhibition of PI3K by LY294002, prevented transepithelial transport of Na^+ ions that was previously induced by aldosterone (Zhou *et al.*, 2014). The phosphorylation of NKCC1 is suggested to be mediated via a PI3K-dependant mechanism, which in turn leads to an enhancement in migration of glioma cells (Garzon-Muvdi *et al.*, 2012). In addition to *PIK3CA*, the transcription factor *GATA3* is mutated in MCF-7 cells only (Usary *et al.*, 2004). This is an insertional frameshift mutation at amino acid position D336, resulting from an insertion of a guanine nucleotide. The *FGFR2* and *TP53* genes are mutated in EFM-19 cells. The gene *FGFR2* identified previously by genome wide association studies is associated with breast cancer risk (Easton *et al.*, 2007). The mutations identified are unlikely to account for the differential responses of the cells to anti-oestrogens.

In order to determine the clinical relevance of the three genes, I evaluated the supplementary data from a number of published studies that explored agonist and antagonist effects of anti-oestrogens and aromatase inhibitors on the expression of oestrogen regulated genes. The gene *PDZK1* whose expression

is known to be increased by oestrogen has been shown previously to be decreased by treatment of MCF-7 cells with 1 μM of the anti-oestrogens, fulvestrant and raloxifene (Frasor *et al.*, 2004). In two clinical studies, in which breast tumours were isolated from postmenopausal women who had previously been treated for 14 days with the aromatase inhibitors; anastrozole and letrozole, the expression of *PDZK1* was consistently downregulated in response to treatment (Mackay *et al.*, 2007; Miller *et al.*, 2007). The other two genes *SLC12A2* and *SCNN1B* were not detected in any of these clinical studies.

Furthermore, future directions including immunohistochemical studies would provide valuable analysis of the expression and localisation of the proteins NKCC1, NHERF3 and ENaC-β in breast tumours isolated from patients. Investigations could be extended to evaluate expression of the three proteins in xenograft models and patient derived breast cancer samples that retain characteristics of the original tumour. Such models would enable greater understanding of clinically-relevant prognostic and predictive information for the potential development of personalised therapeutic strategies. The generation of 3D spheroids and organoids may provide a close resemblance to the physiology of cancer cells *in vivo*. These 3D cultures can form well-organised epithelial structures, complete with cell polarity and formation of tight junctions.

The role of oestrogen in altering the expression and activity of proteins involved in ion transport was confirmed. Modification of this cell phenotype may favour breast cancer progression. The results from this study, particularly NKCC1 and NHERF3 will be of great benefit in terms of identifying suitable treatment conditions and to forecast disease progression.

Abbreviations

µM	Micro molar
µm	Micro metre
17β-HSD1	17β-hydroxysteroid dehydrogenase type 1
4OHT	4-hydroxytamoxifen
ADP	Adenosine diphosphate
AF-1	Activation function domain 1
AF-2	Activation function domain 2
AFF2	AF4/FMR2 family member 2
ANKLE1	Ankyrin repeat and LEM domain containing 1
ANOVA	Analysis of variance
APS	Ammonium Persulphate
ATCC	American Type Culture Collection
ATM	Ataxia-telangiectasia mutated
BABAM1	BRISC and BRCA1 A complex member 1
BCA	Bicinchoninic Acid
BCECF-AM	2',7'-bis-(2-carboxyethyl)-5-(and-6)-carboxyfluorescein acetoxymethyl ester
bp	base pair
BRCA (1, 2)	Breast Cancer Associated (susceptibility gene 1 and 2)
BSA	Bovine Serum Albumin
BZA	Bazedoxifene
$CaCl_2$	Calcium chloride
cAMP	Cyclic adenosine monophosphate
CASC16	Cancer susceptibility candidate 16
CASC21	Cancer susceptibility candidate 21
CASC8	Cancer susceptibility candidate 8
CCND1	Cyclin D1
CCND3	Cyclin D3
CDK4	Cyclin-dependent kinase 4
CDK6	Cyclin-dependent kinase 6
cDNA	Complementary deoxyribonucleic acid
CFTR	Chloride transport receptor
CNA	Copy number aberrations
COMT	Catechol-o-methyltransferase
COSMIC	Catalogue of somatic mutations in cancer
CPM	Counts per minute
CRUK	Cancer Research United Kingdom
Cu^{+}	Cuprous ion
Cu^{2+}	Cupric ion
CYP2C19	Cytochrome P450, family 2, subfamily C, polypeptide 19
DAPI	4',6-diamidino-2-phenylindole
DBD	DNA Binding Domain
DCC-CS	Dextran-Coated Charcoal-treated Calf Serum
DCIS	Ductal Carcinoma *In Situ*
DMEM	Dulbecco's modified eagles medium

DMSO	Di-Methyl Sulphoxide
DNA	Deoxyribo Nucleic Acid
DNA-PK	DNA-Protein Kinase
E_1	oestrone
E_2	oestradiol
E_3	oestriol
EDTA	Ethylene Diamine Tetra Acetic Acid
EGF	Epidermal Growth Factor
EGFR	Epidermal Growth Factor Receptor
EIPA	ethyl-isopropyl-amiloride
ELISA	Enzyme Linked Immunosorbant Assay
EMSY	EMSY, BRCA2-interacting transcriptional repressor
ENaC	Epithelial sodium channel
ENaC-α	Epithelial sodium channel alpha subunit
ENaC-β	Epithelial sodium channel beta subunit
ENaC-γ	Epithelial sodium channel gamma subunit
ENaC-δ	Epithelial sodium channel delta subunit
ERE	Oestrogen Response Elements
ERs	Oestrogen Receptors
ERα	Oestrogen receptor alpha
ERβ	Oestrogen receptor beta
FACS	Flow activated cell sorting
FAK	Focal adhesion kinase
FBS	Foetal Bovine Serum
FDA	Food and Drug Administration
FGFR2	Fibroblast growth factor receptor 2
Fig.	Figure
FISH	Fluorescent in situ hybridisation
FTO	Fat mass and obesity associated
FUL	Fulvestrant
G_1/S	Gap 1 / Synthesis
GAPDH	Glyceraldehyde 3-Phosphate Dehydrogenase
GATA3	GATA binding protein 3
GWAS	Genome wide association studies
HCl	Hydrochloric acid
HEPES N-2	hydroxyethylpiperazine-N'-2-ethanesulfonic acid
HER2	Human Epidermal Growth Factor Receptor 2
HRP	Horse Radish Peroxidase
IDC	Invasive Ductal Carcinoma
IGF-1	Insulin-like Growth Factor 1
IGF-IR	Type I IGF receptor
IHC	Immunohistochemistry
ILC	Invasive Lobular Carcinoma
IntClust	Integrative Cluster
IP3	Inositol-1,4,5 triphosphate
IR	Insulin receptor
K_2HPO_4	Dipotassium hydrogen orthophosphate
Kb	Kilobase

KCl	Potassium chloride
kDa	KiloDalton
KH_2PO_4	Potassium dihydrogen phosphate
KHH	Krebs' Henseleit HEPES-buffered solution
LAS	Lasofoxifene
LBD	Ligand Binding Domain
LCIS	Lobular Carcinoma *In Situ*
LGR6	Leucine-rich repeat containing G-protein coupled receptor 6
LSP1	Lymphocyte specific protein 1
M	Molar
mA	Milliamps
MAP17	Membrane-associated protein 17
MAP2K4	Mitogen activated protein kinase kinase 4
MAP3K1	Mitogen activated protein kinase kinase kinase 1
MAPK	Mitogen Activated Protein Kinase
Mb	Megabase
MDM4	Mouse Double Minute 4, p53 regulator
MEK	Mitogen activated protein kinase kinase
MES hydrate	2-(N-morpholino)ethanesulfonic hydrate
MgCl2	Magnesium chloride
$MgSO_4$	Magnesium sulphate
mM	Milli molar
mm	Milli metre
mRNA	Messenger RNA
mTOR	Mammalian target of rapamycin
NaCl	Sodium chloride
NaH_2PO_4	Sodium dihydrogen phosphate
NCS	New-born Calf Serum
NF1	Neurofibromin 1
NHE	Sodium hydrogen exchanger
NHERF	Sodium hydrogen exchange regulatory co-factor
NKCC1	Sodium potassium chloride co-transporter 1
NKCC2	Sodium potassium chloride co-transporter 2
nM	Nano molar
NP-40	Nonylphenoxy Polyethoxy Ethanol
NRIP1	Nuclear receptor interacting protein 1
NTD	N-terminal domain
OH	Hydroxyl
OSR1	Oxidative stress-responsive kinase 1
PBS	Phosphate Buffered Saline
PCR	Polymerase Chain Reaction
PDVF	Polyvinylidene Difluoride
pH_i	Intracellular pH
PI	Propidium iodide
PI3K	Phosphatidyl Inositol 3-Kinase related Kinases
PIK3CA	Phosphatidylinositol-4,5-bisphosphate 3-

	kinase catalytic subunit alpha
PMSF	Phenylemethoxysulphonyl Fluoride
PO_4	Phosphate
PR	Progesterone receptor
PRF	Phenol red free
PTEN	Phosphatase and Tensin homologue
PTFE	polytetrafluoroethylene
PTHLH	Parathyroid hormone-like hormone
PTPN22	Protein tyrosine phosphatase non-receptor type 22
qRT PCR	Quantitative Real Time Reverse Transcription Polymerase Chain Reaction
RAL	Raloxifene
RALY	RALY heterogeneous nuclear ribonucleoprotein
RIPA	Radioimmunoprecipitation assay
RNA	Ribo Nucleic Acid
RPM	Revolutions per minute
RUNX1	Runt-related transcription factor 1
SDS	Sodium Dodecyl Sulphate
SDW	Sterile Distilled Water
SEM	Standard error of the mean
SERD	Selective oestrogen receptor downregulator
SERM	Selective oestrogen receptor modulator
SGK	Serum glucocorticoid kinase
SHC	Src homology domain containing protein
siRNA	Small interfering RNA
SLC	Solute carrier family
SNP	Single nucleotide polymorphisms
SPAK	SPS1-related proline/alanine-rich kinase
TAM	Tamoxifen
TBS	Tris-Buffered Saline
TBST	Tris-Buffered Saline/Tween 20
TBX3	T-box 3
TCGA	The cancer genome atlas
TE	Tris-HCl EDTA
TEMED	Tetramethylethylenediamine
TERT	Telomerase reverse transcriptase
TM	Transmembrane
TNF	Tumour Necrosis Factor
TNM	Tumour, node, metastasis
TNRC9	Trinucleotide repeat containing 9
TOR	Toremifene
TP53	Tumour protein 53 gene
UV	Ultra-violet
UV-light	Ultra Violet Light
v/v	volume / volume
VEGF	Vascular Endothelial Growth Factor
w/v	weight / volume
w/w	weight / weight

WHO	World Health Organisation
WNK	With no lysine kinase
x g	Gravity
γ-ray	Gamma-Ray

References

Ackerman, G.E. and Carr, B.R. (2002) 'Estrogens', *Rev Endocr Metab Disord*, 3(3), pp. 225-30.

Aiton, J.F. and Simmons, N.L. (1984) 'An effect of piretanide upon the intracellular cation contents of cells subjected to partial chronic (Na-K) pump blockade by ouabain', *Biochem Pharmacol*, 33(21), pp. 3425-31.

Allen, N.E., Beral, V., Casabonne, D., Kan, S.W., Reeves, G.K., Brown, A. and Green, J. (2009) 'Moderate alcohol intake and cancer incidence in women', *J Natl Cancer Inst*, 101(5), pp. 296-305.

Alvarez-Baron, C.P., Jonsson, P., Thomas, C., Dryer, S.E. and Williams, C. (2011) 'The two-pore domain potassium channel KCNK5: induction by estrogen receptor alpha and role in proliferation of breast cancer cells', *Mol Endocrinol*, 25(8), pp. 1326-36.

Amith, S.R., Wilkinson, J.M., Baksh, S. and Fliegel, L. (2015) 'The Na(+)/H(+) exchanger (NHE1) as a novel co-adjuvant target in paclitaxel therapy of triple-negative breast cancer cells', *Oncotarget*, 6(2), pp. 1262-75.

Antoniou, A., Pharoah, P.D., Narod, S., Risch, H.A., Eyfjord, J.E., Hopper, J.L., Loman, N., Olsson, H., Johannsson, O., Borg, A., Pasini, B., Radice, P., Manoukian, S., Eccles, D.M., Tang, N., Olah, E., Anton-Culver, H., Warner, E., Lubinski, J., Gronwald, J., Gorski, B., Tulinius, H., Thorlacius, S., Eerola, H., Nevanlinna, H., Syrjakoski, K., Kallioniemi, O.P., Thompson, D., Evans, C., Peto, J., Lalloo, F., Evans, D.G. and Easton, D.F. (2003) 'Average risks of breast and ovarian cancer associated with BRCA1 or BRCA2 mutations detected in case Series unselected for family history: a combined analysis of 22 studies', *Am J Hum Genet*, 72(5), pp. 1117-30.

Antoniou, A.C., Wang, X., Fredericksen, Z.S., McGuffog, L., Tarrell, R., Sinilnikova, O.M., Healey, S., Morrison, J., Kartsonaki, C., Lesnick, T., Ghoussaini, M., Barrowdale, D., Embrace, Peock, S., Cook, M., Oliver, C., Frost, D., Eccles, D., Evans, D.G., Eeles, R., Izatt, L., Chu, C., Douglas, F., Paterson, J., Stoppa-Lyonnet, D., Houdayer, C., Mazoyer, S., Giraud, S., Lasset, C., Remenieras, A., Caron, O., Hardouin, A., Berthet, P., Collaborators, G.S., Hogervorst, F.B., Rookus, M.A., Jager, A., van den Ouweland, A., Hoogerbrugge, N., van der Luijt, R.B., Meijers-Heijboer, H., Gomez Garcia, E.B., Hebon, Devilee, P., Vreeswijk, M.P., Lubinski, J., Jakubowska, A., Gronwald, J., Huzarski, T., Byrski, T., Gorski, B., Cybulski, C., Spurdle, A.B., Holland, H., kConFab, Goldgar, D.E., John, E.M., Hopper, J.L., Southey, M., Buys, S.S., Daly, M.B., Terry, M.B., Schmutzler, R.K., Wappenschmidt, B., Engel, C., Meindl, A., Preisler-Adams, S., Arnold, N., Niederacher, D., Sutter, C., Domchek, S.M., Nathanson, K.L., Rebbeck, T., Blum, J.L., Piedmonte, M., Rodriguez, G.C., Wakeley, K., Boggess, J.F., Basil, J., Blank, S.V., Friedman, E., Kaufman, B., Laitman, Y., Milgrom, R., Andrulis, I.L., Glendon, G., Ozcelik,

H., Kirchhoff, T., Vijai, J., Gaudet, M.M., Altshuler, D., Guiducci, C., Swe, B., Loman, N., Harbst, K., Rantala, J., Ehrencrona, H., Gerdes, A.M., Thomassen, M., Sunde, L., et al. (2010) 'A locus on 19p13 modifies risk of breast cancer in BRCA1 mutation carriers and is associated with hormone receptor-negative breast cancer in the general population', *Nat Genet*, 42(10), pp. 885-92.

Archer, D.F., Pinkerton, J.V., Utian, W.H., Menegoci, J.C., de Villiers, T.J., Yuen, C.K., Levine, A.B., Chines, A.A. and Constantine, G.D. (2009) 'Bazedoxifene, a selective estrogen receptor modulator: effects on the endometrium, ovaries, and breast from a randomized controlled trial in osteoporotic postmenopausal women', *Menopause*, 16(6), pp. 1109-15.

Baines, D. (2013) 'Kinases as targets for ENaC regulation', *Curr Mol Pharmacol*, 6(1), pp. 50-64.

Beral, V. (2003) 'Breast cancer and hormone-replacement therapy in the Million Women Study', *Lancet*, 362(9382), pp. 419-27.

Bhatnagar, A.S. (2007) 'The discovery and mechanism of action of letrozole', *Breast Cancer Res Treat*, 105 Suppl 1, pp. 7-17.

Blair, R.M., Fang, H., Branham, W.S., Hass, B.S., Dial, S.L., Moland, C.L., Tong, W., Shi, L., Perkins, R. and Sheehan, D.M. (2000) 'The estrogen receptor relative binding affinities of 188 natural and xenochemicals: structural diversity of ligands', *Toxicol Sci*, 54(1), pp. 138-53.

Boyd, C. and Naray-Fejes-Toth, A. (2007) 'Steroid-mediated regulation of the epithelial sodium channel subunits in mammary epithelial cells', *Endocrinology*, 148(8), pp. 3958-67.

Boyd, N.F., Stone, J., Vogt, K.N., Connelly, B.S., Martin, L.J. and Minkin, S. (2003) 'Dietary fat and breast cancer risk revisited: a meta-analysis of the published literature', *Br J Cancer*, 89(9), pp. 1672-85.

Breitwieser, G.E., Altamirano, A.A. and Russell, J.M. (1990) 'Osmotic stimulation of Na(+)-K(+)-Cl- cotransport in squid giant axon is [Cl-]i dependent', *Am J Physiol*, 258(4 Pt 1), pp. C749-53.

Brueggemeier, R.W., Hackett, J.C. and Diaz-Cruz, E.S. (2005) 'Aromatase inhibitors in the treatment of breast cancer', *Endocr Rev*, 26(3), pp. 331-45.

Brzozowski, A.M., Pike, A.C., Dauter, Z., Hubbard, R.E., Bonn, T., Engstrom, O., Ohman, L., Greene, G.L., Gustafsson, J.A. and Carlquist, M. (1997) 'Molecular basis of agonism and antagonism in the oestrogen receptor', *Nature*, 389(6652), pp. 753-8.

Burris, T.P., Solt, L.A., Wang, Y., Crumbley, C., Banerjee, S., Griffett, K., Lundasen, T., Hughes, T. and Kojetin, D.J. (2013) 'Nuclear receptors and their selective pharmacologic modulators', *Pharmacol Rev*, 65(2), pp. 710-78.

Cancer Genome Atlas, N. (2012) 'Comprehensive molecular portraits of human breast tumours', *Nature*, 490(7418), pp. 61-70.

Cancer Statistics, CRUK (2014).

CGHFBC (1996) 'Breast cancer and hormonal contraceptives: collaborative reanalysis of individual data on 53 297 women with breast cancer and 100 239 women without breast cancer from 54 epidemiological studies. Collaborative Group on Hormonal Factors in Breast Cancer', *Lancet*, 347(9017), pp. 1713-27.

CGHFBC (2001) 'Familial breast cancer: collaborative reanalysis of individual data from 52 epidemiological studies including 58,209 women with breast cancer and 101,986 women without the disease', *Lancet*, 358(9291), pp. 1389-99.

Chalbos, D., Vignon, F., Keydar, I. and Rochefort, H. (1982) 'Estrogens stimulate cell proliferation and induce secretory proteins in a human breast cancer cell line (T47D)', *J Clin Endocrinol Metab*, 55(2), pp. 276-83.

Chan, A.M. and Weber, T. (2002) 'A putative link between exocytosis and tumor development', *Cancer Cell*, 2(6), pp. 427-8.

Chinigarzadeh, A., Muniandy, S. and Salleh, N. (2015) 'Estrogen, progesterone, and genistein differentially regulate levels of expression of alpha-, beta-, and gamma-epithelial sodium channel (ENaC) and alpha-sodium potassium pump (Na/K-ATPase) in the uteri of sex steroid-deficient rats', *Theriogenology*.

Coezy, E., Borgna, J.L. and Rochefort, H. (1982) 'Tamoxifen and metabolites in MCF7 cells: correlation between binding to estrogen receptor and inhibition of cell growth', *Cancer Res*, 42(1), pp. 317-23.

COSMIC. Available at: http://cancer.sanger.ac.uk.

Couch, F.J., Wang, X., McGuffog, L., Lee, A., Olswold, C., Kuchenbaecker, K.B., Soucy, P., Fredericksen, Z., Barrowdale, D., Dennis, J., Gaudet, M.M., Dicks, E., Kosel, M., Healey, S., Sinilnikova, O.M., Lee, A., Bacot, F., Vincent, D., Hogervorst, F.B., Peock, S., Stoppa-Lyonnet, D., Jakubowska, A., kConFab, I., Radice, P., Schmutzler, R.K., Swe, B., Domchek, S.M., Piedmonte, M., Singer, C.F., Friedman, E., Thomassen, M., Ontario Cancer Genetics, N., Hansen, T.V., Neuhausen, S.L., Szabo, C.I., Blanco, I., Greene, M.H., Karlan, B.Y., Garber, J., Phelan, C.M., Weitzel, J.N., Montagna, M., Olah, E., Andrulis, I.L., Godwin, A.K., Yannoukakos, D., Goldgar, D.E., Caldes, T., Nevanlinna, H., Osorio, A., Terry, M.B., Daly, M.B., van Rensburg, E.J., Hamann, U., Ramus, S.J., Toland, A.E.,

Caligo, M.A., Olopade, O.I., Tung, N., Claes, K., Beattie, M.S., Southey, M.C., Imyanitov, E.N., Tischkowitz, M., Janavicius, R., John, E.M., Kwong, A., Diez, O., Balmana, J., Barkardottir, R.B., Arun, B.K., Rennert, G., Teo, S.H., Ganz, P.A., Campbell, I., van der Hout, A.H., van Deurzen, C.H., Seynaeve, C., Gomez Garcia, E.B., van Leeuwen, F.E., Meijers-Heijboer, H.E., Gille, J.J., Ausems, M.G., Blok, M.J., Ligtenberg, M.J., Rookus, M.A., Devilee, P., Verhoef, S., van Os, T.A., Wijnen, J.T., Hebon, Embrace, Frost, D., Ellis, S., Fineberg, E., Platte, R., Evans, D.G., Izatt, L., Eeles, R.A., Adlard, J., et al. (2013) 'Genome-wide association study in BRCA1 mutation carriers identifies novel loci associated with breast and ovarian cancer risk', *PLoS Genet*, 9(3), p. e1003212.

Cuddapah, V.A. and Sontheimer, H. (2011) 'Ion channels and transporters [corrected] in cancer. 2. Ion channels and the control of cancer cell migration', *Am J Physiol Cell Physiol*, 301(3), pp. C541-9.

Cummings, S.R., Ensrud, K., Delmas, P.D., LaCroix, A.Z., Vukicevic, S., Reid, D.M., Goldstein, S., Sriram, U., Lee, A., Thompson, J., Armstrong, R.A., Thompson, D.D., Powles, T., Zanchetta, J., Kendler, D., Neven, P., Eastell, R. and Investigators, P.S. (2010) 'Lasofoxifene in postmenopausal women with osteoporosis', *N Engl J Med*, 362(8), pp. 686-96.

Curtis, C., Shah, S.P., Chin, S.F., Turashvili, G., Rueda, O.M., Dunning, M.J., Speed, D., Lynch, A.G., Samarajiwa, S., Yuan, Y., Graf, S., Ha, G., Haffari, G., Bashashati, A., Russell, R., McKinney, S., Group, M., Langerod, A., Green, A., Provenzano, E., Wishart, G., Pinder, S., Watson, P., Markowetz, F., Murphy, L., Ellis, I., Purushotham, A., Borresen-Dale, A.L., Brenton, J.D., Tavare, S., Caldas, C. and Aparicio, S. (2012) 'The genomic and transcriptomic architecture of 2,000 breast tumours reveals novel subgroups', *Nature*, 486(7403), pp. 346-52.

Dalvai, M. and Bystricky, K. (2010) 'Cell cycle and anti-estrogen effects synergize to regulate cell proliferation and ER target gene expression', *PLoS One*, 5(6), p. e11011.

Davenport, T.G., Jerome-Majewska, L.A. and Papaioannou, V.E. (2003) 'Mammary gland, limb and yolk sac defects in mice lacking Tbx3, the gene mutated in human ulnar mammary syndrome', *Development*, 130(10), pp. 2263-73.

Davison, Z., de Blacquiere, G.E., Westley, B.R. and May, F.E. (2011) 'Insulin-like growth factor-dependent proliferation and survival of triple-negative breast cancer cells: implications for therapy', *Neoplasia*, 13(6), pp. 504-15.

DeFriend, D.J., Anderson, E., Bell, J., Wilks, D.P., West, C.M., Mansel, R.E. and Howell, A. (1994a) 'Effects of 4-hydroxytamoxifen and a novel pure antioestrogen (ICI 182780) on the clonogenic growth of human breast cancer cells in vitro', *Br J Cancer*, 70(2), pp. 204-11.

DeFriend, D.J., Howell, A., Nicholson, R.I., Anderson, E., Dowsett, M., Mansel, R.E., Blamey, R.W., Bundred, N.J., Robertson, J.F., Saunders, C. and et al. (1994b) 'Investigation of a new pure antiestrogen (ICI 182780) in women with primary breast cancer', *Cancer Res*, 54(2), pp. 408-14.

Delpire, E. and Gagnon, K.B. (2011) 'Kinetics of hyperosmotically stimulated Na-K-2Cl cotransporter in Xenopus laevis oocytes', *Am J Physiol Cell Physiol*, 301(5), pp. C1074-85.

Deng, C.X. (2006) 'BRCA1: cell cycle checkpoint, genetic instability, DNA damage response and cancer evolution', *Nucleic Acids Res*, 34(5), pp. 1416-26.

Donaldson, S.H. and Boucher, R.C. (2007) 'Sodium channels and cystic fibrosis', *Chest*, 132(5), pp. 1631-6.

Dooley, R., Angibaud, E., Yusef, Y.R., Thomas, W. and Harvey, B.J. (2013) 'Aldosterone-induced ENaC and basal Na+/K+-ATPase trafficking via protein kinase D1-phosphatidylinositol 4-kinaseIIIbeta trans Golgi signalling in M1 cortical collecting duct cells', *Mol Cell Endocrinol*, 372(1-2), pp. 86-95.

Early Breast Cancer Trialists' Collaborative, G. (2001) 'Tamoxifen for early breast cancer', *Cochrane Database Syst Rev*, (1), p. CD000486.

Early Breast Cancer Trialists' Collaborative, G., Darby, S., McGale, P., Correa, C., Taylor, C., Arriagada, R., Clarke, M., Cutter, D., Davies, C., Ewertz, M., Godwin, J., Gray, R., Pierce, L., Whelan, T., Wang, Y. and Peto, R. (2011a) 'Effect of radiotherapy after breast-conserving surgery on 10-year recurrence and 15-year breast cancer death: meta-analysis of individual patient data for 10,801 women in 17 randomised trials', *Lancet*, 378(9804), pp. 1707-16.

Early Breast Cancer Trialists' Collaborative, G., Davies, C., Godwin, J., Gray, R., Clarke, M., Cutter, D., Darby, S., McGale, P., Pan, H.C., Taylor, C., Wang, Y.C., Dowsett, M., Ingle, J. and Peto, R. (2011b) 'Relevance of breast cancer hormone receptors and other factors to the efficacy of adjuvant tamoxifen: patient-level meta-analysis of randomised trials', *Lancet*, 378(9793), pp. 771-84.

Easton, D.F., Pooley, K.A., Dunning, A.M., Pharoah, P.D., Thompson, D., Ballinger, D.G., Struewing, J.P., Morrison, J., Field, H., Luben, R., Wareham, N., Ahmed, S., Healey, C.S., Bowman, R., collaborators, S., Meyer, K.B., Haiman, C.A., Kolonel, L.K., Henderson, B.E., Le Marchand, L., Brennan, P., Sangrajrang, S., Gaborieau, V., Odefrey, F., Shen, C.Y., Wu, P.E., Wang, H.C., Eccles, D., Evans, D.G., Peto, J., Fletcher, O., Johnson, N., Seal, S., Stratton, M.R., Rahman, N., Chenevix-Trench, G., Bojesen, S.E., Nordestgaard, B.G., Axelsson, C.K., Garcia-Closas, M., Brinton, L., Chanock, S., Lissowska, J., Peplonska, B., Nevanlinna, H., Fagerholm, R., Eerola, H., Kang, D., Yoo, K.Y., Noh, D.Y., Ahn, S.H., Hunter, D.J., Hankinson, S.E., Cox, D.G., Hall, P., Wedren, S., Liu, J., Low, Y.L., Bogdanova, N., Schurmann, P., Dork, T.,

Tollenaar, R.A., Jacobi, C.E., Devilee, P., Klijn, J.G., Sigurdson, A.J., Doody, M.M., Alexander, B.H., Zhang, J., Cox, A., Brock, I.W., MacPherson, G., Reed, M.W., Couch, F.J., Goode, E.L., Olson, J.E., Meijers-Heijboer, H., van den Ouweland, A., Uitterlinden, A., Rivadeneira, F., Milne, R.L., Ribas, G., Gonzalez-Neira, A., Benitez, J., Hopper, J.L., McCredie, M., Southey, M., Giles, G.G., Schroen, C., Justenhoven, C., Brauch, H., Hamann, U., Ko, Y.D., Spurdle, A.B., Beesley, J., Chen, X., kConFab, Group, A.M., Mannermaa, A., Kosma, V.M., et al. (2007) 'Genome-wide association study identifies novel breast cancer susceptibility loci', *Nature*, 447(7148), pp. 1087-93.

Edge, S., Byrd, D.R., Compton, C.C., Fritz, A.G., Greene, F.L., Trotti, A Editors (2010) *AJCC Cancer Staging Manual, 7th Edition* New York: Springer.

Elledge, R.M. and Allred, D.C. (1998) 'Prognostic and predictive value of p53 and p21 in breast cancer', *Breast Cancer Res Treat*, 52(1-3), pp. 79-98.

Englert, N.A., Spink, B.C. and Spink, D.C. (2011) 'Persistent and non-persistent changes in gene expression result from long-term estrogen exposure of MCF-7 breast cancer cells', *J Steroid Biochem Mol Biol*, 123(3-5), pp. 140-50.

Ettinger, B., Black, D.M., Mitlak, B.H., Knickerbocker, R.K., Nickelsen, T., Genant, H.K., Christiansen, C., Delmas, P.D., Zanchetta, J.R., Stakkestad, J., Gluer, C.C., Krueger, K., Cohen, F.J., Eckert, S., Ensrud, K.E., Avioli, L.V., Lips, P. and Cummings, S.R. (1999) 'Reduction of vertebral fracture risk in postmenopausal women with osteoporosis treated with raloxifene: results from a 3-year randomized clinical trial. Multiple Outcomes of Raloxifene Evaluation (MORE) Investigators', *JAMA*, 282(7), pp. 637-45.

Fabbri, A., Carcangiu, M. and Carbone, A. (2008) *Histological Classification of Breast Cancer*. in Bombardieri, E., Gianni, L. and Bonadonna, G. (eds.) Breast Cancer: Springer Berlin Heidelberg.

Favoni, R.E. and de Cupis, A. (1998) 'Steroidal and nonsteroidal oestrogen antagonists in breast cancer: basic and clinical appraisal', *Trends Pharmacol Sci*, 19(10), pp. 406-15.

Fenske, S.A., Yesilaltay, A., Pal, R., Daniels, K., Barker, C., Quinones, V., Rigotti, A., Krieger, M. and Kocher, O. (2009) 'Normal hepatic cell surface localization of the high density lipoprotein receptor, scavenger receptor class B, type I, depends on all four PDZ domains of PDZK1', *J Biol Chem*, 284(9), pp. 5797-806.

Fernando, R.I. and Wimalasena, J. (2004) 'Estradiol abrogates apoptosis in breast cancer cells through inactivation of BAD: Ras-dependent nongenomic pathways requiring signaling through ERK and Akt', *Mol Biol Cell*, 15(7), pp. 3266-84.

Fraser, S.P., Diss, J.K., Chioni, A.M., Mycielska, M.E., Pan, H., Yamaci, R.F., Pani, F., Siwy, Z., Krasowska, M., Grzywna, Z., Brackenbury, W.J., Theodorou, D., Koyuturk, M., Kaya, H., Battaloglu, E., De Bella, M.T., Slade, M.J., Tolhurst, R., Palmieri, C., Jiang, J., Latchman, D.S., Coombes, R.C. and Djamgoz, M.B. (2005) 'Voltage-gated sodium channel expression and potentiation of human breast cancer metastasis', *Clin Cancer Res*, 11(15), pp. 5381-9.

Frasor, J., Danes, J.M., Komm, B., Chang, K.C., Lyttle, C.R. and Katzenellenbogen, B.S. (2003) 'Profiling of estrogen up- and down-regulated gene expression in human breast cancer cells: insights into gene networks and pathways underlying estrogenic control of proliferation and cell phenotype', *Endocrinology*, 144(10), pp. 4562-74.

Frasor, J., Stossi, F., Danes, J.M., Komm, B., Lyttle, C.R. and Katzenellenbogen, B.S. (2004) 'Selective estrogen receptor modulators: discrimination of agonistic versus antagonistic activities by gene expression profiling in breast cancer cells', *Cancer Res*, 64(4), pp. 1522-33.

Friday, E., Oliver, R., 3rd, Welbourne, T. and Turturro, F. (2007) 'Role of epidermal growth factor receptor (EGFR)-signaling versus cellular acidosis via Na+/H+ exchanger1(NHE1)-inhibition in troglitazone-induced growth arrest of breast cancer-derived cells MCF-7', *Cell Physiol Biochem*, 20(6), pp. 751-62.

Frindt, G. and Palmer, L.G. (2012) 'Regulation of epithelial Na+ channels by adrenal steroids: mineralocorticoid and glucocorticoid effects', *Am J Physiol Renal Physiol*, 302(1), pp. F20-6.

Gambling, L., Dunford, S., Wilson, C.A., McArdle, H.J. and Baines, D.L. (2004) 'Estrogen and progesterone regulate alpha, beta, and gammaENaC subunit mRNA levels in female rat kidney', *Kidney Int*, 65(5), pp. 1774-81.

Gamper, N. and Shapiro, M.S. (2007) 'Regulation of ion transport proteins by membrane phosphoinositides', *Nat Rev Neurosci*, 8(12), pp. 921-34.

Garcia-Closas, M., Couch, F.J., Lindstrom, S., Michailidou, K., Schmidt, M.K., Brook, M.N., Orr, N., Rhie, S.K., Riboli, E., Feigelson, H.S., Le Marchand, L., Buring, J.E., Eccles, D., Miron, P., Fasching, P.A., Brauch, H., Chang-Claude, J., Carpenter, J., Godwin, A.K., Nevanlinna, H., Giles, G.G., Cox, A., Hopper, J.L., Bolla, M.K., Wang, Q., Dennis, J., Dicks, E., Howat, W.J., Schoof, N., Bojesen, S.E., Lambrechts, D., Broeks, A., Andrulis, I.L., Guenel, P., Burwinkel, B., Sawyer, E.J., Hollestelle, A., Fletcher, O., Winqvist, R., Brenner, H., Mannermaa, A., Hamann, U., Meindl, A., Lindblom, A., Zheng, W., Devillee, P., Goldberg, M.S., Lubinski, J., Kristensen, V., Swerdlow, A., Anton-Culver, H., Dork, T., Muir, K., Matsuo, K., Wu, A.H., Radice, P., Teo, S.H., Shu, X.O., Blot, W., Kang, D., Hartman, M., Sangrajrang, S., Shen, C.Y., Southey, M.C., Park, D.J., Hammet, F., Stone, J., Veer, L.J., Rutgers, E.J., Lophatananon, A., Stewart-Brown, S., Siriwanarangsan, P., Peto, J., Schrauder, M.G., Ekici, A.B., Beckmann, M.W., Dos Santos Silva, I., Johnson, N., Warren, H., Tomlinson, I.,

Kerin, M.J., Miller, N., Marme, F., Schneeweiss, A., Sohn, C., Truong, T., Laurent-Puig, P., Kerbrat, P., Nordestgaard, B.G., Nielsen, S.F., Flyger, H., Milne, R.L., Perez, J.I., Menendez, P., Muller, H., Arndt, V., Stegmaier, C., Lichtner, P., Lochmann, M., Justenhoven, C., et al. (2013) 'Genome-wide association studies identify four ER negative-specific breast cancer risk loci', *Nat Genet*, 45(4), pp. 392-8, 398e1-2.

Garty, H. and Palmer, L.G. (1997) 'Epithelial sodium channels: function, structure, and regulation', *Physiol Rev*, 77(2), pp. 359-96.

Garzon-Muvdi, T., Schiapparelli, P., ap Rhys, C., Guerrero-Cazares, H., Smith, C., Kim, D.H., Kone, L., Farber, H., Lee, D.Y., An, S.S., Levchenko, A. and Quinones-Hinojosa, A. (2012) 'Regulation of brain tumor dispersal by NKCC1 through a novel role in focal adhesion regulation', *PLoS Biol*, 10(5), p. e1001320.

Geck, P., Pietrzyk, C., Burckhardt, B.C., Pfeiffer, B. and Heinz, E. (1980) 'Electrically silent cotransport on Na+, K+ and Cl- in Ehrlich cells', *Biochim Biophys Acta*, 600(2), pp. 432-47.

Gennari, L., Merlotti, D., Martini, G. and Nuti, R. (2006) 'Lasofoxifene: a third-generation selective estrogen receptor modulator for the prevention and treatment of osteoporosis', *Expert Opin Investig Drugs*, 15(9), pp. 1091-103.

Gennari, L., Merlotti, D. and Nuti, R. (2010) 'Selective estrogen receptor modulator (SERM) for the treatment of osteoporosis in postmenopausal women: focus on lasofoxifene', *Clin Interv Aging*, 5, pp. 19-29.

Ghosh, M.G., Thompson, D.A. and Weigel, R.J. (2000) 'PDZK1 and GREB1 are estrogen-regulated genes expressed in hormone-responsive breast cancer', *Cancer Res*, 60(22), pp. 6367-75.

Ghoussaini, M., Fletcher, O., Michailidou, K., Turnbull, C., Schmidt, M.K., Dicks, E., Dennis, J., Wang, Q., Humphreys, M.K., Luccarini, C., Baynes, C., Conroy, D., Maranian, M., Ahmed, S., Driver, K., Johnson, N., Orr, N., dos Santos Silva, I., Waisfisz, Q., Meijers-Heijboer, H., Uitterlinden, A.G., Rivadeneira, F., Netherlands Collaborative Group on Hereditary, B., Ovarian, C., Hall, P., Czene, K., Irwanto, A., Liu, J., Nevanlinna, H., Aittomaki, K., Blomqvist, C., Meindl, A., Schmutzler, R.K., Muller-Myhsok, B., Lichtner, P., Chang-Claude, J., Hein, R., Nickels, S., Flesch-Janys, D., Tsimiklis, H., Makalic, E., Schmidt, D., Bui, M., Hopper, J.L., Apicella, C., Park, D.J., Southey, M., Hunter, D.J., Chanock, S.J., Broeks, A., Verhoef, S., Hogervorst, F.B., Fasching, P.A., Lux, M.P., Beckmann, M.W., Ekici, A.B., Sawyer, E., Tomlinson, I., Kerin, M., Marme, F., Schneeweiss, A., Sohn, C., Burwinkel, B., Guenel, P., Truong, T., Cordina-Duverger, E., Menegaux, F., Bojesen, S.E., Nordestgaard, B.G., Nielsen, S.F., Flyger, H., Milne, R.L., Alonso, M.R., Gonzalez-Neira, A., Benitez, J., Anton-Culver, H., Ziogas, A., Bernstein, L., Dur, C.C., Brenner, H., Muller, H., Arndt, V., Stegmaier, C., Familial Breast Cancer, S., Justenhoven, C., Brauch, H., Bruning,

T., Gene Environment Interaction of Breast Cancer in Germany, N., Wang-Gohrke, S., Eilber, U., Dork, T., Schurmann, P., Bremer, M., Hillemanns, P., Bogdanova, N.V., Antonenkova, N.N., Rogov, Y.I., Karstens, J.H., Bermisheva, M., Prokofieva, D., et al. (2012) 'Genome-wide association analysis identifies three new breast cancer susceptibility loci', *Nat Genet*, 44(3), pp. 312-8.

Gillen, C.M. and Forbush, B., 3rd (1999) 'Functional interaction of the K-Cl cotransporter (KCC1) with the Na-K-Cl cotransporter in HEK-293 cells', *Am J Physiol*, 276(2 Pt 1), pp. C328-36.

Gilmore, E.S., Stutts, M.J. and Milgram, S.L. (2001) 'SRC family kinases mediate epithelial Na+ channel inhibition by endothelin', *J Biol Chem*, 276(45), pp. 42610-7.

Glanville, M., Kingscote, S., Thwaites, D.T. and Simmons, N.L. (2001) 'Expression and role of sodium, potassium, chloride cotransport (NKCC1) in mouse inner medullary collecting duct (mIMCD-K2) epithelial cells', *Pflugers Arch*, 443(1), pp. 123-31.

GLOBOCAN (2012) *Estimated Cancer Incidence, Mortality and Prevalence Worldwide in 2012. World Health Organization.* Available at: http://globocan.iarc.fr/Default.aspx.

Grenman, R., Laine, K.M., Klemi, P.J., Grenman, S., Hayashida, D.J. and Joensuu, H. (1991) 'Effects of the antiestrogen toremifene on growth of the human mammary carcinoma cell line MCF-7', *J Cancer Res Clin Oncol*, 117(3), pp. 223-6.

Guijarro, M.V., Leal, J.F., Fominaya, J., Blanco-Aparicio, C., Alonso, S., Lleonart, M., Castellvi, J., Ruiz, L., Ramon, Y.C.S. and Carnero, A. (2007) 'MAP17 overexpression is a common characteristic of carcinomas', *Carcinogenesis*, 28(8), pp. 1646-52.

Gunter, M.J., Hoover, D.R., Yu, H., Wassertheil-Smoller, S., Rohan, T.E., Manson, J.E., Li, J., Ho, G.Y., Xue, X., Anderson, G.L., Kaplan, R.C., Harris, T.G., Howard, B.V., Wylie-Rosett, J., Burk, R.D. and Strickler, H.D. (2009) 'Insulin, insulin-like growth factor-I, and risk of breast cancer in postmenopausal women', *J Natl Cancer Inst*, 101(1), pp. 48-60.

Haas, B.R. and Sontheimer, H. (2010) 'Inhibition of the Sodium-Potassium-Chloride Cotransporter Isoform-1 reduces glioma invasion', *Cancer Res*, 70(13), pp. 5597-606.

Hager, H., Kwon, T.H., Vinnikova, A.K., Masilamani, S., Brooks, H.L., Frokiaer, J., Knepper, M.A. and Nielsen, S. (2001) 'Immunocytochemical and immunoelectron microscopic localization of alpha-, beta-, and gamma-ENaC in rat kidney', *Am J Physiol Renal Physiol*, 280(6), pp. F1093-106.

Haiman, C.A., Chen, G.K., Vachon, C.M., Canzian, F., Dunning, A., Millikan, R.C., Wang, X., Ademuyiwa, F., Ahmed, S., Ambrosone, C.B., Baglietto, L., Balleine, R., Bandera, E.V., Beckmann, M.W., Berg, C.D., Bernstein, L., Blomqvist, C., Blot, W.J., Brauch, H., Buring, J.E., Carey, L.A., Carpenter, J.E., Chang-Claude, J., Chanock, S.J., Chasman, D.I., Clarke, C.L., Cox, A., Cross, S.S., Deming, S.L., Diasio, R.B., Dimopoulos, A.M., Driver, W.R., Dunnebier, T., Durcan, L., Eccles, D., Edlund, C.K., Ekici, A.B., Fasching, P.A., Feigelson, H.S., Flesch-Janys, D., Fostira, F., Forsti, A., Fountzilas, G., Gerty, S.M., Gene Environment, I., Breast Cancer in Germany, C., Giles, G.G., Godwin, A.K., Goodfellow, P., Graham, N., Greco, D., Hamann, U., Hankinson, S.E., Hartmann, A., Hein, R., Heinz, J., Holbrook, A., Hoover, R.N., Hu, J.J., Hunter, D.J., Ingles, S.A., Irwanto, A., Ivanovich, J., John, E.M., Johnson, N., Jukkola-Vuorinen, A., Kaaks, R., Ko, Y.D., Kolonel, L.N., Konstantopoulou, I., Kosma, V.M., Kulkarni, S., Lambrechts, D., Lee, A.M., Marchand, L.L., Lesnick, T., Liu, J., Lindstrom, S., Mannermaa, A., Margolin, S., Martin, N.G., Miron, P., Montgomery, G.W., Nevanlinna, H., Nickels, S., Nyante, S., Olswold, C., Palmer, J., Pathak, H., Pectasides, D., Perou, C.M., Peto, J., Pharoah, P.D., Pooler, L.C., Press, M.F., Pylkas, K., Rebbeck, T.R., Rodriguez-Gil, J.L., Rosenberg, L., Ross, E., et al. (2011) 'A common variant at the TERT-CLPTM1L locus is associated with estrogen receptor-negative breast cancer', *Nat Genet*, 43(12), pp. 1210-4.

Hamann, S., Herrera-Perez, J.J., Zeuthen, T. and Alvarez-Leefmans, F.J. (2010) 'Cotransport of water by the Na+-K+-2Cl(-) cotransporter NKCC1 in mammalian epithelial cells', *J Physiol*, 588(Pt 21), pp. 4089-101.

Hampton, T. (2005) 'Monoclonal antibody therapies shine in breast cancer clinical trials', *JAMA*, 293(24), pp. 2985-9.

Hannaert, P., Alvarez-Guerra, M., Pirot, D., Nazaret, C. and Garay, R.P. (2002) 'Rat NKCC2/NKCC1 cotransporter selectivity for loop diuretic drugs', *Naunyn Schmiedebergs Arch Pharmacol*, 365(3), pp. 193-9.

Hartley, D.E. and Forsling, M.L. (2002) 'Renal response to arginine vasopressin during the oestrous cycle in the rat: comparison of glucose and saline infusion using physiological doses of vasopressin', *Exp Physiol*, 87(1), pp. 9-15.

Hebert, S.C., Mount, D.B. and Gamba, G. (2004) 'Molecular physiology of cation-coupled Cl- cotransport: the SLC12 family', *Pflugers Arch*, 447(5), pp. 580-93.

Howell, S.J., Johnston, S.R. and Howell, A. (2004) 'The use of selective estrogen receptor modulators and selective estrogen receptor down-regulators in breast cancer', *Best Pract Res Clin Endocrinol Metab*, 18(1), pp. 47-66.

Huang, P., Chandra, V. and Rastinejad, F. (2010) 'Structural overview of the nuclear receptor superfamily: insights into physiology and therapeutics', *Annu Rev Physiol*, 72, pp. 247-72.

Hunter, D.J., Kraft, P., Jacobs, K.B., Cox, D.G., Yeager, M., Hankinson, S.E., Wacholder, S., Wang, Z., Welch, R., Hutchinson, A., Wang, J., Yu, K., Chatterjee, N., Orr, N., Willett, W.C., Colditz, G.A., Ziegler, R.G., Berg, C.D., Buys, S.S., McCarty, C.A., Feigelson, H.S., Calle, E.E., Thun, M.J., Hayes, R.B., Tucker, M., Gerhard, D.S., Fraumeni, J.F., Jr., Hoover, R.N., Thomas, G. and Chanock, S.J. (2007) 'A genome-wide association study identifies alleles in FGFR2 associated with risk of sporadic postmenopausal breast cancer', *Nat Genet*, 39(7), pp. 870-4.

Hutcheson, I.R., Goddard, L., Barrow, D., McClelland, R.A., Francies, H.E., Knowlden, J.M., Nicholson, R.I. and Gee, J.M. (2011) 'Fulvestrant-induced expression of ErbB3 and ErbB4 receptors sensitizes oestrogen receptor-positive breast cancer cells to heregulin beta1', *Breast Cancer Res*, 13(2), p. R29.

Imkampe, A.K. and Bates, T. (2012) 'Correlation of age at oral contraceptive pill start with age at breast cancer diagnosis', *Breast J*, 18(1), pp. 35-40.

Inskip, H.M., Kinlen, L.J., Taylor, A.M., Woods, C.G. and Arlett, C.F. (1999) 'Risk of breast cancer and other cancers in heterozygotes for ataxia-telangiectasia', *Br J Cancer*, 79(7-8), pp. 1304-7.

Isenring, P., Jacoby, S.C., Chang, J. and Forbush, B. (1998) 'Mutagenic mapping of the Na-K-Cl cotransporter for domains involved in ion transport and bumetanide binding', *J Gen Physiol*, 112(5), pp. 549-58.

Jakesz, R., Smith, C.A., Aitken, S., Huff, K., Schuette, W., Shackney, S. and Lippman, M. (1984) 'Influence of cell proliferation and cell cycle phase on expression of estrogen receptor in MCF-7 breast cancer cells', *Cancer Res*, 44(2), pp. 619-25.

Johnson, M.D., Westley, B.R. and May, F.E. (1989) 'Oestrogenic activity of tamoxifen and its metabolites on gene regulation and cell proliferation in MCF-7 breast cancer cells', *Br J Cancer*, 59(5), pp. 727-38.

Kalluri, R. and Zeisberg, M. (2006) 'Fibroblasts in cancer', *Nat Rev Cancer*, 6(5), pp. 392-401.

Kapoor, N., Bartoszewski, R., Qadri, Y.J., Bebok, Z., Bubien, J.K., Fuller, C.M. and Benos, D.J. (2009) 'Knockdown of ASIC1 and epithelial sodium channel subunits inhibits glioblastoma whole cell current and cell migration', *J Biol Chem*, 284(36), pp. 24526-41.

Key, T., Appleby, P., Barnes, I. and Reeves, G. (2002) 'Endogenous sex hormones and breast cancer in postmenopausal women: reanalysis of nine prospective studies', *J Natl Cancer Inst*, 94(8), pp. 606-16.

Kim, H., Abd Elmageed, Z.Y., Ju, J., Naura, A.S., Abdel-Mageed, A.B., Varughese, S., Paul, D., Alahari, S., Catling, A., Kim, J.G. and Boulares, A.H. (2013) 'PDZK1 is a novel factor in breast cancer that is indirectly regulated by estrogen through IGF-1R and promotes estrogen-mediated growth', *Mol Med*, 19, pp. 253-62.

Kim, N.H., Cheong, K.A., Lee, T.R. and Lee, A.Y. (2012) 'PDZK1 Upregulation in Estrogen-Related Hyperpigmentation in Melasma', *J Invest Dermatol*.

Kimura, T. (1969) '[Electron microscopic study of the mechanism of secretion of milk]', *Nihon Sanka Fujinka Gakkai Zasshi*, 21(3), pp. 301-8.

Kiyotani, K., Mushiroda, T., Nakamura, Y. and Zembutsu, H. (2012) 'Pharmacogenomics of tamoxifen: roles of drug metabolizing enzymes and transporters', *Drug Metab Pharmacokinet*, 27(1), pp. 122-31.

Knight, K.K., Olson, D.R., Zhou, R. and Snyder, P.M. (2006) 'Liddle's syndrome mutations increase Na+ transport through dual effects on epithelial Na+ channel surface expression and proteolytic cleavage', *Proc Natl Acad Sci U S A*, 103(8), pp. 2805-8.

Kocher, O., Comella, N., Gilchrist, A., Pal, R., Tognazzi, K., Brown, L.F. and Knoll, J.H. (1999) 'PDZK1, a novel PDZ domain-containing protein up-regulated in carcinomas and mapped to chromosome 1q21, interacts with cMOAT (MRP2), the multidrug resistance-associated protein', *Lab Invest*, 79(9), pp. 1161-70.

Kocher, O., Comella, N., Tognazzi, K. and Brown, L.F. (1998) 'Identification and partial characterization of PDZK1: a novel protein containing PDZ interaction domains', *Lab Invest*, 78(1), pp. 117-25.

Koide, A., Zhao, C., Naganuma, M., Abrams, J., Deighton-Collins, S., Skafar, D.F. and Koide, S. (2007) 'Identification of regions within the F domain of the human estrogen receptor alpha that are important for modulating transactivation and protein-protein interactions', *Molecular Endocrinology*, 21(4), pp. 829-42.

Komm, B.S., Kharode, Y.P., Bodine, P.V., Harris, H.A., Miller, C.P. and Lyttle, C.R. (2005) 'Bazedoxifene acetate: a selective estrogen receptor modulator with improved selectivity', *Endocrinology*, 146(9), pp. 3999-4008.

Kumar, R., Zakharov, M.N., Khan, S.H., Miki, R., Jang, H., Toraldo, G., Singh, R., Bhasin, S. and Jasuja, R. (2011) 'The dynamic structure of the estrogen receptor', *J Amino Acids*, 2011, p. 812540.

Kumar V, F.N. (2004) *Robbins and Cotran pathologic basis of disease*. Philadelphia : Saunders Elsevier.

Kunzelmann, K. (2005) 'Ion channels and cancer', *J Membr Biol*, 205(3), pp. 159-73.

Kushner, P.J., Agard, D.A., Greene, G.L., Scanlan, T.S., Shiau, A.K., Uht, R.M. and Webb, P. (2000) 'Estrogen receptor pathways to AP-1', *J Steroid Biochem Mol Biol*, 74(5), pp. 311-7.

Lamb, J.F., Ogden, P. and Simmons, N.L. (1981) 'Autoradiographic localisation of [3H]ouabain bound to cultured epithelial cell monolayers of MDCK cells', *Biochim Biophys Acta*, 644(2), pp. 333-40.

Lamprecht, G. and Seidler, U. (2006) 'The emerging role of PDZ adapter proteins for regulation of intestinal ion transport', *Am J Physiol Gastrointest Liver Physiol*, 291(5), pp. G766-77.

Laube, M., Kuppers, E. and Thome, U.H. (2011) 'Modulation of sodium transport in alveolar epithelial cells by estradiol and progesterone', *Pediatr Res*, 69(3), pp. 200-5.

Le Romancer, M., Treilleux, I., Bouchekioua-Bouzaghou, K., Sentis, S. and Corbo, L. (2010) 'Methylation, a key step for nongenomic estrogen signaling in breast tumors', *Steroids*, 75(8-9), pp. 560-4.

Lewis-Wambi, J.S., Kim, H., Curpan, R., Grigg, R., Sarker, M.A. and Jordan, V.C. (2011) 'The selective estrogen receptor modulator bazedoxifene inhibits hormone-independent breast cancer cell growth and down-regulates estrogen receptor alpha and cyclin D1', *Mol Pharmacol*, 80(4), pp. 610-20.

Li, M. and Xiong, Z.G. (2011) 'Ion channels as targets for cancer therapy', *Int J Physiol Pathophysiol Pharmacol*, 3(2), pp. 156-66.

Li, Z., Yan, M., Li, Z., Vuki, M., Wu, D., Liu, F., Zhong, W., Zhang, L. and Xu, D. (2012) 'A multiplexed screening method for agonists and antagonists of the estrogen receptor protein', *Anal Bioanal Chem*, 403(5), pp. 1373-84.

Liang, X., Butterworth, M.B., Peters, K.W. and Frizzell, R.A. (2010) 'AS160 modulates aldosterone-stimulated epithelial sodium channel forward trafficking', *Mol Biol Cell*, 21(12), pp. 2024-33.

Liao, S., Li, J., Wei, W., Wang, L., Zhang, Y., Wang, C. and Sun, S. (2011) 'Association between diabetes mellitus and breast cancer risk: a meta-analysis of the literature', *Asian Pac J Cancer Prev*, 12(4), pp. 1061-5.

Lin, R. and Tripuraneni, P. (2011) 'Radiation therapy in early-stage invasive breast cancer', *Indian J Surg Oncol*, 2(2), pp. 101-11.

Linzell, J.L. and Peaker, M. (1971) 'Intracellular concentrations of sodium, potassium and chloride in the lactating mammary gland and their relation to the secretory mechanism', *J Physiol*, 216(3), pp. 683-700.

Liu, S., Han, S.J. and Smith, C.L. (2013) 'Cooperative activation of gene expression by agonists and antagonists mediated by estrogen receptor heteroligand dimer complexes', *Mol Pharmacol*, 83(5), pp. 1066-77.

Loffing, J., Zecevic, M., Feraille, E., Kaissling, B., Asher, C., Rossier, B.C., Firestone, G.L., Pearce, D. and Verrey, F. (2001) 'Aldosterone induces rapid apical translocation of ENaC in early portion of renal collecting system: possible role of SGK', *Am J Physiol Renal Physiol*, 280(4), pp. F675-82.

Lonning, P.E. (2011) 'The potency and clinical efficacy of aromatase inhibitors across the breast cancer continuum', *Ann Oncol*, 22(3), pp. 503-14.

Lorincz, A.M. and Sukumar, S. (2006) 'Molecular links between obesity and breast cancer', *Endocr Relat Cancer*, 13(2), pp. 279-92.

Lu, J. (2015) 'Palbociclib: a first-in-class CDK4/CDK6 inhibitor for the treatment of hormone-receptor positive advanced breast cancer', *J Hematol Oncol*, 8, p. 98.

Lyons, S.A., O'Neal, J. and Sontheimer, H. (2002) 'Chlorotoxin, a scorpion-derived peptide, specifically binds to gliomas and tumors of neuroectodermal origin', *Glia*, 39(2), pp. 162-73.

Lytle, C. and Forbush, B., 3rd (1992) 'The Na-K-Cl cotransport protein of shark rectal gland. II. Regulation by direct phosphorylation', *J Biol Chem*, 267(35), pp. 25438-43.

Lytle, C. and McManus, T. (2002) 'Coordinate modulation of Na-K-2Cl cotransport and K-Cl cotransport by cell volume and chloride', *Am J Physiol Cell Physiol*, 283(5), pp. C1422-31.

Mackay, A., Urruticoechea, A., Dixon, J.M., Dexter, T., Fenwick, K., Ashworth, A., Drury, S., Larionov, A., Young, O., White, S., Miller, W.R., Evans, D.B. and Dowsett, M. (2007) 'Molecular response to aromatase inhibitor treatment in primary breast cancer', *Breast Cancer Res*, 9(3), p. R37.

Mamenko, M., Zaika, O., Doris, P.A. and Pochynyuk, O. (2012) 'Salt-dependent inhibition of epithelial Na+ channel-mediated sodium reabsorption in the aldosterone-sensitive distal nephron by bradykinin', *Hypertension*, 60(5), pp. 1234-41.

Mehdawi, H., Alkhalaf, M. and Khan, I. (2012) 'Role of Na+/H+ exchanger in resveratrol-induced growth inhibition of human breast cancer cells', *Med Oncol*, 29(1), pp. 25-32.

Miller, P.D., Chines, A.A., Christiansen, C., Hoeck, H.C., Kendler, D.L., Lewiecki, E.M., Woodson, G., Levine, A.B., Constantine, G. and Delmas, P.D. (2008) 'Effects of bazedoxifene on BMD and bone turnover in postmenopausal women: 2-yr results of a randomized, double-blind, placebo-, and active-controlled study', *J Bone Miner Res*, 23(4), pp. 525-35.

Miller, W.R. and Dixon, J.M. (2000) 'Antiaromatase agents: preclinical data and neoadjuvant therapy', *Clin Breast Cancer*, 1 Suppl 1, pp. S9-14.

Miller, W.R., Larionov, A.A., Renshaw, L., Anderson, T.J., White, S., Murray, J., Murray, E., Hampton, G., Walker, J.R., Ho, S., Krause, A., Evans, D.B. and Dixon, J.M. (2007) 'Changes in breast cancer transcriptional profiles after treatment with the aromatase inhibitor, letrozole', *Pharmacogenet Genomics*, 17(10), pp. 813-26.

Miyoshi, Y., Murase, K., Saito, M., Imamura, M. and Oh, K. (2010) 'Mechanisms of estrogen receptor-alpha upregulation in breast cancers', *Medical Molecular Morphology*, 43(4), pp. 193-196.

Molloy, C.A., May, F.E. and Westley, B.R. (2000) 'Insulin receptor substrate-1 expression is regulated by estrogen in the MCF-7 human breast cancer cell line', *J Biol Chem*, 275(17), pp. 12565-71.

Monette, M.Y. and Forbush, B. (2012) 'Regulatory activation is accompanied by movement in the C terminus of the Na-K-Cl cotransporter (NKCC1)', *J Biol Chem*, 287(3), pp. 2210-20.

Monninkhof, E.M., Elias, S.G., Vlems, F.A., van der Tweel, I., Schuit, A.J., Voskuil, D.W. and van Leeuwen, F.E. (2007) 'Physical activity and breast cancer: a systematic review', *Epidemiology*, 18(1), pp. 137-57.

Morrison, M.M., Hutchinson, K., Williams, M.M., Stanford, J.C., Balko, J.M., Young, C., Kuba, M.G., Sanchez, V., Williams, A.J., Hicks, D.J., Arteaga, C.L., Prat, A., Perou, C.M., Earp, H.S., Massarweh, S. and Cook, R.S. (2013) 'ErbB3 downregulation enhances luminal breast tumor response to antiestrogens', *J Clin Invest*, 123(10), pp. 4329-43.

Mosselman, S., Polman, J. and Dijkema, R. (1996) 'ER beta: identification and characterization of a novel human estrogen receptor', *FEBS Lett*, 392(1), pp. 49-53.

Nicco, C., Wittner, M., DiStefano, A., Jounier, S., Bankir, L. and Bouby, N. (2001) 'Chronic exposure to vasopressin upregulates ENaC and sodium

transport in the rat renal collecting duct and lung', *Hypertension*, 38(5), pp. 1143-9.

O'Regan, R.M. and Jordan, V.C. (2001) 'Tamoxifen to raloxifene and beyond', *Semin Oncol*, 28(3), pp. 260-73.

Osborne, C.K. (1998) 'Tamoxifen in the treatment of breast cancer', *N Engl J Med*, 339(22), pp. 1609-18.

Osborne, C.K. and Schiff, R. (2005) 'Estrogen-receptor biology: continuing progress and therapeutic implications', *J Clin Oncol*, 23(8), pp. 1616-22.

Parkin, D.M. (2011) '15. Cancers attributable to reproductive factors in the UK in 2010', *Br J Cancer*, 105 Suppl 2, pp. S73-6.

Parkin, D.M. and Boyd, L. (2011) '8. Cancers attributable to overweight and obesity in the UK in 2010', *Br J Cancer*, 105 Suppl 2, pp. S34-7.

Parkin, D.M. and Darby, S.C. (2011) '12. Cancers in 2010 attributable to ionising radiation exposure in the UK', *Br J Cancer*, 105 Suppl 2, pp. S57-65.

Payne, J.A., Xu, J.C., Haas, M., Lytle, C.Y., Ward, D. and Forbush, B., 3rd (1995) 'Primary structure, functional expression, and chromosomal localization of the bumetanide-sensitive Na-K-Cl cotransporter in human colon', *J Biol Chem*, 270(30), pp. 17977-85.

PC, O.L., Penny, S.A., Dolan, R.T., Kelly, C.M., Madden, S.F., Rexhepaj, E., Brennan, D.J., McCann, A.H., Ponten, F., Uhlen, M., Zagozdzon, R., Duffy, M.J., Kell, M.R., Jirstrom, K. and Gallagher, W.M. (2013) 'Systematic antibody generation and validation via tissue microarray technology leading to identification of a novel protein prognostic panel in breast cancer', *BMC Cancer*, 13, p. 175.

Pechere-Bertschi, A., Maillard, M., Stalder, H., Brunner, H.R. and Burnier, M. (2002) 'Renal segmental tubular response to salt during the normal menstrual cycle', *Kidney Int*, 61(2), pp. 425-31.

Perez, E.A. and Spano, J.P. (2012) 'Current and emerging targeted therapies for metastatic breast cancer', *Cancer*, 118(12), pp. 3014-25.

Perou, C.M., Sorlie, T., Eisen, M.B., van de Rijn, M., Jeffrey, S.S., Rees, C.A., Pollack, J.R., Ross, D.T., Johnsen, H., Akslen, L.A., Fluge, O., Pergamenschikov, A., Williams, C., Zhu, S.X., Lonning, P.E., Borresen-Dale, A.L., Brown, P.O. and Botstein, D. (2000) 'Molecular portraits of human breast tumours', *Nature*, 406(6797), pp. 747-52.

Piccart, M., Hortobagyi, G.N., Campone, M., Pritchard, K.I., Lebrun, F., Ito, Y., Noguchi, S., Perez, A., Rugo, H.S., Deleu, I., Burris, H.A., 3rd, Provencher, L., Neven, P., Gnant, M., Shtivelband, M., Wu, C., Fan, J., Feng, W., Taran, T. and Baselga, J. (2014) 'Everolimus plus exemestane for hormone-receptor-positive, human epidermal growth factor receptor-2-negative advanced breast cancer: overall survival results from BOLERO-2dagger', *Ann Oncol*, 25(12), pp. 2357-62.

Pike, M.C., Spicer, D.V., Dahmoush, L. and Press, M.F. (1993) 'Estrogens, progestogens, normal breast cell proliferation, and breast cancer risk', *Epidemiol Rev*, 15(1), pp. 17-35.

Platet, N., Cathiard, A.M., Gleizes, M. and Garcia, M. (2004) 'Estrogens and their receptors in breast cancer progression: a dual role in cancer proliferation and invasion', *Crit Rev Oncol Hematol*, 51(1), pp. 55-67.

Platet, N., Cunat, S., Chalbos, D., Rochefort, H. and Garcia, M. (2000) 'Unliganded and liganded estrogen receptors protect against cancer invasion via different mechanisms', *Molecular Endocrinology*, 14(7), pp. 999-1009.

Prevarskaya, N., Skryma, R. and Shuba, Y. (2010) 'Ion channels and the hallmarks of cancer', *Trends Mol Med*, 16(3), pp. 107-21.

Pribanic, S., Gisler, S.M., Bacic, D., Madjdpour, C., Hernando, N., Sorribas, V., Gantenbein, A., Biber, J. and Murer, H. (2003) 'Interactions of MAP17 with the NaPi-IIa/PDZK1 protein complex in renal proximal tubular cells', *Am J Physiol Renal Physiol*, 285(4), pp. F784-91.

Pritchard, K. (2005) 'Endocrinology and hormone therapy in breast cancer: endocrine therapy in premenopausal women', *Breast Cancer Res*, 7(2), pp. 70-6.

Pyrhonen, S., Ellmen, J., Vuorinen, J., Gershanovich, M., Tominaga, T., Kaufmann, M. and Hayes, D.F. (1999) 'Meta-analysis of trials comparing toremifene with tamoxifen and factors predicting outcome of antiestrogen therapy in postmenopausal women with breast cancer', *Breast Cancer Res Treat*, 56(2), pp. 133-43.

Qi, D., He, J., Wang, D., Deng, W., Zhao, Y., Ye, Y. and Feng, L. (2014) '17beta-estradiol suppresses lipopolysaccharide-induced acute lung injury through PI3K/Akt/SGK1 mediated up-regulation of epithelial sodium channel (ENaC) in vivo and in vitro', *Respir Res*, 15, p. 159.

Quesnell, R.R., Erickson, J. and Schultz, B.D. (2007a) 'Apical electrolyte concentration modulates barrier function and tight junction protein localization in bovine mammary epithelium', *Am J Physiol Cell Physiol*, 292(1), pp. C305-18.

Quesnell, R.R., Han, X. and Schultz, B.D. (2007b) 'Glucocorticoids stimulate ENaC upregulation in bovine mammary epithelium', *Am J Physiol Cell Physiol*, 292(5), pp. C1739-45.

Razandi, M., Pedram, A., Park, S.T. and Levin, E.R. (2003) 'Proximal events in signaling by plasma membrane estrogen receptors', *J Biol Chem*, 278(4), pp. 2701-12.

Reyes, A.J. and Leary, W.P. (1993) 'Clinicopharmacological reappraisal of the potency of diuretics', *Cardiovasc Drugs Ther*, 7 Suppl 1, pp. 23-8.

Riazi, S., Maric, C. and Ecelbarger, C.A. (2006) '17-beta Estradiol attenuates streptozotocin-induced diabetes and regulates the expression of renal sodium transporters', *Kidney Int*, 69(3), pp. 471-80.

Robinson, S.P. and Jordan, V.C. (1988) 'Metabolism of steroid-modifying anticancer agents', *Pharmacol Ther*, 36(1), pp. 41-103.

Robinson, S.P. and Jordan, V.C. (1989) 'Antiestrogenic action of toremifene on hormone-dependent, -independent, and heterogeneous breast tumor growth in the athymic mouse', *Cancer Res*, 49(7), pp. 1758-62.

Ronkin, S., Northington, R., Baracat, E., Nunes, M.G., Archer, D.F., Constantine, G. and Pickar, J.H. (2005) 'Endometrial effects of bazedoxifene acetate, a novel selective estrogen receptor modulator, in postmenopausal women', *Obstet Gynecol*, 105(6), pp. 1397-404.

Rosati, R.L., Da Silva Jardine, P., Cameron, K.O., Thompson, D.D., Ke, H.Z., Toler, S.M., Brown, T.A., Pan, L.C., Ebbinghaus, C.F., Reinhold, A.R., Elliott, N.C., Newhouse, B.N., Tjoa, C.M., Sweetnam, P.M., Cole, M.J., Arriola, M.W., Gauthier, J.W., Crawford, D.T., Nickerson, D.F., Pirie, C.M., Qi, H., Simmons, H.A. and Tkalcevic, G.T. (1998) 'Discovery and preclinical pharmacology of a novel, potent, nonsteroidal estrogen receptor agonist/antagonist, CP-336156, a diaryltetrahydronaphthalene', *J Med Chem*, 41(16), pp. 2928-31.

Ross, S.B., Fuller, C.M., Bubien, J.K. and Benos, D.J. (2007) 'Amiloride-sensitive Na+ channels contribute to regulatory volume increases in human glioma cells', *Am J Physiol Cell Physiol*, 293(3), pp. C1181-5.

Rossier, B.C., Pradervand, S., Schild, L. and Hummler, E. (2002) 'Epithelial sodium channel and the control of sodium balance: interaction between genetic and environmental factors', *Annu Rev Physiol*, 64, pp. 877-97.

Rossouw, J.E., Anderson, G.L., Prentice, R.L., LaCroix, A.Z., Kooperberg, C., Stefanick, M.L., Jackson, R.D., Beresford, S.A., Howard, B.V., Johnson, K.C., Kotchen, J.M., Ockene, J. and Writing Group for the Women's Health Initiative, I. (2002) 'Risks and benefits of estrogen plus progestin in healthy

postmenopausal women: principal results From the Women's Health Initiative randomized controlled trial', *JAMA*, 288(3), pp. 321-33.

Russell, J.M. (2000) 'Sodium-potassium-chloride cotransport', *Physiol Rev*, 80(1), pp. 211-76.

Saarto, T., Vehmanen, L., Elomaa, I., Valimaki, M., Makela, P. and Blomqvist, C. (2001) 'The effect of clodronate and antioestrogens on bone loss associated with oestrogen withdrawal in postmenopausal women with breast cancer', *Br J Cancer*, 84(8), pp. 1047-51.

Sabel, M.S. (2009) *Essentials of Breast Surgery*. Elsevier.

Safe, S. (2001) 'Transcriptional activation of genes by 17 beta-estradiol through estrogen receptor-Sp1 interactions', *Vitam Horm*, 62, pp. 231-52.

Sasieni, P.D., Shelton, J., Ormiston-Smith, N., Thomson, C.S. and Silcocks, P.B. (2011) 'What is the lifetime risk of developing cancer?: the effect of adjusting for multiple primaries', *Br J Cancer*, 105(3), pp. 460-5.

Sauter, D., Fernandes, S., Goncalves-Mendes, N., Boulkroun, S., Bankir, L., Loffing, J. and Bouby, N. (2006) 'Long-term effects of vasopressin on the subcellular localization of ENaC in the renal collecting system', *Kidney Int*, 69(6), pp. 1024-32.

Selvaraj, N.G., Omi, E., Gibori, G. and Rao, M.C. (2000) 'Janus kinase 2 (JAK2) regulates prolactin-mediated chloride transport in mouse mammary epithelial cells through tyrosine phosphorylation of Na+-K+-2Cl- cotransporter', *Mol Endocrinol*, 14(12), pp. 2054-65.

Shao, W. and Brown, M. (2004) 'Advances in estrogen receptor biology: prospects for improvements in targeted breast cancer therapy', *Breast Cancer Res*, 6(1), pp. 39-52.

Shennan, D.B. (1989) 'Evidence for furosemide-sensitive Na+-K+-Cl- co-transport in lactating rat mammary tissue', *Q J Exp Physiol*, 74(6), pp. 927-38.

Shennan, D.B. and McNeillie, S.A. (1990) 'Efflux of chloride from lactating rat mammary tissue slices', *Comp Biochem Physiol A Comp Physiol*, 95(3), pp. 367-71.

Shennan, D.B. and Peaker, M. (2000) 'Transport of milk constituents by the mammary gland', *Physiol Rev*, 80(3), pp. 925-51.

Shillingford, J.M., Miyoshi, K., Flagella, M., Shull, G.E. and Hennighausen, L. (2002) 'Mouse mammary epithelial cells express the Na-K-Cl cotransporter,

NKCC1: characterization, localization, and involvement in ductal development and morphogenesis', *Mol Endocrinol*, 16(6), pp. 1309-21.

Siddiq, A., Couch, F.J., Chen, G.K., Lindstrom, S., Eccles, D., Millikan, R.C., Michailidou, K., Stram, D.O., Beckmann, L., Rhie, S.K., Ambrosone, C.B., Aittomaki, K., Amiano, P., Apicella, C., Australian Breast Cancer Tissue Bank, I., Baglietto, L., Bandera, E.V., Beckmann, M.W., Berg, C.D., Bernstein, L., Blomqvist, C., Brauch, H., Brinton, L., Bui, Q.M., Buring, J.E., Buys, S.S., Campa, D., Carpenter, J.E., Chasman, D.I., Chang-Claude, J., Chen, C., Clavel-Chapelon, F., Cox, A., Cross, S.S., Czene, K., Deming, S.L., Diasio, R.B., Diver, W.R., Dunning, A.M., Durcan, L., Ekici, A.B., Fasching, P.A., Familial Breast Cancer, S., Feigelson, H.S., Fejerman, L., Figueroa, J.D., Fletcher, O., Flesch-Janys, D., Gaudet, M.M., Consortium, G., Gerty, S.M., Rodriguez-Gil, J.L., Giles, G.G., van Gils, C.H., Godwin, A.K., Graham, N., Greco, D., Hall, P., Hankinson, S.E., Hartmann, A., Hein, R., Heinz, J., Hoover, R.N., Hopper, J.L., Hu, J.J., Huntsman, S., Ingles, S.A., Irwanto, A., Isaacs, C., Jacobs, K.B., John, E.M., Justenhoven, C., Kaaks, R., Kolonel, L.N., Coetzee, G.A., Lathrop, M., Le Marchand, L., Lee, A.M., Lee, I.M., Lesnick, T., Lichtner, P., Liu, J., Lund, E., Makalic, E., Martin, N.G., McLean, C.A., Meijers-Heijboer, H., Meindl, A., Miron, P., Monroe, K.R., Montgomery, G.W., Muller-Myhsok, B., Nickels, S., Nyante, S.J., Olswold, C., Overvad, K., Palli, D., Park, D.J., Palmer, J.R., Pathak, H., et al. (2012) 'A meta-analysis of genome-wide association studies of breast cancer identifies two novel susceptibility loci at 6q14 and 20q11', *Hum Mol Genet*, 21(24), pp. 5373-84.

Sieri, S., Krogh, V., Ferrari, P., Berrino, F., Pala, V., Thiebaut, A.C., Tjonneland, A., Olsen, A., Overvad, K., Jakobsen, M.U., Clavel-Chapelon, F., Chajes, V., Boutron-Ruault, M.C., Kaaks, R., Linseisen, J., Boeing, H., Nothlings, U., Trichopoulou, A., Naska, A., Lagiou, P., Panico, S., Palli, D., Vineis, P., Tumino, R., Lund, E., Kumle, M., Skeie, G., Gonzalez, C.A., Ardanaz, E., Amiano, P., Tormo, M.J., Martinez-Garcia, C., Quiros, J.R., Berglund, G., Gullberg, B., Hallmans, G., Lenner, P., Bueno-de-Mesquita, H.B., van Duijnhoven, F.J., Peeters, P.H., van Gils, C.H., Key, T.J., Crowe, F.L., Bingham, S., Khaw, K.T., Rinaldi, S., Slimani, N., Jenab, M., Norat, T. and Riboli, E. (2008) 'Dietary fat and breast cancer risk in the European Prospective Investigation into Cancer and Nutrition', *Am J Clin Nutr*, 88(5), pp. 1304-12.

Simmons, N.L. (1984) 'Epithelial cell volume regulation in hypotonic fluids: studies using a model tissue culture renal epithelial cell system', *Q J Exp Physiol*, 69(1), pp. 83-95.

Smith, L., Smallwood, N., Altman, A. and Liedtke, C.M. (2008) 'PKCdelta acts upstream of SPAK in the activation of NKCC1 by hyperosmotic stress in human airway epithelial cells', *J Biol Chem*, 283(32), pp. 22147-56.

Song, R.X., Barnes, C.J., Zhang, Z., Bao, Y., Kumar, R. and Santen, R.J. (2004) 'The role of Shc and insulin-like growth factor 1 receptor in mediating the

translocation of estrogen receptor alpha to the plasma membrane', *Proc Natl Acad Sci U S A*, 101(7), pp. 2076-81.

Sorlie, T., Tibshirani, R., Parker, J., Hastie, T., Marron, J.S., Nobel, A., Deng, S., Johnsen, H., Pesich, R., Geisler, S., Demeter, J., Perou, C.M., Lonning, P.E., Brown, P.O., Borresen-Dale, A.L. and Botstein, D. (2003) 'Repeated observation of breast tumor subtypes in independent gene expression data sets', *Proc Natl Acad Sci U S A*, 100(14), pp. 8418-23.

Soroceanu, L., Gillespie, Y., Khazaeli, M.B. and Sontheimer, H. (1998) 'Use of chlorotoxin for targeting of primary brain tumors', *Cancer Res*, 58(21), pp. 4871-9.

Spector, N.L. and Blackwell, K.L. (2009) 'Understanding the mechanisms behind trastuzumab therapy for human epidermal growth factor receptor 2-positive breast cancer', *J Clin Oncol*, 27(34), pp. 5838-47.

Stacey, S.N., Manolescu, A., Sulem, P., Rafnar, T., Gudmundsson, J., Gudjonsson, S.A., Masson, G., Jakobsdottir, M., Thorlacius, S., Helgason, A., Aben, K.K., Strobbe, L.J., Albers-Akkers, M.T., Swinkels, D.W., Henderson, B.E., Kolonel, L.N., Le Marchand, L., Millastre, E., Andres, R., Godino, J., Garcia-Prats, M.D., Polo, E., Tres, A., Mouy, M., Saemundsdottir, J., Backman, V.M., Gudmundsson, L., Kristjansson, K., Bergthorsson, J.T., Kostic, J., Frigge, M.L., Geller, F., Gudbjartsson, D., Sigurdsson, H., Jonsdottir, T., Hrafnkelsson, J., Johannsson, J., Sveinsson, T., Myrdal, G., Grimsson, H.N., Jonsson, T., von Holst, S., Werelius, B., Margolin, S., Lindblom, A., Mayordomo, J.I., Haiman, C.A., Kiemeney, L.A., Johannsson, O.T., Gulcher, J.R., Thorsteinsdottir, U., Kong, A. and Stefansson, K. (2007) 'Common variants on chromosomes 2q35 and 16q12 confer susceptibility to estrogen receptor-positive breast cancer', *Nat Genet*, 39(7), pp. 865-9.

Stadler, C., Skogs, M., Brismar, H., Uhlen, M. and Lundberg, E. (2010) 'A single fixation protocol for proteome-wide immunofluorescence localization studies', *J Proteomics*, 73(6), pp. 1067-78.

Steeg, P.S. (2005) 'New insights into the tumor metastatic process revealed by gene expression profiling', *Am J Pathol*, 166(5), pp. 1291-4.

Tabuchi, Y., Matsuoka, J., Gunduz, M., Imada, T., Ono, R., Ito, M., Motoki, T., Yamatsuji, T., Shirakawa, Y., Takaoka, M., Haisa, M., Tanaka, N., Kurebayashi, J., Jordan, V.C. and Naomoto, Y. (2009) 'Resistance to paclitaxel therapy is related with Bcl-2 expression through an estrogen receptor mediated pathway in breast cancer', *Int J Oncol*, 34(2), pp. 313-9.

Thastrup, J.O., Rafiqi, F.H., Vitari, A.C., Pozo-Guisado, E., Deak, M., Mehellou, Y. and Alessi, D.R. (2012) 'SPAK/OSR1 regulate NKCC1 and WNK activity:

analysis of WNK isoform interactions and activation by T-loop trans-autophosphorylation', *Biochem J*, 441(1), pp. 325-37.

Thompson, E.W., Reich, R., Shima, T.B., Albini, A., Graf, J., Martin, G.R., Dickson, R.B. and Lippman, M.E. (1988) 'Differential regulation of growth and invasiveness of MCF-7 breast cancer cells by antiestrogens', *Cancer Res*, 48(23), pp. 6764-8.

Thomson, R.B., Wang, T., Thomson, B.R., Tarrats, L., Girardi, A., Mentone, S., Soleimani, M., Kocher, O. and Aronson, P.S. (2005) 'Role of PDZK1 in membrane expression of renal brush border ion exchangers', *Proc Natl Acad Sci U S A*, 102(37), pp. 13331-6.

Tolcher, A.W., Patnaik, A., Papadopoulos, K.P., Rasco, D.W., Becerra, C.R., Allred, A.J., Orford, K., Aktan, G., Ferron-Brady, G., Ibrahim, N., Gauvin, J., Motwani, M. and Cornfeld, M. (2015) 'Phase I study of the MEK inhibitor trametinib in combination with the AKT inhibitor afuresertib in patients with solid tumors and multiple myeloma', *Cancer Chemother Pharmacol*, 75(1), pp. 183-9.

Turner, N.C., Ro, J., Andre, F., Loi, S., Verma, S., Iwata, H., Harbeck, N., Loibl, S., Huang Bartlett, C., Zhang, K., Giorgetti, C., Randolph, S., Koehler, M., Cristofanilli, M. and Group, P.S. (2015) 'Palbociclib in Hormone-Receptor-Positive Advanced Breast Cancer', *N Engl J Med*, 373(3), pp. 209-19.

Turturro, F., Friday, E., Fowler, R., Surie, D. and Welbourne, T. (2004) 'Troglitazone acts on cellular pH and DNA synthesis through a peroxisome proliferator-activated receptor gamma-independent mechanism in breast cancer-derived cell lines', *Clin Cancer Res*, 10(20), pp. 7022-30.

Usary, J., Llaca, V., Karaca, G., Presswala, S., Karaca, M., He, X., Langerod, A., Karesen, R., Oh, D.S., Dressler, L.G., Lonning, P.E., Strausberg, R.L., Chanock, S., Borresen-Dale, A.L. and Perou, C.M. (2004) 'Mutation of GATA3 in human breast tumors', *Oncogene*, 23(46), pp. 7669-78.

Vajdos, F.F., Hoth, L.R., Geoghegan, K.F., Simons, S.P., LeMotte, P.K., Danley, D.E., Ammirati, M.J. and Pandit, J. (2007) 'The 2.0 A crystal structure of the ERalpha ligand-binding domain complexed with lasofoxifene', *Protein Sci*, 16(5), pp. 897-905.

Vic, P., Vignon, F., Derocq, D. and Rochefort, H. (1982) 'Effect of estradiol on the ultrastructure of the MCF7 human breast cancer cells in culture', *Cancer Res*, 42(2), pp. 667-73.

Walker, G., MacLeod, K., Williams, A.R., Cameron, D.A., Smyth, J.F. and Langdon, S.P. (2007) 'Estrogen-regulated gene expression predicts response to endocrine therapy in patients with ovarian cancer', *Gynecol Oncol*, 106(3), pp. 461-8.

Walker, K., Bratton, D.J. and Frost, C. (2011) 'Premenopausal endogenous oestrogen levels and breast cancer risk: a meta-analysis', *Br J Cancer*, 105(9), pp. 1451-7.

Wang, J., Knight, Z.A., Fiedler, D., Williams, O., Shokat, K.M. and Pearce, D. (2008) 'Activity of the p110-alpha subunit of phosphatidylinositol-3-kinase is required for activation of epithelial sodium transport', *Am J Physiol Renal Physiol*, 295(3), pp. F843-50.

Wang, J., Xu, H., Wang, Q., Zhang, H., Lin, Y., Zhang, H., Li, Q. and Pang, T. (2015) 'CIAPIN1 targets Na(+)/H(+) exchanger 1 to mediate MDA-MB-231 cells' metastasis through regulation of MMPs via ERK1/2 signaling pathway', *Exp Cell Res*, 333(1), pp. 60-72.

Wang, Q. and Schultz, B.D. (2014) 'Cholera toxin enhances Na(+) absorption across MCF10A human mammary epithelia', *Am J Physiol Cell Physiol*, 306(5), pp. C471-84.

Warnmark, A., Wikstrom, A., Wright, A.P., Gustafsson, J.A. and Hard, T. (2001) 'The N-terminal regions of estrogen receptor alpha and beta are unstructured in vitro and show different TBP binding properties', *J Biol Chem*, 276(49), pp. 45939-44.

Westley, B.R. and May, F.E. (2006) 'Identification of steroid hormone-regulated genes in breast cancer', *Methods Mol Med*, 120, pp. 363-88.

Winer, E.P., Hudis, C., Burstein, H.J., Wolff, A.C., Pritchard, K.I., Ingle, J.N., Chlebowski, R.T., Gelber, R., Edge, S.B., Gralow, J., Cobleigh, M.A., Mamounas, E.P., Goldstein, L.J., Whelan, T.J., Powles, T.J., Bryant, J., Perkins, C., Perotti, J., Braun, S., Langer, A.S., Browman, G.P. and Somerfield, M.R. (2005) 'American Society of Clinical Oncology technology assessment on the use of aromatase inhibitors as adjuvant therapy for postmenopausal women with hormone receptor-positive breast cancer: status report 2004', *J Clin Oncol*, 23(3), pp. 619-29.

Wright, P.K. (2008) 'Targeting vesicle trafficking: an important approach to cancer chemotherapy', *Recent Pat Anticancer Drug Discov*, 3(2), pp. 137-47.

Wright, P.K., May, F.E., Darby, S., Saif, R., Lennard, T.W. and Westley, B.R. (2009) 'Estrogen regulates vesicle trafficking gene expression in EFF-3, EFM-19 and MCF-7 breast cancer cells', *Int J Clin Exp Pathol*, 2(5), pp. 463-75.

Wysolmerski, J.J. and Stewart, A.F. (1998) 'The physiology of parathyroid hormone-related protein: an emerging role as a developmental factor', *Annu Rev Physiol*, 60, pp. 431-60.

Xu, J.C., Lytle, C., Zhu, T.T., Payne, J.A., Benz, E., Jr. and Forbush, B., 3rd (1994) 'Molecular cloning and functional expression of the bumetanide-sensitive Na-K-Cl cotransporter', *Proc Natl Acad Sci U S A*, 91(6), pp. 2201-5.

Xue, F., Willett, W.C., Rosner, B.A., Hankinson, S.E. and Michels, K.B. (2011) 'Cigarette smoking and the incidence of breast cancer', *Arch Intern Med*, 171(2), pp. 125-33.

Yamamura, H., Ugawa, S., Ueda, T. and Shimada, S. (2008) 'Expression analysis of the epithelial Na+ channel delta subunit in human melanoma G-361 cells', *Biochem Biophys Res Commun*, 366(2), pp. 489-92.

Yang, J., Singleton, D.W., Shaughnessy, E.A. and Khan, S.A. (2008) 'The F-domain of estrogen receptor-alpha inhibits ligand induced receptor dimerization', *Mol Cell Endocrinol*, 295(1-2), pp. 94-100.

Yusef, Y.R., Thomas, W. and Harvey, B.J. (2014) 'Estrogen increases ENaC activity via PKCdelta signaling in renal cortical collecting duct cells', *Physiol Rep*, 2(5).

Zachos, N.C., Li, X., Kovbasnjuk, O., Hogema, B., Sarker, R., Lee, L.J., Li, M., de Jonge, H. and Donowitz, M. (2009) 'NHERF3 (PDZK1) contributes to basal and calcium inhibition of NHE3 activity in Caco-2BBe cells', *J Biol Chem*, 284(35), pp. 23708-18.

Zaman, K., Winterhalder, R., Mamot, C., Hasler-Strub, U., Rochlitz, C., Mueller, A., Berset, C., Wiliders, H., Perey, L., Rudolf, C.B., Hawle, H., Rondeau, S. and Neven, P. (2015) 'Fulvestrant with or without selumetinib, a MEK 1/2 inhibitor, in breast cancer progressing after aromatase inhibitor therapy: a multicentre randomised placebo-controlled double-blind phase II trial, SAKK 21/08', *Eur J Cancer*, 51(10), pp. 1212-20.

Zhang, Y., Moerkens, M., Ramaiahgari, S., de Bont, H., Price, L., Meerman, J. and van de Water, B. (2011) 'Elevated insulin-like growth factor 1 receptor signaling induces antiestrogen resistance through the MAPK/ERK and PI3K/Akt signaling routes', *Breast Cancer Res*, 13(3), p. R52.

Zhou, Y., Chen, X., Liu, X., Lu, H., Li, Y., Zhu, H., An, G., Zhang, N., Zhang, J., Ma, Q. and Zhang, Y. (2014) 'Phosphoinositide 3-kinase pathway mediates early aldosterone action on morphology and epithelial sodium channel in mammalian renal epithelia', *J Membr Biol*, 247(6), pp. 461-8.